

Functionalization of Silsesquioxanes: From Linkage of Unsaturated Silicon Clusters and Framework Expansion to Lewis Acid-Base Chemistry

Dissertation

zur Erlangung des Grades

des Doktors der Naturwissenschaften

der Naturwissenschaftlich-Technischen Fakultät

der Universität des Saarlandes

von

M.Sc. Marc Christian Hunsicker

Saarbrücken

2024

Tag des Kolloquiums: 04.06.2025

Dekan: Prof. Dr.-Ing. Dirk Bähre

Berichterstatter: Prof. Dr. David Scheschkewitz

Prof. Dr. Guido Kickelbick

Vorsitz: Prof. Dr. Andreas Speicher

Akademischer Mitarbeiter: Dr. Angelika Ullrich

Meiner Familie gewidmet

The present dissertation was prepared in the time between June 2019 to December 2024 at the Institute of General and Inorganic Chemistry of the Faculty of Natural Science and Engineering at the Saarland University under the supervision of Prof. Dr. David Scheschkewitz.

Die vorliegende Dissertation wurde in der Zeit von Juni 2019 bis Dezember 2024 am Institut für Allgemeine und Anorganische Chemie der Naturwissenschaftlich-Technischen Fakultät der Universität des Saarlandes unter der Aufsicht von Prof. Dr. David Scheschkewitz erstellt.

Abstract

Silsesquioxanes as organic-inorganic hybrid species are established polymer additives and fillers due to their beneficial contributions to the mechanical and thermal properties of the resulting material. Most investigations therefore focus on the organic substituents of the silsesquioxane, often ignoring the chemistry of the siloxane framework. This PhD thesis focuses on three aspects of silsesquioxane chemistry going significantly beyond such limitations: (1) a T_8R_8 silsesquioxane is connected with an unsaturated silicon cluster in search of a potential molecular silicon monoxide model system, (2) the straightforward trifluoromethanesulfonic acid-catalyzed condensation of two $T_7R_7(OH)_3$ units towards the so far largest structurally fully characterized silsesquioxane with organic substituents is demonstrated and a tris(triflate) derivative as intermediate explored, (3) the Lewis basicity of phospho-substituted silsesquioxanes of the T_7R_7P type is systematically studied for the first time including the unambiguous demonstration of the coordination of a phenyl-substituted derivative to sterically demanding Lewis acids.

Zusammenfassung

Silsesquioxane als organisch-anorganische Hybridspezies sind etablierte Polymer Additive und Füllmaterialien, aufgrund ihrer vorteilhaften Beiträge zu den mechanischen und thermischen Eigenschaften des resultierenden Materials. Die meisten Untersuchungen fokussieren sich daher auf die organischen Substituenten des Silsesquioxans, während die Chemie des Siloxangerüsts meist ignoriert wird. Diese Doktorarbeit fokussiert sich auf drei Aspekte der Silsesquioxanchemie, die signifikant weiter als diese Einschränkungen gehen: (1) ein T_8R_8 Silsesquioxan wird mit einem ungesättigten Siliziumcluster verbunden, auf der Suche nach einem potenziellen molekularen Siliziummonoxid Modellsystem, (2) die zielgerichtete, Trifluormethansulfonsäure katalysierte Kondensation von zwei $T_7R_7(OH)_3$ Einheiten hin zum bislang größten strukturell voll charakterisierten Silsesquioxan mit organischen Substituenten ist demonstriert und ein tris(triflat) Derivat als Intermediat erforscht, (3) die Lewis Basizität eines phospho-substituierten Silsesquioxans des T_7R_7P Typs ist systematisch zum ersten Mal untersucht, inklusive der eindeutigen Demonstration der Koordination eines phenylsubstituierten Derivats an sterisch anspruchsvolle Lewis Säuren.

List of publications

The present dissertation was published in parts in:

M. Hunsicker, N. E. Poitiers, V. Huch, B. Morgenstern, M. Zimmer, D. Scheschkewitz, Interlinkage of a siliconoid with a silsesquioxane: en route to a molecular model system for silicon monoxide, *Z. Anorg. Allg. Chem.* **2022**, 648, e202200239.

<https://doi.org/10.1002/zaac.202200239>

M. Hunsicker, Ankur, B. Morgenstern, M. Zimmer, D. Scheschkewitz, Polyhedral Oligomeric Silsesquioxane D_{3h} -(RSiO_{1.5})₁₄, *Chem. Eur. J.* **2024**, 30, e202303640.

<https://doi.org/10.1002/chem.202303640>

M. Hunsicker, J. Krebs, M. Zimmer, B. Morgenstern, V. Huch, D. Scheschkewitz, Synthesis and Ligand Properties of Silsesquioxane-Caged Phosphite T₇Ph₇P, *Z. Anorg. Allg. Chem.* **2024**, 650, e202400068

<https://doi.org/10.1002/zaac.202400068>

Acknowledgements/Danksagung

Ich bedanke mich zunächst ganz herzlich bei **Professor Dr. David Scheschkewitz** dafür, dass er mir die vorliegende Themenstellung anvertraut hat und ich diese Arbeit in seiner Gruppe anfertigen durfte. Silsesquioxane erwiesen sich als sehr spannende Herausforderung, die meine Fähigkeiten auch außerhalb des Experimentierens vertiefte. Dazu gehört ebenfalls die Weiterentwicklung des eigenen Charakters, bei welchem er stets mit gutem Beispiel vorangeht. Die durch die Dissertation ermöglichte Teilnahme an Fachkonferenzen und dem damit verbundenen Austausch bereitete mir großes Vergnügen, ebenso bin ich froh darüber, dass er mich ermutigte, dem Skifahren doch noch einmal eine Chance zu geben. :) Insgesamt fühlte ich mich stets willkommen, gut aufgehoben und wertgeschätzt. Danke!

Weiterhin bedanke ich mich bei **Professor Dr. Guido Kickelbick** für das Zweitgutachten dieser Arbeit und das bereits auf Konferenzen bekundete Interesse an meiner Forschung.

Professor Dr. Ralf Kautenburger danke ich für die Rolle meines wissenschaftlichen Begleiters.

Bei **Dr. Carsten Präsang** bedanke ich mich für die großartige Unterstützung im Labor, sowohl bei konkreten Fragen am Abzug als auch bei organisatorischen Details.

Dr. Volker Huch und **Dr. Bernd Morgenstern** danke ich sowohl für die Messung meiner Kristalle und Verfeinerung der Strukturen als auch für die Geduld die sie mit meinen oftmals schwierig zu messenden Proben mitbrachten.

Dr. Michael Zimmer danke ich für die Messung der VT- und Festkörper NMR Spektren, sowie für den Betrieb und die Wartung der NMR-Geräte, ohne die Routinemessungen und der Laboralltag kaum möglich wären.

Susanne Harling danke ich für die Messung der CHN-Analysen, meinen Kollegen aus dem AK Kickelbick **Svenja Pohl**, **Jan-Falk Kannengießer** und **Elias Gießelmann** für die Durchführung von DSC, TGA und Festkörper NMR Messungen.

Den beiden ehemaligen Sekretärinnen **Bianca Iannuzzi** und **Dominika Posse** danke ich für die Bearbeitung aller möglichen bürokratischen Angelegenheiten, sowie für ihre freundliche und offene Art.

Ich bedanke mich bei meinen Coautoren **Dr. Nadine Poitiers**, **Ankur** und **Johannes Krebs** für die wertvollen Beiträge zu meinen Publikationen, die sie wissenschaftlich abrundeten.

Den ehemaligen Mitgliedern des Arbeitskreis Scheschkewitz zur Zeit meiner Masterarbeit und frühen Doktorarbeit, bestehend aus **Dr. Kinga Leszczyńska**, **Dr. Paresh Kumar Majhi**, **Dr. Cem B. Yildiz**, **Dr. Nadine Poitiers**, **Dr. Lukas Klemmer**, **Dr. Yannic Heider**, **Dr. Yvonne Kaiser**, **Eveline Altmeyer** und **Lena Pesch**, danke ich für die überaus freundliche Aufnahme in die Gruppe, aus der auch Freundschaften hervorgegangen sind, und das vermittelte Wissen.

Dem aktuellen Arbeitskreis, insbesondere **Dr. Andreas Rammo**, **Dr. Diego Andrada**, **Dr. Nasrina Parvin**, **Andreas Adolf**, **Britta Schreiber**, **Henrike Waller**, **Thomas Büttner**, **Anna-Lena Thömmes**, **Luisa Giarrana**, **Daniel Mühlhausen**, **Philipp Grewelinger**, **Peter A.M. Spieß**, **Ankur (Urpils)**, **Liane Müller**, **Tim Wiesmeier**, **Michel Böhmert** und **Vanessa Grabowski** danke ich für die gute Zusammenarbeit, den vielen denk- und merkwürdigen Gesprächen und der wirklich tollen Zeit die wir auf Konferenzen (und Skipisten) hatten, die ich nicht missen möchte!

Den sich aus Partnerschafts- und Nachwuchsgründen stetig erweiternden Freundeskreisen möchte ich für die andauernde Freundschaft und den Zusammenhalt danken, die nun teilweise seit drei Jahrzehnten Bestand haben und dass wir es

(größtenteils) schaffen, uns trotz unserer unterschiedlichen Situationen alle paar Wochen zu sehen!

Meinen Eltern möchte ich für die anhaltende Unterstützung danken, die sie mir von Beginn an zuteilwerden ließen.

Content

| | |
|---|----|
| List of Abbreviations | 1 |
| List of Figures | 3 |
| List of Schemes | 4 |
| Preface | 7 |
| 1 Introduction | 9 |
| 1.1 Silsesquioxanes | 9 |
| 1.1.1 Overview, early synthetic procedures and analysis | 9 |
| 1.1.2 Synthesis of functionalized T ₈ R ₈ Silsesquioxanes | 13 |
| 1.1.3 Incompletely condensed silsesquioxanes | 14 |
| 1.1.4 Larger Silsesquioxane cage systems..... | 23 |
| 1.1.5 Applications of silsesquioxanes | 25 |
| 1.2 Lewis acid-base chemistry and frustrated Lewis pairs | 28 |
| 1.3 Stable unsaturated molecular silicon clusters | 30 |
| 1.3.1 Overview | 30 |
| 1.3.2 Stable neutral unsaturated Siliconoids..... | 30 |
| 1.3.3 Stable anionic unsaturated siliconoids | 32 |
| 1.4 Silicon monoxide..... | 34 |
| 1.4.1 Synthesis of silicon monoxide..... | 34 |
| 1.4.2 Model systems for SiO | 35 |
| 2 Aims and scope | 38 |
| 3 Publications..... | 42 |
| 3.1 Interlinkage of a siliconoid with a silsesquioxane: en route to a molecular model system for silicon monoxide | 42 |
| 3.2 Polyhedral Oligomeric Silsesquioxane D _{3h} -(RSiO _{1.5}) ₁₄ | 49 |
| 3.3 Synthesis and ligand properties of silsesquioxane-caged phosphite T ₇ Ph ₇ P | 56 |

| | | |
|-----|---|-----|
| 4 | Conclusion and Outlook..... | 63 |
| 5 | References..... | 68 |
| 6 | Supporting Information..... | 84 |
| 6.1 | Interlinkage of a siliconoid with a silsesquioxane: en route to a molecular model system for silicon monoxide | 84 |
| 6.2 | Polyhedral Oligomeric Silsesquioxane $D_{3h}-(R\text{SiO}_{1.5})_{14}$ | 119 |
| 6.3 | Synthesis and Ligand Properties of Silsesquioxane-Caged Phosphite $T_7\text{Ph}_7\text{P}$ | 143 |
| 7 | Permission of Redistribution and Licensing | 168 |

List of Abbreviations

| | |
|-------------|---|
| 222-crypt | {4,7,13,16,21,24-hexaoxa-1,10-diaza-bicyclo[8.8.8]hexacosane} |
| Å | Angstrom |
| °C | Celsius |
| cal | calories |
| CHN | Carbon, Hydrogen, Nitrogen Elemental Analysis |
| CP/MAS | Cross-polarization/magic angle spinning |
| CVD | Chemical vapour deposition |
| Cy | Cyclohexyl, -C ₆ H ₁₁ |
| dme | 1,2-Dimethoxyethane |
| eq | equivalent |
| Et | Ethyl, -C ₂ H ₅ |
| exc. | Excess |
| FLP | Frustrated Lewis pair |
| FTIR | Fourier Transform Infrared Spectroscopy |
| h | hour |
| HR | High-Resolution |
| HSQ | Hydrogen silsesquioxane |
| Hz | Hertz |
| ICM model | Interface clusters mixture model |
| <i>i</i> Pr | <i>iso</i> -Propyl, -C ₃ H ₇ |
| IR | Infrared |
| K | Kelvin |
| k | kilo |
| L | Liter |
| LA | Lewis-acid |
| LB | Lewis-base |
| M | Molar |
| Me | Methyl, -CH ₃ |
| Mes | Mesityl, 2,4,6-Trimethylphenyl, -(2,4,6-Me ₃ C ₆ H ₂) |
| min | Minute |

List of Abbreviations

| | |
|-------------------|---|
| m.p. | M elting p oint |
| NMR | N uclear M agnetic R esonance |
| Ph | P henyl, -C ₆ H ₅ |
| ppm | P arts p er m illion |
| RB model | R andom b onding model |
| RM model | R andom m ixture model |
| rt | r oom t emperature |
| ^t Bu | t ert- B utyl, -C(CH ₃) ₃ |
| TEM | T ransmission e lectron m icroscopy |
| TfOH | T rifluoromethanesulfonic a cid, F ₃ CSO ₃ H |
| Tf ₂ O | T rifluoromethanesulfonic a nhydride, (F ₃ CSO ₂) ₂ O |
| TGA | T hermo g ravimetric A nalysis |
| thf | t etra h ydro f urane |
| Tip | 2,4,6- T riisopropyl p henyl |
| UV/vis | U ltraviolet / v isible |
| VT-NMR | V ariable T emperature N uclear M agnetic R esonance |

List of Figures

| | |
|---|----|
| Figure 1. Exemplary structures of different silsesquioxane types. A: T_6R_6 , B: T_8R_8 , C: $T_{10}R_{10}$, D: incompletely condensed $T_7R_7(OH)_3$, E: ladder-like, F: random polymeric. R designates hydrogen or organic functional groups. | 10 |
| Figure 2. Schematic of processes from silanol (A ; $HSi(OH)_3$) to T_8 (U). The numbers are the MP2//B3LYP/6-31G(d) + ZPC reaction energies. The number of intramolecular hydrogen bonds shorter than 2.5 Å are indicated in parentheses. Figure reproduced with permission from the American Chemical Society. ^[37d] | 13 |
| Figure 3. Examples of isolated larger silsesquioxane frameworks: $T_{12}R_{12}$ (G ^[65a-e]), C_{2v} isomer of $T_{14}R_{14}$ (H ^[67a]), D_{3h} isomer of $T_{14}R_{14}$ (I ^[34a]), $T_{18}R_{18}$ (J ^[66]). | 24 |
| Figure 4. Examples of an Si_8Me_{14} polycyclic silane 29 , ^[97] a $[Si_9]^{4-}$ Zintl anion 30 ^[99a] and a Si_5Tip_6 siliconoid 31 . ^[102] The counter ions of 30 are omitted for clarity, the unsubstituted silicon atom of 31 is highlighted in bold (Tip = 2,4,6-triisopropylphenyl). | 30 |
| Figure 5. Selected siliconoids (Mes = 2,4,6-trimethylphenyl, Dip = 2,6-diisopropylphenyl, Tip = 2,4,6-triisopropylphenyl, R = $SiMe_3$). ^[110] | 32 |
| Figure 6. Targeted proof-of-principle molecule 46 consisting of hexasilabenzpolarene linked to a T_8Ph_7R silsesquioxane. The stoichiometry of silicon to oxygen (about 1:0.86) approximates the overall 1:1 ratio of silicon monoxide, while the components themselves represent silicon and oxygen rich domains..... | 39 |

List of Schemes

- Scheme 1.** Synthesis of T_8H_8 **1** via “scarce-water” hydrolysis of trichlorosilane with $FeCl_3$.^[34b] 11
- Scheme 2.** Selected functionalization strategies of hydridosilsesquioxanes T_nH_n . For **2** to **6**: $n = 8$, for **7**: $n = 12$, for **8**: $n = 14$.^[34a;39] 14
- Scheme 3.** Treatment of fully condensed T_8Cy_8 **9** silsesquioxane with a) tetrafluoroboric acid and b) triflic acid. In both cases, one edge of the cubic framework is opened and two silyl fluoride (**10**) or triflate (**12**) moieties are produced. $Cy=C_6H_{11}$.^[44] 15
- Scheme 4.** Edge-capping of bis(triflate) **12** with an excess of aniline results in an incompletely condensed silsesquioxane functionalized with two silyl amide moieties **15**. A formally fully condensed T_8Cy_8 structure such as **14** can be obtained with one oxygen replaced by nitrogen, by treatment of the bistriflate with an equimolar amount of aniline.^[45] 16
- Scheme 5.** Synthesis of incompletely condensed silsesquioxanes $T_7R_7(OH)_3$ type **16** with C_{3v} symmetry and of the double decker type **17** from the same starting material. $R =$ in general organic substituents, for $R = Ph$: **16a**,^[38,46b;48] $R = Cy$: **16b**,^[46c] $R' =$ alkoxysubstituents. 17
- Scheme 6.** Corner capping reaction of incompletely condensed $T_7Cy_7(OH)_3$ silsesquioxane **16b** with chlorosilanes and an auxiliary base producing a completely condensed framework **18** akin to structure **B** (Figure 1) with one different substituent. $R' = H$ or organic substituent.^[32a;49] 18
- Scheme 7.** Corner-opening reaction of a completely condensed monofunctional silsesquioxane **19** with tetraethylammonium hydroxide resulting in functionalized trisilanol **20**.^[50] 18
- Scheme 8.** Incompletely condensed silsesquioxanes **16b** react with (transition-)metals react with in such a way, that a M_2O_2 bridge between two T_7 fragments is created. $M = Ti$: **21a**,^[52a] $M = Al$: **21b**,^[52b] $M = V$: **21c**.^[52c;53a] 19
- Scheme 9.** a) Treatment of incompletely condensed silsesquioxane $T_7Cy_7(OH)_3$ **16b** with BI_3 in the presence of NEt_3 results in dimer **22**, in which two boron atoms bridge two separate T_7 fragments, while keeping their trigonal planar coordination

| | |
|--|----|
| environment. ^[58] b) The reaction of $T_7Cy_7(OH)_3$ with $AlMe_3$ yields dimer 21b , in which the two Al atoms are tetrahedrally coordinated and form an Al_2O_2 ring. ^[52b] | 21 |
| Scheme 10. Cleavage of aluminium dimer 21b with proposed occurrence of intermediate monomeric species 23 on the way to Lewis adducts 24a ((a) = R = $OPPh_3$, n = 0), 24b ((b) = R = Me_3NO , n = 0), ^[52b] 24c ((c) = $Me_4SbOTMS$, R = TMS, n = 1, X = Me_4Sb ; TMS = trimethylsilyl) ^[59a] and 24d ((d) = Me_4SbOH , R = H, n = 1, X = Me_4Sb). ^[59b] | 21 |
| Scheme 11. Treatment of incompletely condensed silsesquioxane 25 with 0.5 equivalents of $LiBH_4$ produces the bridged species 26 R = C_5H_9 . ^[59c] | 22 |
| Scheme 12. The concept of Frustrated Lewis pairs (FLPs) illustrated with dihydrogen activation by prototypical 27 . ^[89] | 28 |
| Scheme 13. Treatment of lithium-disilenide 32 ^[108] with 0.25 eq of tetrachlorosilane yields the first siliconoid 31 ^[107] with tetrasilabutadiene 33 ^[109] as by-product (Tip = 2,4,6-triisopropylphenyl). | 31 |
| Scheme 14. a) Syntheses of anionic siliconoids from the dismutative isomer of hexasilabenzpolarene 36 in different positions. ^[112a-c] (Reagents: (a): $BH_3 \cdot SME_2$; (b): $tBuC(O)Cl$; (c): $PhC(O)Cl$; (d): $SiCl_4$; (e): $CIP(NMe_2)_2$; (f): $ClSiMe_3$; E = main group element electrophiles: 41a : E = BH_3^- , 41b : E = $tBuCO$, 41c : E = $PhCO$, 41d : E = $SiCl_3$, 41e : E = $P(NMe_2)_2$, 41f : E = $SiMe_3$, Tip = 2,4,6-triisopropylphenyl). b) Formation of anionic siliconoids 44 and 45 through silylation of $K_{12}Si_{17}$. 45 is formed in small amounts during crystallization of 44 (222crypt = {4,7,13,16,21,24-hexaoxa-1,10-diaza-bicyclo[8.8.8]hexacosane}). ^[110g] | 33 |
| Scheme 15. Heating of silicon and silicon dioxide forms diatomic silicon monoxide, which disproportionates partially again upon cooling or thermal treatment into silicon and silicon dioxide. ^[117] | 34 |
| Scheme 16. Proposed treatment of the phenyl substituted incompletely condensed silsesquioxane $T_7Ph_7(OH)_3$ 16a with trifluoromethanesulfonic acid..... | 40 |
| Scheme 17. Treatment of incompletely condensed silsesquioxane 16b with PCl_3 corner caps the missing vertex with a phosphorus atom. The hereby generated phosphite 47 was shown to coordinate to Lewis acidic center of trimethylaluminium to form the Lewis adduct 48 . ^[61a] | 41 |
| Scheme 18. Reaction of silsesquioxane substituted phosphite 49 with various sterically demanding Lewis acids R_3A can potentially lead to frustrated Lewis pairs with interesting properties (R = organic substituent, A = Lewis acidic center). | 41 |

- Scheme 19.** a) Combining the linker substituted silsesquioxane **50** with anionic siliconoid **40** yields the proof-of-concept model system **46**. b) Due to steric compatibility, even shorter linking units such as used in silsesquioxane **51** are accepted to form the smaller linked congener **52**..... 63
- Scheme 20.** a) Treatment of incompletely condensed silsesquioxane **16a** with an excess of TfOH substitutes the silanol moieties, however only small amounts of triflate **53** could be obtained in the form of low-quality crystals. An overall partial substitution in the reaction mixture towards $T_7Ph_7(OH)_{3-x}(OTf)_x$ is tentatively suggested. b) Adding 10 mol% of TfOH to silsesquioxane **16a** produces the $T_{14}Ph_{14}$ silsesquioxane **54**... 65
- Scheme 21.** Corner capping of phenyl substituted incompletely condensed silsesquioxane **16a** with PCl_3 yields phosphite **49**. Treatment of **49** with several Lewis acids affords the Lewis acid-base adducts **55a-d** (E = main group or transition metal element, R = organic substituent **55a**: $ER_n = BPh_3$, **55b**: $ER_n = B(C_6F_5)_3$, **55c**: $ER_n = BCl_3$, **55d**: $ER_n = Fe(CO)_4$). 67

Preface

Modern society is unimaginable without the technological advances seen in recent history. Of all elements in the periodic table, silicon is a critical component with regards to its role in semiconductors. It is only second to oxygen with regards to the abundance in earth's crust^[1] and occurs in the form of silicon dioxide and silicate minerals. Since its first isolation in amorphous form by Berzelius in 1824^[2] and the discovery of its semiconducting properties, the development and improvement of industrial manufacturing processes opened the door for mass production of everyday devices.^[3] The increase in annual production of (ferro-)silicon (from about 3.4 million tons in the year 2000 to over 9 million tons as of 2023) reflects the great demand of silicon-based materials.^[4] The impact of the so-called semiconductor crisis^[5] on the supply chains of silicon and the resulting delay in technological goods demonstrates the importance of the element in our daily lives.

To further the technological progress even more, it is vital to understand more about different silicon compounds and their effect on semiconducting materials. Established processes, like the top-down approach of etching circuitry into silicon wafers via photolithography, frequently reach their resolution limit in creating smaller structures and new techniques must be explored. While extreme ultraviolet (EUV) lithography^[6] enabled the patterning below the diffraction limit of previous photolithography methods, it faces challenges to further minimize semiconductor circuitry. Promising new techniques are investigated to replace EUV lithography,^[6b;7a] as well as fundamentally new transistor components.^[7b] On the other hand, bottom-up approaches^[8] can be a complementary tool which in principle allows for a structural build-up from silicon surfaces. The investigation of relevant intermediates is hence a priority of increasing importance.

Molecular silicon clusters were reported to resemble intermediates of bulk silicon produced by chemical vapor deposition (CVD) of silanes,^[9] and can be versatile model systems of these processes and resulting materials. Silicon monoxide (SiO), which is known since 1886^[10] and heavily investigated in industrial applications such as lithium-ion battery materials,^[11] is a prominent example as its exact atomic composition is still a matter of debate.

Aside from the semiconductor field, various forms of silicon compounds found their way into every nook and cranny of homes around the globe in the form of polysiloxanes. A special class of siloxane compounds are silsesquioxanes, organic-inorganic hybrid materials consisting of a siloxane framework with organic substituents in the form of polymeric networks or discrete molecules. Due to their structural proximity to silicon dioxide, they are sometimes regarded as the smallest possible silica structure, albeit with some restrictions due to their substituents.^[12] Closely resembling sphaerosilicates^[13] (with organic substituents on each vertex), their synthetic access was troublesome in the beginning, but later breakthroughs^[14] enabled their widespread use in industrial applications. Employed as copolymers, they transfer unique properties such as thermal and mechanical stability^[15] to materials,^[16] and are also relevant in the aforementioned bottom-up procedures.^[17] Functionalization strategies of silsesquioxanes have been investigated thoroughly for certain readily accessible species such as the series from the T_8R_8 to $T_{12}R_{12}$ representatives, while synthetic access of larger frameworks and their structure-property relationships remain mostly obscure to this day. The goal of this thesis is to contribute to functionalization strategies from a molecular chemical point of view, regarding model systems of subvalent silicon oxides with the silsesquioxane acting as silica model, facile access to larger frameworks through catalyzed condensation, as well as Lewis-acid-base chemistry.

1 Introduction

1.1 Silsesquioxanes

1.1.1 Overview, early synthetic procedures and analysis

Silsesquioxanes are a class of organic-inorganic hybrid materials with the stoichiometric formula of $[\text{RSiO}_{1.5}]_n$. The term “sesqui”, translating to “one and a half” in Latin, reflects the silicon to oxygen ratio of 1.5 in silsesquioxanes. A variety of structures is known, ranging from cage- or ladder-like representatives to random polymeric mixtures as shown in Figure 1. The functional group R can designate hydrogen or organic substituents suitable for a vast amount of functionalizations. As agreed upon in siloxane chemistry, the abbreviation T_n distinguishes the cage size with the index n ($n \geq 4$) being the number of trifunctional silicon vertices T in the silsesquioxane. Additionally, the name “POSS” for polyhedral oligomeric silsesquioxanes has been established, differentiating the cage-like from cyclic and polymeric structures. The size of the T_8R_8 siloxane cages is usually in the range of 1.2 to 1.4 nm,^[18a] while the very rigid inorganic siloxane core^[18b] itself amounts to about 0.5 nm^[18c] which makes them one of the smallest classes of nanoparticles.^[19]

First reports hinting at the formation of – by then – structurally unverified siloxane frameworks that could today be classified as silsesquioxanes were published as early as 1873 by Ladenburg.^[20] The hydrolysis product of phenyltrichlorosilane was described as “silicobenzoic acid”, reaction with potassium hydroxide in alcohol and carbonic acid resulted in a solid product given the formula of $(\text{SiC}_6\text{H}_5\text{O})_2\text{O}$ via molecular weight determination, wrongly identified as “siliconic anhydride”. Kipping and coworkers argued from their own observations with silane diols,^[21] that the more realistic interpretation would be hydrolysis followed by condensation into more complex structures. The nature of these condensation products was also pointed out to be highly influenced by the hydrolysis conditions employed, usually resulting in mixtures. Reported by Scott in 1946,^[22] thermal rearrangement of a MeSiCl_3 and Me_2SiCl_2 condensate forms different siloxane products, one of which was tentatively attributed to the formula $[\text{MeSiO}_{1.5}]_{2n}$, with n being an integer. Overall low yields (below 1%) and bad solubilities hindered a more detailed analysis. A patent by Barry and Gilkey

published in 1949^[23] details the separation of supposedly T_8R_8 to $T_{24}R_{24}$ monomers – distinguished via their molecular weight – from a mixture of alkylsilsesquioxane hydrolysate and sodium hydroxide, with some of the proposed conformations being correct in hindsight, though at the time still unverified.

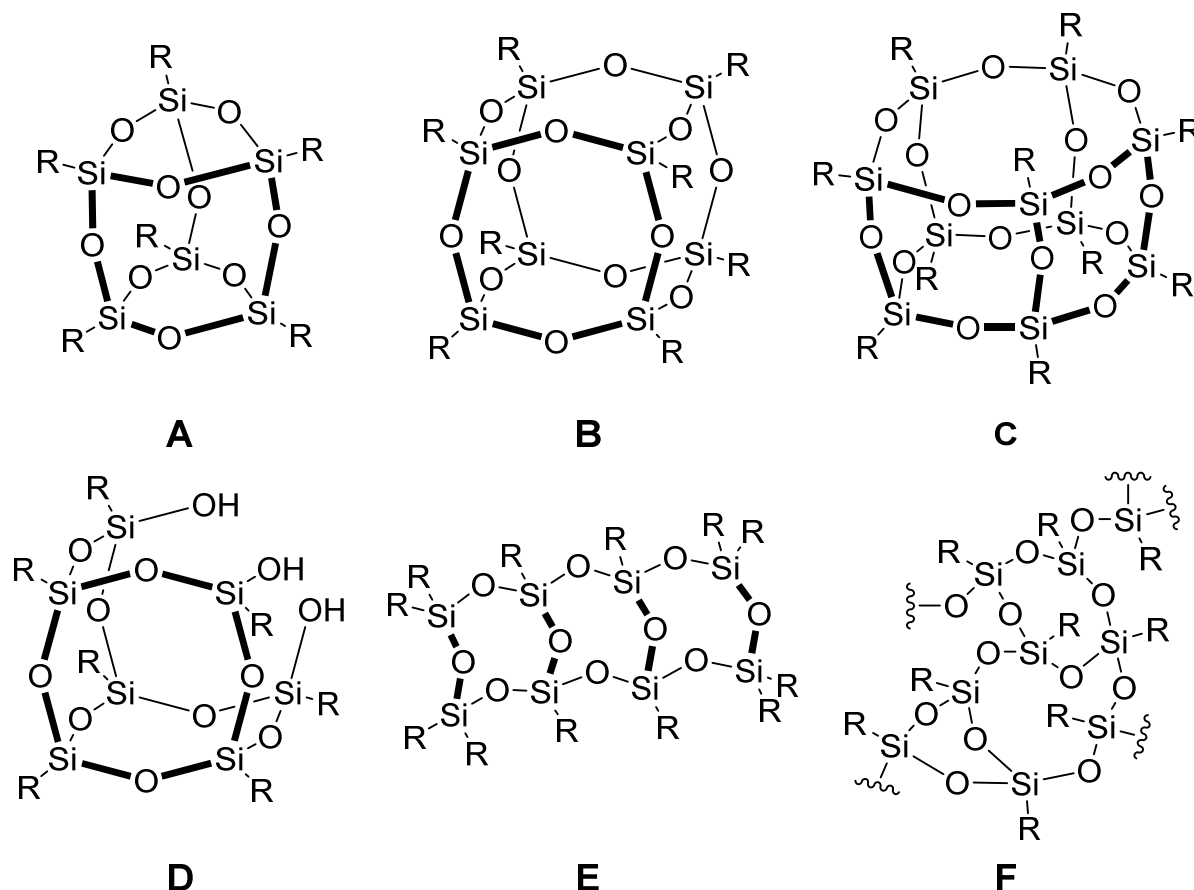
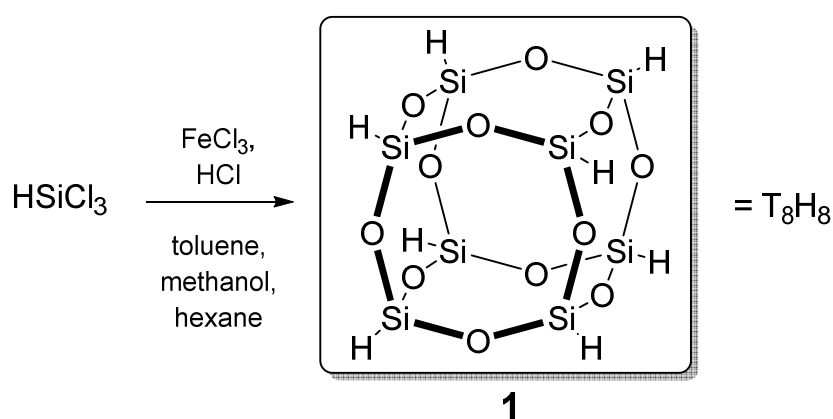


Figure 1. Exemplary structures of different silsesquioxane types. **A:** T_6R_6 , **B:** T_8R_8 , **C:** $T_{10}R_{10}$, **D:** incompletely condensed $T_7R_7(OH)_3$, **E:** ladder-like, **F:** random polymeric. R designates hydrogen or organic functional groups.

In 1955, several reports were published in rapid succession by the groups of Guenther, Gilkey and Wiberg, describing indication for T_6Me_6 , T_8Me_8 ,^[24a,c] T_6Ph_6 ,^[25] T_8Et_8 ,^[24b;25] $T_{10}Me_{10}$ ^[25] and $T_4^tBu_4$ as well as $T_4^iPr_4$ ^[26] units. It should be noted that some of the structural assumptions were allegedly wrong (T_6Ph_6)^[25,27] or remained tentative until subsequently realized from different starting materials (T_4R_4).^[26,28] The approach of Sprung and Guenther differed from the so far established procedures. Instead of thermally rearranging (co-)hydrolysates of di- and trichlorosilanes produced in an excess of water, they employed co-hydrolysis of trialkoxysilanes and trichlorosilanes

in the presence of up to three molar equivalents of water,^[24a,b] with additional acid catalysis^[24c] depending on the silane employed. In case of basic catalysis, the addition of tetraethylammonium hydroxide increased yields somewhat as well as shown by the same authors.^[29] Structural conformations of T_8Et_8 and T_8Cy_8 were finally obtained by Gilkey via XRD-analysis,^[25] followed by the works of Sliwinski^[30] in 1959 (reporting the first synthesis of the octahydridosilsesquioxane T_8H_8) and Larrson^[31] in 1960, detailing several other alkylsubstituted silsesquioxane solid-state structures.

After these seminal reports, the next decades encompassed the synthesis of many structures from $n=6$ upward in one reaction mixture from chloro- or alkoxy silanes. In addition, most silsesquioxanes could only be isolated in very low yields after being crystallized or precipitated over the course of weeks or even months.^[25,32] During this time, the first incompletely condensed frameworks (such as Structure **D** from Figure 1) were reported by Brown and Vogt,^[32a,b] which will be the focus of Chapter 1.1.3. In 1970, Frye and Collins reported the synthesis of T_8H_8 under “scarce-water” conditions, in contrast to previous syntheses, which had employed water in excess. Controlling the exact equivalents of water in the reaction mixture allowed the authors to isolate T_8H_8 in about 13% yield, along with the first higher hydridosubstituted structures from $T_{10}H_{10}$ to $T_{16}H_{16}$ in combined yields of 15-35%.^[33] Further improved protocols with additional characterization data based on Collins work were published in 1987 and 1991 by Agaskar and coworkers,^[34] reaching an overall yield of 17.5% of T_8H_8 **1** (Scheme 1).



Scheme 1. Synthesis of T_8H_8 **1** via “scarce-water” hydrolysis of trichlorosilane with $FeCl_3$.^[34b]

Another report of Agaskar and Klemperer in 1995^[35] details the synthesis and isolation protocols of silsesquioxanes ranging from T_8H_8 **1** to $T_{18}H_{18}$ from one and the same reaction mixture in a long and resource-intensive procedure. Breakthroughs such as reported by Bassindale and coworkers^[14] enabled the synthesis of T_8R_8 silsesquioxanes with yields of up to 90%, finally giving broader access to functionalized T_8R_8 frameworks without the need of hydrosilylation of T_8H_8 .

The remarkable and apparently quite selective formation of discrete molecules from monomeric silanes instead of random polymeric structures has been subject of many investigations. The observations of Brown and Vogt^[32a,b] infer cyclic oligosiloxanes ((SiO)₃ and (SiO)₄ rings) emerging from dimers. Fourier Transform infrared spectroscopy (FTIR) monitoring the condensation process of alkoxy silanes under basic conditions alludes to a four membered (SiO)₄ ring as well, two of which then condense into T_8 frameworks.^[36] Kudo and coworkers investigated the formation of the T_8H_8 framework theoretically from the role of solvents and starting materials' substituents to the fully condensed products.^[37] Water is ascribed a significant beneficial effect in the initial condensation and formation of small three and four membered rings with SiO units by stabilizing all-*cis* transition states with hydrogen bonds.^[37a,b] Supporting the findings of Brown, Vogt^[32a,b] and Li,^[36] the (SiO)₄ ring (structure C in Figure 2) is understood as initial precursor for larger frameworks as well, although alternative rearrangement processes of for example three membered ring systems were not considered in the calculations.^[37d] In addition to four consecutive condensations of two (SiO)₄ rings towards the T_8 framework, Kudo and coworkers describe (energetically less favored) alternative stepwise constructions from the four membered ring onward: ancillary siloxane mono- or dimers are being added in such a way, that the greatest possible stabilizing effect through hydrogen bonding is achieved. This leads to many possible intermediates on the way to the fully condensed octahydridosilsesquioxane T_8H_8 (Figure 2).^[37d] Nevertheless, research concerning the choice of reaction conditions such as the solvent is still ongoing, which can significantly influence the structural outcome.^[38]

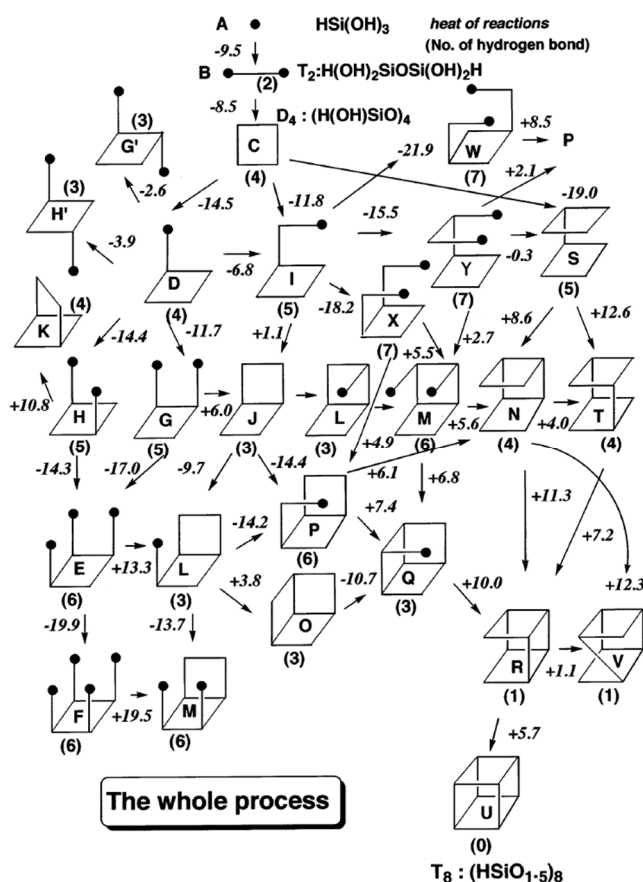
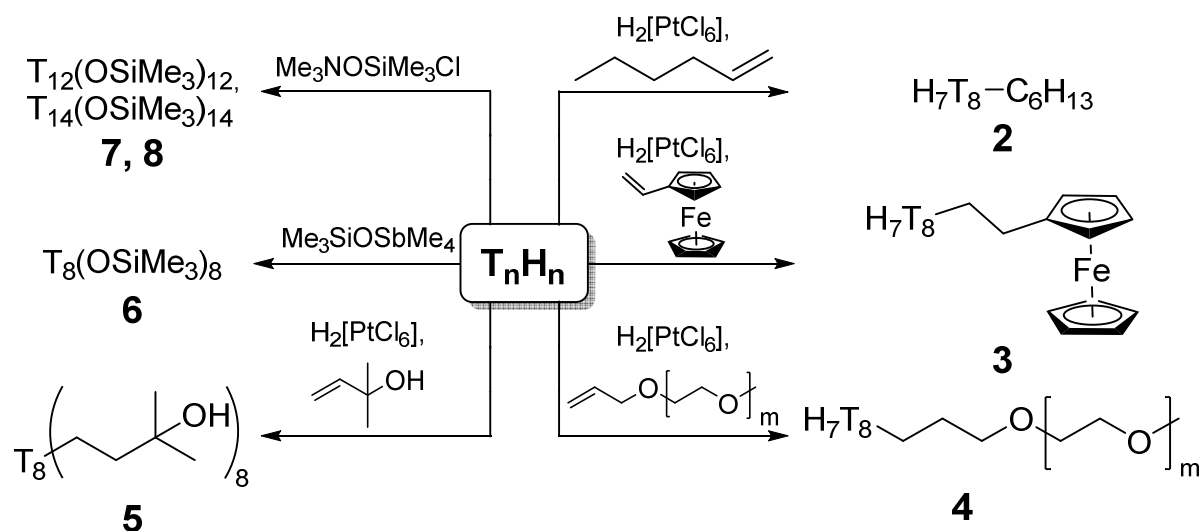


Figure 2. Schematic of processes from silanol (A; $HSi(OH)_3$) to T_8 (U). The numbers are the MP2//B3LYP/6-31G(d) + ZPC reaction energies. The number of intramolecular hydrogen bonds shorter than 2.5 Å are indicated in parentheses. Figure reproduced with permission from the American Chemical Society.^[37d]

1.1.2 Synthesis of functionalized T_8R_8 Silsesquioxanes

The T_8R_8 framework is the by far most investigated representative of the silsesquioxanes. Several pathways to certain functionality patterns are known, depending on the starting material. The parent molecule, T_8H_8 is formed through the improved “scarce-water”-method of Agaskar and Klemperer as described above.^[34b] The silicon-hydrogen functionalities allow different modifications such as hydrosilylation, usually carried out with Speier’s or Karstedt’s catalysts.^[39] The versatility of these approaches is limited by indiscriminate conversion of the Si-H functionalities, as in most cases all of them react in the same manner, although some reports do give insight into selective monofunctionalization via this route, as shown in Scheme 2.^[39a-c]



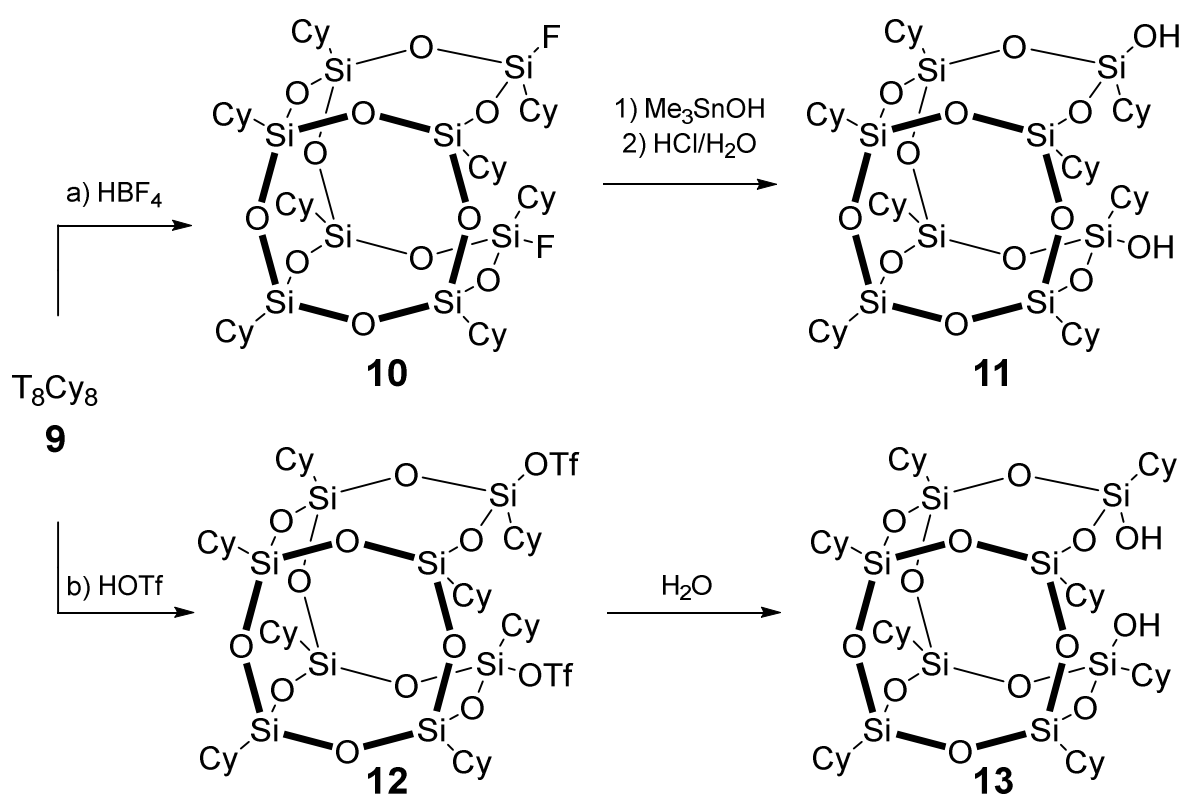
Scheme 2. Selected functionalization strategies of hydridosilsesquioxanes T_nH_n . For **2** to **6**: $n = 8$, for **7**: $n = 12$, for **8**: $n = 14$.^[34a;39]

Organically substituted T_8R_8 frameworks can be synthesized from accordingly substituted starting materials as well, provided the functional group tolerates the necessary condensation conditions. Common organic manipulations have been used to create silsesquioxanes tailored to the desired application, as most reactions are targeting the functional organic groups, not the siloxane core itself.^[40] Perhaps the most important requirement in this case is the compatibility of the siloxane core with regards to harsh reaction conditions, as it can be cleaved by strong acids and bases, which will be discussed in the next chapter. Silsesquioxanes are also investigated regarding the encapsulation of hydrogen^[41] and fluoride inside the siloxane core.^[18c;42]

1.1.3 Incompletely condensed silsesquioxanes

As in the T_8H_8 parent case, monofunctionalization of only one functional group from a fully condensed T_8R_8 silsesquioxane is a difficult task. While condensations of differently substituted chloro- or alkoxy-silanes in the desired stoichiometric ratio can indeed be used to isolate partially functionalized frameworks, very low yields and mixtures of different isomers are the result of such reaction conditions.^[43] A different reaction pathway solves this problem by utilizing incompletely condensed silsesquioxanes, where at least one siloxane bond of the framework is missing. From general investigations, such as shown in Figure 2, it can be rationalized that

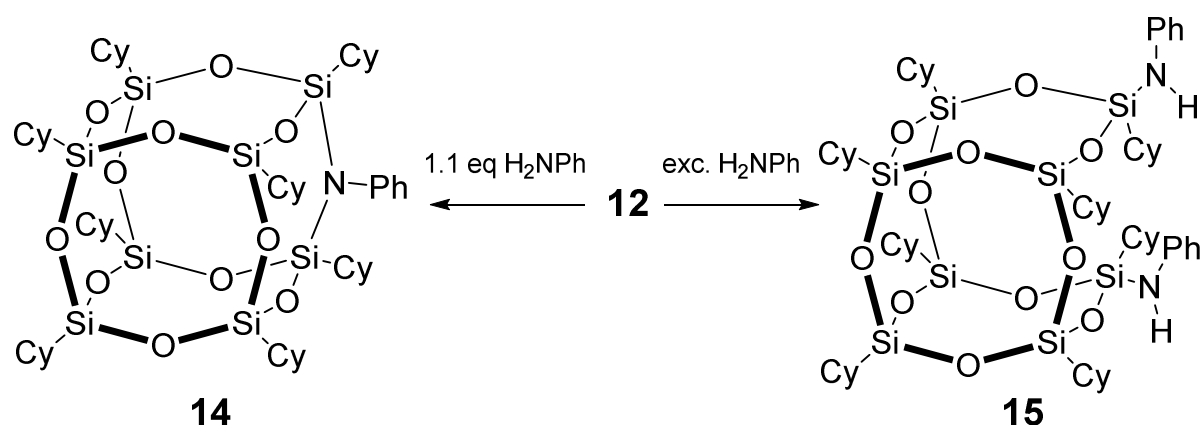
incompletely condensed structures are suitable precursors for various framework manipulations through condensation. As mentioned in Chapter 1.1.1, such open frameworks were already reported by Brown and Vogt in the 1960's, although their significant synthetic value had not been recognized at the time.^[32a] Two general methods are established: Siloxane bond cleavage of a completely condensed cage with strong acids or bases or preventing the condensation process from finishing the framework during the synthesis. Feher's pioneering work details the edge-opening reactions of T_8Cy_8 silsesquioxane **9** using trifluoromethanesulfonic acid (TfOH) or $HBF_4 \cdot OEt_2$.^[44] Upon bond cleavage, either a triflate group or fluorine substitutes the oxygen on the silicon atoms formerly part of the siloxane bond. The disilyl fluoride **10** allows substitution with trimethylstannanol, followed by hydrolyzation towards the exodisilanol **11**. The bis(triflate) **12** is prone to hydrolysis and can form the endodisilanol **13** or reform the completely condensed T_8 framework **9** to varying degrees.^[44] With both reaction pathways, stereochemical control over the position of the silanol groups enables the endo- and exohedral functionalization of the framework (Scheme 3).



Scheme 3. Treatment of fully condensed T_8Cy_8 **9** silsesquioxane with a) tetrafluoroboric acid and b) triflic acid. In both cases, one edge of the cubic framework is opened and two silyl fluoride (**10**) or triflate (**12**) moieties are produced. Cy= C_6H_{11} .^[44]

While the disilyl fluoride **10** is a very stable species due to its silicon-fluoride bond and is restricted to a few manipulations, the more versatile bis(triflate) **12** can be functionalized with suitable nucleophiles. Treatment with either stoichiometric amounts or an excess of aniline results in the silsesquioxane framework **14** with an oxygen atom substituted by nitrogen, or in the disilylamide **15**, respectively (Scheme 4).^[45]

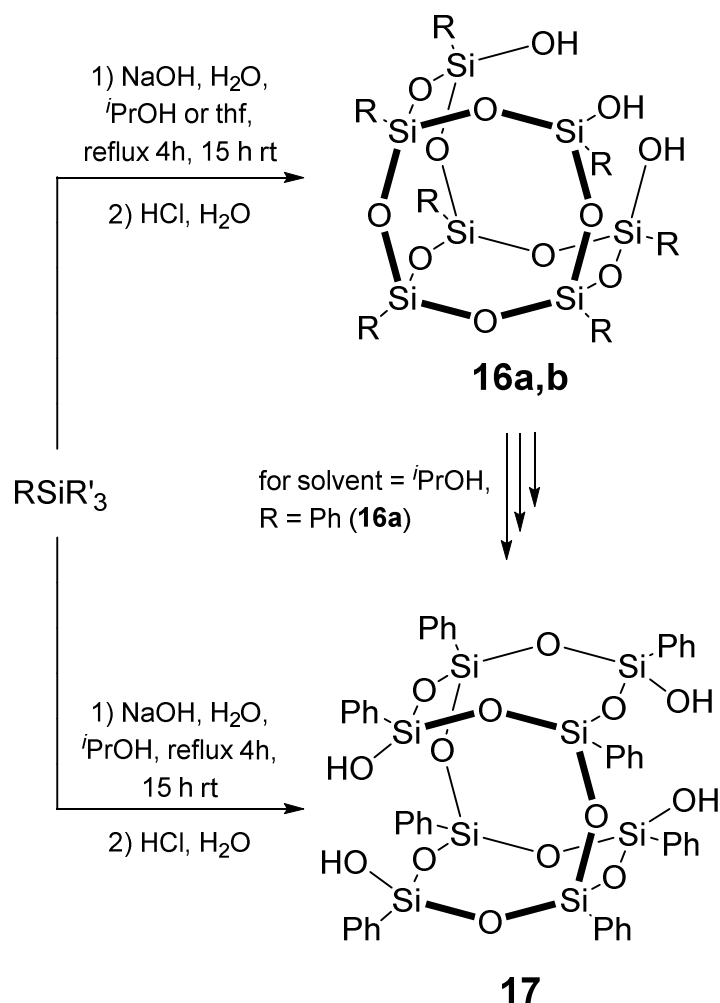
The incompletely condensed silsesquioxanes with one vertex missing have garnered more attention than the previously discussed mono edge-opened frameworks, as their synthetic access is far easier. The approximately C_{3v} symmetric T_7 silsesquioxane structure **16** is formed through the hydrolysis and condensation of trichloro- or alkoxy silanes. The early reports detail chlorosilane hydrolysis procedures lasting months to years,^[32] a period of time that can be shortened considerably by the presence of a base such as lithium or sodium hydroxide and a slight excess (1.1 to 1.3 equivalents) of water (Scheme 5).^[46] The synthesized silanolates can then be protonated to obtain the incompletely condensed $R_7T_7(OH)_3$ species.



Scheme 4. Edge-capping of bis(triflate) **12** with an excess of aniline results in an incompletely condensed silsesquioxane functionalized with two silyl amide moieties **15**. A formally fully condensed T_8Cy_8 structure such as **14** can be obtained with one oxygen replaced by nitrogen, by treatment of the bistriflate with an equimolar amount of aniline.^[45]

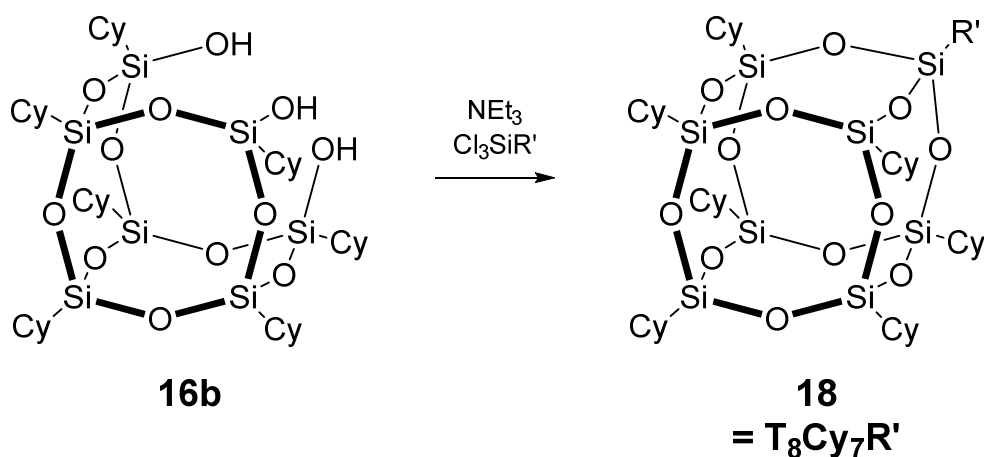
Notably, almost the same reaction conditions are employed to obtain the incompletely condensed framework **17**, usually termed double decker silsesquioxane (DDSQ).^[47] Applying alcohols as solvents instead of aprotic ethers such as thf and longer reaction times is the key for this reactivity, as intermolecular hydrogen bonding to the solvent molecule suppresses dimer formation of two $T_7R_7(OH)_3$ fragments.^[38,48] The $T_7Ph_7(OH)_3$ trisilanol **16a** was found to act as the precursor for DDSQ **17**, which is

obtained after about 44 h of continuous stirring (Scheme 5), in line with previous findings reporting siloxane bond cleavage in silsesquioxane frameworks under basic conditions in alcoholic media.^[36]



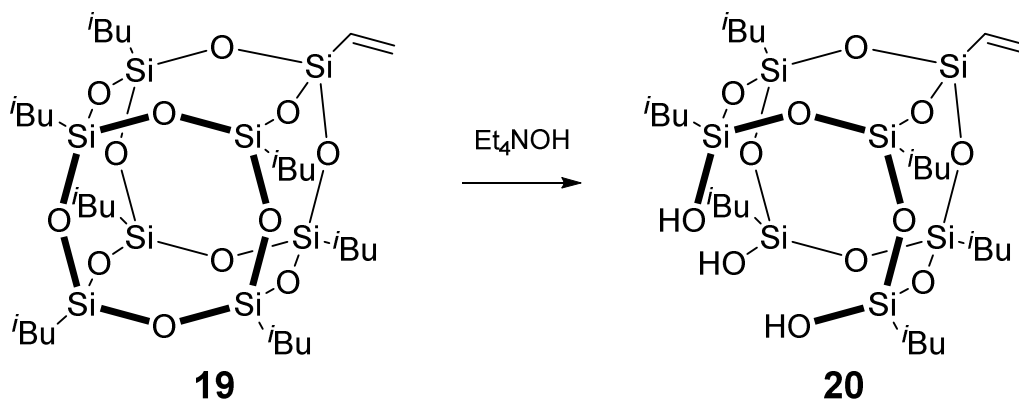
Scheme 5. Synthesis of incompletely condensed silsesquioxanes $\text{T}_7\text{R}_7(\text{OH})_3$ type **16** with C_{3v} symmetry and of the double decker type **17** from the same starting material. R = in general organic substituents, for $\text{R} = \text{Ph}$: **16a**,^[38,46b,48] $\text{R} = \text{Cy}$: **16b**,^[46c] R' = alkoxysubstituents.

The silanol functionalities of incompletely condensed silsesquioxanes make them an extremely versatile starting material, enabling the incorporation of a differently substituted silicon atom in so-called corner capping reactions. Capping the structure with silicon vertices is conveniently achieved with trichlorosilanes and an amine as auxiliary base (Scheme 6).^[32a,c;49] In general, any functional group can be introduced this way, as long as the necessary reaction conditions do not decompose the siloxane framework.



Scheme 6. Corner capping reaction of incompletely condensed T₇Cy₇(OH)₃ silsesquioxane **16b** with chlorosilanes and an auxiliary base producing a completely condensed framework **18** akin to structure **B** (Figure 1) with one different substituent. R' = H or organic substituent.^[32a;49]

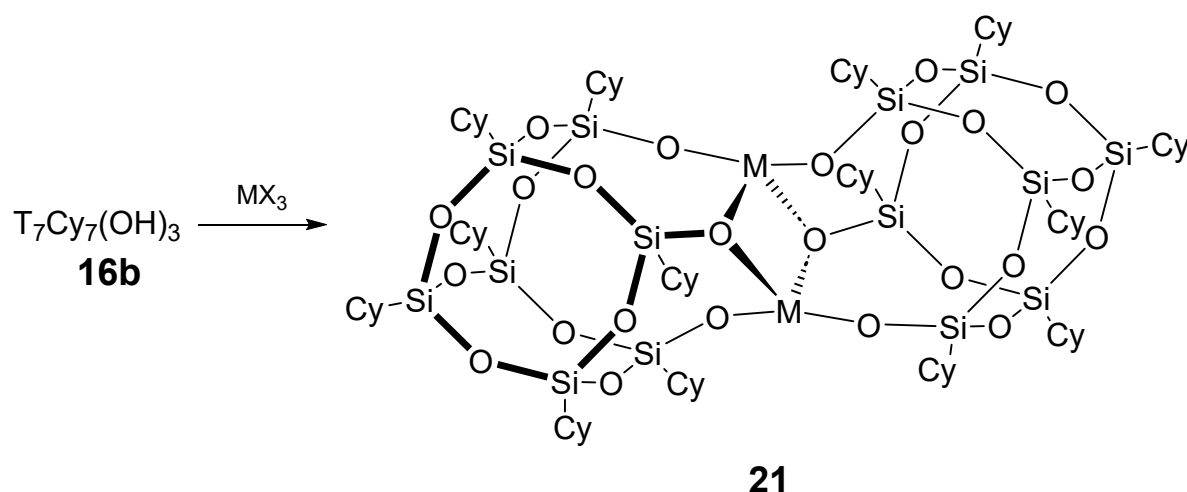
Introduction of a second functional group can be accomplished by cleaving a silicon vertex of a previously corner-capped silsesquioxane (**20**) with Et₄NOH,^[50] although it has to be emphasized that the selective cleavage of a particular vertex can be challenging, and a mixture of corner-opened products can result (Scheme 7).^[50f] Corner-capping with a suitable trichlorosilane enables two-fold functionalization, e.g. for the crosslinking of polymers.



Scheme 7. Corner-opening reaction of a completely condensed monofunctional silsesquioxane **19** with tetraethylammonium hydroxide resulting in functionalized trisilanol **20**.^[50]

Aside from silicon atoms, many other elements of the periodic table can be introduced by corner-capping reactions of incompletely condensed frameworks. In general, the heteroelement atoms introduced to the silsesquioxane framework do not have to coordinate exclusively to the oxygen atoms of just one silsesquioxane, most

prominently seen in metallasilsesquioxanes. While the T_7 framework **D** from Figure 1 is able to accommodate even large transition metals such as zirconium into a single vertex,^[51] dimeric structures are frequently obtained, especially when trivalent metal precursors are employed.^[52] One commonly adopted structure (**21**) is shown in Scheme 8, though depending on the metal and silsesquioxane framework, a different number of bridging blocks and coordination environments are possible.



Scheme 8. Incompletely condensed silsesquioxanes **16b** react with (transition-)metals react with in such a way, that a M_2O_2 bridge between two T_7 fragments is created. M = Ti: **21a**;^[52a] M = Al: **21b**;^[52b] M = V: **21c**.^[52c;53a]

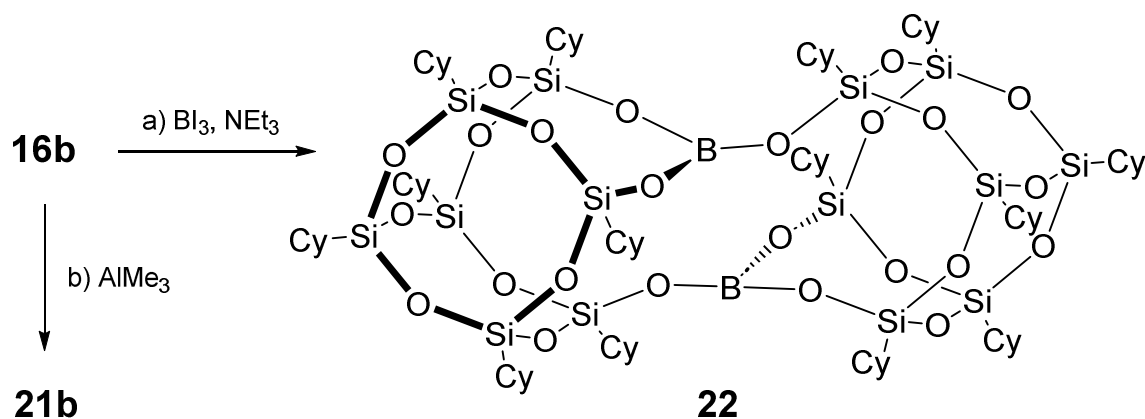
For example, in addition to structure **21**, molybdenum and tungsten form $Mo\equiv Mo$ and $W\equiv W$ triple bonds^[52d] and a single transition metal can connect two corner opened $T_7R_7(OR')(OH)_2$ ^[52e,f] or edge-opened $T_8R_8(OH)_2$ moieties.^[52h] Some species exhibit an equilibrium between the mono- and dimeric state,^[53] tentatively attributed to the poorer orbital overlap between the silsesquioxane to the transition metal in the monomer,^[53a] as well as steric demand of the corresponding ligand coordinating to the metal center.^[53c] Through treatment of these dimers with strong bases such as pyridine or acetonitrile, species with two additional ligands located at one of the two transition metals are obtained, some of which are surprisingly stable against dissociation into monomers.^[52a,c;53a] In other examples, a donor on each metal is reported for titanium dimers in chloroform solution (prepared from $Ti(iPrO)_4$ and a T_7 trisilanol), after addition of methanol.^[53b]

Alkali metals such as lithium and sodium are introduced either through the condensation process using NaOH or LiOH as discussed above,^[46] or through

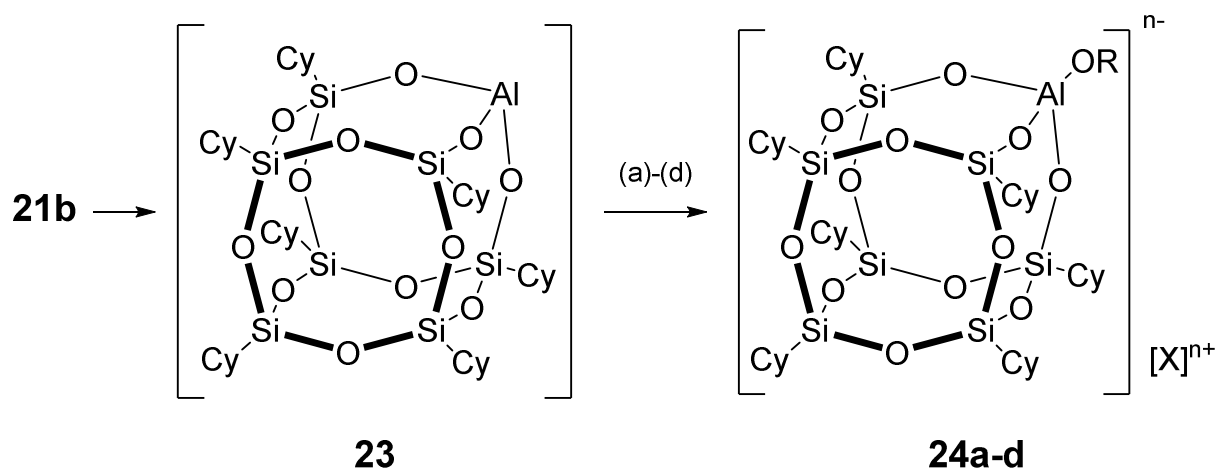
deprotonation of the trisilanol **D** with suitable bases. While stronger alkali metal bases such as sodium *tert*-butoxide^[54a] tend to quickly destroy the silsesquioxane framework, sodium hydride^[54b] or *n*-butyllithium^[55a,c] are sufficient deprotonation agents. The structure of $[T_7R_7(OLi_3)]_2$ in the solid state is a matter of debate, as Edelmann and coworkers^[55b] reported a dimer featuring a Li_6O_6 bridging unit between the two T_7Cy_7 fragments, while Gómez and coworkers^[55c] published a $[T_7^iBu_7(OLi_3)]_4$ tetramer. In the latter case, bad crystal quality might factor into ambiguous results^[55c] and DFT optimized studies^[55d] support the former Li_6O_6 dimer reported by Edelmann.^[55b]

Group 2 elements are less common for corner-capping and can form more intricate structures. Magnesium features an example of three Mg_2O_2 rings bridging two T_7 parts, but is nonetheless equally useful for the synthesis of silicon or titanium capped silsesquioxanes.^[56] In contrast, treatment of $T_7Cy_7(OH)_3$ **16b** in thf with calcium in liquid ammonia led to cage rearrangement towards the complex $[(T_8Cy_8O)_2Ca(dme)Ca(thf)_2]$ with two edge-opened T_8 fragments.^[57]

Group 13 elements produce different bridging modes: in contrast to aluminium (forming dimer **21b**^[52b]), boron tends to arrange its substituents in such a way that allows the retention of the trigonal planar coordination environment when incorporated into incompletely condensed T_7 frameworks, as shown by Feher and coworkers (Scheme 9, reaction a).^[58] The reported $[T_7Cy_7B]_2$ dimer **22** shows a remarkable stability against various bases and so far, no isolated species with a single boron atom capping a T_7 fragment was reported. Boron dimer **22** exhibits behavior indicative of switching the coordination of the oxygen ligands between the two borate esters, producing an intermediate structurally akin to the dimeric motif **21**.^[52b] Upon addition of Ph_3PO or Me_3NO to aluminium dimer **21b**, the authors describe **21b** as a “latent source”^[52b] of the monomeric T_7Cy_7Al intermediate **23**, forming according to a dissociative mechanism even before a reaction with Ph_3PO or Me_3NO takes place, as shown in Scheme 10.^[52b;59a,b] In contrast to other monomer-dimer equilibria, however,^[53b,c] the authors observe only one species in solution via spectroscopic methods,^[52b] and the reactions take several hours at room temperature, so that an equilibrium producing noteworthy amounts of a reactive, Lewis acidic monomer seems unlikely.



Scheme 9. a) Treatment of incompletely condensed silsesquioxane $T_7\text{Cy}_7(\text{OH})_3$ **16b** with BI_3 in the presence of NEt_3 results in dimer **22**, in which two boron atoms bridge two separate T_7 fragments, while keeping their trigonal planar coordination environment.^[58] b) The reaction of $T_7\text{Cy}_7(\text{OH})_3$ with AlMe_3 yields dimer **21b**, in which the two Al atoms are tetrahedrally coordinated and form an Al_2O_2 ring.^[52b]

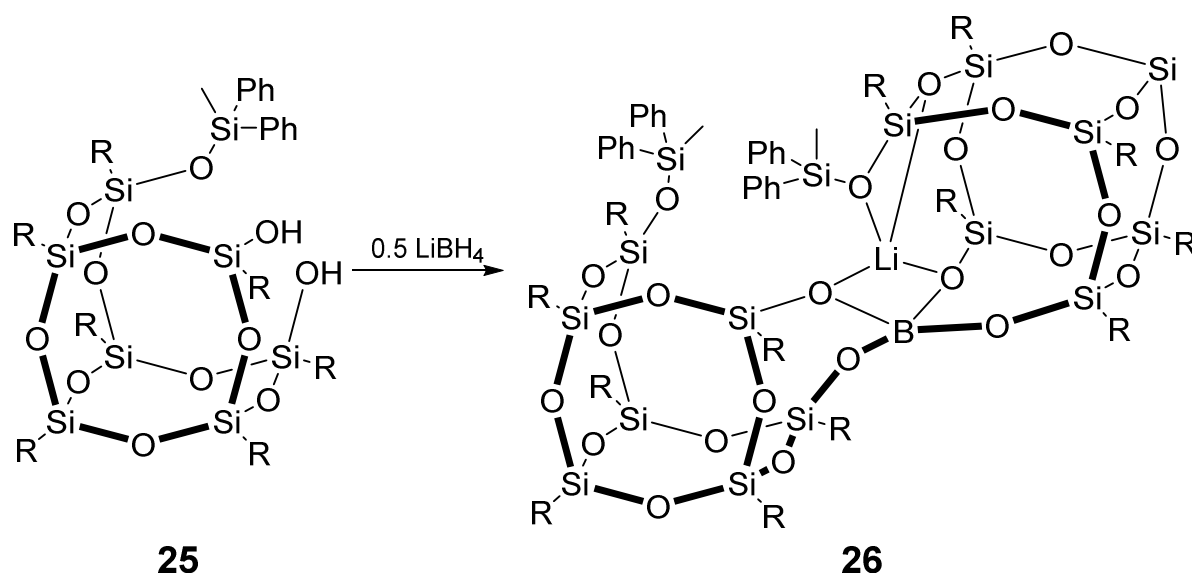


Scheme 10. Cleavage of aluminium dimer **21b** with proposed occurrence of intermediate monomeric species **23** on the way to Lewis adducts **24a** ((a) = $\text{R} = \text{OPPh}_3$, $n = 0$), **24b** ((b) = $\text{R} = \text{Me}_3\text{NO}$, $n = 0$),^[52b] **24c** ((c) = Me_4SbOTMS , $\text{R} = \text{TMS}$, $n = 1$, $\text{X} = \text{Me}_4\text{Sb}$; $\text{TMS} = \text{trimethylsilyl}$)^[59a] and **24d** ((d) = Me_4SbOH , $\text{R} = \text{H}$, $n = 1$, $\text{X} = \text{Me}_4\text{Sb}$).^[59b]

$T_7\text{R}_7(\text{OH})_3$ frameworks treated with gallium trichloride or trimethylgallium share similar dimeric structures as aluminium, though also Lewis base-coordinated monomers and more extensive dimers with multiple four-membered Ga_2O_2 rings can be obtained with an excess of GaMe_3 .^[59c]

Group 14 and 15 trihalides usually cap the missing vertex to complete the framework condensation,^[60,61] if used in a 1:1 stoichiometric ratio. The heavier group 14 elements behave similar to silicon in the capping process,^[32c,d;60] while group 15 elements can

act as Lewis bases due to their electron lone pair.^[61a] Employing an excess of the main group element, a threefold substitution of a trisilanol with pentamethylantimony affords stibonium substituted silsesquioxanes amenable as precursors for a variety of electrophilic substitution reactions,^[62a] although their propensity for side reactions such as cyclodehydrations limits their synthetic use. A trimeric Sb(V) species in which a single antimony atom is coordinated by three T₇ frameworks was recently reported.^[61c] Adding one equivalent of a mono- or dihalide to a trisilanol can introduce different functionalities, or exclude one or more silanols from participating in further reactions by capping them with inert groups.^[62] Incompletely condensed T₇R₇(OSiR'₃)(OH)₂ silsesquioxanes with one inert siloxane moiety can produce interesting structures, for example when treated with LiBH₄ a lithium and a boron atom bridging two T₇ silsesquioxanes are introduced to give structure **26** (Scheme 11).^[59c] In contrast to the [T₇B]₂ dimer **22**, the boron atom adopts a tetrahedral coordination environment.



Scheme 11. Treatment of incompletely condensed silsesquioxane **25** with 0.5 equivalents of LiBH₄ produces the bridged species **26** R = C₅H₉.^[59c]

Lanthanoids were introduced into silsesquioxane frameworks as well, adopting silsesquioxane dimer, trimer and tetramer structures.^[55a;63] Sometimes other elements such as lithium are mixed into the bridging units,^[63b] and such species are investigated as potential components of semiconductor surfaces.^[63c] Yttrium exhibits a dimer, in which framework oxygen atoms are used to satisfy the coordination sphere of the metal atoms.^[55a;63a] Applied in transition metal complexes,^[51,52,64] many incompletely

condensed silsesquioxanes tend to dimerize as with group 1, 2 or 13 metals, though some interesting features can be observed. For example, pleochroic mixed-metal species are obtained in solid solutions by treating the silsesquioxane trisilanol consecutively with the different metal precursors.^[52c]

1.1.4 Larger Silsesquioxane cage systems

While the syntheses of larger congeners of T_8H_8 were reported early on,^[33-35] simple and high-yielding procedures were lacking. The organically functionalized $T_{10}R_{10}$ (Structure **C**) and $T_{12}R_{12}$ (**G**) silsesquioxanes turned out to be the most accessible larger silsesquioxanes, prepared either from T_8 and polysilsesquioxane structures with acid or base induced cleavage and subsequent rearrangement processes,^[65a-c,e,f] or through TfOH-catalyzed hydrolysis of alkoxysilanes.^[65d,g] So far, the largest isolated organically substituted silsesquioxane $T_{18}R_{18}$ (R = styryl, $PhCH=CH-$) framework (**J**) was reported by Wong Chi Man et al. in 2021,^[66] albeit without characterization in the solid state. Functionalization strategies of $T_{10}R_{10}$, $T_{12}R_{12}$ and the $T_{18}R_{18}$ silsesquioxanes are largely the same compared to T_8R_8 , as most reactions occur at the organic substituents.

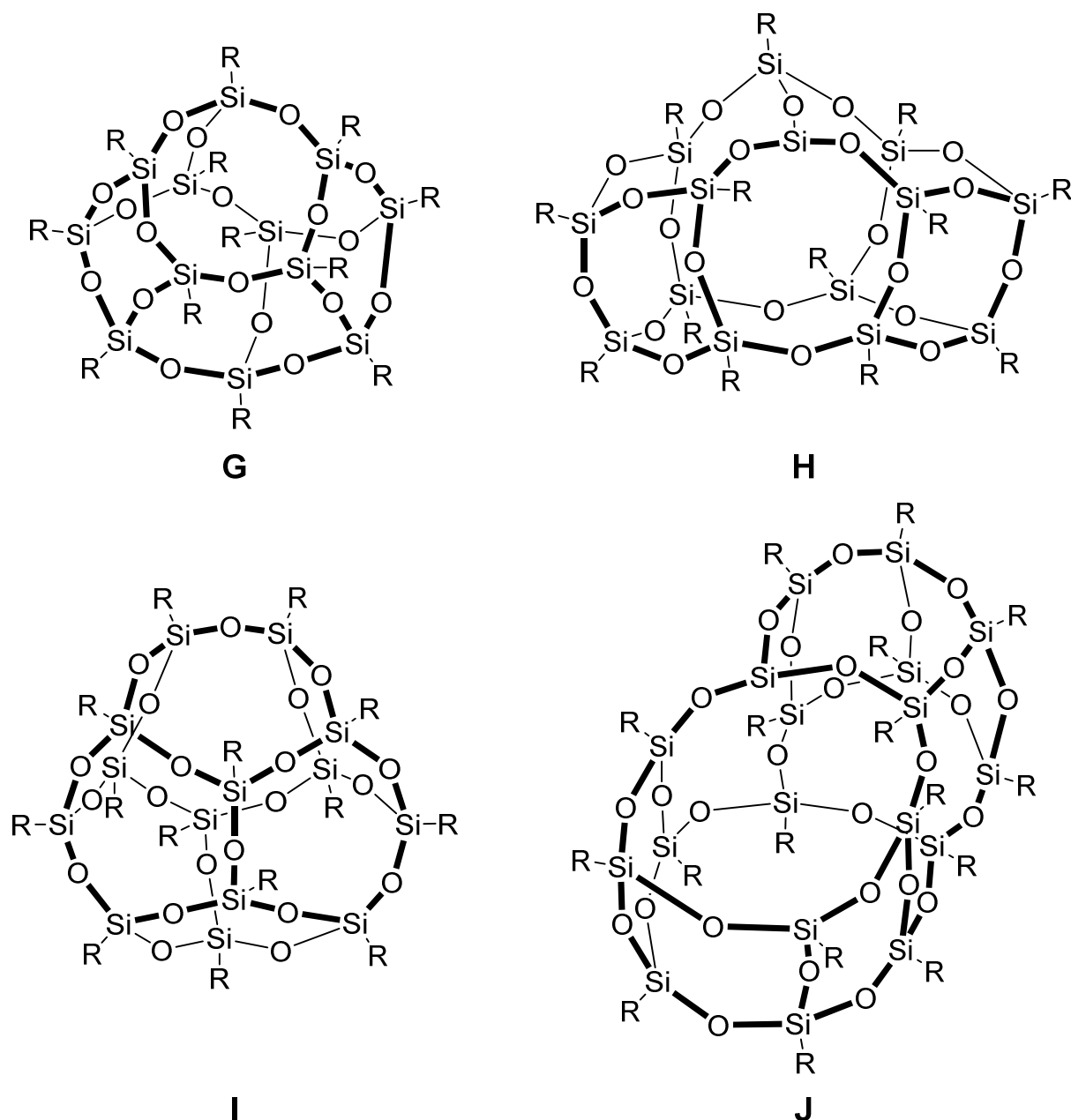


Figure 3. Examples of isolated larger silsesquioxane frameworks: $T_{12}R_{12}$ (**G**^[65a-e]), C_{2v} isomer of $T_{14}R_{14}$ (**H**^[67a]), D_{3h} isomer of $T_{14}R_{14}$ (**I**^[34a]), $T_{18}R_{18}$ (**J**^[66]).

So far, the systematic construction of a broad variety of larger silsesquioxanes other than T_{10} and T_{12} is considerably underdeveloped: many cage systems are formed in one-pot reactions without explicit control over the cluster size (aside from the previously mentioned NEt_4F templated T_8R_8 synthesis). A few reports mention the selective formation of distinct silsesquioxanes where C_{2v} or D_{3h} $T_{14}R_{14}$ species

(Frameworks **H** and **I**, respectively) were either obtained as crystals in minute amounts or postulated as thermal rearrangement products of smaller silsesquioxanes.^[67]

Theoretical studies explored the possible isomers of $T_{14}H_{14}$ and $T_{16}H_{16}$ compositions. Usually, one distinguishes by the number of four-, five- and six-membered rings (with regards to the $RSiO$ unit). The established nomenclature indicates as superscript how many ring motifs are present in a given silsesquioxane. For example, $6^05^64^3$ refers to the D_{3h} isomer **I** of $T_{14}R_{14}$ displayed in Figure 3. While Freeman^[68] and Kudo^[41b] investigated only three of the four^[35] possible $T_{14}R_{14}$ isomers, they found significant differences in relative stability. Freeman and coworkers^[68] argued that larger structures favor larger ring systems to decrease ring strain, which is also reflected in the empirical observations by Agaskar,^[35] Wong Chi Man^[66] and Marsmann^[65a] in their respective systems. Extrapolation of the number of rings from spectroscopic data would help identifying the framework isomers in a reaction mixture if isolation of single crystals is unsuccessful.

1.1.5 Applications of silsesquioxanes

Feher and coworkers first recognized the resemblance of incompletely condensed $T_7R_7(OH)_3$ silsesquioxanes with hydroxylated silica surfaces.^[32c;51a] Synthetically, T_7 silsesquioxanes are therefore useful silica model systems, resembling the (111) octahedral face of β -cristobalite.^[32c] Coordination to a transition metal follows the same rationale, allowing for the development of structure-property relationships of silica supported catalytic systems.^[69,70] Early reports showcased vanadium and chromium silsesquioxanes as efficient catalysts for olefin polymerization.^[70a,b] Since then many combinations of silsesquioxanes and (transition) metals have been evaluated on their catalytic activity. Along with useful insights into catalytically active sites in silica-supported catalysts, these efforts led to interesting structural findings such as a tetrameric neodymium silsesquioxane complex initiating the 1,4 polymerization of isoprene,^[70c] or two T_7 fragments bridged by perpendicular Zn_2O_2 rings useful for polylactide polymerization.^[70d]

The completely condensed silsesquioxane framework can also act as monodentate ligand, for example in the molybdenum catalyzed alkyne metathesis.^[71a] Non-

metallated silsesquioxanes are used as catalysts as well, for example in the formation of cyclic carbonates from CO₂ and epoxides,^[71b] and C-O bond reduction with multiborylated T₈ silsesquioxanes.^[71c]

Closely related to the function as silica surface model, the T₈R₈ framework was recognized to resemble the building blocks of zeolites.^[59a,b] The vibrational spectra of hydrogen substituted silsesquioxanes, also in case of larger systems, match the zeolite data to such a degree, that they can act as model systems for the ring-opening vibrations of the latter.^[72a-c] Kuroda and coworkers synthesized macrocyclic structures from dihydroxysilsesquioxanes resembling zeolite apertures,^[72d] while Feher and coworkers prepared R₇T₇Al-O-T₈R₇^[59a] and [R₇T₇Al]₂O^[59b] species. The latter example violates Loewenstein's rule^[73a] (prohibition of (O₃)Al-O-Al(O₃) motifs in zeolites), which has seen some other violations and expansions emerge in recent times.^[73b,c] Treatment of a T₇R₇(OH)₂(OSiMe₃) incompletely condensed silsesquioxane with aluminium sources such as AlEt₃^[74a] or AlCl₃^[74b] along with an amine base result in a monoanionic dimer, in which one aluminium atom bridges two difunctional T₇ fragments, a feature usually observed in transition metal complexes of incompletely condensed silsesquioxanes.^[52e,f]

Since more synthetic procedures targeting the T₈R₈ silsesquioxanes produced better yields and shorter reaction times, T₈ systems have been widely applied in industrial settings, mainly as nano building blocks^[75a,b] of organic-inorganic hybrid systems. The inherent symmetrical structure and high core rigidity^[18b] of T₈ frameworks enables their use in dendrimers,^[76a] chemical sensors^[76b,c,d] and in OLED applications.^[77]

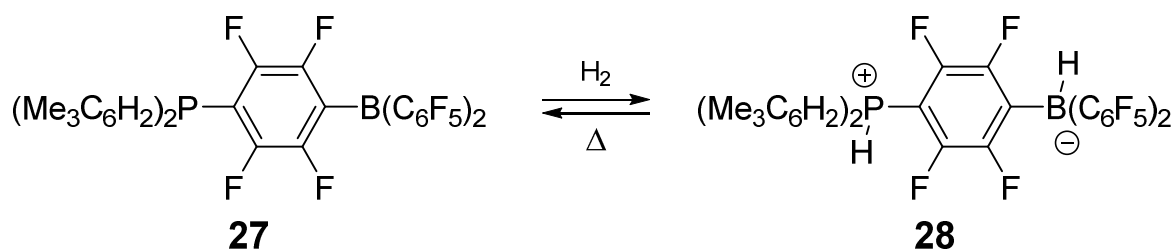
Calcination of metallasilsesquioxanes produces evenly distributed metal oxide particles in the resulting material, due to the preconfigured selective incorporation of heteroelements into the T_n framework.^[78a,b] The same rationale prompted the groups of Thieuleux and Grandier to dope germanium wafers with an antimony monolayer surface, applying silsesquioxane stibines as precursor.^[78c,d] Their high thermal and mechanical stability^[15] makes them attractive additives for fire-resistant materials, additionally introducing a protective char layer in the material during combustion.^[79]

Aside of the organically functionalized T₈R₈ framework, other forms of silsesquioxanes are of industrial interest as well. HSQ, a resin consisting of hydrogen-functionalized T_nH_n silsesquioxanes, can function as negative electron-beam and extreme ultraviolet

lithography resists for integrated circuitry with intriguing results for potential future nanofabrications below 10 nm.^[80a,b] Organically functionalized silsesquioxane copolymers are promising electron-beam lithography resist candidates as well.^[80c] Ladder-like silsesquioxanes (Type **E** in Figure 1) were recently shown to exhibit thermoplastic behavior, useful for thermally stable hybrid glass applications.^[81]

1.2 Lewis acid-base chemistry and frustrated Lewis pairs

The Lewis acid-base concept is one of the fundamental principles of chemistry. Lewis bases, electron pair donors as per definition,^[82] are key components in transition metal chemistry, acting as ligands to the metal and exerting electronical as well as steric influence.^[83] The almost unlimited combinations of Lewis basic centers with organic substituents enable specifically tailored electron pair donors, such as trisubstituted amines and phosphines amenable for C-C bond formation^[84] and catalysis.^[85] Lewis acids act as electron acceptors, and can likewise be tuned through their substituents.^[86] Lewis acids are – for instance – employed as catalysts in a number of organic reactions^[87] and as anion transporters.^[88] In 2006, Lewis acids and bases attracted considerable renewed attention with the introduction of the concept of Frustrated Lewis Pairs (FLPs) by Stephan and co-workers.^[89] In their pioneering work, they showed that the intermolecular combination of sterically shielded strongly Lewis acidic and strongly Lewis basic centers in **27** was capable of metal-free reversible dihydrogen activation to yield **28** (Scheme 12). The lone pair of the Lewis base and the empty p-orbital of the acid exhibit essentially unquenched reactivity if sterically hindered from forming the adduct.



Scheme 12. The concept of Frustrated Lewis pairs (FLPs) illustrated with dihydrogen activation by prototypical **27**.^[89]

Such hindrance is achieved intermolecularly with bulky substituents on preferably both components.^[89b;90d] The reactive centers can additionally be incorporated intramolecularly into a rigid scaffold with a suitable distance between the two.^[90a-c] Since their introduction, numerous FLPs with diverse structural features have been reported and investigated regarding their scope of substituents^[91] and the mechanisms of activating small molecules.^[92] Lewis acidity^[93] and basicity^[94] scales along with theoretical calculations^[95] have been helpful to rationalize the general reactivity trends,

though the factors responsible for successful activation, or no reaction at all, are not always obvious.^[96]

1.3 Stable unsaturated molecular silicon clusters

1.3.1 Overview

In general, silicon cluster chemistry can be divided into three categories shown in Figure 1: the polyhedral oligosilanes,^[97,98] commonly referred to as saturated clusters, in which every silicon atom is tetrahedrally coordinated to either stabilizing substituents or other cluster vertices; the Zintl anions,^[99-101] completely substituent-free, negatively charged deltahedral clusters; and siliconoids,^[102] which must feature at least one unsubstituted, hemispheroidally coordinated silicon atom. Regarding silicon clusters in this thesis, the focus will be on siliconoids and the following section will give a brief overview of their syntheses, structures and properties.

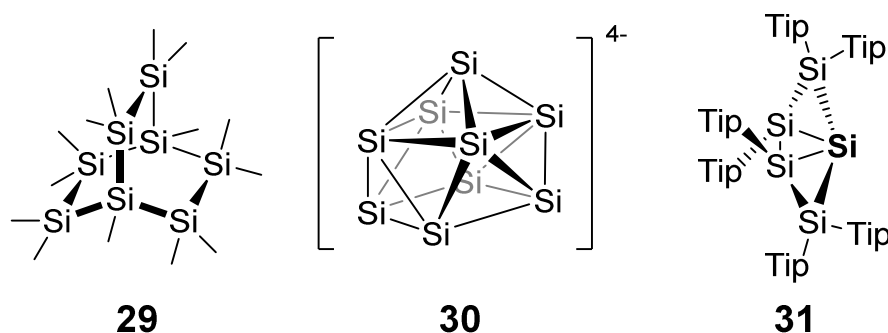
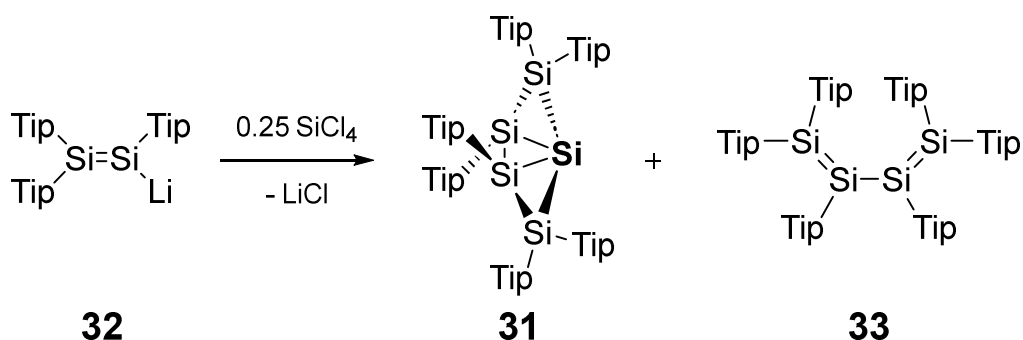


Figure 4. Examples of an Si₈Me₁₄ polycyclic silane **29**,^[97] a [Si₉]⁴⁻ Zintl anion **30**^[99a] and a Si₅Tip₆ siliconoid **31**.^[102] The counter ions of **30** are omitted for clarity, the unsubstituted silicon atom of **31** is highlighted in bold (Tip = 2,4,6-triisopropylphenyl).

1.3.2 Stable neutral unsaturated Siliconoids

Schnöckel and coworkers^[103] developed synthetic protocols for the preparation of group 13 clusters via the corresponding monohalides, termed metalloids. A metalloid consists of more metal-metal than metal-ligand bonds and ligand free, “naked”, cluster vertices,^[103a] with an average oxidation state between 0 and +I.^[103d] The name was chosen to reflect on the atomic arrangement of these clusters, which is reminiscent of that in the corresponding bulk metal.^[103b,c] Schnepf^[104] later expanded the metalloid concept to group 14 elements, although the preference of this main group for oxidation states of +II rather than +I gives rise to a certain ambiguity. Scheschkewitz et al.^[105] therefore coined the term siliconoids for unsaturated silicon clusters in 2012: while the

average oxidation state is ignored, a siliconoid only requires the presence of at least one unsaturated, hemispheroidally coordinated cluster atom. The hemispheroidality parameter Φ ^[106] was introduced to distinguish unambiguously from the tetrahedral coordinated case. The term siliconoid reflects on the resemblance to potential intermediates during the deposition of elemental silicon from the gas to the condensed phase.^[105,107] The first siliconoid **31** (adhering to this definition in hindsight) was reported in 2005 by Scheschkewitz^[102] and is obtained through treatment of SiCl₄ with a fourfold excess of lithium-disilenide **32**.^[108]



Scheme 13. Treatment of lithium-disilenide **32**^[108] with 0.25 eq of tetrachlorosilane yields the first siliconoid **31**^[107] with tetrasilabutadiene **33**^[109] as by-product (Tip = 2,4,6-triisopropylphenyl).

In the following years, more examples of siliconoids were reported by the groups of Veith, Wiberg, Breher, Scheschkewitz, Iwamoto, Kyushin, Fässler and Lips (Figure 5).^[110] Some of them are obtained through thermal rearrangement of their isomers or smaller siliconoids, such as the global minimum isomer of hexasilabenzpolarene **37**^[110d] or Iwamoto's Si₈ siliconoid **38**.^[110f]

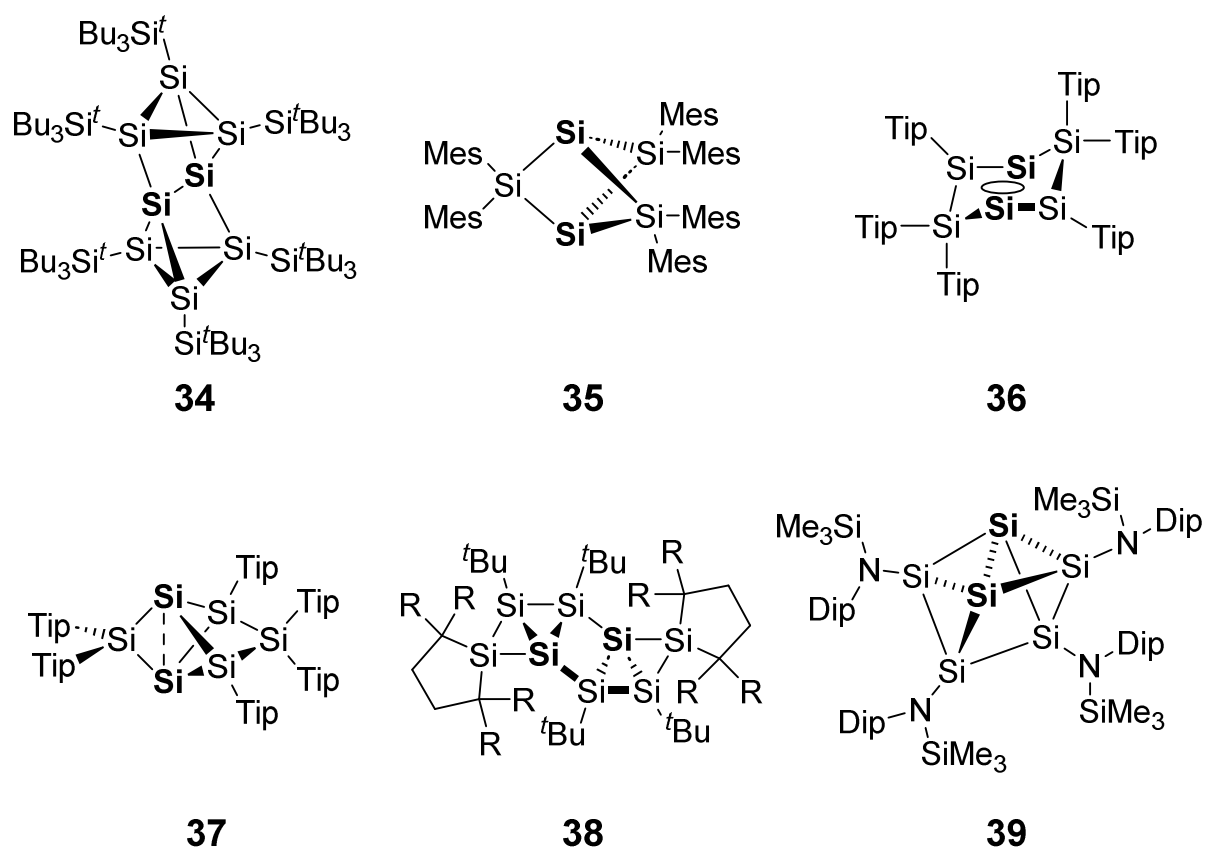
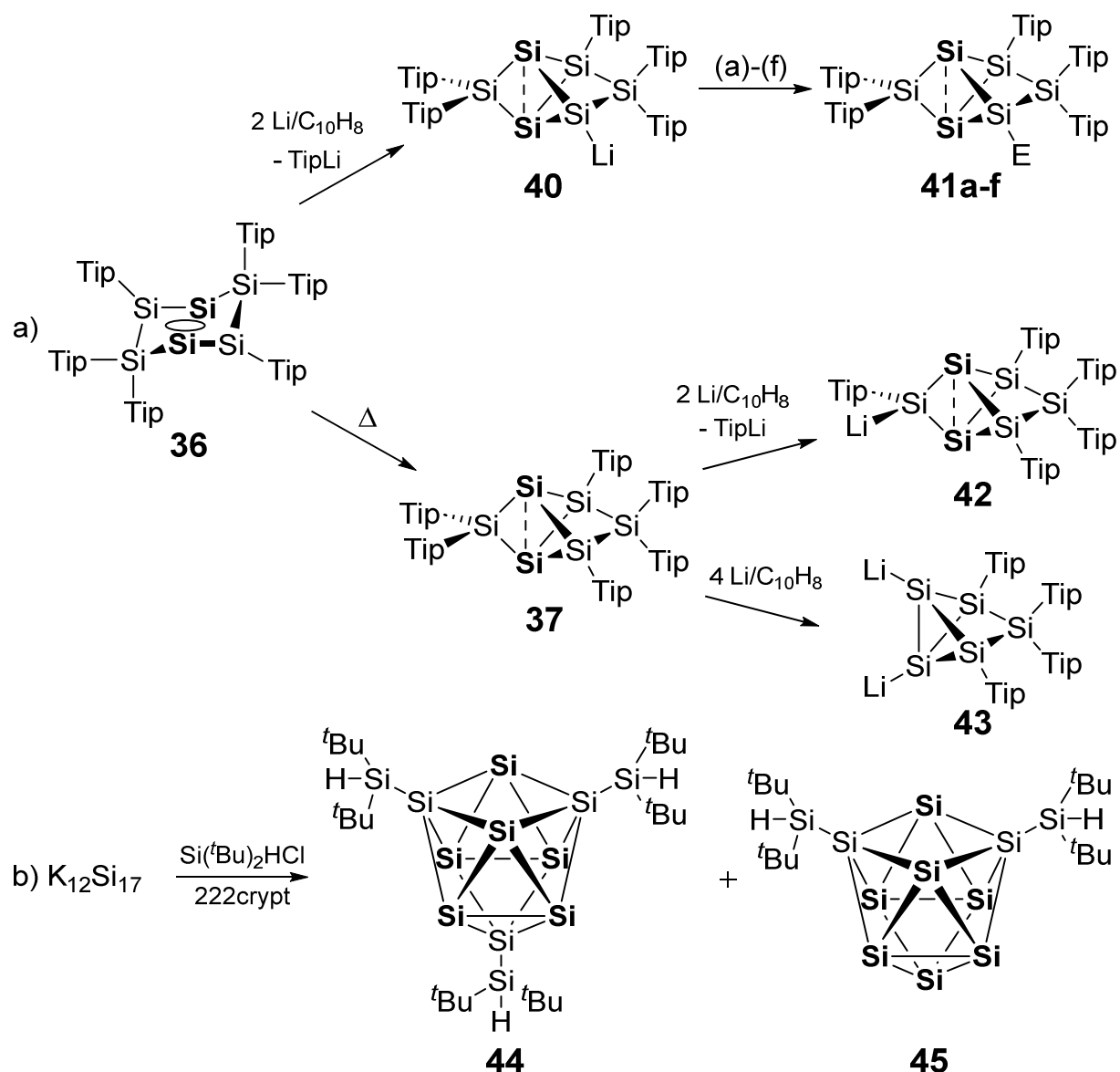


Figure 5. Selected siliconoids (Mes = 2,4,6-trimethylphenyl, Dip = 2,6-diisopropylphenyl, Tip = 2,4,6-triisopropylphenyl, R = SiMe₃).^[110]

1.3.3 Stable anionic unsaturated siliconoids

A common feature of many siliconoids is the propellane-like structure, which was also found to be a plausible structure of 2D silicon films such as the still elusive silicene.^[111] Siliconoids thus constitute suitable molecular models stabilized kinetically by their large organic substituents. The unsubstituted vertices in siliconoids resemble the “dangling bonds” of a silicon surface and are heavily studied with regards to their reactivity and structure-property relationships. Scheschkewitz and coworkers reported (di)anionic unsaturated siliconoids,^[112] which enable the transfer of the intact siliconoid moiety, or (among other methods^[113]) the incorporation of heteroatoms into the cluster framework.^[112c] Such anionic, partially substituted siliconoids represent a valuable contribution regarding the relationship of Zintl clusters of silicon with neutral saturated and unsaturated clusters.^[110g] Silylation of a Si₉ Zintl anion accesses the anionic siliconoid **44** with an exceptionally high number of unsubstituted vertices.



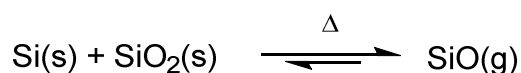
Scheme 14. a) Syntheses of anionic siliconoids from the dismutative isomer of hexasilabenzpolarene **36** in different positions.^[112a-c] (Reagents: (a): $\text{BH}_3 \cdot \text{SMe}_2$; (b): tBuC(O)Cl ; (c): PhC(O)Cl ; (d): SiCl_4 ; (e): $\text{ClP(NMe}_2)_2$; (f): ClSiMe_3 ; E = main group element electrophiles: **41a**: E = BH_3^- , **41b**: E = tBuCO , **41c**: E = PhCO , **41d**: E = SiCl_3 , **41d**: E = $\text{P(NMe}_2)_2$, **41f**: E = SiMe_3 , Tip = 2,4,6-triisopropylphenyl). b) Formation of anionic siliconoids **44** and **45** through silylation of $\text{K}_{12}\text{Si}_{17}$. **45** is formed in small amounts during crystallization of **44** (222crypt = {4,7,13,16,21,24-hexaoxa-1,10-diaza-bicyclo[8.8.8]hexacosane}).^[110g]

With the basic set of differently sized siliconoid frameworks and manipulation tools at hand, transition metal chemistry and cluster expansions are currently being explored.^[114]

1.4 Silicon monoxide

1.4.1 Synthesis of silicon monoxide

The material commonly known as silicon monoxide (SiO) was first reported by Mabery in 1886 by reduction of silicon dioxide (SiO₂) in an electrical furnace.^[10] Mabery described a green-yellow amorphous substance with a nominal composition between elemental silicon (Si) and unreduced silicon dioxide, variable in color and yield depending on the reaction and condensation conditions. To this day, the exact structure of SiO in the condensed phase is unknown. The heavier group 14 monoxides of tin and lead^[115] adopt well-characterized crystalline lattices, while the structure of solid GeO is also amorphous and still somewhat ambiguous.^[116] SiO is commonly prepared by heating elemental silicon and silicon dioxide and condensing the generated gaseous SiO on cold surfaces (Scheme 7).^[117]



Scheme 15. Heating of silicon and silicon dioxide forms diatomic silicon monoxide, which disproportionates partially again upon cooling or thermal treatment into silicon and silicon dioxide.^[117]

Other preparation methods employ the reduction of silica with reductive agents other than elemental Si. As described by Hass,^[117] these methods generate systematic by-products and thus proceed with lower atom economy. Different cooling rates of the diatomic gas^[118] result in several different modifications in the condensed phase, ranging from green-yellow to black in color.^[10,117] The condensed material tends to disproportionate over time into Si and SiO₂, which complicates the analysis and interpretation considerably. SiO is an amorphous substance, and the lack of spatial resolution approximating the long-range order of the material turns the deduction of structural information into a tedious task. Despite the so far unknown composition at the atomic level, it has been explored for many decades as component in optical coatings,^[117,119] and is an extensively studied potential anode material in lithium ion batteries,^[11,120] as well as precursor for Si nanowires, nanotubes and porous silicon.^[121] Essentially since its first report, scientists debated if SiO consists of a mixture of amorphous silicon (a-Si) and amorphous silicon dioxide (a-SiO₂)^[122] or rather a macroscopic phase of silicon(II) oxide.^[123] Regardless of their actual composition, the

various known modifications are all amorphous. Studies claiming that a crystalline SiO (c-SiO) modification exists^[124] were proven wrong by describing the “c-SiO” to be a mixture of β -silicon carbide and β -cristobalite,^[125a] and no credible report on c-SiO was published so far. Theoretical investigations regarding the crystallinity of SiO at pressures of 1 atm and above were performed by Hoffmann and coworkers,^[126] in which they found many possible structures at ambient conditions deviating only slightly in energy. Crystallization of pure silicon from SiO however was experimentally proven through the aforementioned disproportionation into Si and SiO₂ at temperatures above 850 °C.^[127]

1.4.2 Model systems for SiO

The works of Brady in 1959^[122a] attributed the radial distribution functions of amorphous SiO to a stoichiometric mixture of a-Si and a-SiO₂. The random mixture (RM) model later on presented by Temkin^[128] regards SiO as a mixture of a-Si and a-SiO₂ in the short-range order. The individual phases were assumed to be 10 Å in size with thin intermediary regions. On the other hand, Philipp proposed the random bonding (RB) model,^[129] in which silicon, being tetrahedrally coordinated, is bonded in a statistical distribution to silicon and oxygen atoms, which would result in a macroscopically unique phase of Si(II)oxide. Schmid-Fetzer and coworkers^[125b] reviewed the literature, also highlighting the aforementioned disproportionation. This renders comparisons without further knowledge about the actual preparation method, age, and storage conditions of the investigated samples problematic.

More intricate model systems have been proposed since then, essentially blending both aspects of the two pioneering models together. High resolution transmission electron microscopy (HRTEM)^[130] analysis of commercially obtained, otherwise thermally untreated SiO samples only produces the image of an amorphous powder while samples annealed at 1000 °C exhibit small microcrystallites of silicon.^[127,131] Pair distribution function (PDF) analysis hints at intermediate layers between silicon and silicon dioxide domains in which Si atoms are being coordinated by both silicon and oxygen, forming Si(Si_xO_{4-x}) tetrahedra.^[130] At the same time, energy-loss near edge structure (ELNES) fails to give any information about the intermediate regions. Schulmeister and Mader^[130] suggest the Si and SiO₂ domains to be about 3 to 4 nm in size, about six to eight times larger than assumed by Temkin.^[128] The thickness of the

intermediate layer was suggested to be about 0.3 nm, interpreted as the edge length of one tetrahedrally coordinated $\text{Si}(\text{Si}_x\text{O}_{4-x})$ silicon unit, reaching a proportion of 20 to 25% of all silicon atoms in SiO_2 .^[130]

The interface clusters mixture model (ICM model, Figure 3, left hand side)^[131] describes SiO_2 as a nano-composite being divided into a-Si and a- SiO_2 domains. The bulk SiO_2 is described as a “frozen non-equilibrium state”, the disproportionation having stopped sometime after the initial onset. The interface between the Si/ SiO_2 regions is described to be as thin as possible, while having a contribution of about 10 at.%.

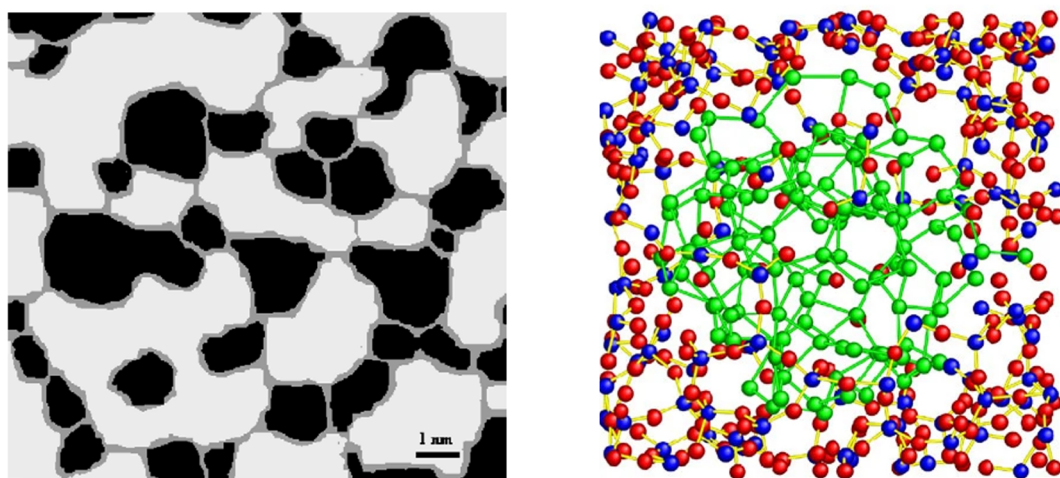


Figure 3. Left: Schematic illustration of the interface clusters mixture structure of a- SiO_2 . The ultrathin sub-oxidic interface (gray) has a matrix-like structure (roughly 10 vol%) between clusters of SiO_2 (light gray) and more numerous smaller convex clusters of Si (black). Figure and caption reproduced with permission from Elsevier.^[131] Right: Reconstructed heterostructure model of amorphous SiO_2 . The inner part corresponds to an amorphous Si cluster and the outer part is amorphous SiO_2 matrix. The blue, red and green circles denote Si and O in amorphous SiO_2 and Si in the Si cluster, respectively. Figure and caption reproduced with permission from the literature.^[132]

Taking different oxidation states and bond lengths into account, 79 different $\text{Si}(\text{Si}_x\text{O}_{4-x})$ tetrahedra would be possible. The TEM investigations of the authors hinted at a maximum Si cluster size of less than 2 nm.

In more recent times, Chen et al.^[132] published a heterogeneous structure model of a-Si incorporated into an a- SiO_2 matrix as shown in Figure 3 (right hand side), separated by the aforementioned interface. Angstrom beam electron diffraction analysis detected tetrahedral suboxidic species, reiterating the interface clusters mixture model. The existence of $\text{Si}(\text{Si}_x\text{O}_{4-x})$ tetrahedra reinforces the hypothesis of disproportionation suggested by earlier publications.^[125b] Very recently, machine-learning based models were applied to the SiO_x system:^[133] silicon domains after disproportionation were

estimated to average between 24 to 54 Å, in line with observations of Schulmeister and Mader.^[130] Overall, the atomic composition of SiO might be approximated for the short-range order, but a concise description through experimental evidence is still elusive.

2 Aims and scope

After the breakthrough of silsesquioxanes with regards to industrial applications and as ligands in transition metals, the majority of publications revolve around the well-known $T_7R_7(OH)_3$ and T_8R_8 species as well as the double-decker derivatives, with many silsesquioxanes finding their way into polymers. Aside from the use as transition metal ligands, the potentially interesting chemistry of the frameworks themselves has received less attention than the functionalization with organic groups. Considering larger structures, only a handful of reports detail the synthesis of silsesquioxanes larger than T_{12} systems, let alone detail more of their properties due to limited quantities available. The following summarizes the scope of this PhD thesis.

The first contribution of the present work is the design and synthesis of a molecular proof-of-principle prototype, which can open the door to novel molecular model systems of SiO. So far, discrete silicon oxides such as silanones, resembling linear SiO in the gas phase, rely on stabilizing contributions of substituents, due to their inherent reactive nature.^[134] A different approach combining Zintl anions and silicates approximates the necessary stoichiometry: obtained by the reaction of elemental Si, SiO₂ and alkali metals at about 700 °C, SiO is also reported as byproduct.^[135] As described in the introduction, SiO models of the actual material are in general realized as silicon clusters of variable sizes embedded into a subvalent silicon and silicon dioxide matrix^[132] and of theoretical rather than experimental nature.^[131] To circumvent such problems molecular model systems are a viable approach. Examples of other molecular suboxidic model systems employ strong Lewis basic substituents for stabilization,^[136] whereas the model presented herein consists of donor free components and is in parts kinetically stabilized. The goal of any molecular model is to create a species with which more targeted experimental investigations regarding the thermal breakdown into SiO resembling domains can be realized. Such a model system must a) consist of a silicon to oxygen stoichiometry as close as possible to SiO (1:1) and b) be thermally decomposable in a way that mimics the synthesis procedure/formation of SiO. The high thermal stability silsesquioxanes makes them the ideal species to resemble the oxygen-rich domains of SiO (in analogy to the application of silsesquioxanes as silica models), which is preserved until organic components tend to be removed during heating. Silicon clusters on the other hand can

function as the pure silicon domains, evidenced by their inherent resemblance to bulk silicon intermediates during the condensation from the gas phase.^[107] A Si₆ silicon cluster together with a T₈ silsesquioxane exhibit a stoichiometric ratio of about SiO_{0.86}, as shown in the proof-of principle molecule **46**. Both parts usually contain carbon-rich substituents, which (ideally) evaporate above temperatures of the usual decomposition of organic matter, leaving mainly silicon and oxygen phases.

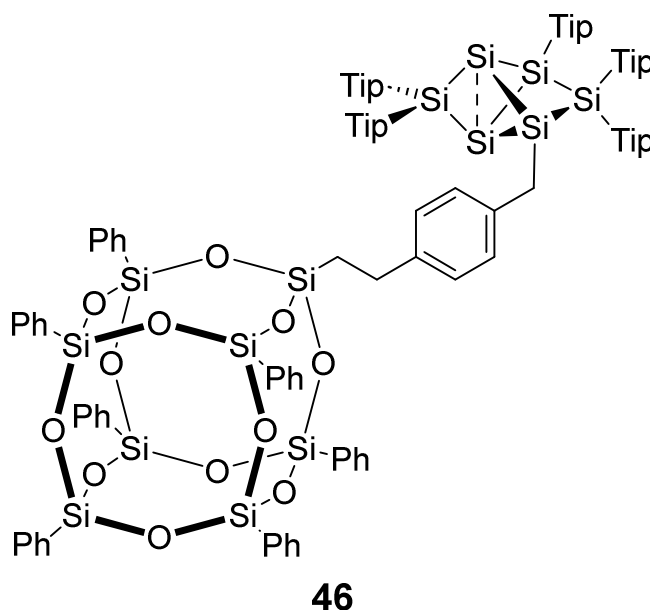
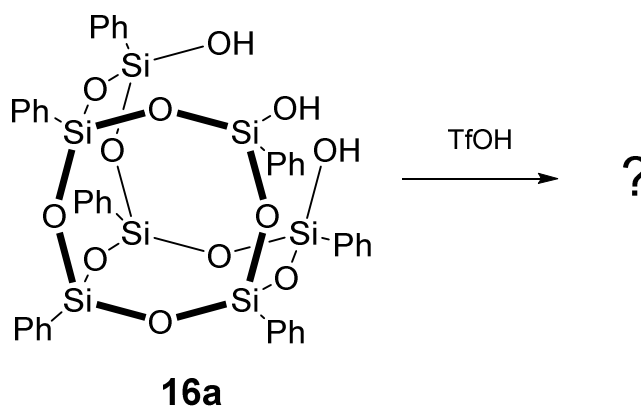


Figure 6. Targeted proof-of-principle molecule **46** consisting of hexasilabenzpolarene linked to a T₈Ph₇R silsesquioxane. The stoichiometry of silicon to oxygen (about 1:0.86) approximates the overall 1:1 ratio of silicon monoxide, while the components themselves represent silicon and oxygen rich domains.

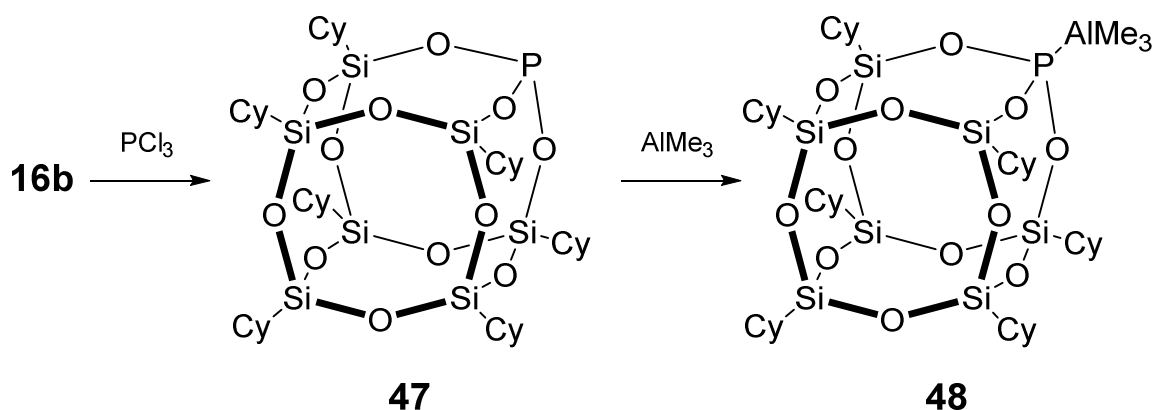
The creation of a straightforward synthetic procedure for larger silsesquioxanes would enable the application of extended systems in various applications, and in particular as larger SiO₂ part of the model system. So far, all synthetic methods known involve tedious separation of larger frameworks from a mixture of many different cages, making broad reactivity and property related investigations cumbersome. Combining a few reports concerning the condensation of two cyclotetrasiloxanes,^[137] siloxane bond (re)formation of silyltriflates in silsesquioxane frameworks^[44] and the dimeric stabilization of incompletely condensed frameworks,^[32a;138] the general idea of linking such open-cage systems with suitable catalytic support arose. Treatment of such incompletely condensed silsesquioxanes with TfOH should allow for the transformation of silanol functionalities at the open face into triflates, which may even be isolable and serve as precursors for a whole variety of subsequent manipulations including

condensation to larger silsesquioxanes. The use of silyl triflates was recognized by Feher and coworkers^[44,45] for edge-opened silsesquioxanes as versatile intermediates, but an isolated incompletely condensed $T_7R_7(OTf)_3$ had yet to be reported.



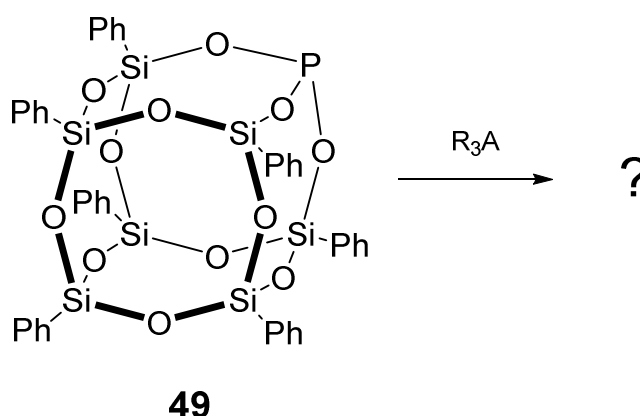
Scheme 16. Proposed treatment of the phenyl substituted incompletely condensed silsesquioxane $T_7Ph_7(OH)_3$ **16a** with trifluoromethanesulfonic acid.

In light of the near endless possibilities of incompletely condensed silsesquioxanes to produce functionalized frameworks, it is curious that phosphites embedded into a silsesquioxane framework have not received much attention since their initial report by Feher.^[61a] The few available publications provide an incomplete picture, especially regarding the variation of steric demand. The initial report cautioned that the large Tolman cone angle of the phosphite **47**^[61a;139] may be detrimental for its ligand properties towards transition metals. As, however, phosphite **47** readily coordinates to trimethylaluminium^[61a] but shows no catalytic activity,^[140] and the isooctyl-substituted congener actively hinders catalysis,^[54b] the role of different substituents and Lewis acids should be evaluated. Even more so, since Tolman's initial report about the cone angle, several more sophisticated methods have been established, such as the crystallographic cone angle of Müller and Mingos,^[141] and the percent buried volume parameter.^[142]



Scheme 17. Treatment of incompletely condensed silsesquioxane **16b** with PCl_3 corner caps the missing vertex with a phosphorus atom. The hereby generated phosphite **47** was shown to coordinate to Lewis acidic center of trimethylaluminium to form the Lewis adduct **48**.^[61a]

A comparison and possible reevaluation of the steric demand of **47** seems appropriate in context of the more refined methods. Furthermore, many FLP systems focus on boranes and phosphanes, due to their inherent natures as Lewis acids and bases, respectively. Silsesquioxane substituted phosphites might be suitable candidates as basic components, as the large Tolman cone angle can hint at an ideal structural prerequisite for steric shielding of the Lewis base. The synthesis and properties of phosphite **49** are to be investigated with regards to general Lewis acid-base reactivity, as well as FLP chemistry. The phenyl substituent is chosen as less sterically demanding functional group compared to the reported cyclohexyl congener to elucidate the reactivity and steric constraints.



Scheme 18. Reaction of silsesquioxane substituted phosphite **49** with various sterically demanding Lewis acids R_3A can potentially lead to frustrated Lewis pairs with interesting properties (R = organic substituent, A = Lewis acidic center).

3 Publications

3.1 Interlinkage of a siliconoid with a silsesquioxane: en route to a molecular model system for silicon monoxide

M. Hunsicker, N. E. Poitiers, V. Huch, B. Morgenstern, M. Zimmer, D. Scheschkewitz, *Z. Anorg. Allg. Chem.* **2022**, 648, e202200239. Copyright © 2022 The Authors.

<https://doi.org/10.1002/zaac.202200239>

This article has been published by Wiley-VCH Verlag GmbH & Co. KGaA as an “Open Access” Article and is licensed under a “Creative Commons Attribution-NonCommercial-NoDerivatives 4.0 International (CC BY-NC-ND-4.0)” License (<https://creativecommons.org/licenses/by-nc-nd/4.0/>).

The article is reproduced with permission of Wiley-VCH Verlag GmbH & Co. KGaA and all authors. No modifications were made. The results are additionally concluded and put into context in Chapter 4.

Contribution of authors:

Marc Hunsicker: Equal (D. S.): Conceptualization; Lead: Data curation, Formal analysis, Investigation, Methodology, Validation, Visualization, Writing and Editing.

Nadine E. Poitiers: Supporting: Investigation, Data curation, Formal analysis of Si₆-CH₂-Ph.

Volker Huch: Equal (B. M.): Lead: X-ray analysis.

Bernd Morgenstern: Equal (V. H.) Lead: X-ray analysis.

Michael Zimmer: Lead: CP/MAS NMR, VT-NMR and TOCSY NMR analysis.

David Scheschkewitz: Lead: Conceptualization, Project administration, Supervision, Acquisition of Funding and Resources, Supporting: Methodology, Writing - Review and Editing.

DOI: 10.1002/zaac.202200239

Interlinkage of a siliconoid with a silsesquioxane: en route to a molecular model system for silicon monoxide

Marc Hunsicker,^[a] Nadine E. Poitiers,^[a] Volker Huch,^[a] Bernd Morgenstern,^[a] Michael Zimmer,^[a] and David Scheschkewitz^{*[a]}

Dedicated to Prof. Cameron Jones on occasion of his 60th birthday.

A new potential model system for silicon monoxide (SiO) is synthesized by the interlinkage of an unsaturated silicon cluster (siliconoid) with a polyhedral silsesquioxane cage. Two derivatives with variable linker size are obtained by the corner-capping reaction of $\text{Ph}_7\text{T}_7(\text{ONa})_3$ with a trichlorosilane featuring a remote benzylic chloride functionality and the subsequent

nucleophilic substitution of the latter by the anionic hexasila-benzpolarene-type Si_6 siliconoid. Based on the recently proposed heterogeneous cluster model for the SiO structure, the stoichiometry between silicon and oxygen reiterates the suboxidic interface of the nano-composite in a Si:O ratio of 14:12.

Introduction

Silicon monoxide (SiO) has been reported more than 130 years ago,^[1] yet relatively little is known about the structure of this commercially available material, which is nonetheless extensively employed, e.g. as antireflective coating.^[2d,e] More recently, it is being investigated along with suboxidic SiO_x species as a component of anode materials in lithium ion batteries^[2a-c,f,g] and as pivotal component of silicon nanowires in light-enhanced hydrogen generation.^[2h]

SiO is usually prepared by thermal evaporation of elemental Si and SiO_2 . In the gas phase at high temperatures it predominantly exists as a diatomic molecule, which is subsequently condensed by cooling.^[3] Depending on the cooling rate, different modifications of SiO are obtained of which the amorphous dark powder is typically employed for the various applications.^[4] In contrast to SiO_2 ,^[5] the solid state structure of SiO is still a controversial subject,^[6] and is either described as a single phase^[7] or an amorphous, nanoscale composite of Si and SiO_2 .^[6,8] Earlier suggestions of a simple macroscopic mixture of Si and SiO_2 ^[9] are neither in line with the distinct reactivity of SiO,^[6] nor with spectroscopic findings.^[10] The random bonding model proposed by Philipp assumes a continuous network of

arbitrarily distributed covalent Si–O and Si–Si bonds.^[11] Such a network could be regarded as a single macroscopic phase of SiO, but would not account for the aforementioned thermodynamically driven disproportionation of SiO. Recently, Chen et al. developed a heterogeneous structure model consisting of elemental silicon clusters incorporated into an amorphous SiO_2 matrix with interfacial $\text{Si}(\text{Si}_4\text{O}_4)_x$ tetrahedra.^[12]

In view of the lack of empirical evidence for the SiO structure, several (potential) model systems have been conceived. Ionic phases approximating the Si/O ratio of 1:1 incorporate both discrete Si-based Zintl anions and silicate anions as reported by the groups of Fässler and Röhr.^[13] In fact, SiO was suspected as byproduct of this synthesis. Molecular species with silicon suboxide motifs have been reported as well, all containing strong external donors to increase stability: Filippou et al. prepared a chromium complex of NHC-stabilized SiO ,^[14] while Robinson et al. isolated several disilicon suboxides coordinated by NHC ligands.^[15]

Herein, we report the synthesis of a well-defined and stable potential molecular model system, which combines an unsaturated Si_6 siliconoid with a T_8 silsesquioxane in one and the same molecule and thus reiterates Chen's model with local molecular Si and SiO clusters.^[12] While silsesquioxanes have been suggested as models for silica surfaces and silica supported transition metal catalysts,^[16] siliconoids are implied as intermediates in gas phase deposition processes of elemental silicon^[17] and – in the form of stable molecular representatives regarded as model systems for silicon surfaces (Figure 1).^[18]

Results and Discussion

Anionically functionalized siliconoids are easily derivatized in a straightforward manner by reactions with various electrophiles, which mostly proceed without compromising the integrity of the Si_6 cluster scaffold.^[19] Yet, attempts to introduce the 4-vinylbenzoyl group (as a group potentially amenable to

[a] M. Hunsicker, Dr. N. E. Poitiers, Dr. V. Huch, Dr. B. Morgenstern, Dr. M. Zimmer, Prof. Dr. D. Scheschkewitz
Krupp-Chair of Inorganic and General Chemistry
Saarland University
66123 Saarbrücken (Germany)
E-mail: scheschkewitz@mx.uni-saarland.de

Supporting information for this article is available on the WWW under <https://doi.org/10.1002/zaac.202200239>

© 2022 The Authors. *Zeitschrift für anorganische und allgemeine Chemie* published by Wiley-VCH GmbH. This is an open access article under the terms of the Creative Commons Attribution Non-Commercial NoDerivs License, which permits use and distribution in any medium, provided the original work is properly cited, the use is non-commercial and no modifications or adaptations are made.

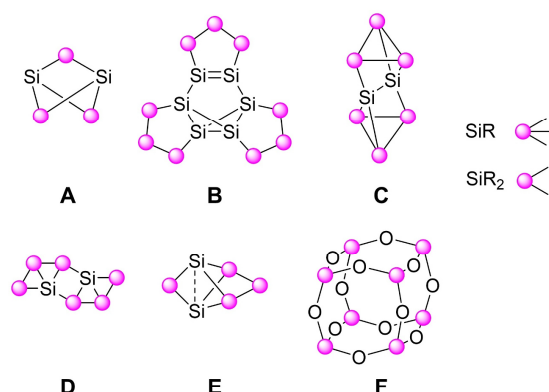
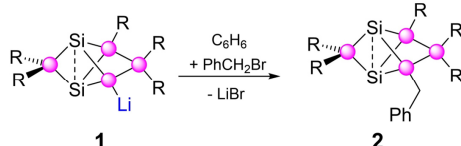


Figure 1. Selected examples of unsaturated neutral siliconoids **A** to **E**^[18] and of polyhedral molecular silsesquioxanes **F**^[16] (●: saturated silicon vertex, Si: unsubstituted silicon vertex).

subsequent hydrosilylation by T_8Ph_7H in *ligato*-position^[20] of a hexasilabenzpolarene scaffold gave complex and intractable product mixtures. Although hydro silsesquioxanes are routinely modified by hydrosilylation procedures,^[21] the reverse approach of initial grafting of the linker units to T_8Ph_7H by reaction with suitably functionalized terminal alkenes in the presence of either the Karstedt catalyst or palladium on charcoal only resulted in partial conversion of the silsesquioxane. In contrast, corner-capping reactions^[22] of incompletely condensed T_7 silsesquioxanes using highly electrophilic trichlorosilanes tolerate less reactive remote functionalities potentially amenable to later introduction of the hexasilabenzpolarene motif. In terms of grafting the substituted T_8 to the anionic *ligato* lithiated hexasilabenzpolarene **1**, we selected a remote benzylic halide functionality in *para*-position to the ethylene moiety.^[23] Encouragingly, the test reaction of the *ligato*-lithiated hexasilabenzpolarene **1** with benzyl bromide yielded the benzyl-substituted **2** in 75% isolated yield (Scheme 1).

The desired trichlorosilane **3** with remote benzylic chloride was obtained by hydrosilylation of *para*-vinylbenzyl chloride with trichlorosilane through an adapted literature procedure (see Supporting Info).^[24] In our hands, the anti-Markovnikov selectivity of the reaction heavily depended on the choice of catalyst. The use of Pt/C finally allowed for the isolation of **3** by vacuum distillation in 67% yield.

The subsequent treatment of $Ph_7T_7(ONa)_3$ with a slight excess of trichlorosilane **3** in tetrahydrofuran at 0 °C indeed



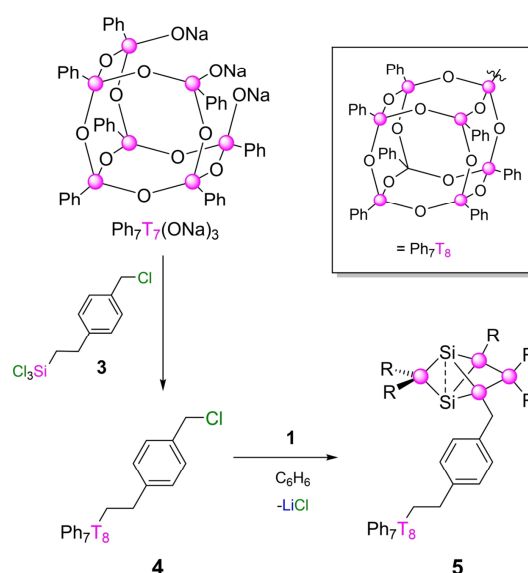
Scheme 1. Test reaction of anionic siliconoid **1** with benzyl bromide to obtain benzyl functionalized hexasilabenzpolarene.

affords the T_8 -substituted benzyl chloride **4** as a white solid in 46% yield after aqueous work-up (Scheme 2).

The ethylene moiety in **4** gives rise to characteristic 1H NMR multiplets between 2.79 and 2.75 ppm as well as 1.16 and 1.12 ppm, respectively. The ^{13}C NMR signals of the corresponding carbon atoms are observed at 28.83 and 14.14 ppm. The benzylic group gives rise to a 1H NMR singlet at 4.08 ppm and a ^{13}C NMR signal at 46.19 ppm. The ^{29}Si NMR resonances in C_6D_6 of the T_8 cage in **4** are observed at -65.4 , -77.6 and -78.0 ppm. While the local C_{3v} symmetry would demand four signals, monofunctionalized T_8 cages often only show three ^{29}Si signals due to incidental isochronism of the phenyl-substituted corners of the T_8 cage.^[25] A 1H - ^{29}Si NMR correlation experiment assigned the resonance at -65.4 ppm to the newly introduced silicon vertex (Experimental Section/SI). In contrast, the parent species T_8Ph_8 exhibits one signal at -78.3 ppm in $CDCl_3$,^[26] while silsesquioxane **4** gives rise to resonances at -65.8 , -78.3 and -78.6 ppm in this solvent.

Reaction with the anionic silicon cluster **1** in benzene at 25 °C quantitatively afforded the anticipated benzpolarene-grafted T_8 cage **5**. Crystallization from a benzene solution afforded orange crystals of **5** in 31% yield (Figure 2). Single crystals suitable for X-ray diffraction were grown from a 10:1 mixture of toluene and hexane.

The Si1–Si3 distance of the *nudo*-silicon atoms of 2.640(1) Å is at the short end of the typical range for neutral hexasilabenzpolarenes.^[19b] Despite the difference in carbon hybridization, the bond between the T_8 silicon vertex to the



Scheme 2. Corner capping reaction of the incompletely condensed heptaphenyl silsesquioxane $T_7Ph_7(ONa)_3$ with trichlorosilane **3** containing the linking group ($R = \text{Tip} = 2,4,6$ -triisopropylphenyl), as well as grafting reaction to lithiated hexasilabenzpolarene motif by nucleophilic substitution of chloride at benzylic carbon atom to yield the potential SiO model system **5**.

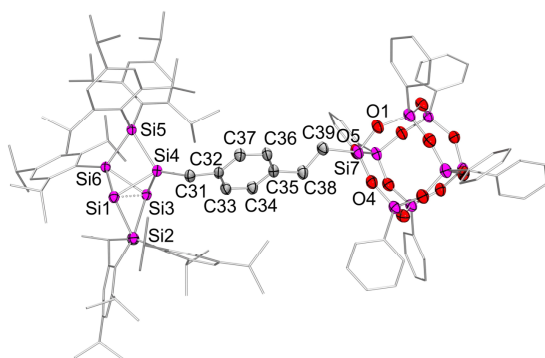


Figure 2. Molecular structure of potential SiO model system **5** in the solid state. Thermal ellipsoids at 50% probability, hydrogen atoms and co-crystallized solvent molecules omitted for clarity. Selected bond lengths [Å] and angles [°]: Si1–Si2 2.357(1), Si1–Si3 2.640(1), Si1–Si4 2.374(1), Si1–Si6 2.329(1), Si2–Si3 2.395(1), Si3–Si4 2.315(1), Si3–Si6 2.376(1), Si4–Si5 2.345(1), Si5–Si6 2.388(1), Si4–C31 1.894(3), C31–C32 1.513(4), C32–C37 1.384(4), C37–C36 1.393(4), C36–C35 1.381(4), C35–C38 1.512(4), C38–C39 1.514(4), C39–Si7 1.838(3); O1–Si7–O4 109.7(1), O4–Si7–O5 108.2(1), O1–Si7–O5 109.4(1), O1–Si7–C39 109.1(1), O4–Si7–C39 110.2(1), O5–Si7–C39 110.3(1).

pending ethylene moiety (Si7–C39 1.838(3) Å) is identical within the margin of error to the Si–C distances involving the T_8 -phenyl substituents and indistinguishable from those reported for T_8Ph_8 ^[27] (1.838(2) to 1.843(2) Å) as well as an octa(*p*-carboxyphenylethyl)- T_8 (1.840(4) to 1.851(4) Å).^[28] The SiO bond lengths of the T_8 cage are between 1.606(2) Å and 1.627(2) Å, thus showing slightly more variance compared to T_8Ph_8 (1.6166(11) to 1.6258(11) Å). As a consequence of the reduced symmetry, the silicon atoms of **5** deviate slightly more from the ideal tetrahedral coordination with angles between 103.9(3) and 116.3(3)°. In comparison, the silicon atoms of T_8Ph_8 exhibit bond angles from 107.72(6) to 111.58(6)°. The same applies to the angles at the oxygen cage atoms with values between 137.6(1)° and 168.0(2)° compared to T_8Ph_8 (min. 142.28(7) and max. 153.22(8)°). The ethylene signals undergo downfield shifts to 2.98–2.91 ppm and 1.41–1.34 ppm (previously 2.79–2.75 ppm and 1.16–1.12 ppm) in the ¹H NMR and 28.93 and 15.34 ppm in the ¹³C NMR respectively (**4**: 28.83 and 14.14 ppm).

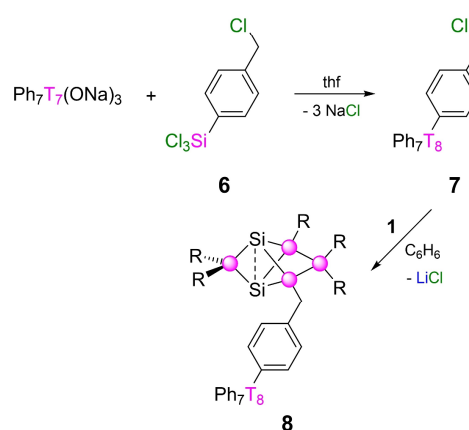
As to be expected for the substitution of the electron-withdrawing chloro group, the ¹H NMR signal of the benzylic proton in **5** is no longer observed at 4.08 ppm but most likely obscured by the Tip groups of the hexasilabenzpolarene through an upfield shift. The benzylic carbon atom of **5** is observed at 20.34 ppm (**4**: 46.19 ppm). The ²⁹Si NMR shows diagnostic signals for an intact hexasilabenzpolarene motif^[19a,b] at 170.6 ppm for the *privo*-position, 14.1, 8.4 and 1.0 ppm for the two *ligato*- and the *remoto*-vertices as well as –261.1 and –275.9 ppm for the two *nudo*-positions. The silsesquioxane signals observed at –65.3, –77.6 and –77.9 ppm are comparable to the precursor **4** (–65.4, –77.6 and –78.0 ppm). The ²⁹Si CP/MAS NMR spectrum shows almost identical signals to those

in solution, indicating a very similar structure in the solid state (Experimental Section/SI).

The longest wavelength absorption in the UV/Vis spectrum of **5** at 470 nm ($\epsilon = 540 \text{ M}^{-1} \text{ cm}^{-1}$) is marginally blue-shifted compared to the all-Tip substituted hexasilabenzpolarene **E** (473 nm).^[18d]

With compound **5** as proof-of-principle in hand, we attempted the installation of a shorter linking unit between the siliconoid and silsesquioxane motifs, that is without the ethylene bridge between the T_8 cage and the *para*-phenylene spacer. Corner capping the incompletely condensed silsesquioxane $Ph_7T_7(ONa)_3$ through a modified literature procedure^[29] with commercially available 4-(chloromethyl)phenyltrichlorosilane **6** gives **7** in 11% isolated yield. Subsequent treatment of **7** with the anionic siliconoid **1** indeed results in **8**, which was isolated in 74% crystalline yield by slowly cooling down a 75 °C hot benzene solution during 15 h (Scheme 3).

Unfortunately, no single crystals of **8** could be obtained so that the comparison of physical data with those of **5** is limited to the NMR spectroscopic investigations. As in **5**, the hexasilabenzpolarene motif of **8** shows the typical distribution of ²⁹Si NMR signals.^[18d;19a,b] The shortened linking unit has close to no discernible effect on the chemical shifts. The absence of the ethylene bridge at the silsesquioxane side of the linker is reflected in the ²⁹Si NMR spectrum of **8**. All corners of the T_8 unit are directly substituted by aryl groups giving rise to four signals (instead of three in **5**), which are closely grouped together at chemical shifts of –76.8, –77.5, –77.6 and –77.7 ppm. A total correlation spectroscopy (TOCSY) experiment was used to verify the linkage of the cluster compounds spectroscopically. Cross signals in the TOCSY experiment indicate the successful connection of the silsesquioxane (see Supporting Info). Compound **8** also exhibits a longest wavelength absorption of 470 nm ($\epsilon = 540 \text{ M}^{-1} \text{ cm}^{-1}$).



Scheme 3. Corner-capping reaction using trichlorosilane with shorter linking group **6** to yield monofunctionalized T_8 as well as subsequent reaction with *ligato*-lithiated hexasilabenzpolarene to yield the potential SiO model system **8** (R = Tip = 2,4,6-triisopropylphenyl).

Conclusions

Suitably functionalized T_8 -silsesquioxanes react with a lithiated hexasilabenzpolarene to yield interconnected molecular species featuring both uncompromised silicon-rich and oxygen-rich moieties, the siliconoid and the T_8 silsesquioxane, respectively. With the overall Si:O ratio of 14:12 these molecules approximately reflect the stoichiometry of silicon monoxide and thus represent potential molecular model systems. With the non-conjugated linkers employed here, however, only very small structural and spectroscopic effects result. One of the inter-linked species was fully characterized by single-crystal X-ray diffraction leaving no doubt regarding the constitution of the other based on the similarity of spectroscopic data. The synthesis of derivatives with fully π -conjugated linking units and possibly more realistic σ -conjugated oligosilane linkers is currently being investigated in our laboratory.

Experimental Section

General. All manipulations were conducted under a protective argon atmosphere using standard Schlenk techniques or a glovebox. Non-chlorinated solvents were dried over Na/benzophenone (in the presence of tetraglyme in case of aromatic and aliphatic solvents) and distilled under argon atmosphere. Deuterated solvents were dried by reflux over potassium and distilled under argon atmosphere prior to use. Chlorinated deuterated solvents were refluxed and distilled over P_4O_{10} and stored under Argon atmosphere. NMR spectra were recorded on either a Bruker Avance III 300 NMR spectrometer (1H : 300.13 MHz, ^{13}C : 75.46 MHz, ^{29}Si : 59.63 MHz) or a Bruker Avance III 400 spectrometer (1H : 400.12 MHz, ^{13}C : 100.61 MHz, ^{29}Si : 79.49 MHz) at 300 K. UV/VIS spectra were recorded on a Shimadzu UV-2600 spectrometer in quartz cells with a path length of 0.1 cm. Melting points were measured in sealed NMR caps under Ar atmosphere. Elemental analysis was carried out with an elemental analyzer Leco CHN-900. $T_7Ph_7(OH)_3$ was obtained from Hybrid Plastics and dried under vacuum prior to use. 4-vinylbenzyl chloride was obtained from Sigma Aldrich and degassed before use. Platinum on activated carbon was obtained from abcr. Trichlorosilane was obtained from abcr and distilled prior to use. Sodium hydride was obtained from Sigma Aldrich, washed with hexane and stored under argon atmosphere. Triethylamine was obtained from Merck, stirred over calcium hydride overnight and distilled prior to use. Calcium hydride was obtained from Acros Organics and used as received. (2,2,5,5,6-Pentakis(2',4',6'-trisopropylphenyl)tetracyclo[2.2.0.0^{1,3}.0^{3,6}]hexasilan-4-yl)lithium **1** was synthesized according to the published procedure.^[19a]

Deprotonation of heptaphenylsilsesquioxanetriol with sodium hydride. The synthesis was carried out according to a modified literature procedure.^[30] A solution of 21.17 g (22.70 mmol) of $T_7Ph_7(OH)_3$ in 80 mL thf was added dropwise to a suspension of 1.69 g (70.4 mmol) sodium hydride in 30 mL thf at room temperature in three hours. The reaction mixture was stirred for 24 hours, after which the solvent was evaporated. 23.20 g (90%) of a white solid were obtained. 1H NMR (400 MHz, $CDCl_3$, 300 K): 8.08–5.87 (m, 35 H, Ar-H), 3.40 (m, 8 H, thf), 1.54 (m, 8 H, thf) ppm.

Preparation of the benzyl-functionalized siliconoid **2.** The *ligato*-lithiated hexasilabenzpolarene **1** (200 mg; 0.127 mmol) is dissolved in 2 mL benzene and 1.1 eq benzylbromide (23.96 mg; 16.64 μ L; 0.14 mmol) are added at room temperature under stirring. After stirring the dark orange solution for 15 h, the precipitation of LiBr as white solid can be observed. Benzene is distilled off in vacuum

at room temperature. The orange residue is digested with 4 mL hexane and extracted with hexane at room temperature. After evaporation of hexane in vacuum, the crude product is dissolved in 0.5 mL pentane to afford 122 mg (75%) of **2** as orange crystals. 1H -NMR (300.13 MHz, C_6D_6 , 300 K): 7.62, 7.24 ($C_{10}H_8$), 7.13–6.69 (br, 9 H, Ar-H), 5.91–4.37 (br, 1 H, Tip-H), 4.37–3.91 (br, 2 H, Tip-Pr-CHMe₂), 2.85–2.57, 2.47–2.36 (each br, together 4 H, Tip-Pr-CHMe₂), 2.21–0.02 (br, overlapping with thf, all together 72 H, Tip-Pr-CH₃) ppm. ^{29}Si -NMR (59.62 MHz, C_6D_6 , 300 K): 170.6 (Tip₂-Si), 14.0 (Tip-Si), 8.5 (Tip₂-Si), 1.3 (s, Si-C-Ph), –260.9, –276.0 (each br, Si-Si₃) ppm.

4-(Chloromethyl)phenethyltrichlorosilane **3.** The synthesis was carried out according to a modified literature procedure.^[24] A mixture of 0.19 g platinum on activated carbon, 200 mL toluene, 13.50 mL (95.80 mmol) of 4-vinylbenzyl chloride and 14.50 mL (143.45 mmol) of trichlorosilane was refluxed at 80 °C for 4 hours, stirring was continued at room temperature for another 17 h. The mixture was filtered over Celite 545 and all volatiles were distilled off at 10^{–2} mbar. Distillation at 10^{–5} mbar using an oil diffusion pump and 120 °C afforded 18.55 g (67%) of **3** as a deep yellow liquid. 1H NMR (400 MHz, $CDCl_3$, 300 K): 7.36–7.22 (m, 4 H, Ar-H), 4.59 (s, 2 H, Ar-CH₂-Cl), 2.93–2.89 (m, 2 H, Ar-CH₂-CH₂), 1.78–1.73 (m, 2 H, Si-CH₂-CH₂) ppm. ^{13}C NMR (100 MHz, $CDCl_3$, 300 K): 141.81, 135.87, 129.09, 128.42 (each Ar-C), 46.13 (Ar-CH₂-Cl), 28.08 (Ar-CH₂-CH₂), 26.08 (Si-CH₂-CH₂) ppm. ^{29}Si NMR (79.5 MHz, $CDCl_3$, 300 K): 11.8 ppm.

Corner-capping reaction of $Ph_7T_7(ONa)_3$ with 4-(chloromethyl)phenethyltrichlorosilane. Preparation of **4** (T_8Ph_8R ; R = 4-(chloromethyl)phenethyl). This synthesis was carried out according to a modified literature procedure.^[23] A suspension of 14.68 g (14.72 mmol) of $T_7(ONa)_3$ and 6.60 mL (47 mmol) NEt_3 in 250 mL dry thf was stirred for 30 minutes and then cooled down in an ice-water bath for 1 h. A solution of 3.85 mL (17.66 mmol) of 4-(chloromethyl)phenethyltrichlorosilane **3** in 150 mL of dry thf was added dropwise during 3.5 h and stirring continued for 14 h in the thawing ice-bath. The solvent was evaporated, and the white residue dissolved in 150 mL of chloroform. The organic phase was washed three times with water and dried over magnesium sulfate. The product was precipitated by pouring the organic phase into 100 mL of MeOH. Drying in vacuum yielded 7.47 g (6.73 mmol, 46%) of **4** as a white solid (m.p. > 300 °C). 1H NMR (400 MHz, C_6D_6 , 300 K): 7.89–7.81 (m, 14 H, T_8 -*m*-Ar-H), 7.15–7.00 (m, 21 H, T_8 -*o,p*-Ar-H), 6.93–6.83 (m, 4 H, *o,m*-Ar-H), 4.08 (s, 2 H, Ar-CH₂-Cl), 2.79–2.75 (m, 2 H, Ar-CH₂-CH₂), 1.16–1.12 (m, 2 H, T_8 -CH₂-CH₂) ppm. ^{13}C NMR (100 MHz, C_6D_6 , 300 K): 144.12, 135.28, 134.64, 134.60, 131.27, 131.24, 130.69, 130.45, 130.39, 128.89, 128.43, 128.36, 128.20, 127.94 (each Ar-C), 46.19 (Ar-CH₂-Cl), 28.83 (Ar-CH₂-CH₂), 14.14 (T_8 -CH₂-CH₂) ppm. ^{29}Si NMR (79.5 MHz, C_6D_6 , 300 K): –65.4 (O_3Si -CH₂), –77.6 (O_3Si -Ph), –78.0 (O_3Si -Ph) ppm. ^{29}Si NMR (79.5 MHz, $CDCl_3$, 300 K): –65.8 (O_3Si -CH₂), –78.3 (O_3Si -Ph), –78.6 (O_3Si -Ph) ppm.

Preparation of hybrid system **5.** A solution of the *ligato*-lithiated hexasilabenzpolarene **1** in C_6H_6 (7.5 mL) was added dropwise to 388 mg (0.35 mmol) of the linker-substituted silsesquioxane **4** in 5 mL benzene during 25 minutes. The mixture was stirred at room temperature for another 45 minutes and filtered. The solvent was reduced to half of its volume and 213 mg (31%) of orange crystals of **5** were grown by heating the solution to 75 °C in an oil bath and letting it cool down slowly to rt overnight. Single crystals suitable for an X-ray diffraction study were grown by adding hexane to the amorphous solid to form a suspension. Dropwise addition of toluene while heating gently dissolved all solids and standing for three days at room temperature produced orange needles of **5** as single crystals. (m.p. 200–201 °C, no dec.). 1H NMR (400 MHz, C_6D_6 , 300 K): 7.97–7.79 (m, 14 H, T_8 -*m*-Ar-H), 7.63, 7.25 ($C_{10}H_8$), 7.19–7.00 (m, 27 H, overlapping T_8 -*o,p*-Ar-H with Tip-CH), 6.97 (br, 2 H, Tip-CH), 6.95–6.82 (m, 4 H, *o,m*-Ar-H), 6.80 (br, 1 H, Tip-CH), 5.11, 4.57

(each br, 1 H, ¹H-CH), 4.24 (br, 2 H, ¹H-CH), 4.17–3.99 (m, overlapping, 2 H, ¹H-CH), 3.44, 3.31, 3.12 (each br, 1 H, ¹H-CH), 2.98–2.91 (m, 2 H, Ar-CH₂-CH₃), 2.69, 2.68 (each sept., overlapping, 4 H, ¹H-CH), 2.39 (sept., ³J_{HH} = 6.90 Hz, 1 H, ¹H-CH), 2.17 (br, 3 H, ¹H-CH₃), 1.93 (br, 1 H, ¹H-CH), 1.75, 1.63 (each br, 6 H, ¹H-CH₃), 1.60–1.42 (m, 19 H, ¹H-CH₃), 1.41–1.34 (m, 2 H, Si-CH₂-CH₃), 1.33–1.01 (m, overlapping, 32 H, ¹H-CH₃), 0.85–0.68 (br, overlapping, 20 H, ¹H-CH₃), 0.65, 0.36, 0.23 (each br, 3 H, ¹H-CH₃) ppm. ¹³C NMR (100 MHz, C₆D₆, 300 K): 157.30, 155.13, 154.11, 153.50, 152.70, 150.82, 150.78, 150.63, 149.36, 140.88, 137.78, 136.73, 134.70, 134.67, 134.64, 131.26, 131.21, 130.76, 130.50, 130.45, 130.05, 127.40, 126.07, 124.02, 123.52, 123.42, 123.05, 122.46, 122.07, 121.45, (each Ar-C), 37.77, 36.56, 36.11, 34.74, 34.42, 34.38, 31.97, (each Tip-¹H-CH and Tip-¹H-CH₃), 28.93 (Ar-C, 27.50, 27.14, 26.51, 25.61, 24.48, 24.18, 24.06, 23.86, 23.47, 23.07, 22.55 (each Tip-¹H-CH and Tip-¹H-CH₃), 20.33 (Ar-CH₂-Si), 15.34 (Si-CH₂-CH₃), 14.39 ppm. ²⁹Si NMR (79.5 MHz, C₆D₆, 300 K): 170.6 (Tip₂-Si), 14.1 (Tip-Si), 8.4 (Tip₂-Si), 1.0 (Si-C-Ar), –65.3 (O₃Si-CH₂), –77.6, –77.9 (each O₃Si-Ph), –261.1, –275.9 (each Si-Si₃) ppm. CP-MAS ²⁹Si NMR (79.5 MHz, 11 kHz, C₆D₆, 300 K): 168.3 (Tip₂-Si), 18.1, 5.0, 1.9 (RSi₃Si), –67.4 (O₃Si-CH₂), –79.0 (O₃Si-Ph), –264.8, –274.3 (each Si-Si₃) ppm. UV/VIS (n-hexane): λ_{max}(ε) = 470 nm (540 M^{–1} cm^{–1}), 375 nm (8190 M^{–1} cm^{–1}). Elemental Analysis: Calc. for C₁₂₆H₁₆₀O₁₂Si₁₄: C, 66.96; H, 7.15; Found: C, 67.03; H, 7.43.

Corner-capping reaction of T₇Ph₇(ONa)₃ with 4-((chloromethyl)phenyl)-trichlorosilane. Preparation of 7 (T₈Ph₇R; R = 4-((chloromethyl)phenyl)). This synthesis was carried out according to a modified literature procedure.^[29] A suspension of 26.50 g (26.57 mmol) of T₇(ONa)₃ and 12.5 mL (89.70 mmol) NEt₃ in 300 mL thf was stirred for 20 minutes and cooled in an ice-water bath for one hour. 4-(Chloromethyl)phenyltrichlorosilane **6** in 125 mL of thf was added dropwise during 2 h in the cold. The reaction mixture was allowed to reach room temperature and stirring continued for another 15 hours. All volatiles were removed under vacuum and 500 mL of CH₂Cl₂ were added. The mixture was filtered and the solvent reduced until precipitation started to occur. The residue was collected and washed with 100 mL dichloromethane. The product **7** (3.15 g; 2.92 mmol) was collected as a white solid in 11 % yield (m.p. > 300 °C). ¹H NMR (400 MHz, C₆D₆, 300 K): 7.86–7.84 (m, 14 H, T₈-m-Ar-H), 7.74–7.72 (m, 2 H, Ar-o,m-H), 7.11–7.01 (m, 21 H, T₈-o,p-H), 6.90–6.88 (m, 2 H, Ar-o,m-H), 3.92 (s, 2 H, Ar-CH₂) ppm. ¹H NMR (400 MHz, CD₂Cl₂, 300 K): 7.80–7.78 (m, 14 H, T₈-m-Ar-H), 7.50–7.39 (m, 26 H, Ar-o,m-H overlapping with T₈-o,p-H), 4.60 (s, 2 H, Ar-CH₂) ppm. ¹³C NMR (100 MHz, CD₂Cl₂, 300 K): 140.66, 134.88, 134.41, 131.33, 130.79, 130.45, 130.41, 128.50, 128.40 (each Ar-C), 46.42 (Ar-CH₂-Cl) ppm. ²⁹Si NMR (79.5 MHz, CD₂Cl₂, 300 K): –78.31, –78.35, –78.6 ppm.

Preparation of hybrid system 8. A mixture of 273 mg (0.253 mmol) of silsesquioxane **7** and 372 mg (0.256 mmol) of the *ligato*-lithiated hexasilabenzopolarane **1** in benzene (5 mL) was stirred at room temperature for 75 min. The resulting dark orange mixture was filtered by cannula and the filtrate reduced in vacuum until a viscous solution was obtained. Orange crystals of **8** (417 mg, 74 %) were obtained by heating the benzene solution to 75 °C in an oil bath and letting it cool down slowly during 14 h (m.p. 200–201 °C, no dec.). ¹H NMR (400 MHz, C₆D₆, 300 K): 8.04–7.97 (m, 7 H, Ar-H), 7.89–7.77 (m, 14 H, Ar-H), 7.29–7.21 (m, 13 H, Ar-H), 7.13–7.01 (m, 20 H, Ar-H), 7.00–6.88 (m, 10 H, Ar-H and Tip-CH), 6.85 (br, 2 H, Tip-CH), 6.79 (br, 1 H, Tip-CH), 5.10 (br, 1 H, ¹H-CH), 4.56 (br, 1 H, ¹H-CH), 4.23 (br, 1 H, ¹H-CH), 4.08 (br, 4 H, overlapping, ¹H-CH), 3.41, 3.29, 3.10 (each br, 1 H, ¹H-CH), 2.76–2.59 (m, 5 H, overlapping, ¹H-CH), 2.28 (sept, 1 H, ¹H-CH), 2.16 (br, 3 H, ¹H-CH), 1.76–1.04 (m, 79 H, overlapping, ¹H-CH₃), 0.80 (br, 5 H, ¹H-CH₃), 0.72 (br, 8 H, overlapping, ¹H-CH₃), 0.62 (br, 17 H, overlapping, ¹H-CH₃), 0.35, 0.22 (each br, 4 H, ¹H-CH₃) ppm. ¹³C NMR (100 MHz, C₆D₆, 300 K): 156.90,

154.70, 153.65, 153.01, 152.29, 150.68, 150.50, 150.32, 148.92, 148.77, 144.11, 137.83, 136.17, 135.44, 134.46, 134.36, 134.30, 133.74, 133.69, 130.87, 130.82, 130.49, 130.12, 129.47, 128.23, 128.01, 127.94, 127.89, 127.82, 127.70, 127.58, 127.46, 125.71, 123.62, 123.07, 122.66, 122.07, 121.72, 121.10, (each Ar-C) 37.44, 36.28, 36.05, 35.78, 35.39, 34.86, 34.46, 34.37, 34.01, 33.95, 28.36, 27.59, 26.99, 26.75, 26.10, 25.33, 24.28, 24.12, 23.82, 23.68, 23.50, 22.98, 22.71, 22.23, (each Tip-¹H-CH and Tip-¹H-CH₃), 20.94 (Ar-CH₂-Si) ppm. ²⁹Si NMR (79.5 MHz, C₆D₆, 300 K): 170.8 (Tip₂-Si), 14.3 (Tip-Si), 8.8 (Tip₂-Si), 1.9 (Si-C-Ar), –76.8, –77.5, –77.6, –77.7 (each O₃Si-Ar), –260.5, –276.2 (each Si-Si₃) ppm. CP-MAS ²⁹Si NMR (79.5 MHz, 11 kHz, 300 K): 167.1 (Tip₂-Si), 9.1, 5.0 (each RSi₃Si), –78.9 (O₃Si-Ar), –255.0, –281.7 (each Si₃Si) ppm. UV/VIS (n-hexane): λ_{max}(ε) = 470 nm (540 M^{–1} cm^{–1}), 362 nm (8510 M^{–1} cm^{–1}). Elemental Analysis: Calc. for C₁₂₄H₁₅₆O₁₂Si₁₄: C, 66.73; H, 7.05; Found: C, 68.86; H, 5.98.

Acknowledgements

The single crystal X-ray diffraction study was carried out at the Service Center X-ray Diffraction with financial support from Saarland University and the Deutsche Forschungsgemeinschaft (INST 256/506-1). Open Access funding enabled and organized by Projekt DEAL.

Conflict of Interest

The authors declare no conflict of interest.

Data Availability Statement

The data that support the findings of this study are available in the supplementary material of this article.

Keywords: silicon monoxide • silsesquioxane • siliconoid • hybrid • model system

- [1] a) C. F. Mabery, *J. Franklin Inst.* **1886**, 122, 271–274; b) C. F. Mabery, *Am. Chem. J.* **1887**, 9, 11–15.
- [2] a) A. Netz, R. A. Huggins, W. Weppner, *J. Power Sources* **2003**, 119–121, 95–100; b) C.-M. Park, W. Choi, Y. Hwa, J.-H. Kim, G. Jeong, H.-J. Sohn, *J. Mater. Chem.* **2010**, 20, 4854–4860; c) J.-H. Kim, C.-M. Park, H. Kim, Y.-J. Kim, H.-J. Sohn, *J. Electroanal. Chem.* **2011**, 661, 245–249; d) B. G. Gribov, K. V. Zinov'ev, O. N. Kalashnik, N. N. Gerasimenko, D. I. Smirnov, V. N. Sukhanov, *Semiconductors* **2012**, 46, 1576–1579; e) B. G. Gribov, K. V. Zinov'ev, O. N. Kalashnik, N. N. Gerasimenko, D. I. Smirnov, V. N. Sukhanov, N. N. Kononov, S. G. Dorofeev, *Semiconductors* **2017**, 51, 1675–1680; f) R. Fu, K. Zhang, R. P. Zaccaria, H. Huang, Y. Xia, Z. Liu, *Nano Energy* **2017**, 39, 546–553; g) S. Lu, B. Wu, Y. Sun, Y. Cheng, F. Liao, M. Shao, *J. Mater. Chem. C* **2017**, 5, 6713–6717; h) T. Ming, S. Turishchev, A. Schleusener, E. Parinova, D. Koyuda, O. Chuvankova, M. Schulz, B. Dietzek, V. Sivakov, *Small* **2021**, 17, 2007650.
- [3] a) H.-H. Emons, P. Hellmold, H. Knoll, *Zeit. Anorg. Allg. Chem.* **1965**, 11, 78–87; b) S. Schnurre, J. Gröbner, R. Schmid-Fetzer, *J. Non-Cryst. Solids* **2003**, 336, 1–25.

- [4] A. Hohl, T. Wieder, P. A. Van Aken, T. E. Weirich, G. Denninger, M. Vidal, S. Oswald, C. Deneke, J. Mayer, H. Fuess, *J. Non-Cryst. Solids* **2003**, 320, 255–280.
- [5] S. S. Nekrashevich, V. A. Gritsenko, *Phys. Solid State* **2014**, 46, 207–222.
- [6] B. Friede, M. Jansen, *J. Non-Cryst. Solids* **1996**, 204, 202–203.
- [7] a) M. Nagamori, J.-A. Boivin, A. Claveau, *J. Non-Cryst. Solids* **1995**, 189, 270–276; b) D. C. Gunduz, A. Tankut, S. Sedani, M. Karaman, R. Turan, *Phys. Status Solidi C* **2015**, 12, 1229–1235.
- [8] K. Schulmeister, W. Mader, *J. Non-Cryst. Solids* **2003**, 320, 143–150.
- [9] a) G. W. Brady, *J. Phys. Chem.* **1959**, 63, 1119–1120; b) R. J. Temkin, *J. Non-Cryst. Solids* **1975**, 17, 215–230.
- [10] A. Yasaitis, R. J. Kaplow, *J. Appl. Phys.* **1972**, 43, 995–1000.
- [11] H. R. Philipp, *J. Phys. Chem. Solids* **1971**, 32, 1935–1945.
- [12] A. Hirata, S. Kohara, T. Asada, M. Arao, C. Yogi, H. Imai, Y. Tan, T. Fujita, M. Chen, *Nat. Commun.* **2016**, 7, 11591.
- [13] S. Hoffmann, T. F. Fässler, C. Hoch, C. Röhr, *Angew. Chem.* **2001**, 113, 4527–4529; *Angew. Chem. Int. Ed.* **2001**, 40, 4398–4400.
- [14] A. C. Filippou, B. Baars, O. Chernov, Y. N. Lebedev, G. Schnakenburg, *Angew. Chem.* **2014**, 126, 576–581; *Angew. Chem. Int. Ed.* **2014**, 53, 565–570.
- [15] Y. Wang, M. Chen, Y. Xie, P. Wei, H. F. Schaefer III, P. v. R. Schleyer, G. H. Robinson, *Nat. Chem.* **2015**, 7, 509–513.
- [16] a) J. Brown, L. Vogt, *J. Am. Chem. Soc.* **1965**, 87, 4313–4317; b) F. J. Feher, *J. Am. Chem. Soc.* **1986**, 108, 3850–3852; c) F. J. Feher, D. A. Newman, J. F. Walzer, *J. Am. Chem. Soc.* **1989**, 111, 1741–1748.
- [17] G. Hadjisavvas, G. Kipodakis, P. C. Kelires, *Phys. Rev. B: Condens. Matter Mater. Phys.* **2001**, 64, 125413.
- [18] a) D. Scheschkewitz, *Angew. Chem. Int. Ed.* **2005**, 44, 2954–2956; *Angew. Chem.* **2005**, 117, 3014–3016; b) G. Fischer, V. Huch, P. Mayer, S. K. Vasisht, M. Veith, N. Wiberg, *Angew. Chem.* **2005**, 117, 8096–8099; *Angew. Chem. Int. Ed.* **2005**, 44, 7884–7887; c) D. Nied, R. Köppe, W. Kloppe, H. Schnöckel, F. Breher, *J. Am. Chem. Soc.* **2010**, 132, 10264–10265; d) K. Abersfelder, A. J. P. White, R. J. F. Berger, H. S. Rzepa, D. Scheschkewitz, *Angew. Chem.* **2011**, 123, 8082–8086; *Angew. Chem. Int. Ed.* **2011**, 50, 7936–7939; e) A. Tsurusaki, C. Iizuka, K. Otsuka, S. Kyushin, *J. Am. Chem. Soc.* **2013**, 135, 16340–16343; f) T. Iwamoto, N. Akasaka, S. Ishida, *Nat. Commun.* **2014**, 5, 5353; g) L. J. Schiegl, A. J. Karttunen, W. Klein, T. F. Fässler, *Chem. Eur. J.* **2018**, 24, 19171–19174; h) L. J. Schiegl, A. J. Karttunen, W. Klein, T. F. Fässler, *Chem. Sci.* **2019**, 10, 9130–9139; i) J. Keuter, C. Schwermann, A. Hepp, K. Bergander, J. Droste, M. R. Hansen, N. L. Doltsinis, C. Mück-Lichtenfeld, F. Lips, *Chem. Sci.* **2020**, 11, 5895–5901.
- [19] a) P. Willmes, K. Leszczyńska, Y. Heider, K. Abersfelder, M. Zimmer, V. Huch, D. Scheschkewitz, *Angew. Chem.* **2016**, 128, 2959–2963; *Angew. Chem. Int. Ed.* **2016**, 55, 2907–2910; b) Y. Heider, N. Poitiers, P. Willmes, K. Leszczyńska, V. Huch, D. Scheschkewitz, *Chem. Sci.* **2019**, 10, 4523–4530; c) Y. Heider, P. Willmes, V. Huch, M. Zimmer, D. Scheschkewitz, *J. Am. Chem. Soc.* **2019**, 141, 19498–19504; d) K. I. Leszczyńska, V. Huch, C. Präsang, J. Schwabedissen, R. J. F. Berger, D. Scheschkewitz, *Angew. Chem.* **2019**, 131, 5178–5182; *Angew. Chem. Int. Ed.* **2019**, 58, 5124–5128; e) L. Klemmer, V. Huch, A. Jana, D. Scheschkewitz, *Chem. Commun.* **2019**, 55, 10100–10103.
- [20] The nomenclature of the individual silicon vertices and their substitution patterns is reminiscent of disubstituted six-membered aromatic ring systems. The two mono substituted vertices are given the prefix *ligato*, while the two unsubstituted silicon atoms are referred to as *nudo*-positions. The low field shift in the ^{29}Si NMR of the disubstituted *privo*-silicon atom gave rise to its prefix (*privo* meaning deprived in latin, referring to the electrons) and the remaining disubstituted vertex is referred to as *remoto* due to its position being the most remote from the *nudo*-atoms.^[19b]
- [21] a) Y. Cao, S. Xu, L. Li, S. Zheng, *J. Polym. Sci., Part B: Polym. Phys.* **2017**, 55, 587–600; b) J. Duszczak, K. Mitula, R. Januszewski, P. Żak, B. Dudziec, B. Marciniec, *ChemCatChem* **2019**, 11, 1086–1091; c) Y. Sato, H. Imoto, K. Naka, *J. Polym. Sci.* **2020**, 58, 1456–1462; d) A. Igarashi, H. Imoto, K. Naka, *Polym. Chem.* **2022**, 13, 1228–1235.
- [22] a) K. Ohno, S. Sugiyama, K. Koh, Y. Tsujii, T. Fukuda, M. Yamahiro, H. Oikawa, Y. Yamamoto, N. Ootake, K. Watanabe, *Macromolecules* **2004**, 37, 8517–8522; b) M. Janssen, J. Wilting, C. Müller, D. Vogt, *Angew. Chem.* **2010**, 122, 7904–7907; *Angew. Chem. Int. Ed.* **2010**, 49, 7738–7741; c) C.-Y. Yu, S.-W. Kuo, *Ind. Eng. Chem. Res.* **2018**, 57, 2546–2559; d) D. Zhang, Y. Liu, Y. Shi, G. Huang, *RSC Adv.* **2014**, 4, 6275–6283.
- [23] JNC Corp (Y. Urata, K. Hashimoto, M. Nishimura, J. Terasawa, M. Nakayama), JP2013032340 A (February 14, 2013).
- [24] D. Kessler, P. Theato, *Macromolecules* **2008**, 41, 5237–5244.
- [25] a) E. G. Shockey, A. G. Bolf, P. F. Jones, J. J. Schwab, K. P. Chaffee, T. S. Haddad, J. D. Lichtenhan, *Appl. Organomet. Chem.* **1999**, 13, 311–327; b) P. Żak, C. Pietraszuk, B. Marciniec, G. Spólnik, W. Danikiewicz, *Adv. Synth. Catal.* **2009**, 351, 2675–82.
- [26] M. A. Hoque, Y. H. Cho, Y. Kawakami, *React. Funct. Polym.* **2007**, 67, 1192–1199.
- [27] P. R. Chinnam, M. R. Gau, J. Schwab, M. J. Zdzilla, S. L. Wunder, *Acta Crystallogr., Sect. C: Struct. Chem.* **2014**, 70, 971–974.
- [28] D. Voisin, D. Flot, A. Van der Lee, O. J. Dautel, J. J. E. Moreau, *CrystEngComm* **2017**, 19, 492–502.
- [29] F. Liu, H. Guo, Y. Zhao, X. Qiu, L. Gao, Y. Zhang, *Polym. Degrad. Stab.* **2019**, 168, 108959.
- [30] I. Kownacki, B. Marciniec, K. Szubert, M. Kubicki, M. Jankowska, H. Steinberger, S. Rubinsztajn, *Appl. Catal., A* **2010**, 380, 105–112.

Manuscript received: July 11, 2022
 Revised manuscript received: August 30, 2022
 Accepted manuscript online: September 5, 2022

3.2 Polyhedral Oligomeric Silsesquioxane D_{3h} -(RSiO_{1.5})₁₄

M. Hunsicker, Ankur, B. Morgenstern, M. Zimmer, D. Scheschkewitz, *Chem. Eur. J.* **2024**, 30, e202303640. Copyright © 2023 The Authors.

<https://doi.org/10.1002/chem.202303640>

This article has been published by Wiley-VCH Verlag GmbH & Co. KGaA as an “Open Access” Article and is licensed under a “Creative Commons Attribution-NonCommercial-NoDerivatives 4.0 International (CC BY-NC-ND-4.0)” License (<https://creativecommons.org/licenses/by-nc-nd/4.0/>).

The article is reproduced with permission of Wiley-VCH Verlag GmbH & Co. KGaA and all authors. No modifications were made. The results are additionally concluded and put into context in Chapter 4.

Author contributions:

Marc Hunsicker: Equal (D. S.): Conceptualization, Lead: Data curation, Formal analysis, Investigation, Methodology, Validation, Visualization, Writing and Editing.

Ankur: Lead: Theoretical calculations.

Bernd Morgenstern: Lead: X-ray analysis.

Michael Zimmer: Supporting: Hetero-NMR and 2D-NMR analysis.

David Scheschkewitz: Lead: Conceptualization, Project administration, Supervision, Acquisition of Funding and Resources, Supporting: Methodology, Writing – Review and Editing.



Hot Paper

Polyhedral Oligomeric Silsesquioxane D_{3h} -(RSiO_{1.5})₁₄
 Marc Hunsicker,^[a] Ankur,^[a] Bernd Morgenstern,^[b] Michael Zimmer,^[a] and
David Scheschkewitz^{*[a]}

Dedicated to the memories of Robert West and Petey Young

While smaller polyhedral oligomeric silsesquioxanes T_nR_n (POSS) are readily accessible or even commercially available, unambiguously authenticated larger systems ($n > 12$) have barely been reported. Synthesis and isolation procedures are lengthy, and yields are often very low. Herein, we present the surprisingly straightforward and high-yielding access to the phenyl-substituted derivative of a so far only postulated second D_{3h} -symmetric T_{14} isomer and with that the largest crystallographically characterized POSS cage with organic substituents.

Treatment of the commercially available incompletely condensed $T_7Ph_7(OH)_3$ silsesquioxane with catalytic amounts of trifluoromethanesulfonic acid results in high yields of the $T_{14}Ph_{14}$ framework, which is isolated in crystalline form by a simple work-up. D_{3h} - $T_{14}Ph_{14}$ was analyzed by single crystal X-ray diffraction, multinuclear NMR spectroscopy and thermal analysis. The relative energies of all four theoretically possible $T_{14}Ph_{14}$ isomers were determined by optimization of the corresponding structure using DFT methods.

Introduction

Silsesquioxanes $[RSiO_{1.5}]_n$ are polymeric or oligomeric materials with a wide variety of applications in materials chemistry, e.g. as building blocks in inorganic-organic copolymers and other hybrid materials,^[1a] precursors for silicon nanocrystals,^[1b] electron beam resists,^[1c] chemical sensors,^[1d] and as model systems for silicon surfaces.^[2] Many oligomeric silsesquioxanes adopt cage-like molecular structures (polyhedral oligomeric silsesquioxanes POSS, $R = H$, alkyl, aryl). Their high stability gives rise to a broad range of further manipulations in the POSS framework periphery.^[3] The common abbreviation T_nR_n refers to the number n of trifunctional silicon centers T each carrying a single substituent R . Early synthetic procedures^[4a–c] employed the controlled hydrolysis of trihalo- or trialkoxysilanes followed by the condensation to often complicated mixtures of variously sized molecular cages as well as polymers. Long reaction times, low yields and tedious separation procedures limited the potential applications initially. The use of NBu_4F as catalyst improved yields in case of T_8R_8 significantly (Figure 1, A) despite

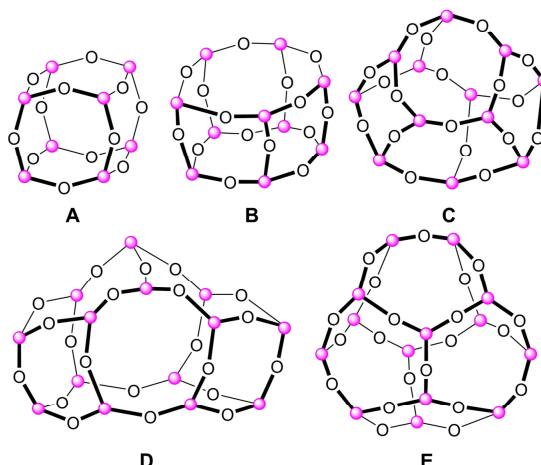


Figure 1. Exemplary POSS derivatives characterized in the solid state by X-ray crystallography. A: T_8R_8 ; B: $T_{10}R_{10}$; C: D_{2d} isomer of $T_{12}H_{12}$; D: D_{3h} isomer of $T_{14}H_{14}$; E: C_{2v} isomer of $T_{14}H_{14}$ (● = SiR).

[a] M. Hunsicker, Ankur, Dr. M. Zimmer, Prof. Dr. D. Scheschkewitz
Krupp-Chair of General and Inorganic Chemistry
Saarland University
66123 Saarbrücken, Germany
E-mail: scheschkewitz@mx.uni-saarland.de

[b] Dr. B. Morgenstern
Service Center X-Ray Diffraction
Saarland University
66123 Saarbrücken, Germany

Supporting information for this article is available on the WWW under
<https://doi.org/10.1002/chem.202303640>

© 2023 The Authors. Chemistry - A European Journal published by Wiley-VCH GmbH. This is an open access article under the terms of the Creative Commons Attribution Non-Commercial NoDerivs License, which permits use and distribution in any medium, provided the original work is properly cited, the use is non-commercial and no modifications or adaptations are made.

much shorter reaction times.^[4e] A large number of T_8R_8 derivatives have thus been crystallographically characterized, as well as a few examples of the larger cages $T_{10}R_{10}$ (B) and $T_{12}R_{12}$ (C).^[5] The largest POSS cages with unambiguously determined solid state structure are two of the four possible $T_{14}H_{14}$ isomers with D_{3h} and C_{2v} symmetry (D and E).^[4c,6] Recently, a styryl-functionalized $T_{18}R_{18}$ isomer was isolated in low yield from a complex product mixture, but its structural characterization was restricted to spectroscopic observations and DFT calculations.^[7] Using larger silsesquioxane cages as precursors for materials may lead to altered, possibly improved properties, for example in hybrid porous polymers and materials with low dielectric constants.^[8]

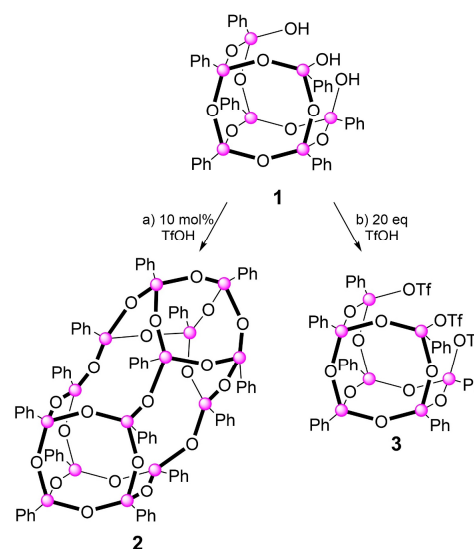
Herein, we report the simple and systematic preparation of one of the two elusive T_{14} framework isomers as crystalline material. With its phenyl-substituents, the obtained $T_{14}Ph_{14}$ represents the largest organic POSS derivative with unambiguously determined solid state structure to date. Its straightforward and reliable high yield synthesis by condensation of the commercially available trisilanol $T_7Ph_7(OH)_3$ is enabled by the catalytic action of trifluoromethanesulfonic acid (TfOH). We also obtained circumstantial evidence for the formation of triflates of the type $T_7Ph_7(OTf)_n(OH)_{3-n}$ under closely related reaction conditions.

Results and Discussion

Given the resemblance of the commercially available trisilanol $T_7Ph_7(OH)_3$ to one half of the postulated, yet experimentally elusive second D_{3h} isomer in the $T_{14}H_{14}$ system, we speculated that a condensation reaction may result in an analogous $T_{14}R_{14}$ structure. Pietschnig et al. previously reported that the corresponding *tert*-butyl-substituted $T_7Bu_7(OH)_3$ forms a dimer in which two T_7 units are connected by hydrogen bonding through the silanol groups.^[9] Thermal rearrangement above 200 °C was postulated to form the aforementioned second D_{3h} $T_{14}R_{14}$ isomer among other possible condensation products, based on MALDI-TOF-MS data.^[10] As spontaneous self-condensation at ambient temperature does apparently not occur in either case, and considering the NBu_4F catalyzed condensation of silanetriols towards T_8R_8 silsesquioxane frameworks,^[11] we concluded that a catalyst would be required in order to enable a nucleophilic attack of the OH groups of one molecule at the open face of a second.

Trifluoromethanesulfonic acid (triflic acid, TfOH) is reported to cleave Si–O–Si linkages of silsesquioxane cages under formation of bis(triflates), a reaction plausibly involving silanol intermediates.^[12,13] Despite reports on cage rearrangements during the acid-catalyzed hydrolysis of $T_7Ph_7(OH)_3$ and related incompletely condensed species,^[14] we speculated that TfOH may either substitute the Si–OH groups of the incompletely condensed $T_7Ph_7(OH)_3$ 1 or catalyze the condensation to $T_{14}Ph_{14}$.

In an initial attempt targeting the tris(triflate) $T_7Ph_7(OTf)_3$, three equivalents of TfOH were added to 1 in toluene at room temperature (Scheme 1). This resulted in a product mixture from which low amounts of a product with three ^{29}Si NMR signals at $\delta = -76.1$, -77.5 and -79.1 ppm in C_6D_6 were obtained by cooling a hot, concentrated toluene solution to room temperature. The absence of OH signals in the 1H NMR and of any ^{19}F NMR signal suggested that instead of substitution of OH by OTf condensation to a symmetrical $T_{14}Ph_{14}$ derivative had occurred. As in this case triflic acid would be needed in catalytic quantities only, we repeated the reaction with 10 mol% of TfOH and in the presence of molecular sieves (to capture the released water upon substitution) in toluene and indeed obtained the same product in 39% yield after evaporation of the volatiles and precipitation from minimal amounts of toluene.



Scheme 1. a) Synthesis of the D_{3h} - $T_{14}Ph_{14}$ isomer 2 from incompletely condensed silsesquioxane $Ph_7T_7(OH)_3$ 1 catalyzed by TfOH (●: silicon vertex). b) Treatment of $T_7Ph_7(OH)_3$ with 20 equivalents of triflic acid results in a mixture quantity of $T_7Ph_7(OTf)_3$ among other non-isolated $T_7Ph_7(OTf)_n(OH)_{3-n}$ species.

Single crystals were grown by slowly cooling a concentrated toluene solution from approx. 100 °C to room temperature in the course of 16 h. An X-ray diffraction study (Figure 2)^[15] indeed confirmed the formation of the condensation product of two molecules of $T_7Ph_7(OH)_3$ 1 across the three silanol functions. The $T_{14}Ph_{14}$ cage 2 thus shows approximated D_{3h} symmetry with the three edge-sharing $(RSiO)_4$ rings of each T_7 unit connected by three $(RSiO)_6$ motifs ($6^35^04^6$; the base referring to the number of SiO units in a given ring motif and the exponent to the

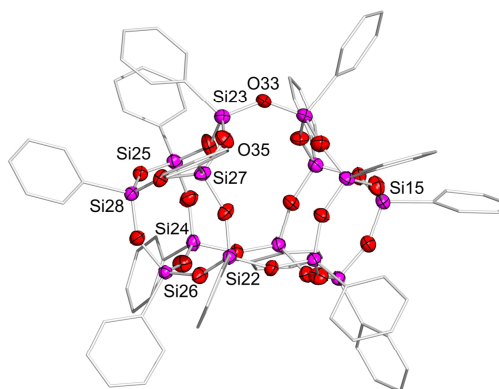


Figure 2. Molecular structure of $T_{14}Ph_{14}$ silsesquioxane 2 in the solid state. The idealized D_{3h} symmetry has no crystallographic correspondence. Thermal ellipsoids at 50% probability level, two of the three molecules in the asymmetric unit as well as hydrogen atoms and co-crystallized solvent molecules are omitted for clarity.

number of occurrences).^[4d] This connectivity is in marked contrast to the two crystallographically characterized isomers of the $T_{14}H_{14}$ parent species isolated by Agaskar et al. in a multiple step separation effort and with the very small combined yield of 1.1 %.^[4d] The D_{3h} - $T_{14}H_{14}$ isomer shows $6^05^64^3$ and its C_{2v} isomer $6^15^44^4$ connectivity. The $6^35^04^6$ isomer of $T_{14}H_{14}$ had been proposed to be part of the reaction mixture together with a fourth isomer of $6^25^24^5$ connectivity on the basis of GC-MS analysis, although no further information on its structure had been given in the absence of analytical data in solution and the solid state.^[4d] In subsequent computations on $T_{14}H_{14}$, however, only the two experimentally confirmed isomers plus the elusive $6^35^04^6$ motif reported in here as phenyl-substituted version **2** were considered^[16] revealing its strong energetic disadvantage by approximately $14.7 \text{ kcal mol}^{-1}$ at the MP2/SBK level of theory.^[16b]

The asymmetric unit of the crystals of **2** consists of three crystallographically independent molecules with noticeable differences in the bonding parameters although all show approximate D_{3h} symmetry. The silicon-oxygen bond lengths in the three molecules vary between $1.583(7) \text{ \AA}$ and $1.638(6) \text{ \AA}$ as opposed to the relatively uniform case of T_8Ph_8 (with Si-O bond lengths between 1.617 \AA and 1.626 \AA).^[17] In contrast, the OSiO bond angles are rather uniform and differ just slightly from T_8Ph_8 . The range of SiOSi bond angles in **2** ($T_{14}Ph_{14}(1)$: $138.8(4)^\circ$ to $172.0(6)^\circ$, $T_{14}Ph_{14}(2)$: $138.0(4)^\circ$ to $162.6(4)^\circ$ and $T_{14}Ph_{14}(3)$: $141.0(4)^\circ$ to $155.3(4)^\circ$) is larger than in T_8Ph_8 (142.28° to 153.22°) for all three independent molecules. Figure S14 shows superpositions of two molecules each in order to visualize the geometrical deviations (see Supporting Information).

The $T_{14}Ph_{14}$ silsesquioxane **2** gives rise to three signals in the ^{29}Si NMR at -76.2 , -77.6 and -79.1 ppm in C_6D_6 as depicted in Figure 3, which is in the usual range of phenyl-substituted silsesquioxanes.^[18] Compared to the $Ph_7T_7(OH)_3$ starting material (-68.3 , -76.9 and -77.8 ppm) the chemical shifts of **2** are closer together due to the very similar coordination environment at each silicon center. A 1H - ^{29}Si correlation NMR experiment in $CDCl_3$ (Figure S8) indicates the signal at -76.9 ppm to represent the two silicon atoms located on the C_3 rotation axis

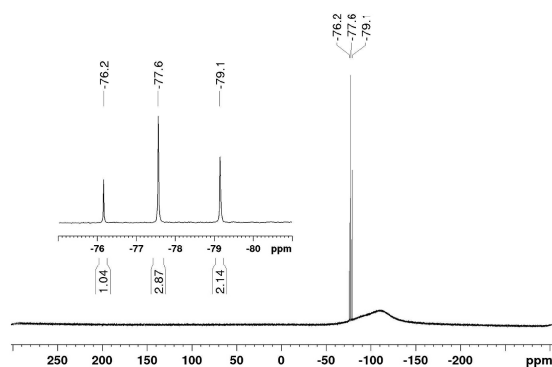


Figure 3. ^{29}Si NMR spectrum of the $T_{14}Ph_{14}$ silsesquioxane **2** in C_6D_6 at 25°C . The insert shows the signals with their relative intensities.

in the T_7 fragments (Si28 and Si15 atoms in Figure 2), by assignment of the corresponding 1H NMR resonances to the *meta* hydrogen atoms of the phenyl groups based on the relative intensities (see Figures S1 and S2). The $^{29}\text{Si}/\text{CP}$ MAS spectrum of the crystalline material (Figure S7) shows an unresolved single broad peak at -77.8 ppm . The reported $T_{12}Ph_{12}$ $^{29}\text{Si}/\text{CP}$ MAS spectrum shows two well-resolved signals at -76.8 and -80.4 ppm ,^[4e] in accordance with the two distinctly different chemical environments of the Si atoms. In our case, it is not surprising that the different silicon environments cannot be resolved in the solid state given the 42 silicon atoms of the three crystallographically inequivalent $T_{14}Ph_{14}$ molecules with only slightly different chemical environments. Diagnostically, the IR spectrum in Figure S10 of silsesquioxane **2** (ATR) lacks the distinct OH bands of the $T_7Ph_7(OH)_3$ precursor ($\nu_{OH} = 3234 \text{ cm}^{-1}$, $\nu_{SiOH} = 885 \text{ cm}^{-1}$, Figure S9)^[18] but is otherwise almost identical. Thermogravimetric analysis and differential scanning calorimetry of the $T_{14}Ph_{14}$ isomer show a behavior similar to that of the T_8Ph_8 to $T_{12}Ph_{12}$ systems (see Supporting Information for details).

DFT optimization of the four isomers in the $T_{14}Ph_{14}$ system at the B3LYP/6-311G level of theory (Figure 4) revealed the D_{3h} ($6^05^64^3$) (framework **E** in Figure 1) to be the most stable representative, while the herein synthesized D_{3h} ($6^35^04^6$) isomer **2** is the least stable at 13 kcal mol^{-1} . This reflects the previously reported findings for $T_{14}H_{14}$.^[16] The most stable D_{3h} isomer features the largest ratio of five-membered SiO rings to four- or six membered ones. This is in line with the observation that the five membered SiO ring systems are less strained and thus more stable.^[7,16b] As can be seen in Figure 4, the higher the number of four and six membered rings, the higher the relative energy of the $T_{14}Ph_{14}$ isomer. In contrast to the experimental

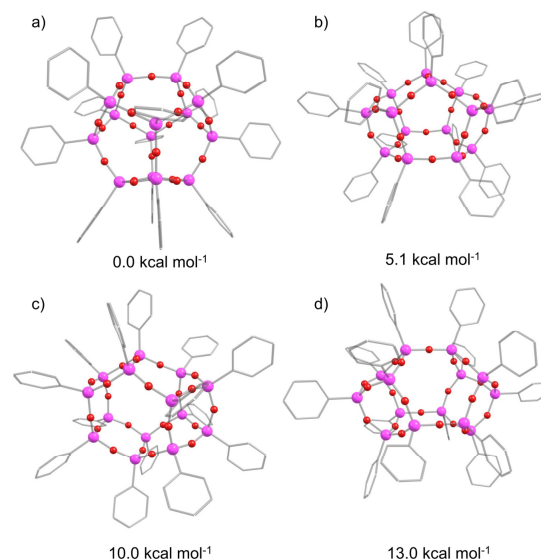


Figure 4. Optimized structures of the $T_{14}Ph_{14}$ isomers. a) D_{3h} ($6^05^64^3$) isomer, b) C_{2v} ($6^15^44^4$) isomer, c) C_{2v} isomer ($6^25^24^5$), d) D_{3h} ($6^35^04^6$) isomer.

solid state structure, the SiOSi bond angles are relatively uniform between 178.001° and 179.335° . Due to the well-established facile variation of the siloxane linkage, packing effects in the crystal lattice readily explain the deformation of the SiOSi angles in silsesquioxanes and can deviate by a large margin from calculations in the gas phase.^[3,19] The SiO bond lengths vary between 1.653 and 1.684 Å, which is overall slightly longer than in the experimental case as well-known for many DFT-functionals. In concert with the tendency of TfOH to cleave siloxane bonds under thermodynamic conditions, the high relative energy of the here reported D_{3h} ($6^3 5^0 4^6$) isomer suggests that silsesquioxane **2** represents the kinetic product of the reaction.

In order to broaden the scope of the systematic preparation of large silsesquioxanes, we attempted to isolate the incompletely condensed silsesquioxane as tris(triflate) derivative **3**, despite clear indications that it was unlikely to be an intermediate in the catalyzed formation of **2**. The reverse addition of the trisilanol **1** as suspension in toluene to a large extent of TfOH (20 eq) was expected to favor the stoichiometric reaction. Indeed, the biphasic mixture produced a small quantity of colorless single crystals after layering the separated toluene phase with hexane (Scheme 1). X-ray diffraction analysis revealed the heavily disordered structure of **3** (Figure 5), which may serve as strong indication for its formation but does not allow for the discussion of structural parameters. Unfortunately, the extreme sensitivity of **3** prevented a spectroscopic characterization of the minute amount obtained. In addition, as water is released during the substitution of OH by TfOH under the conditions described above, an unfavorable equilibrium reaction may complicate the isolation of **3** in larger quantities. The use of triflic anhydride Tf_2O instead of TfOH was expected to avoid this issue but did not produce satisfying results, as depending on the reaction conditions variable amounts of $\text{T}_{14}\text{Ph}_{14}$ along with unidentified byproducts at ambient temperatures or intractable product mixtures (between -78°C and 0°C) are obtained. Attempts to quench potential triflate species with suitable nucleophiles such as MeOH resulted in incon-

clusive NMR spectra. Increasing the excess of triflic acid even further was not considered a viable option as it may favor competing side reactions such as ring opening and cage-rearrangements as reported by Feher and coworkers for other silsesquioxanes.^[20]

Based on above findings and considerations, it can be safely assumed that the mechanism of the condensation dimerization of **1** to the here reported D_{3h} -symmetric $\text{T}_{14}\text{Ph}_{14}$ isomer **2** does not involve intermediate tris(triflates) to any significant extent although they undoubtedly occur in low concentration under the reaction conditions. Instead we assume a catalytic cycle that closes the three required SiOSi linkages in a stepwise manner.

Conclusions

We conclude that whereas all hitherto reported polyhedral silsesquioxanes ($\text{RSiO}_{1.5}$)_n of cage sizes beyond $n = 8$ have been obtained as side-products of the smaller congeners in typically low yield and required complicated separation protocols, the here presented approach via an unprecedented catalytic condensation dimerization of $\text{T}_7\text{Ph}_7(\text{OH})_3$ to give $\text{T}_{14}\text{Ph}_{14}$ is simple and straightforward. This allowed for the first complete characterization of a $\text{T}_{14}\text{Ph}_{14}$ silsesquioxane, a substituted representative of the elusive second D_{3h} isomer of $\text{T}_{14}\text{H}_{14}$. The high yielding and reproducible TfOH-catalyzed synthesis of the largest organically substituted polyhedral silsesquioxane from commercially available $\text{Ph}_7\text{T}_7(\text{OH})_3$ opens the door to the development of an entirely new field of silsesquioxane chemistry. The reactivity of $\text{T}_{14}\text{Ph}_{14}$ is currently being investigated in our laboratory.

Experimental

General. All manipulations were conducted under a protective argon atmosphere using standard Schlenk techniques unless otherwise stated. Non-chlorinated solvents were dried over Na/benzophenone (in the presence of tetraglyme in case of aromatic and aliphatic solvents) and distilled under argon atmosphere. Deuterated solvents were dried by reflux over potassium and distilled under argon atmosphere prior to use. NMR spectra were recorded on either a Bruker Avance III 300 NMR spectrometer (^1H : 300.13 MHz, ^{13}C : 75.46 MHz, ^{19}F : 282.4 MHz, ^{29}Si : 59.63 MHz) or a Bruker Avance III 400 spectrometer (^1H : 400.12 MHz, ^{13}C : 100.61 MHz, ^{29}Si : 79.49 MHz) at 300 K. Thermogravimetric Analysis (TGA) was performed on a TGA/DSC Stare System 1 (Mettler-Toledo) and applying a heating rate of 10 K/min between 30 and 1000°C . The Ar gas flow was set to 60 mL/min. Differential Scanning Calorimetry (DSC) was performed on a DSC 204 F1 Phoenix calorimeter (NETZSCH-Gerätebau GmbH) using an aluminum crucible with a pierced lid under nitrogen atmosphere (60 mL/min). A heating rate of 10 K/min from 25 to 415°C was applied, with an isothermal step for 5 min at 415°C . A cooling rate of 15 K/min from 415°C to 25°C was applied. Elemental analysis was carried out with an elemental analyzer Leco CHN-900. $\text{T}_7\text{Ph}_7(\text{OH})_3$ was obtained from Hybrid Plastics, Inc. and dried under vacuum prior to use. Trifluoromethanesulfonic acid was obtained from TCI Belgium and distilled over a small amount of trifluoromethanesulfonic anhydride. Trifluoromethanesulfonic anhydride was obtained from Fluorochem and distilled over P_4O_{10} prior to use.

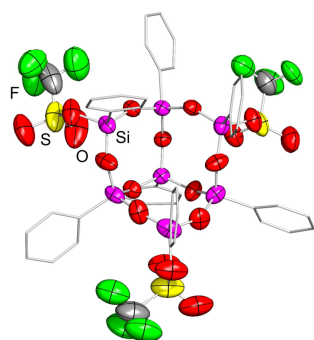


Figure 5. Highly disordered structure of silsesquioxanes tris(triflate) **3** in the solid state. Hydrogen atoms and disorder of phenyl and OTf groups are omitted for clarity. While the structure confirms the formation of the $\text{T}_7\text{Ph}_7(\text{OTf})_3$ species, the pronounced disorder of the OTf groups is prohibitive with regards to a discussion of bonding parameters.

Preparation of $T_{14}Ph_{14}$. 2. A suspension of 1.27 g $T_7Ph_7(OH)_3$ in 13 mL of toluene is treated with 0.13 mL of a 1 M stock solution of freshly distilled trifluoromethanesulfonic acid in dichloromethane at room temperature in the presence of molecular sieve 4 Å. The reaction mixture is stirred for 30 minutes at ambient temperature, then for 15 minutes at 50 °C. The volatiles are evaporated under reduced pressure using a warm water bath. From here on, protective atmosphere or dry solvents are no longer necessary. The obtained residue is washed with another 2 mL of toluene at 0 °C. The product is again dissolved in 2 mL of dichloromethane and separated from the molecular sieves via filtration. 7 mL of toluene are used to separate the $T_{14}Ph_{14}$ from residual toluene-insoluble byproducts. Evaporation of toluene gives 475 mg of a white powder (39% yield). (m.p. 407 °C). 1H NMR (400 MHz, C_6D_6 , 300 K): 7.96–7.92 (m, 4H, *m*-Ph-H), 7.79–7.70 (m, 24H, *m*-Ph-H), 7.14–7.01 (m, 12H, *o*, *p*-Ph-H, overlapping with toluene-H), 6.97–6.93 (m, 18H, *o*, *p*-Ar-H), 6.86–6.82 (m, 12H, *o*, *p*-Ph-H) ppm. 1H NMR (400 MHz, $CDCl_3$, 300 K): 7.76–7.74 (m, 4H, *m*-Ph-H), 7.56–7.54 (m, 12H, *m*-Ph-H), 7.47–7.44 (m, 12H, *m*-Ph-H), 7.38–7.33 (m, 10H, *o*, *p*-Ph-H), 7.27–7.20 (m, 20H, *o*, *p*-Ph-H, overlapping with toluene-H), 7.10–7.06 (m, 12H, *o*, *p*-Ph-H) ppm. ^{13}C NMR (100 MHz, C_6D_6 , 300 K): 134.6, 134.5, 132.0, 131.3, 131.1, 130.9, 130.7, 130.5, 129.3, 128.6, 128.5, 128.2, 125.7 (each Ph-C) ppm. ^{13}C NMR (100 MHz, $CDCl_3$, 300 K): 134.3, 134.2, 134.1, 131.7, 131.2, 130.9, 130.8, 130.4, 130.2, 128.1, 127.8, 127.7 (each Ph-C) ppm. ^{29}Si NMR (79.5 MHz, C_6D_6 , 300 K): –76.2, –77.6, –79.1 ppm. ^{29}Si NMR (79.5 MHz, $CDCl_3$, 300 K): –76.9, –78.3, –80.1 ppm. CP-MAS- ^{29}Si NMR: (79.5 MHz, 13 kHz, 300 K) –77.8 ppm. **Elemental Analysis:** Calc. for $C_{64}H_{70}O_7Si_{14}$: C, 55.78; H, 3.90; Found: C, 56.11; H, 3.86.

Supporting Information

Plots of NMR and IR spectra as well as details of thermal analysis, X-ray structures and DFT calculations. The authors have cited additional references within the Supporting Information.^[21–28]

Acknowledgements

We gratefully acknowledge the funding by Saarland University. We acknowledge the Service Center X-ray Diffraction established with financial support from Saarland University and the Deutsche Forschungsgemeinschaft (INST 256/506-1). We thank Svenja Pohl, Jan-Falk Kannengießner and Elias Gießelmann for the TGA, DSC and solid state NMR measurements. Open Access funding enabled and organized by Projekt DEAL.

Conflict of Interests

The authors declare no conflict of interest.

Data Availability Statement

The data that support the findings of this study are available in the supplementary material of this article.

Keywords: Cage structures • Reactive Intermediates • silsesquioxanes • silyl triflates

- [1] a) S. M. Ramirez, Y. J. Diaz, C. M. Sahagun, M. W. Duff, O. B. Lawal, S. T. Ianoco, J. M. Mabry, *Polym. Chem.* **2013**, *4*, 2230–2234; b) R. J. Clark, M. Aghajamali, C. M. Gonzalez, L. Hadidi, M. A. Islam, M. Javadi, M. H. Mobarok, T. K. Purkait, C. J. T. Robidillo, R. Sinelnikov, A. N. Thiessen, J. Washington, H. Yu, J. C. C. Veinot, *Chem. Mater.* **2017**, *29*, 80–89; c) J. Shen, F. Aydinoglu, M. Soltani, B. Cui, *J. Vac. Sci. Technol. B* **2019**, *37*, 021601; d) M. Gon, K. Tanaka, Y. Chujo, *Chem. Asian J.* **2022**, *17*, e2202200144.
- [2] F. J. Feher, D. A. Newman, J. F. Walzer, *J. Am. Chem. Soc.* **1989**, *111*, 1741–1748.
- [3] D. B. Cordes, P. D. Lickiss, F. Rataboul, *Chem. Rev.* **2010**, *110*, 2081–2173.
- [4] a) A. J. Barry, W. H. Daudt, J. J. Domicone, J. W. Gilkey, *J. Am. Chem. Soc.* **1955**, *77*, 4248–4252; b) J. F. Brown, L. H. Vogt, *J. Am. Chem. Soc.* **1965**, *87*, 4313–4317; c) P. A. Agaskar, V. W. Day, W. G. Klemperer, *J. Am. Chem. Soc.* **1987**, *109*, 5554–5556; d) P. A. Agaskar, W. G. Klemperer, *Inorg. Chim. Acta* **1995**, *229*, 355–364; e) A. R. Bassindale, Z. Liu, I. A. MacKinnon, P. G. Taylor, Y. Yang, M. E. Light, P. N. Horton, M. B. Hursthouse, *Dalton Trans.* **2003**, 2945–2949.
- [5] a) D. Hossain, C. U. Pittman, S. Saebø, F. Hagelberg, *J. Phys. Chem. C* **2007**, *111*, 6199–6206; b) M. Z. Asuncion, R. M. Laine, *J. Am. Chem. Soc.* **2010**, *132*, 3723–3736; c) S. Chimjarn, R. Kunthom, P. Chancharone, R. Sodkhomkhum, P. Sangtrirutnugul, V. Ervithayasuporn, *Dalton Trans.* **2015**, *44*, 916–919; d) K. Imai, Y. Kaneko, *Inorg. Chem.* **2017**, *56*, 4133–4140.
- [6] Y. Kawakami, K. Yamaguchi, T. Yokozawa, T. Serizawa, M. Hasegawa, Y. Kabe, *Chem. Lett.* **2007**, *36*, 792–793.
- [7] M. Laird, N. Hermann, N. Ramsahye, C. Totée, C. Carcel, M. Unno, J. R. Bartlett, M. Wong Chi Man, *Angew. Chem.* **2021**, *133*, 3059–3064; *Angew. Chem. Int. Ed.* **2021**, *60*, 3022–3027.
- [8] a) X. Lin, Y.-Y. Deng, Q. Zhang, D. Han, Q. Fu, *Macromolecules* **2023**, *56*, 1243–1252; b) J. Wang, X. Lin, D.-L. Zhou, S.-R. Fu, Q. Zhang, H. Bai, D. Han, Q. Fu, *Macromol. Mater. Eng.* **2023**, *308*, 2300076.
- [9] S. Spirk, M. Nieger, F. Belaj, R. Pietschnig, *Dalton Trans.* **2009**, 163–167.
- [10] D. Brzakalski, R. E. Przekop, B. Sztorch, P. Jakubowska, M. Jalbzykowski, B. Marciniak, *Polymer* **2020**, *12*, 2269.
- [11] N. Hurkes, C. Bruhn, F. Belaj, R. Pietschnig, *Organometallics* **2014**, *33*, 7299–7306.
- [12] F. J. Feher, F. Nguyen, D. Soulivong, J. W. Ziller, *Chem. Commun.* **1999**, 1705–1706.
- [13] F. J. Feher, D. Soulivong, A. G. Eklund, *Chem. Commun.* **1998**, 399–400.
- [14] J. C. Furgal, T. Goodson III, R. M. Laine, *Dalton Trans.* **2016**, *45*, 1025–1039.
- [15] Deposition numbers 2300495 (for 2) and 2300496 (for 3) contain the supplementary crystallographic data for this paper. These data are provided free of charge by the joint Cambridge Crystallographic Data Centre and Fachinformationszentrum Karlsruhe Access Structures service.
- [16] a) K.-H. Xiang, R. Pandey, U. C. Pernisz, C. Freeman, *J. Phys. Chem. B* **1998**, *102*, 8704–8711; b) T. Kudo, *J. Phys. Chem. A* **2009**, *113*, 12311–12321.
- [17] P. R. Chinnam, M. R. Gau, J. Schwab, M. J. Zdilla, S. L. Wunder, *Acta Crystallogr. Sect. C* **2014**, *70*, 971–974.
- [18] Y. Sato, R. Hayami, T. Gunji, *J. Sol-Gel Sci. Technol.* **2022**, *104*, 36–52.
- [19] A. R. Bassindale, H. Chen, Z. Liu, I. A. MacKinnon, D. J. Parker, P. G. Taylor, Y. Yang, M. E. Light, P. N. Horton, M. B. Hursthouse, *J. Organomet. Chem.* **2004**, *689*, 3287–3300.
- [20] F. J. Feher, D. Soulivong, F. Nguyen, *Chem. Commun.* **1998**, 1279–1280.
- [21] C. Pakjamsai, Y. Kawakami, *Des. Monomers Polym.* **2005**, *8*, 423–435.
- [22] P. J. Jones, R. D. Cook, C. N. McWright, R. J. Nalty, V. Choudhary, S. E. Morgan, *Appl. Polym. Sci.* **2011**, *121*, 2945–2956.
- [23] G. M. Sheldrick, *Acta Crystallogr.* **2015**, *A71*, 3–8.
- [24] G. M. Sheldrick, *Acta Crystallogr.* **2015**, *C71*, 3–8.
- [25] C. B. Hübschle, G. M. Sheldrick, B. Dittrich, *J. Appl. Crystallogr.* **2011**, *44*, 1281–1284.
- [26] Gaussian 16, Revision C.01, M. J. Frisch, G. W. Trucks, H. B. Schlegel, G. E. Scuseria, M. A. Robb, J. R. Cheeseman, G. Scalmani, V. Barone, G. A. Petersson, H. Nakatsuji, X. Li, M. Caricato, A. V. Marenich, J. Bloino, B. G. Janesko, R. Gomperts, B. Mennucci, H. P. Hratchian, J. V. Ortiz, A. F. Izmaylov, J. L. Sonnenberg, D. Williams-Young, F. Ding, F. Lipparini, F. Egidi, J. Goings, B. Peng, A. Petrone, T. Henderson, D. Ranasinghe, V. G. Zakrzewski, J. Gao, N. Rega, G. Zheng, W. Liang, M. Hada, M. Ehara, K.

- Toyota, R. Fukuda, J. Hasegawa, M. Ishida, T. Nakajima, Y. Honda, O. Kitao, H. Nakai, T. Vreven, K. Throssell, J. A. Montgomery, Jr., J. E. Peralta, F. Ogliaro, M. J. Bearpark, J. J. Heyd, E. N. Brothers, K. N. Kudin, V. N. Staroverov, T. A. Keith, R. Kobayashi, J. Normand, K. Raghavachari, A. P. Rendell, J. C. Burant, S. S. Iyengar, J. Tomasi, M. Cossi, J. M. Millam, M. Klene, C. Adamo, R. Cammi, J. W. Ochterski, R. L. Martin, K. Morokuma, O. Farkas, J. B. Foresman, and D. J. Fox, Gaussian, Inc., Wallingford CT, 2019.
- [27] a) A. D. Becke, *J. Chem. Phys.* **1993**, *98*, 5648–5652; b) C. Lee, W. Yang, R. G. Parr, *Phys. Rev. B* **1988**, *37*, 785–789; c) A. D. Becke, *Phys. Rev. A* **1988**, *38*, 3098–3100.
- [28] a) R. Krishnan, J. S. Binkley, R. Seeger, J. A. Pople, *J. Chem. Phys.* **1980**, *72*, 650–654; b) A. D. McLean, G. S. Chandler, *J. Chem. Phys.* **1980**, *72*, 5639–5648.

Manuscript received: November 2, 2023
 Accepted manuscript online: December 6, 2023
 Version of record online: January 26, 2024

3.3 Synthesis and ligand properties of silsesquioxane-caged phosphite T₇Ph₇P

M. Hunsicker, J. Krebs, M. Zimmer, B. Morgenstern, V. Huch, D. Scheschkewitz, Z. *Anorg. Allg. Chem.* **2024**, 650, e202400068. Copyright © 2024 The Authors.

<https://doi.org/10.1002/zaac.202400068>

This article has been published by Wiley-VCH Verlag GmbH & Co. KGaA as an “Open Access” Article and is licensed under a “Creative Commons Attribution-NonCommercial-NoDerivatives 4.0 International (CC BY-NC-ND-4.0)” License (<https://creativecommons.org/licenses/by-nc-nd/4.0/>).

The article is reproduced with permission of Wiley-VCH Verlag GmbH & Co. KGaA and all authors. No modifications were made. The results are additionally concluded and put into context in Chapter 4.

Author contributions:

Marc Hunsicker: Equal (D. S.): Conceptualization, Lead: Data curation, Formal analysis, Investigation, Methodology, Validation, Visualization, Writing and Editing.

Johannes Krebs: Supporting: Investigation, Data Curation and Formal Analysis of Ph₇Si₇O₁₂P-B(Ph)₃ (Bachelor Thesis).

Michael Zimmer: Lead: CP/MAS-NMR analysis.

B. Morgenstern: Lead: X-ray analysis.

V. Huch: Supporting: X-ray analysis of Ph₇Si₇O₁₂P-B(Ph)₃.

David Scheschkewitz: Lead: Conceptualization, Project administration, Supervision, Acquisition of Funding and Resources, Supporting: Methodology, Writing – Review and Editing.

DOI: 10.1002/zaac.202400068

Synthesis and Ligand Properties of Silsesquioxane-Caged Phosphite T_7Ph_7P

Marc Hunsicker,^[a] Johannes Krebs,^[a] Michael Zimmer,^[a] Bernd Morgenstern,^[b] Volker Huch,^[a] and David Scheschkewitz*^[a]

Dedicated to Professor Michael Veith on occasion of his 80th birthday

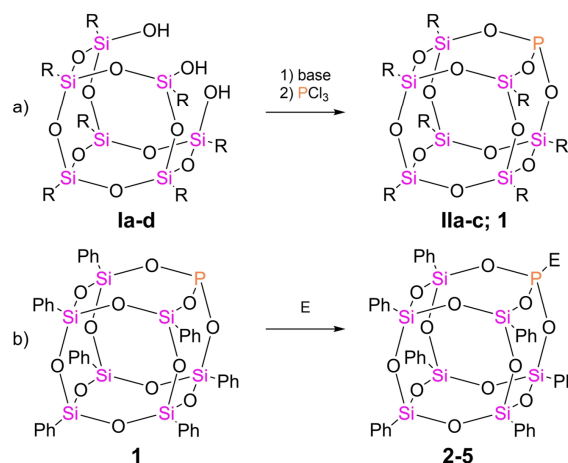
The synthesis of the phosphorus-capped heptaphenylsilsesquioxane T_7Ph_7P is reported. We show that, unlike previous examples, it readily forms Lewis acid-base adducts with boranes of different steric demand and the $FeCO_4$ fragment. All complexes were characterized by multinuclear NMR and IR spectroscopy in solution and the solid state. The molecular

structures of the adducts with BPh_3 and $B(C_6F_5)_3$ were determined from XRD suitable single crystals. The relative conformation of the Ph and C_6F_5 rings in $T_7Ph_7P-B(C_6F_5)_3$ suggests favorable π -interactions, stabilizing the adducts to such a degree that attempts to activate H_2 or CO_2 were unsuccessful.

Introduction

Trisubstituted phosphanes and phosphite esters are ubiquitous as reagents in organic chemistry,^[1] and as ligands in transition metal complexes.^[2] The inherent Lewis basicity associated to the lone pair of electrons leads to the facile formation of adducts with suitable electron deficient Lewis acids.^[3] The strength of this donor-acceptor interaction can be tuned by the electronic nature of the substituents. Framework phosphanes with the donor-center in an oligocyclic bridgehead position can offer additional control of the ligand properties due to their structural rigidity.

In this context, the incompletely condensed $T_7R_7(OH)_3$ silsesquioxanes of type I have proven to be valuable precursors for the incorporation of various heteroelements into the cubic framework.^[4] Feher and coworkers reported the synthesis of the heterosilsesquioxane **IIa** in which a phosphorus atom closes the T_7Cy_7 backbone (Scheme 1).^[5] So far only limited information is available on its coordination chemistry and that of related



Scheme 1. a) Corner capping of partially condensed silsesquioxanes **Ia-c** (a: R=Cy, b: R=Oct, c: R=Bu d: R=Ph) with PCl_3 to heterosilsesquioxane cages with a phosphorus vertex **IIa,c**,^[5,8,11] and **1** (this work). b) Treatment of the phosphorus capped heptaphenylsilsesquioxane **1** with various Lewis acids generates Lewis acid-base adducts **2** to **5** (**2**: E= BPh_3 ; **3**: E= $B(C_6F_5)_3$; **4**: E= BCl_3 ; **5**: E= $Fe(CO)_4$).

[a] M. Hunsicker, J. Krebs, Dr. M. Zimmer, V. Huch, Prof. Dr. D. Scheschkewitz
Krupp-Chair of General and Inorganic Chemistry
Saarland University
66123 Saarbrücken, Germany
E-mail: scheschkewitz@mx.uni-saarland.de

[b] Dr. B. Morgenstern
Service Center X-Ray Diffraction
Saarland University
66123 Saarbrücken, Germany

Supporting information for this article is available on the WWW under <https://doi.org/10.1002/zaac.202400068>

© 2024 The Author(s). Zeitschrift für anorganische und allgemeine Chemie published by Wiley-VCH GmbH. This is an open access article under the terms of the Creative Commons Attribution Non-Commercial NoDerivs License, which permits use and distribution in any medium, provided the original work is properly cited, the use is non-commercial and no modifications or adaptations are made.

compounds: **IIa** reportedly forms a 1:1 adduct with $AlMe_3$ according to NMR spectroscopic evidence, although the lack of suitable single crystals prevented full characterization. The steric demand of the cyclohexyl groups^[5,6] may prevent coordination of **IIa** to transition metal centers as it did not induce catalytic activity when added to $[Rh(acac)(CO)_2]$ under hydroformylation conditions.^[7] In contrast, the heptaisooctyl-substituted **IIb** reported by Marciniec and coworkers acted as inhibitor towards Karstedt's catalyst in hydrosilylation reactions and was proven to coordinate to the platinum center by ^{31}P NMR.^[8]

In the context of the functionalization of polyhedral silsesquioxanes,^[9] we explored their interconnection by donor/acceptor interactions. In particular, we were interested in the phenyl-substituted version of **II** in view of its intermediate steric bulk and the somewhat reduced electron density^[10] compared to the cyclohexyl derivative **IIa**. Herein, we report on the synthesis of the phenyl-substituted cage phosphite T_7Ph_7P and its conversion to Lewis pairs with several boron-centered Lewis acids as well as with the iron tetracarbonyl fragment.

Results and Discussion

Synthesis. In adaption of the reported corner capping reaction of the partially condensed cyclohexyl-substituted **Ia**, $T_7Ph_7(OH)_3$ **Id** was treated with triethylamine and a slight excess of PCl_3 (1.1 eq) in toluene at 0 °C. Filtration after five minutes of stirring followed by removal of the volatiles and washing with minimal amounts of toluene yielded the colorless phosphite T_7Ph_7P **1** in 41 % yield. Phosphite T_7Ph_7P **1** gives rise to a ^{31}P NMR singlet at 86.3 ppm, in C_6D_6 almost identical with those of **IIa** (86.1 ppm),^[5] **IIb** (84.6 ppm)^[8] and **IIc** (84.7 ppm).^[11] The phenyl groups of **1** produce two uniform multiplets in the 1H NMR spectrum in C_6D_6 between 7.85 to 7.79 ppm and 7.15 to 7.00 ppm.

The alternative use of $T_7Ph_7(ONa)_3$ results in the formation of several unidentified byproducts with overlapping 1H NMR resonances in the aromatic region, unlike in case of $T_7Oct_7(ONa)_3$ from which Marciniec et al. obtained near-quantitative yields of T_7Oct_7P .^[8] These byproducts give rise to several ^{31}P NMR signals between 180 and –21 ppm after stirring overnight (see Figure S36). Resonances at –19 and –26 ppm were reported by Copéret et al. for the grafting of T_7Bu_7P to OH-terminated silica and rationalized by the formation of phosphonates through OH transfer from the surface to the P center.^[11]

In an initial attempt to elucidate the geometric constraints between the phosphite and a boron-centred Lewis acid, we prepared Lewis acid-base complex **2** by treatment of T_7Ph_7P with a slight excess of triphenylborane in toluene. Stirring for 35 minutes at room temperature and isolation of the resulting precipitate by filtration yields the colorless product in 51 % yield (reaction of Ph_3BPCl_3 adduct with $T_7Ph_7(OH)_3$ resulted in much lower yields of **2**). 1H NMR spectra confirm a new species, although the ^{11}B and ^{31}P NMR spectra in C_6D_6 do not show any signals (*vide infra*).

Next, tris(pentafluorophenyl)borane was used as Lewis acid component to increase acidity and steric demand of the borane in the hope to induce frustration. Reaction of a 1 : 1 stoichiometric ratio of T_7Ph_7P **1** and $B(C_6F_5)_3$ in toluene for 30 minutes, however, results in the formation of a new adduct as well, as evidenced by its uniform 1H NMR spectrum and ^{11}B and ^{31}P NMR signals at –14.9 ppm and 37.1 ppm, respectively, in C_6D_6 solution. The adduct **3** was isolated by crystallization at room temperature from a hot-saturated toluene solution in 42 % yield. In order to increase steric demand of the Lewis acid even more, a mixture of T_7Ph_7P and tris(4-bromo-2,3,5,6-tetramethylphenyl)borane in toluene was stirred at room temperature,

and indeed no adduct formation took place according to NMR monitoring.

Initial attempts to obtain the boron trichloride adduct $T_7Ph_7P \cdot BCl_3$ **4** by combining toluene solutions of BCl_3 and **1** led to inseparable mixtures with about 35 % of a major product (^{11}B NMR at 1.4 ppm). In an improved procedure, careful layering a concentrated toluene solution of **1** with a stock solution of BCl_3 in toluene affords **4** as a microcrystalline colorless product in 43 % yield.

Stirring a twofold excess of $Fe_2(CO)_9$ (in order to assure complete conversion) and the cage phosphite **1** in toluene results in the immediate formation of a new species at room temperature as well. The $Fe(CO)_4$ adduct **5** shows a single resonance at 124.1 ppm in the ^{31}P NMR spectrum and is thus downfield shifted by $\Delta\delta = 37.8$ ppm. Various alkoxy- and amino-substituted phosphite iron carbonyl complexes (in CH_2Cl_2 or $CDCl_3$) showed ^{31}P NMR signals, downfield shifted by $\Delta\delta$ between 20.2 and 55.1 ppm compared with the free ligands.^[12] The adduct **5** was isolated by extraction from the dried product mixture with toluene in 47 % yield. Unlike in case of **2** and **3**, single crystals of **5** could not be obtained despite crystallization attempts from a saturated toluene solution at room temperature, or from storing slightly more diluted solutions at reduced temperatures between +4 °C and –27 °C.

Crystal structure discussion. Single crystals of the borane adducts **2** and **3** suitable for XRD were obtained from toluene at 4 °C and room temperature, respectively.^[13] The free phosphite ligand **1** and its $Fe(CO)_4$ adduct **5** precipitated in amorphous form, the microcrystals of the BCl_3 adduct **4** proved unsuitable for XRD.

The molecular structures of adducts **2** and **3** in the solid state confirm the anticipated constitutions as borane adduct (Figure 1, left). Both structures show approximate C_3 symmetry. Notably, while the B-bonded phenyl groups of **2** are staggered with respect to the adjacent phenyl groups of the cage phosphite without clear-cut stabilizing interactions, the perfluorinated phenyl groups of **3** adopt an almost eclipsed conformation (Figure 1, right). The centroids of the phenyl and pentafluorophenyl groups of adduct **3** are 4.1794(6) Å apart on average, which is significantly farther than the corresponding distance calculated for the π -stacked benzene-dimer (3.914 Å),^[14] but intriguingly close to those in Lewis adducts of the type $Ph_3E \cdot B(C_6F_5)_3$ with similar eclipsed conformations ($E=P$: 4.169 Å, As : 4.215 Å).^[15a,b] The authors concluded a certain attractive interaction between the aromatic rings in the arsenic case, which was supported by DFT calculations.^[15b] The average angle between the planes of the C_6H_5 and C_6F_5 rings of 7.8(4)° in **3** is much closer to coplanarity than in the abovementioned phosphorus and arsenic Lewis adducts with angles of 24.49° (P) and 22.64° (As). We tentatively attribute the near-coplanarity in **3** to the much smaller distortions from the idealized tetrahedral structure of the Lewis base required for effective π stacking. A theoretical study investigating non covalent interactions (NCI) in several Lewis adducts and FLP systems also found weakly stabilizing effects of π stacking between the aromatic rings in $Ph_3P \cdot B(C_6F_5)_3$.^[15c] Stephan et al. reported parallel alignment of phenyl and C_6F_5 groups in an ethylene bridged P–B adduct and interpreted it as π stacking effect.^[15d]

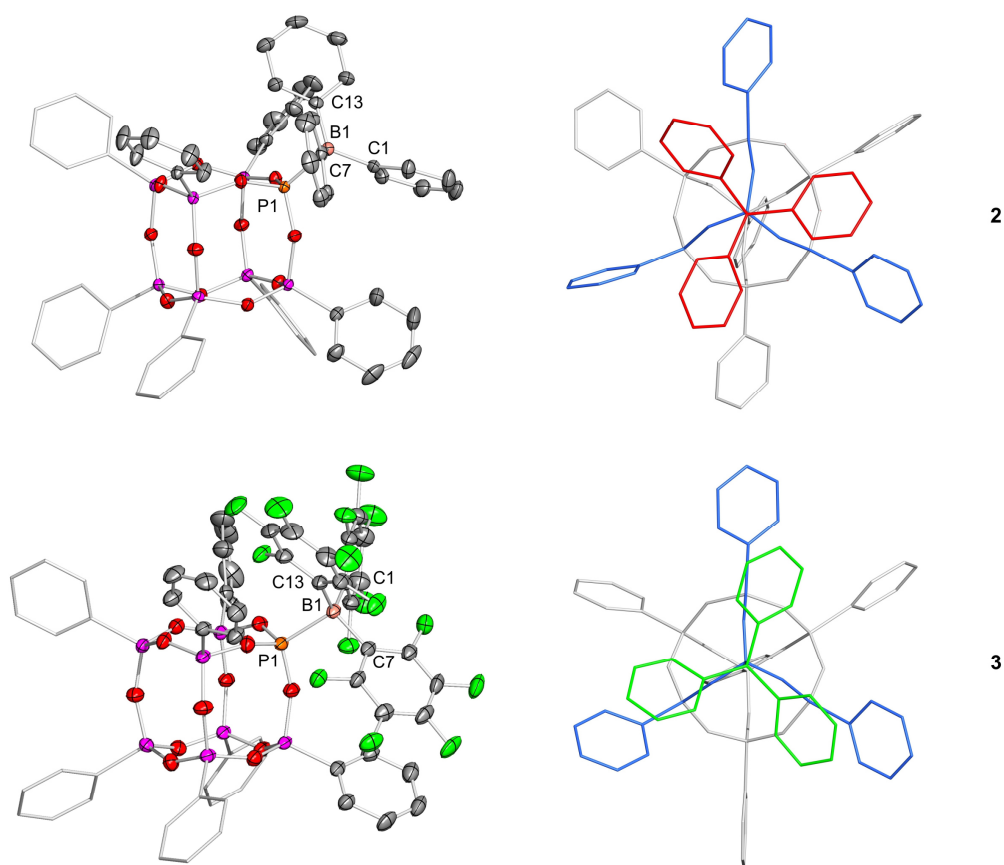


Figure 1. Left: molecular structures of the BPh_3 adduct **2** and $\text{B}(\text{C}_6\text{F}_5)_3$ adduct **3** in the solid state. Co-crystallized solvent molecules, disordered phenyl groups and hydrogen atoms are omitted for clarity. Thermal ellipsoids at 50% probability. Right: top-views of BPh_3 adduct **2** and $\text{B}(\text{C}_6\text{F}_5)_3$ **3** down the boron-phosphorus bonds. **Blue:** phenyl groups on the first substituents attached to phosphorus in both complexes. **Red:** phenyl groups of BPh_3 . **Green:** aromatic rings of the C_6F_5 moieties on boron. Selected bond lengths and angles for **2**: P1-B1: 1.9604(2) Å, P1-O1: 1.5636(1) Å, P1-O4: 1.5652(1) Å, P1-O8: 1.5625(1) Å, B1-C1: 1.629(2) Å, B1-C7: 1.632(2) Å, B1-C13: 1.626(2) Å, O1-P1-O4: 106.34(6)°, O8-P1-O4: 105.05(6)°, O8-P1-O1: 105.39(6)°, C1-B1-C7: 114.62(1)°, C13-B1-C7: 112.54(1)°, C13-B1-C1: 113.47(1)°. Selected bond lengths and angles for **3**: P1-B1: 1.994(4) Å, P1-O6: 1.547(2) Å, P1-O10: 1.545(2) Å, P1-O11: 1.550(2) Å, B1-C1: 1.638(5) Å, B1-C7: 1.638(5) Å, B1-C13: 1.641(5) Å; O6-P1-O11: 106.32(1)°, O10-P1-O11: 106.81(1)°, O10-P1-O6: 107.25(1)°, C1-B1-C7: 114.0(3)°, C1-B1-C13: 112.3(3)°, C7-B1-C13: 115.0(3)°.

The staggered conformation of the triphenylborane adduct **2** with angles of $71.7(6)^\circ$ on average between the planes of adjacent phenyl groups of the PPh_3 and the cage phosphite moieties is best described as a threefold T-shaped interaction between electronically similar benzene rings. The average distance between the centroids of 4.9654(7) Å is substantially longer than in **3** and similar to the distance in the T-shaped benzene dimer (4.913 Å).^[14] The boron-phosphorus bond lengths of **2** and **3** are at the short end of the range of typical Lewis-acid base adducts (for **2**: 1.9604(2) Å, for **3**: 1.994(4) Å). In comparison, the reported $\text{Ph}_3\text{P}-\text{B}(\text{C}_6\text{F}_5)_3$ ^[15a] and $(\text{MeNCH}_2\text{CH}_2)_3\text{N}-\text{B}(\text{C}_6\text{F}_5)_3$ ^[15f] adducts display P–B bond lengths of 2.180 Å, and 2.096 Å, respectively. Phosphite-borane adducts without aromatic substituents at phosphorus also feature significantly longer P–B distances, for instance 2.0209 Å in $(\text{MeO})_3\text{P}-\text{B}(\text{C}_6\text{F}_5)_3$.^[15e]

Due to a lack of single crystals of the free ligand **1**, an unbiased comparison of the steric shielding provided by the substituents with that in $\text{T}_7\text{Cy}_7\text{P}$ **IIa** is difficult. Nonetheless, some trends can be derived from the available solid state structures. Feher and coworkers determined a Tolman cone angle of $\sim 167^\circ$,^[5] by using solely the H–P–L angles as basis for the calculation. A more refined method was introduced shortly thereafter by Mingos et al.,^[16] in which the van der Waals radius of the hydrogen atoms is accounted for when determining the P–L–H angles. According to the latter approach, Tolman cone angles of $\theta = 181.1^\circ$ for **2** and $\theta = 174.3^\circ$ for **3** are obtained from solid state structures truncated to the free $\text{T}_7\text{Ph}_7\text{P}$ ligand. Both cone angles are smaller than that of **IIa** ($\theta = 189^\circ$) recalculated by the same method. As discussed by Sigman and Doyle et al.,^[17] the reactivity of a (phosphine or phosphite) ligand can only be vaguely rationalized on grounds of the Tolman

cone angle. The percent buried volume $\%V_{\text{bur}}^{[18a]}$ parameter (determined with the Sambvca open-source application^[18b] using a distance of 2.28 Å between the phosphorus atom and the center of the putative sphere) is larger for **IIa** (23.8%) than for the phosphite ligands of **2** (23.0%) and **3** (22.2%). This confirms the general trend of the Tolman cone angles and is keeping with other distance values in the $\%V_{\text{bur}}$ calculation, such as the 2.0 Å chosen by Nolan and coworkers,^[18a] albeit at inherently larger values of $\%V_{\text{bur}}$. Overall, the change from cyclohexyl to phenyl, and from phenyl to pentafluorophenyl is 3–4% irrespective of the steric parameter, reflecting the anticipated higher steric bulk of the cyclohexyl substituent and the different conformations of the aromatic groups in **2** and **3**.

NMR spectroscopy. In C_6D_6 solution, the free cage-phosphite **1** gives rise to a diagnostic ^{31}P NMR signal emerging as a singlet at 86.3 ppm along with a satellite doublet with a coupling constant of 37.2 Hz attributed to coupling to the silicon atoms of the silsesquioxane. This compares well with the reported cyclohexyl and isooctyl-substituted congeners (86.1 ($^2J_{\text{P,Si}} = 35.8$ Hz) and 84.6 ppm, respectively).^[5,8] The corresponding CP/MAS spectrum shows two signals of approximately equal intensity at 83.8 and 82.1 ppm, most likely because of at least two symmetry-independent environments in the solid state as previously discussed by Erker et al. for boron-phosphorus frustrated Lewis pairs.^[20] The BPh_3 (**2**) and BCl_3 complexes (**4**) do not show ^{31}P NMR signals in solution, presumably due to coalescence phenomena of temperature dependent processes. Unfortunately, the low solubility of both adducts was prohibitive of VT NMR studies that could have shed further light on this aspect. In the ^{31}P CP/MAS NMR spectra, however, the BPh_3 adduct **2** exhibits a broad signal at 48.1 ppm (full width at half maximum FWHM = 340 Hz, Figure S9), and the BCl_3 adduct **4** a quartet centered at 8.3 ppm, in accordance with the $I = 3/2$ spin of the ^{11}B nucleus. Further signals of minor intensity are strongly concealed by overlap but may be attributable to the ^{10}B isotopomer ($I = 3$) and/or impurities (Figure S26 and S27). The estimated coupling constant of $^1J_{\text{P,B}} \sim 300$ Hz suggests an exceptionally strong donor-acceptor bond in **4** as a result of relatively small steric encumbrance.

The $\text{B}(\text{C}_6\text{F}_5)_3$ and $\text{Fe}(\text{CO})_4$ adducts **3** and **5** in C_6D_6 show ^{31}P NMR resonances in C_6D_6 solution at 37.3 (broad quartet, $^1J_{\text{P,B}} = 150$ Hz) and 124.1 (singlet with a satellite doublet, $^2J_{\text{P,Si}} = 27.4$ Hz) ppm, respectively. The solid-state ^{31}P NMR isotropic shifts of the adducts **3** and **5** match the solution data reasonably well (**3**: 32.8 ppm, $^1J_{\text{P,B}} = 150$ Hz; **5**: 120.2 ppm). The $^1J_{\text{P,B}}$ coupling constant of about 150 Hz (**3**) is comparable to the $\text{B}(\text{C}_6\text{F}_5)_3$ adduct of Verkade's base ($^1J_{\text{P,B}} = 130$ Hz).^[15f] The ^{11}B NMR spectrum in C_6D_6 of **3** shows a broad singlet at -14.9 ppm, while **4** displays a doublet at 1.4 ppm with a $^1J_{\text{B,P}} = 300$ Hz, the same as observed in the ^{31}P CP/MAS spectrum. In solution, no signal for the BPh_3 adduct **2** could be observed, whereas in the solid state two singlets at -4.0 and -7.3 ppm are found with no discernible splitting due to coupling with the ^{11}B nucleus. As in case of **1**, the occurrence of two signals is most likely due to differing solid state environments, as the FWHM of the ^{31}P signal in the solid state is clearly insufficient to conceal a $^1J_{\text{P,B}}$ coupling constant of 420 Hz (corresponding to $\Delta\delta = 3.3$ ppm of the two CP-MAS ^{11}B NMR signals of **2**). The ^{13}C NMR spectrum of the iron carbonyl adduct **5** shows two singlets at 213.2 and 213.0 ppm,

in agreement with the corresponding ^{13}C CP/MAS isotropic shift at 211.4 ppm (broad singlet).

Only the $\text{B}(\text{C}_6\text{F}_5)_3$ and FeCO_4 adducts **3** and **5** are sufficiently soluble in C_6D_6 for the acquisition of ^{29}Si NMR spectra in solution. For **1**, **2**, and **4**, ^{29}Si CP/MAS solid state NMR spectra were obtained instead. The silicon atoms of all compounds give rise to broad, overlapping resonances between -77.1 and -83.2 ppm in the expected region of phenylsubstituted T_7 silsesquioxane backbones without discernible indications for 2J coupling to the ^{31}P nucleus. Phosphite **1**, $\text{B}(\text{C}_6\text{F}_5)_3$ adduct **3** and FeCO_4 adduct **5** give rise to two isotropic shifts in a ratio of 2:1 each, BPh_3 adduct **2** displays three signals (in a ratio of 1:1:2) and BCl_3 adduct **4** shows two barely resolved signals in approximate 1:1 ratio. In contrast, the $\text{B}(\text{C}_6\text{F}_5)_3$ adduct **3** displays three signals at -76.7 , -77.6 and -80.1 ppm (3:1:3) in C_6D_6 solution, the latter as a doublet with a coupling constant of 27.9 Hz, which is again attributed to 2J coupling to phosphorus. The presence of a doublet was furthermore confirmed by a second ^{29}Si NMR experiment at a frequency of 59.62 MHz (before: 79.49 MHz), which produces a $^2J_{\text{P,Si}}$ coupling constant of 28.2 Hz (see Figures S15 to S17). The iron carbonyl adduct **5** shows two singlets at -76.3 , -77.4 and a doublet at -81.3 ppm (3:1:3, $^2J_{\text{Si,P}} = 27.9$ Hz) in C_6D_6 .

The IR spectrum of **5** (ATR) shows a distinct broad signal at 1938 cm^{-1} , and two smaller bands at 1985 and 2064 cm^{-1} for the carbonyl groups, which are at slightly higher wavenumbers compared to $(\text{PhO})_3\text{P}-\text{Fe}(\text{CO})_4$ ($\nu = 1961, 1996, 2070\text{ cm}^{-1}$, pentane solution; $1945, 1985, 2051\text{ cm}^{-1}$ (chloroform solution))^[12,19a] and in reasonable agreement with IR bands reported for $\text{Ph}_3\text{P}-\text{Fe}(\text{CO})_4$ ($1945, 1979, 2044\text{ cm}^{-1}$, heptane solution).^[19b]

Reactivity. In more recent years it was discovered that even classical Lewis adducts may exhibit FLP reactivity.^[15f] Based on computations, it has been proposed that certain adducts should even be more reactive than FLPs.^[21] We therefore investigated the $\text{B}(\text{C}_6\text{F}_5)_3$ adduct **3** and the non-coordinated mixture of $\text{T}_7\text{Ph}_7\text{P}$ and tris(4-bromo-2,3,5,6-tetramethylphenyl)borane with regards to small molecule activation. As adduct **3** contains the most Lewis acidic borane and features the smallest $^1J_{\text{P,B}}$ coupling constant, we treated it with dihydrogen, carbon dioxide and phenylacetylene to gain insight into potential FLP type reactivity. Unfortunately, the adduct proved to be too unreactive; even at elevated temperatures of up to 120°C no reaction took place in either case. From a thermodynamic point of view, even small structural deviations from reactive FLPs can inhibit reactivity completely.^[22] The apparent π interactions between the aromatic systems may stabilize the adduct to a degree that completely prevents any FLP reactivity. Even Lewis pairs with a relatively small tendency towards dissociation were shown to activate phenylacetylene, such as $\text{Ph}_3\text{P}-\text{B}(\text{C}_6\text{F}_5)_3$.^[23] Nonetheless, a mixture of **1** and tris(4-bromo-2,3,5,6-tetramethylphenyl)borane resulted in the consumption of the phosphite, when treated with dihydrogen. However, the ^1H NMR spectrum in C_6D_6 shows an intractable mixture of signals in the aromatic region, whereas the methyl substituents of the duryl groups and the ^{11}B NMR resonance of the starting material remain unchanged. Signals between -14 and -20 ppm in the ^{31}P NMR spectrum suggest the presence of similar (by-) products to the synthesis of phosphite **1**. The obtained spectroscopic information does not allow for any conclusions on the nature of the product(s). In this case, either the phosphites

donor ability is too low due to the aforementioned electron-withdrawing effect of the T_7 backbone, or the boron center is too sterically encumbered to engage in FLP reactivity. Consequently, phosphite **1** does also not react with small molecules on its own in a straightforward manner, as had been observed with more electron-rich phosphines.^[24]

Conclusions

We presented first insights into the donor abilities of phosphite T_7Ph_7P **1** and the properties of adducts with boron-centered Lewis acids. Despite large ligand cone angles, the phenyl-substituted **1** coordinates to Lewis acidic boranes of different steric demand, unlike the previously reported cyclohexyl derivative. The short bond length of $B(C_6F_5)_3$ adduct **3** (1.994(4) Å) indicates that even larger Lewis acids may be accommodated, suggesting the propensity of **1** for a rich coordination chemistry, unlike the cyclohexyl substituted **IIa**. The inability of adduct **3** to engage in FLP type chemistry is tentatively explained by the attractive π stacking between the aromatic substituents of the ligand and the Lewis acid. Cage phosphite **1** does not form a Lewis adduct with tris(4-bromo-2,3,5,6-tetramethylphenyl)borane, indicating a latent FLP in solution yet no according reactivity was observed.

Experimental Section

General. All manipulations were conducted under a protective argon atmosphere using standard Schlenk techniques or a glovebox. Non-chlorinated solvents were dried over Na/benzophenone (in the presence of tetraglyme in case of aromatic and aliphatic solvents) and distilled under argon atmosphere. Deuterated solvents were dried by reflux over potassium and distilled under argon atmosphere prior to use. Chlorinated deuterated solvents were refluxed and distilled over P_4O_{10} and stored under Argon atmosphere. NMR spectra were recorded on either a Bruker Avance III 300 NMR spectrometer (1H : 300.13 MHz, ^{13}C : 75.46 MHz, ^{29}Si : 59.63 MHz, ^{19}F : 282 MHz) or a Bruker Avance III 400 spectrometer (1H : 400.13 MHz, ^{11}B : 128.38 MHz, ^{13}C : 100.61 MHz, ^{29}Si : 79.49 MHz, ^{31}P : 161.98 MHz) at 300 K. Melting points were measured in sealed NMR tubes under Ar atmosphere. Elemental analysis was carried out with an elemental analyzer Leco CHN-900. $T_7Ph_7(OH)_3$ was obtained from Hybrid Plastics, Inc. and dried under vacuum prior to use. Phosphorus trichloride was obtained from commercial sources and distilled prior to use. Tris(pentafluorophenyl)borane was obtained from BLD Pharm. Boron trichloride was obtained from Praxair Deutschland and condensed into toluene before use. Triphenylborane was obtained from abcr and used as received. Diiron nonacarbonyl was obtained from Sigma Aldrich and used as received. Triethylamine was obtained from Sigma Aldrich and distilled over CaH_2 prior to use.

Preparation of T_7Ph_7P **1.** A suspension of 10.35 g of $T_7Ph_7(OH)_3$ in 100 mL toluene is treated with 4.65 mL of NEt_3 and stirred for 10 minutes at room temperature. Then it is cooled down with an ice-water bath for 20 minutes and 1.1 mL of PCl_3 are added. The mixture is stirred for five minutes in the ice bath, then filtered into an equally cooled flask. Another 20 mL of toluene are used to wash the residue. The resulting filtrate is again washed with 20 mL toluene. The mixture is evaporated to dryness to obtain 4.40 g (41%) of a colorless powder (m.p. 200 °C, decomposition). 1H NMR (400.13 MHz, C_6D_6 , 300 K) 7.85–7.79 (m, 14H, *m*-Ar-H), 7.15–7.00 (m, 21H, *o*,*p*-Ar-H, overlapping with toluene H). ^{31}P NMR (161.98 MHz, C_6D_6 , 300 K) 86.3 (s, $^2J_{P-Si}$ = 37.2 Hz for ^{29}Si satellites, (SiO) $_3P$) ppm. CP/MAS ^{29}Si NMR (79.49 MHz, 13 kHz, 300 K)

–77.7, –83.2 (each br, (RO) $_3Si$ -Ar) ppm. CP/MAS ^{31}P NMR (161.98 MHz, 13 kHz, 300 K) 83.8, 82.1 (each br, (SiO) $_3P$) ppm. **Elemental Analysis:** Calc. for $C_{42}H_{35}O_{12}PSi_7$: C: 52.59, H: 3.68, Found: C: 54.90, H: 4.12.

Preparation of T_7Ph_7P -BPh $_3$ **2:** A mixture of 406 mg of T_7P and 117 mg of BPh $_3$ in 5 mL toluene is stirred for 35 minutes at room temperature. The resulting colorless precipitation is separated from the volatiles by filtration and purified by washing with 2 mL of toluene. Drying the product under reduced pressure yields 259 mg (51%) of a colorless solid (m.p. 231–233 °C, decomposition). 1H NMR (400.13 MHz, C_6D_6 , 300 K) 7.81–7.75 (m, 14H, *m*-Ar-H), 7.47–7.45 (m, 6H, *m*-Ar-H), 7.21–7.18 (m, 9H, *o*,*p*-Ar-H, overlapping with C_6D_6), 7.13–6.96 (m, 21H, *o*,*p*-Ar-H, overlapping with toluene-H) ppm. ^{11}B NMR (128.38 MHz, C_6D_6 , 300 K) no signal observed. ^{31}P NMR (161.98 MHz, C_6D_6 , 300 K) no signal observed. CP/MAS ^{11}B NMR (128.38 MHz, 13 kHz, 300 K) –4.0, –7.3 (each s, *P*-BPh $_3$) ppm. CP/MAS ^{13}C NMR (100.61 MHz, 13 kHz, 300 K) 149.0, 138.3, 135.6, 133.3, 131.2, 128.0, 125.5, 122.6 (each s, Ar-C), 47.4, 9.5 ppm. CP/MAS ^{29}Si NMR (79.49 MHz, 13 kHz, 300 K) –77.1, –78.2, –80.4 (each br, (RO) $_3Si$ -Ar) ppm. CP/MAS ^{31}P NMR (161.98 MHz, 13 kHz, 300 K) 48.1 (br, (SiO) $_3P$ -B) ppm. **Elemental Analysis:** Calc. for $C_{60}H_{50}BO_{12}PSi_7$: C: 59.98, H: 4.20, Found: C: 60.40, H: 4.60.

Preparation of T_7Ph_7P -B(C $_6F_5$) $_3$ **3.** A suspension of 458 mg of T_7Ph_7P and 273 mg tris(pentafluorophenyl)borane in 5 mL of toluene is stirred for 30 minutes at room temperature, then it is gently heated until fully dissolved. Standing at room temperature overnight affords colorless crystals, whose yield is increased by keeping the flask at 4 °C for three days. Separation of the crystals from the mother liquor yields 292 mg (42%) of a colorless solid (m.p.: above 300 °C, partial decomposition). 1H NMR (400.13 MHz, C_6D_6 , 300 K) 7.84–7.79 (m, 6H, *m*-Ar-H), 7.77–7.74 (m, 2H, *m*-Ar-H), 7.66–7.62 (m, 6H, *m*-Ar-H), 7.14–7.003 (m, 17H, *o*,*p*-Ar-H, overlapping with toluene-H), 6.996–6.94 (m, 6H, *o*,*p*-Ar-H). ^{11}B NMR (128.38 MHz, C_6D_6 , 300 K) –14.9 (s, *P*-B(C $_6F_5$) $_3$) ppm. ^{13}C NMR (100.61 MHz, C_6D_6 , 300 K) 134.3, 134.2, 133.8, 132.6, 132.0, 131.8, 128.7, 128.5 (overlap with toluene), 128.13, 125.49, 125.46 (each s, Ar-C) ppm. ^{19}F NMR (282 MHz, C_6D_6 , 300 K) –131.3 (s, *o*-Ar-F), –155.6 (dtr, *J* = 21 Hz, 6 Hz, *p*-Ar-F), –163.8 (dtr, *J* = 23 Hz, *J* = 6 Hz, *m*-Ar-F) ppm. ^{29}Si NMR (79.49 MHz, C_6D_6 , 300 K) –76.7, –77.6 (each s, (SiO) $_3Si$ -Ar), –80.1 (d, $^2J_{Si-P}$: 27.9 Hz, (PO)(SiO) $_2Si$ -Ar) ppm. ^{31}P NMR (161.98 MHz, C_6D_6 , 300 K) 37.1 (br) ppm. CP/MAS ^{29}Si NMR (79.49 MHz, 13 kHz, 300 K) –78.3, –82.1 (each br, (RO) $_3Si$ -Ar) ppm. CP/MAS ^{31}P NMR (161.98 MHz, 13 kHz, 300 K) 32.7 (overlapping q, $^1J_{P-B}$: 150 Hz, (SiO) $_3P$ -B) ppm. **Elemental Analysis:** Calc. for $C_{60}H_{35}BF_{15}O_{12}PSi_7$: C: 48.98, H: 2.40, Found: C: 50.50, H: 2.62.

Preparation of T_7Ph_7P -BCl $_3$ **4.** A stock solution of 3 molar boron trichloride in toluene was added slowly to a solution of 348 mg T_7Ph_7P in 18 mL of toluene with a layer of 2 mL toluene in between without stirring. Standing overnight afforded small crystals along with precipitation, which were separated from the volatiles via filtration and purified by washing with another 5 mL of toluene. 169 mg (43%) of a colorless solid were obtained (m.p.: 160 °C, decomposition). 1H NMR (400.13 MHz, C_6D_6 , 300 K) 8.01–7.98 (m, 6H, *m*-Ar-H), 7.80, 7.77 (m, 2H, *m*-Ar-H), 7.61–7.58 (m, 6H, *m*-Ar-H), 7.14–6.94 (m, 21H, *o*,*p*-Ar-H, overlap with toluene). ^{11}B NMR (128.38 MHz, C_6D_6 , 300 K) 1.4 (d, $^1J_{P-B}$ = 301 Hz *P*-BCl $_3$) ppm. CP/MAS ^{13}C NMR (100.61 MHz, 13 kHz, 300 K) 133.5, 131.6, 127.7, 125.0 (each s, Ar-C) ppm. CP/MAS ^{29}Si NMR (79.49 MHz, 13 kHz, 300 K) –78.3, –79.5 (each br, (RO) $_3Si$ -Ar) ppm. CP/MAS ^{31}P NMR (161.98 MHz, 13 kHz, 300 K) 8.3 (overlapping q, $^1J_{P-B}$: 310 Hz, (SiO) $_3P$ -B) ppm. **Elemental Analysis:** Calc. for $C_{42}H_{35}BCl_3O_{12}PSi_7$: C: 46.86, H: 3.28, Found: C: 49.72, H: 3.82.

Preparation of T_7Ph_7P -FeCO $_4$ **5.** A mixture of 301 mg of T_7Ph_7P and 248 mg Fe $_2$ (CO) $_9$ is stirred in 8 mL of toluene for two hours at room temperature. The volatiles are evaporated under reduced pressure using a warm water bath. The mixture is filtered with 6 mL toluene and the residue washed with another 4 mL. The resulting dark brown filtrate is reduced to dryness to obtain 168 mg (47%) of an equally dark brown solid (m.p.: 180 °C, decomposition). 1H NMR (400.13 MHz, C_6D_6 , 300 K)

8.02–7.99 (m, 6H, *m*-Ar-H), 7.80–7.76 (m, 2H, *m*-Ar-H), 7.76–7.73 (m, 6H, *m*-Ar-H), 7.14–6.98 (m, 21H, *o,p*-Ar-H, overlap with toluene). ¹³C NMR (100.61 MHz, C₆D₆, 300 K) 213.2, 213.0 (each s, Fe-CO), 134.52, 134.47, 132.3, 131.7, 131.6, 129.5, 128.9, 128.7, 128.6, 128.54, 128.48, 127.51, 127.49 (each s, Ar-C) ppm. ²⁹Si NMR (79.49 MHz, C₆D₆, 300 K) –76.3, –77.4 (each s, (SiO)₃Si-Ar), –81.3 (d, ²J_{P,Si} = 27.9 Hz, (PO)(SiO)₃Si-Ar) ppm. ³¹P NMR (161.98 MHz, C₆D₆, 300 K) 124.1 (s, ²J_{P,Si} = 27.4 for ²⁹Si satellites, (SiO)₃P-Fe) ppm. CP/MAS ¹³C NMR (100.61 MHz, 13 kHz, 300 K) 211.4 (br, Fe-CO), 133.3, 127.6 (each br, Ar-C) ppm. CP/MAS ²⁹Si NMR (79.49 MHz, 13 kHz, 300 K) –77.5, –83.1 (each br, (RO)₃Si-Ar) ppm. CP/MAS ³¹P NMR (161.98 MHz, 13 kHz, 300 K) 120.2 (s, (SiO)₃P-Fe) ppm. **Elemental Analysis:** Calc. for C₄₆H₃₅FeO₁₆Si₇P: C: 49.02, H: 3.13, Found: C: 50.47, H: 3.63.

Acknowledgements

We gratefully acknowledge the funding by Saarland University. We acknowledge the Service Center X-ray Diffraction established with financial support from Saarland University and the Deutsche Forschungsgemeinschaft (INST 256/506-1 and 256/582-1). Open Access funding enabled and organized by Projekt DEAL.

Conflict of Interest

The authors declare no conflict of interest.

Data Availability Statement

The data that support the findings of this study are available in the supplementary material of this article.

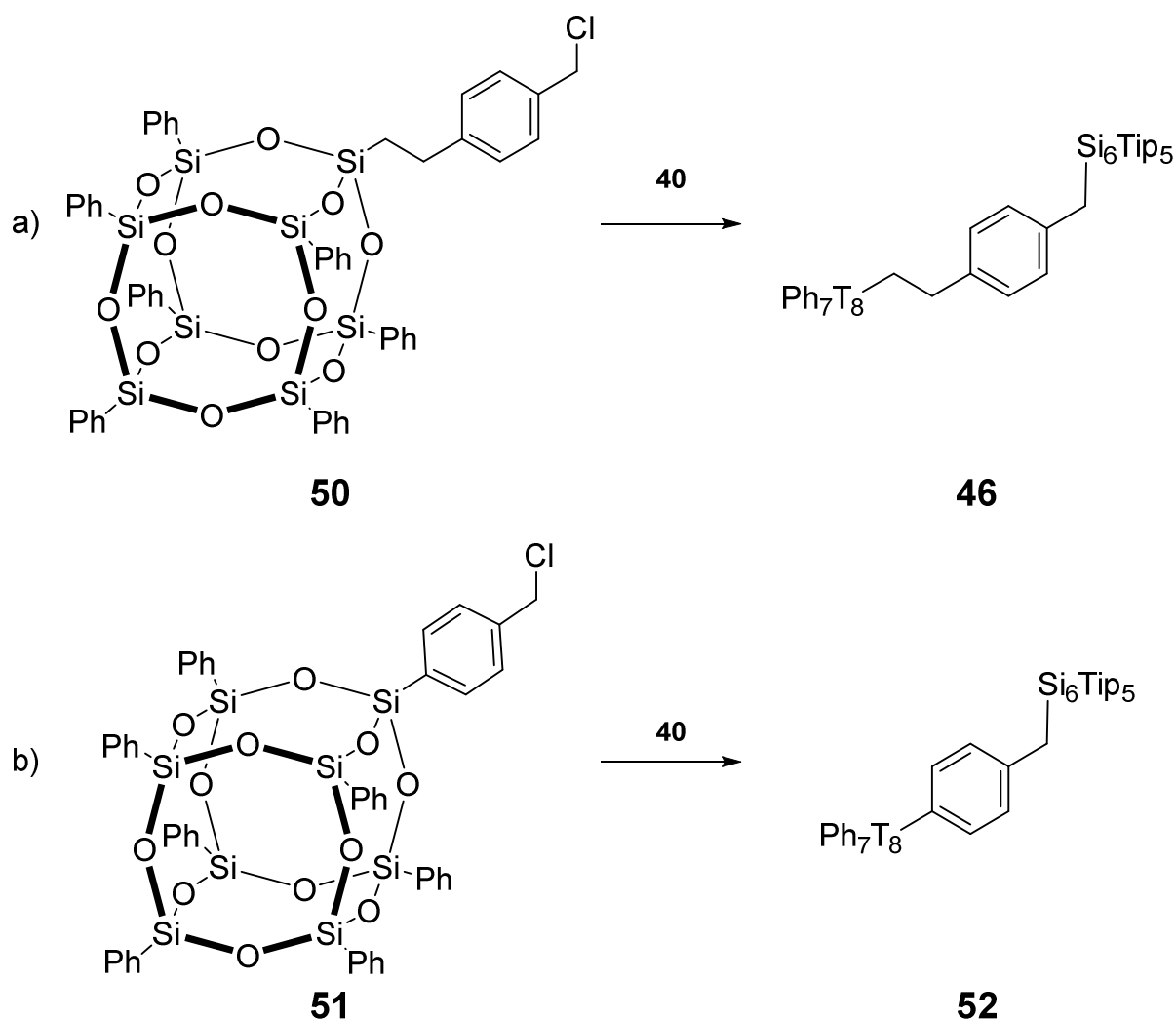
Keywords: boranes · Lewis acid base adducts · phosphanes · phosphite · silsesquioxanes

- [1] a) W. D. Habicher, I. Bauer, J. Pospíšil, *Macromol. Symp.* **2005**, 225, 147–164; b) L.-W. Ye, J. Zhou, Y. Tang, *Chem. Soc. Rev.* **2008**, 37, 1140–1152; c) N. Baral, S. Rani, P. Saikia, P. Maity, *Eur. J. Org. Chem.* **2023**, 26, e202201238; d) S. Kumar, R. Ravi, T. Sahu, V. K. Jha, R. Baweja, A. K. Jha, *Asian J. Org. Chem.* **2024**, 13, e202400028.
- [2] a) P. W. N. M. van Leeuwen, P. C. J. Kamer, C. Claver, O. Pàmies, M. Diéguez, *Chem. Rev.* **2011**, 111, 2077–2118; b) K. Zhao, H. Wang T Li, S. Liu, E. Benassi, X. Li, Y. Yao, X. Wang, X. Cui, F. Shi, *Nat. Commun.* **2024**, 15, 2016.
- [3] a) I. B. Sivaev, V. I. Bregadze, *Coord. Chem. Rev.* **2014**, 270–271, 75–88; b) R. J. Mayer, N. Hampel, A. R. Ofial, *Chem. Eur. J.* **2021**, 27, 4070–4080; c) P. Erdmann, L. Greb, *ChemPhysChem* **2021**, 22, 935–943.
- [4] F. J. Feher, D. A. Newman, J. F. Walzer, *J. Am. Chem. Soc.* **1989**, 111, 1741–1748.
- [5] F. J. Feher, T. A. Budzichowski, *Organometallics* **1991**, 10, 812–815.
- [6] C. A. Tolman, *Chem. Rev.* **1977**, 77, 313–348.
- [7] J. I. van der Vlugt, M. M. P. Grutters, J. Ackerstaff, R. W. J. M. Hanssen, H. C. L. Abbenhuis, D. Vogt, *Tetrahedron Lett.* **2003**, 44, 8301–8305.
- [8] I. Kownacki, B. Marciniak, K. Szubert, M. Kubicki, M. Jankowska, H. Steinberger, S. Rubinsztajn, *Appl. Catal. A* **2010**, 380, 105–112.
- [9] a) F. J. Feher, *J. Am. Chem. Soc.* **1986**, 108, 3850–3852; b) G. Gerritsen, R. Duchateau, R. A. van Santen, G. P. A. Yap, *Organometallics* **2003**, 22, 100–110.
- [10] a) F. J. Feher, T. A. Budzichowski, *J. Organomet. Chem.* **1989**, 379, 33–40; b) J. I. van der Vlugt, M. Fioroni, J. Ackerstaff, R. W. J. M. Hanssen, A. M. Mills, A. L. Spek, A. Meetsma, H. C. L. Abbenhuis, D. Vogt, *Organometallics* **2003**, 22, 5297–5306.
- [11] T. Alphazan, L. Mathey, M. Schwarzwälder, T.-H. Lin, A. J. Rossini, R. Wischert, V. Enyedi, H. Fontaine, M. Veillerot, A. Lesage, L. Emsley, L. Veyre, F. Martin, C. Thieuleux, C. Copéret, *Chem. Mater.* **2016**, 28, 3634–3640.
- [12] H. Inoue, T. Nakagome, T. Kuroiwa, T. Shirai, E. Fluck, Z. *Naturforsch. B: J. Chem. Sci.* **1987**, 42, 573–578.
- [13] Deposition numbers 2353402 (for **2**) and 2353403 (for **3**) contain the supplementary crystallographic data for this paper. These data are provided free of charge by the joint Cambridge Crystallographic Data Centre and Fachinformationszentrum Karlsruhe Access Structures Service.
- [14] S. Grimme, *Angew. Chem. Int. Ed.* **2008**, 47, 3430–3434.
- [15] a) H. Jacobsen, H. Berke, S. Döring, G. Kehr, G. Erker, R. Fröhlich, O. Meyer, *Organometallics* **1999**, 18, 1724–1735; b) S. Ketkov, E. Rychagova, R. Kather, J. Beckmann, *J. Organomet. Chem.* **2021**, 949, 121944; c) G. Skara, B. Pinter, J. Top, P. Geerlings, F. De Proft, F. De Vleeschouwer, *Chem. Eur. J.* **2015**, 21, 5510–5519; d) P. Spies, G. Erker, G. Kehr, K. Bergander, R. Fröhlich, S. Grimme, D. W. Stephan, *Chem. Commun.* **2007**, 5072–5074; e) R. C. Neu, E. Y. Ouyang, S. J. Geier, X. Zhao, A. Ramos, D. W. Stephan, *Dalton Trans.* **2010**, 39, 4285–4294; f) T. C. Johnstone, G. N. J. H. Wee, D. W. Stephan, *Angew. Chem. Int. Ed.* **2018**, 57, 5881–5884.
- [16] T. E. Müller, D. M. P. Mingos, *Transition Met. Chem.* **1995**, 20, 533–539.
- [17] S. H. Newman-Stonebraker, S. R. Smith, J. E. Borowski, E. Peters, T. Gensch, H. C. Johnson, M. S. Sigman, A. G. Doyle, *Science* **2021**, 374, 301–308.
- [18] a) A. C. Hillier, W. J. Sommer, B. S. Yong, J. L. Petersen, L. Cavallo, S. P. Nolan, *Organometallics* **2003**, 22, 4322–4326; A value of 2.28 Å was chosen for the distance of the putative sphere to the P center and H atoms were included in the calculation. All other parameters were kept at their preselected values. b) L. Falivene, Z. Cao, A. Petta, L. Serra, A. Poater, R. Oliva, V. Scarano, L. Cavallo, *Nat. Chem.* **2019**, 11, 872–879.
- [19] a) S. B. Butts, D. F. Shriver, *J. Organomet. Chem.* **1979**, 169, 191–197; b) S. Muhammad, S. Moncho, B. Li, S. J. Kyran, E. N. Brothers, D. J. Darensbourg, A. A. Bengali, *Inorg. Chem.* **2013**, 52, 12655–12660.
- [20] T. Wiegand, H. Eckert, O. Ekkert, R. Fröhlich, G. Kehr, G. Erker, S. Grimme, *J. Am. Chem. Soc.* **2012**, 134, 4236–4249.
- [21] A. V. Pomogaeva, A. Y. Timoshkin, *ACS Omega* **2022**, 7, 48493–48505.
- [22] T. Özgün, K.-Y. Ye, C. G. Daniliuc, B. Wibbeling, L. Liu, S. Grimme, G. Kehr, G. Erker, *Chem. Eur. J.* **2016**, 22, 5988–5995.
- [23] M. A. Dureen, D. W. Stephan, *J. Am. Chem. Soc.* **2009**, 131, 8396–8397.
- [24] F. Buß, P. Mehlmann, C. Mück-Lichtenfeld, K. Bergander, F. Dielmann, *J. Am. Chem. Soc.* **2016**, 138, 1840–1843.

Manuscript received: May 10, 2024
 Revised manuscript received: June 3, 2024
 Accepted manuscript online: June 10, 2024

4 Conclusion and Outlook

The envisioned model system **46** proved to be accessible through corner capping incompletely condensed silsesquioxane **16a** with a suitable electrophilic linking unit, producing silsesquioxane **50**, which is able to connect to the anionic unsaturated siliconoid **40**. Model system **46** was isolated and fully characterized in the solid state and in solution.

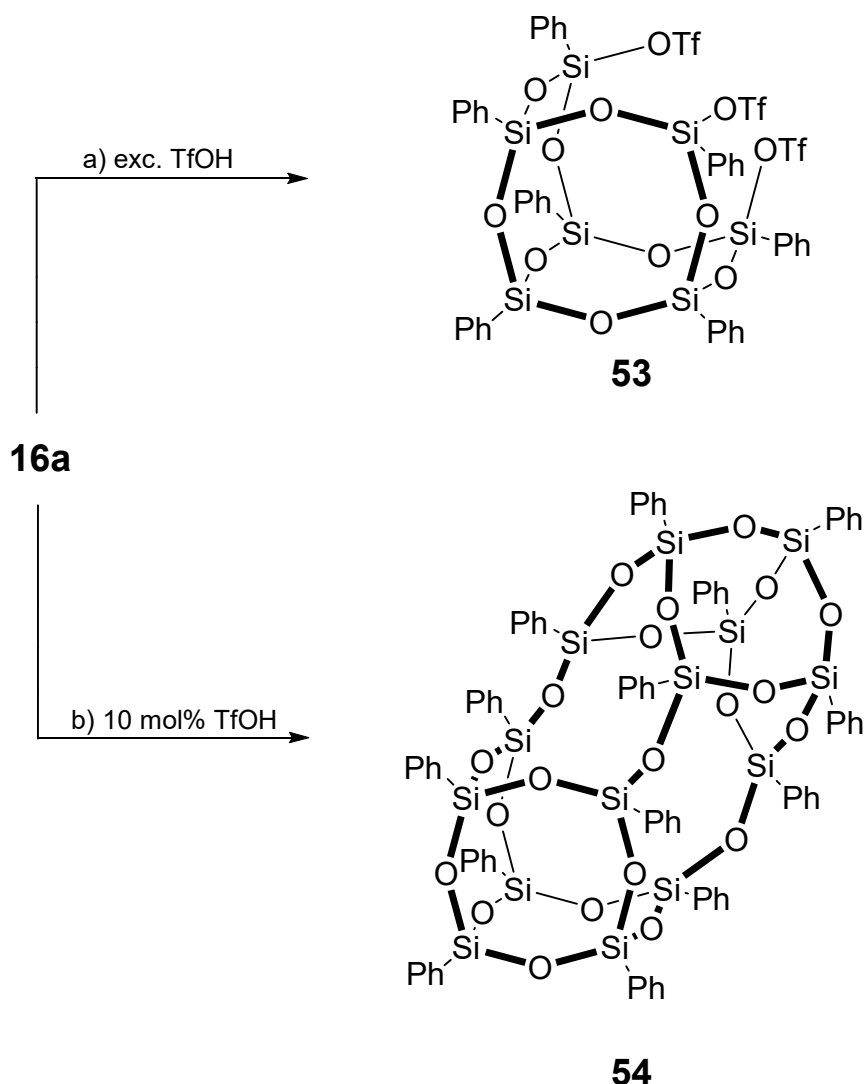


Scheme 19. a) Combining the linker substituted silsesquioxane **50** with anionic siliconoid **40** yields the proof-of-concept model system **46**. b) Due to steric compatibility, even shorter linking units such as used in silsesquioxane **51** are accepted to form the smaller linked congener **52**.

The crystal structure provides information about the steric demand of both parts, which indeed permits shorter linking groups, as demonstrated with the second target

molecule **52**. The next step would constitute the linkage of the silsesquioxane and siliconoid in a π -conjugated manner. As the ^{29}Si NMR and UV/VIS spectra of **46** and **52** demonstrate, the linking of the silsesquioxane to the siliconoid in a non-conjugated manner does not exert significant mutual influence. The unsaturated siliconoid moiety of model system **46** displays spectral data completely in line with other *ligato*-substituted anionic unsaturated siliconoids. Therefore, investigation of electron delocalization effects in a conjugated molecule would shed light on similarities to proper SiO samples. To get a more realistic model with regards to the correct stoichiometry, a siloxane linker could be conceived, mimicking parts of the postulated interface.^[131] Reducing the carbon content in the linking unit and on the silsesquioxane substituents should lessen the formation of silicon oxycarbides from silsesquioxanes during pyrolysis.^[143] Even though very sophisticated theoretical model systems have been established for SiO ,^[132,133] the direct experimental evidence of the long-range order remains elusive. The presented molecule constitutes the starting point for systematic investigations regarding the interfacial $\text{Si}(\text{Si}_x\text{O}_{4-x})$ region, when differently sized silsesquioxanes and siliconoids are considered. Successful functionalization of the also herein presented T_{14} framework with the siliconoid instead of T_8 , the resulting $\text{SiO}_{1.05}$ ratio would be even closer to the actual stoichiometry of silicon monoxide, compared to the $\text{SiO}_{0.86}$ of model systems **46** and **52**.

While several silsesquioxanes larger than T_{12} are accessible,^[33,35,66] the resource intense procedures, low yields and a limited choice of substituents render them almost exclusively interesting to academic investigations. The herein presented formation of a T_{14} framework from two trisilanol silsesquioxanes represents a significant increase in efficiency and yield compared to earlier reports.



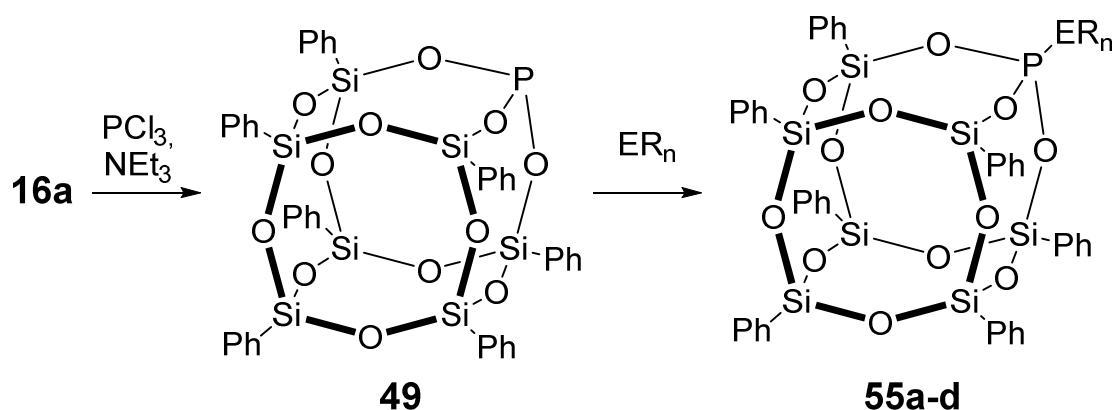
Scheme 20. a) Treatment of incompletely condensed silsesquioxane **16a** with an excess of TfOH substitutes the silanol moieties, however only small amounts of triflate **53** could be obtained in the form of low-quality crystals. An overall partial substitution in the reaction mixture towards $T_7Ph_7(OH)_{3-x}(OTf)_x$ is tentatively suggested. b) Adding 10 mol% of TfOH to silsesquioxane **16a** produces the $T_{14}Ph_{14}$ silsesquioxane **54**.

The straightforward synthesis of a $T_{14}R_{14}$ silsesquioxane framework opens up new strategies toward larger systems, by combining smaller fragments of suitable geometry into bigger frameworks. While such reactions are expected to occur in a typical silsesquioxane reaction mixture, judging from a few possible isomers consisting seemingly of several fused smaller ones,^[68] such an intentional, catalyzed condensation from smaller silsesquioxanes into frameworks larger than T_8R_8 is the first of its kind. Preliminary fragmentation studies by Freeman and coworkers^[68] can provide guidance in selecting appropriate structures, and as was demonstrated herein, even postulated isomers of low stability can be isolated in this manner.

In general, the established chemistry of smaller silsesquioxanes with regards to substituent manipulations with organic chemistry should be transferable to the here presented $T_{14}Ph_{14}$, therefore a larger silsesquioxane with more anchor points could be beneficial as three-dimensional building block in copolymers. More reports urge for the development of synthetic protocols to prepare larger silsesquioxanes in an economic manner in order to explore their so far only postulated properties.^[144] Larger incompletely condensed frameworks – provided methods of their isolation and functionalization are found – could also give more insight into extended silica supported systems.

The observation that $T_7Ph_7(OH)_{3-x}(OTf)_x$ species may be present when the silsesquioxane is treated with an excess of triflic acid strengthens the argument that the siloxane framework itself is prone to more sophisticated manipulations than the simple corner capping methods employed so far. The more general synthetic use would enhance the (already widespread) ability of incompletely condensed frameworks of being closed with heteroatomic vertices unseen so far, or substitution of the pending silanols with completely different functional groups such as, for instance, amines.^[45]

Phosphite **49** was successfully synthesized in an adapted literature procedure, although in comparatively mediocre yield.^[61a,b] While unfortunately no XRD suitable single crystals could be obtained, the spectroscopic data is in line with other silsesquioxane-caged phosphites. It was shown that **49** can indeed coordinate to Lewis acids and transition metals of sizeable steric demand, such as tris(pentafluorophenyl)borane and the $Fe(CO)_4$ fragment.



Scheme 21. Corner capping of phenyl substituted incompletely condensed silsesquioxane **16a** with PCl_3 yields phosphite **49**. Treatment of **49** with several Lewis acids affords the Lewis acid-base adducts **55a-d** (E = main group or transition metal element, R = organic substituent **55a**: $\text{ER}_n = \text{BPh}_3$, **55b**: $\text{ER}_n = \text{B}(\text{C}_6\text{F}_5)_3$, **55c**: $\text{ER}_n = \text{BCl}_3$, **55d**: $\text{ER}_n = \text{Fe}(\text{CO})_4$).

The previously reported Tolman cone angle^[61a;139] of the $\text{T}_7\text{Cy}_7\text{P}$ phosphite **47** is slightly larger than the (approximated) cone angle of the phenyl derivative, when reevaluated with the Mingos method.^[141] This difference is not overly significant, and as such the $\text{T}_7\text{Cy}_7\text{P}$ **47** could also be viable for a broader Lewis acid-base chemistry. In contrast to the successful adduct formation, FLP reactivity was not found for Lewis complex **55b**, which can tentatively be rationalized through a strong donor-acceptor bond. The short P-B bond length and large coupling constants in the ^{11}B and ^{31}P NMR would be in favor of this hypothesis, while the phosphite itself might not be basic enough to instill FLP reactivity, due to the electron withdrawing effect of the silsesquioxane framework.^[40,145] As the crystal structure of Lewis adduct **55b** suggests, threefold π -stacking may be stabilizing the adduct, thus preventing FLP type reactivity. A different combination of silsesquioxane substituents and Lewis acids might be amenable for small molecule activation, as was shown for other Lewis adducts before.^[146] The spectroscopic investigation of a combination of phenyl substituted phosphite **49** with tris(4-bromo-2,3,5,6-tetramethyl)borane provided no hints at adduct formation, nor FLP reactivity. This might be attributed to a severe increase in steric shielding at the Lewis acidic center. In general, the synthetic value of silsesquioxane-caged phosphites could be much greater than anticipated. Likewise, these results demonstrate that incorporation of elements of the periodic table into silsesquioxane frameworks has not reached its conclusion yet, and more unique properties could be uncovered with more exotic species.

5 References

- [1] E. Riedel, C. Janiak, *Anorganische Chemie*, Walter de Gruyter, Berlin, **2007**, p. 511.
- [2] A. F. Hollemann, E. Wiberg, N. Wiberg, *Lehrbuch der Anorganischen Chemie*, Walter de Gruyter, Berlin, **2007**, p. 919.
- [3] a) T. Saga, *NPG Asia Mater.* **2010**, 2, 96-102; b) Z. Sun, X. Chen, Y. He, J. Li, J. Wang, H. Yan, Y. Zhang, *Adv. Energy Mater.* **2022**, 12, 2200015; c) J. Li, J. Wang, L. Liu, Y. Wen, C. Wang, *J. Cryst. Growth* **2024**, 630, 127608.
- [4] a) T.S. Jones, **2001**, *Mineral Commodity Summaries 2001*, U.S. Geological Survey, p. 146-147, <https://doi.org/10.3133/mineral2001>; b) E. K. Schnebele, **2024**, *Mineral Commodity Summaries 2024*, U.S. Geological Survey, 2024, p. 160-161, <https://doi.org/10.3133/mcs2024>.
- [5] a) B. Frieske, S. Stieler, *World Electr. Veh. J.* **2022**, 13, 189; b) W. Mohammad, A. Elomri, L. Kerbach, *IFAC PapersOnLine* **2022**, 55, 476-483.
- [6] a) X. Wang, P. Tao, Q. Wang, R. Zhao, T. Liu, Y. Hu, Z. Hu, Y. Wang, J. Wang, Y. Tang, H. Xu, X. He, *Mater. Today* **2023**, 67, 299-319; b) K. Stokes, K. Clark, D. Odetade, M. Hardy, P. Goldberg Oppenheimer, *Discover Nano* **2023**, 18, 153.
- [7] a) S. Paik, G. Kim, S. Chang, S. Lee, D. Jin, K.-Y. Jeong, I. S. Lee, J. Lee, H. Moon, J. Lee, K. Chang, S. S. Choi, J. Moon, S. Jung, S. Kang, W. Lee, H.-J. Choi, H. Choi, H. J. Kim, J.-H. Lee, J. Cheon, M. Kim, J. Myoung, H.-G. Park, W. Shim, *Nat. Commun.* **2020**, 11, 805; b) H. Ahn, G. Moon, H. Jung, B. Deng, D.-H. Yang, S. Yang, C. Han, H. Cho, Y. Yeo, C.-J. Kim, C.-H. Yang, J. Kim, S.-Y. Choi, H. Park, J. Jeon, J.-H. Park, M.-H. Jo, *Nat. Nanotechnol.* **2024**, 19, 955-961.
- [8] a) J.-E. Hong, Y. Lee, S.-I. Mo, H.-S. Jeong, J.-H. An, H. Song, J. Oh, J. Bang, J.-H. Oh, K.-H. Kim, *Adv. Mater.* **2021**, 33, 2103708; b) T. Arjmand, M. Legallais, T. T. T. Nguyen, P. Serre, M. Vallejo-Perez, F. Morisot, B. Salem, C. TERNON, *Nanomaterials* **2022**, 12, 1043.

- [9] a) W. M. M. Kessels, M. C. M. van de Sanden, D. C. Schram, *Appl. Phys. Lett.* **1998**, *72*, 2397-2399; b) M. T. Swihart, S. L. Girshick, *J. Phys. Chem. B* **1999**, *103*, 64-76.
- [10] a) C.F. Mabery, *J. Franklin Inst.* **1886**, *122*, 271-274; b) C.F. Mabery, *Am. Chem. J.* **1887**, *9*, 11-15.
- [11] a) D. J. Lee, M.-H. Ryou, J.-N. Lee, B. G. Kim, Y. M. Lee, H.-W. Kim, B.-S. Kong, J.-K. Park, J. W. Choi *Electrochem. Commun.* **2013**, *34*, 98-101; b) Z. Liu, Q. Yu, Y. Zhao, R. He, M. Xu, S. Feng, S. Li, L. Zhou, L. Mai, *Chem. Soc. Rev.* **2019**, *48*, 285-309; c) W. Li, L. Zhou, W. Liao, *Int. J. Electrochem. Sci.* **2021**, *16*, 211013.
- [12] a) A. Sellinger, R. M. Laine, *Macromolecules* **1996**, *29*, 2327-2330; b) S.-W. Kuo, F.-C. Chang, *Prog. Polym. Sci.* **2011**, *36*, 1649-1696.
- [13] P. A. Agaskar, *Colloids Surf.* **1992**, *63*, 131-138.
- [14] a) A. R. Bassindale, Z. Liu, I. A. MacKinnon, P. G. Taylor, Y. Yang, M. E. Light, P. N. Horton, M. B. Hursthouse, *Dalton Trans.* **2003**, 2945-2949; b) A. R. Bassindale, H. Chen, Z. Liu, I. A. MacKinnon, D. J. Parker, P. G. Taylor, Y. Yang, M. E. Light, P. N. Horton, M. B. Hursthouse, *J. Organomet. Chem.* **2004**, *689*, 3287-3300.
- [15] a) J. D. Lichtenhan, Y. A. Otonari, M. J. Carr, *Macromolecules* **1995**, *28*, 8435-8437; b) A. Fina, D. Tabuani, F. Carniato, A. Frache, E. Boccaleri, G. Camino, *Thermochim. Acta* **2006**, *440*, 36-42; c) S. O. Hwang, J. Y. Lee, J.-H. Lee, *Prog. Org. Coat.* **2019**, *137*, 105316.
- [16] a) C. Chuanbo, C. Cancan, M. Xiaoyu, Z. Qiong, *J. Appl. Polym. Sci.* **2013**, *130*, 1281-1288; b) C. Zhang, J. Zhang, T. Xu, H. Sima, J. Hou, *Materials* **2020**, *13*, 4570.
- [17] a) R. J. Clark, M. Aghajamali, C. M. Gonzalez, L. Hadidi, M. A. Islam, M. Javadi, M. H. Mobarok, T. K. Purkait, C. J. T. Robidillo, R. Sinelnikov, A. N. Thiessen, J. Washington, H. Yu, J. G. C. Veinot, *Chem. Mater.* **2017**, *29*, 80-89; b) C. Cibaka-Ndaya, K. O'Connor, E. O. Idowu, M. A. Parker, E. Lebraud, S. Lacomme, D. Montero, P. S. Camacho, J. G.-C. Veinot, I.-L. Roiban, G. L. Drisko, *Chem. Mater.* **2023**, *35*, 8551-8560.

- [18] a) R. M. Laine, *J. Mater. Chem.* **2005**, *15*, 3725-3744; b) C.-G. Zhen, U. Becker, J. Kieffer, *J. Phys. Chem. A* **2009**, *113*, 9707-9714; c) Y. El Aziz, A. R. Bassindale, P. G. Taylor, P. N. Horton, R. A. Stephenson, M. B. Hursthouse, *Organometallics* **2012**, *31*, 6032-6040.
- [19] M. Vert, Y. Doi, K.-H. Hellwich, M. Hess, P. Hodge, P. Kubisa, M. Rinaudo, F. Schué, *Pure Appl. Chem.* **2012**, *84*, 377-410.
- [20] a) A. Ladenburg, *Ber. Dtsch. Chem. Ges.* **1873**, *6*, 379-381; b) A. Ladenburg, *Justus Liebigs Ann. Chem.* **1874**, *173*, 143-166.
- [21] J. A. Meads, F. S. Kipping, *J. Chem. Soc. Trans.* **1914**, *105*, 679-690.
- [22] D. W. Scott, *J. Am. Chem. Soc.* **1946**, *68*, 356-358.
- [23] A. J. Barry, J. W. Gilkey (Dow Corning Corporation), US 2465188A, **1949**.
- [24] a) M. M. Sprung, F. O. Guenther, *J. Am. Chem. Soc.* **1955**, *77*, 3990-3996; b) M. M. Sprung, F. O. Guenther, *J. Am. Chem. Soc.* **1955**, *77*, 3996-4002; c) M. M. Sprung, F. O. Guenther, *J. Am. Chem. Soc.* **1955**, *77*, 6045-6047.
- [25] A. J. Barry, W. H. Daudt, J. J. Domicone, J. W. Gilkey, *J. Am. Chem. Soc.* **1955**, *77*, 4248-4252.
- [26] E. Wiberg, W. Simmler, *Z. Anorg. Allg. Chem.* **1955**, *282*, 330-344.
- [27] J. F. Brown, L. H. Vogt, P. I. Prescott, *J. Am. Chem. Soc.* **1964**, *86*, 1120-1125.
- [28] M. Quest, A. Hepp, C. G. Daniliuc, F. Lips, *Chem. Eur. J.* **2024**, *30*, e202302766.
- [29] M. M. Sprung, F. O. Guenther, *J. Polym. Sci.* **1958**, *28*, 17-34.
- [30] R. Müller, R. Köhne, S. Sliwinski, *J. Prakt. Chem.* **1959**, *9*, 71-74.
- [31] a) K. Larsson, *Ark. Kemi* **1960**, *16*, 203-208; b) K. Larsson, *Ark. Kemi* **1960**, *16*, 209-214; c) K. Larsson, *Ark. Kemi* **1960**, *16*, 215-219.
- [32] a) J. F. Brown Jr., L. H. Vogt Jr., *J. Am. Chem. Soc.* **1965**, *87*, 4313-4317; b) J. F. Brown Jr., *J. Am. Chem. Soc.* **1965**, *87*, 4317-4324; c) F. J. Feher, D. A. Newman, J. F. Walzer, *J. Am. Chem. Soc.* **1989**, *111*, 1741-1748; d) F. J. Feher, T. A. Budzichowski, R. L. Blanski, K. J. Weller, J. W. Ziller, *Organometallics* **1991**, *10*, 2526-2528.

- [33] C. L. Frye, W. T. Collins, *J. Am. Chem. Soc.* **1970**, *92*, 5586-5588.
- [34] a) P. A. Agaskar, V. W. Day, W. G. Klemperer, *J. Am. Chem. Soc.* **1987**, *109*, 5554-5556; b) P. A. Agaskar, *Inorg. Chem.* **1991**, *30*, 2707-2708.
- [35] P. A. Agaskar, W. G. Klemperer, *Inorg. Chim. Acta* **1995**, *229*, 355-364.
- [36] Y. Qu, G. Huang, X. Wang, J. Li, *J. Appl. Polym. Sci.* **2012**, *125*, 3658-3665.
- [37] a) T. Kudo, M. S. Gordon, *J. Am. Chem. Soc.* **1998**, *120*, 11432-11438; b) T. Kudo, M. S. Gordon, *J. Phys. Chem. A* **2000**, *104*, 4058-4063; c) T. Kudo, M. S. Gordon, *J. Phys. Chem. A* **2002**, *106*, 11347-11353; d) T. Kudo, K. Machida, M. S. Gordon, *J. Phys. Chem. A* **2005**, *109*, 5424-5429.
- [38] A. Władyczyn, Ł. John, *Inorg. Chem.* **2024**, *63*, 9145-9155.
- [39] a) G. Calzaferri, D. Herren, R. Imhof, *Helv. Chim. Acta* **1991**, *74*, 1278-1280; b) G. Calzaferri, R. Imhof, *J. Chem. Soc. Dalton Trans.* **1992**, 3391-3392; c) R. Knischka, F. Dietsche, R. Hanselmann, H. Frey, R. Mühlhaupt, P. J. Lutz, *Langmuir* **1999**, *15*, 4752-4756, d) M. A. Said, H. W. Roesky, C. Rennekamp, M. Andruh, H.-G. Schmidt, M. Noltemeyer, *Angew. Chem.* **1999**, *111*, 702-705; *Angew. Chem. Int. Ed.* **1999**, *38*, 661-664; e) F. J. Feher, K. J. Weller, *Inorg. Chem.* **1991**, *30*, 880-882.
- [40] a) F. J. Feher, T. A. Budzichowski, *J. Organomet. Chem.* **1989**, *379*, 33-40; b) S. Shanmugan, D. Cani, P. P. Pescarmona, *Chem. Commun.* **2014**, *50*, 11008-11011.
- [41] a) T. Kudo, M. Akasaka, M. S. Gordon, *Theor. Chem. Acc.* **2008**, *120*, 155-166; b) T. Kudo, *J. Phys. Chem. A* **2009**, *113*, 12311-12321; c) T. Kudo, T. Taketsugu, M. S. Gordon, *J. Phys. Chem. A* **2011**, *115*, 2679-2691; d) T. Kudo, T. Taketsugu, M. S. Gordon, *J. Phys. Chem. A* **2016**, *120*, 8699-8715; e) G. Mitrikas, *J. Phys. Chem. Lett.* **2023**, *14*, 9590-9595.
- [42] a) A. R. Bassindale, D. J. Parker, M. Pourny, P. G. Taylor, P. N. Horton, M. B. Hursthouse, *Organometallics* **2004**, *23*, 4400-4405; b) M. Laird, C. Totée, P. Gaveau, G. Silly, A. Van der Lee, C. Carcel, M. Unno, J. R. Bartlett, M. Wong Chi Man, *Dalton Trans.* **2021**, *50*, 81-89; c) M. Laird, P. Gaveau, P. Trens, C.

- Carcel, M. Unno, J. R. Bartlett, M. Wong Chi Man, *New J. Chem.* **2021**, *45*, 4227-4235.
- [43] a) G. Calzaferri, C. Marcolli, R. Imhof, K. W. Törnroos, *J. Chem. Soc. Dalton Trans.* **1996**, 3313-3322; b) B. J. Hendan, H. C. Marsmann, *J. Organomet. Chem.* **1994**, *483*, 33-38.
- [44] F. J. Feher, D. Soulivong, A. G. Eklund, *Chem. Commun.* **1998**, 399-400.
- [45] F. J. Feher, D. Soulivong, F. Nguyen, J. W. Ziller, *Angew. Chem.* **1998**, *110*, 2808-2811; *Angew. Chem. Int. Ed.* **1998**, *37*, 2663-2666.
- [46] a) K. Yoshida, K. Ito, H. Oikawa, M. Yamahiro, Y. Morimoto, K. Ohguma, K. Watanabe, N. Ootake (Chisso Corp.), US 20040068074A1, **2004**; b) W. Wang, Q. Shen, W. Zha, G. Zhu, *J. Polym. Res.* **2011**, *18*, 1119-1124; c) J. Fu, L. Shi, L. Chen, W. Yu, H. Jia, P. Zong, X. Dong (Shanghai University), CN 104311593A, **2015**; d) M. Ye, Y. Wu, W. Zhang, R. Yang, *Res. Chem. Intermed.* **2018**, *44*, 4277-4294.
- [47] a) Y. Morimoto, K. Watanabe, N. Ootake, J.-I. Inagaki, K. Yoshida, K. Ohguma (Chisso Corp.), WO03024870A1, **2003**; b) Y. Morimoto, K. Watanabe, N. Ootake, J.-I. Inagaki, K. Yoshida, K. Ohguma (Chisso Corp.), US2004249103A1, **2004**.
- [48] D. W. Lee, Y. Kawakami, *Polym. J.* **2007**, *39*, 230-238.
- [49] S. Gießmann, A. Fischer, F. T. Edelmann, *Z. Anorg. Allg. Chem.* **2004**, *630*, 1982-1986.
- [50] a) F. Carniato, E. Boccaleri, L. Marchese, *Dalton Trans.* **2008**, 36-39; b) F. Olivero, F. Renò, F. Carniato, M. Rizzi, M. Cannas, L. Marchese, *Dalton Trans.* **2012**, *41*, 7467-7473; c) T. Maegawa, Y. Irie, H. Imoto, H. Fueno, K. Tanaka, K. Naka, *Polym. Chem.* **2015**, *6*, 7500-7504; d) S. Yuasa, H. Imoto, K. Naka, *Polym. J.* **2018**, *50*, 879-887; e) L. Jin, C. Hong, X. Li, Z. Sun, F. Feng, H. Liu, *Chem. Commun.* **2022**, *58*, 1573-1576; f) K. Fuchs, E. Nizioł, J. Ejfler, W. Zierkiewicz, A. Władyczyn, Ł. John, *Dalton Trans.* **2023**, *52*, 16607-16615.

- [51] a) F. J. Feher, *J. Am. Chem. Soc.* **1986**, *108*, 3850-3852; b) M. Ventura, V. Tabernero, T. Cuenca, B. Royo, G. Jiménez, *Eur. J. Inorg. Chem.* **2016**, *2016*, 2843-2849.
- [52] a) F. J. Feher, S. L. Gonzales, J. W. Ziller, *Inorg. Chem.* **1988**, *27*, 3440-3442; b) F. J. Feher, T. A. Budzichowski, K. J. Weller, *J. Am. Chem. Soc.* **1989**, *111*, 7288-7289; c) F. J. Feher, J. F. Walzer, *Inorg. Chem.* **1990**, *29*, 1604-1611; d) T. A. Budzichowski, S. T. Chacon, M. H. Chisholm, F. J. Feher, W. Streib, *J. Am. Chem. Soc.* **1991**, *113*, 689-691; e) M. Crocker, R. H. M. Herold, A. G. Orpen, *Chem. Commun.* **1997**, 2411-2412; f) R. Duchateau, H. C. L. Abbenhuis, R. A. van Santen, A. Meetsma, S. K.-H. Thiele, M. F. H. van Tol, *Organometallics* **1998**, *17*, 5663-5673; g) V. Lorenz, A. Fischer, K. Jacob, F. T. Edelmann, *Inorg. Chem. Commun.* **2003**, *6*, 795-798; h) T. Giovenzana, M. Guidotti, E. Lucenti, A. O. Biroli, L. Sordelli, A. Sironi, R. Ugo, *Organometallics* **2010**, *29*, 6687-6694.
- [53] a) F. J. Feher, J. F. Walzer, *Inorg. Chem.* **1991**, *30*, 1689-1694; b) T. Maschmeyer, M. C. Klunduk, C. M. Martin, D. S. Shepard, J. M. Thomas, B. F. G. Johnson, *Chem. Commun.* **1997**, 1847-1848; c) M. Crocker, R. H. M. Herold, A. G. Orpen, M. T. A. Overgaag, *J. Chem. Soc. Dalton Trans.* **1999**, 3791-3804.
- [54] a) F. J. Feher, T. A. Budzichowski, *Polyhedron* **1995**, *14*, 3239-3253; b) I. Kownacki, B. Marciniak, K. Szubert, M. Kubicki, M. Jankowska, H. Steinberger, S. Rubinsztajn, *Appl. Catal. A* **2010**, *380*, 105-112.
- [55] a) J. Annand, H. C. Aspinall, A. Steiner, *Inorg. Chem.* **1999**, *38*, 3941-3943; b) V. Lorenz, S. Gießmann, Y. K. Gun'ko, A. K. Fischer, J. W. Gilje, F. T. Edelmann, *Angew. Chem.* **2004**, *116*, 4603-4606; *Angew. Chem. Int. Ed.* **2004**, *43*, 4603-4606; c) C. García, M. Gómez, P. Gómez-Sal, J. M. Hernández, *Eur. J. Inorg. Chem.* **2009**, *2009*, 4401-4415; d) N. Prigyi, S. Chanmungkalakul, V. Ervithayasuporn, N. Yodsin, S. Jungsuttiwong, N. Takeda, M. Unno, J. Boonmak, S. Kiatkamjornwong, *Inorg. Chem.* **2019**, *58*, 15110-15117.
- [56] R. W. J. M. Hanssen, A. Meetsma, R. A. van Santen, H. C. L. Abbenhuis, *Inorg. Chem.* **2001**, *40*, 4049-4052.
- [57] V. Lorenz, S. Blaurock, F. T. Edelmann, *Z. Anorg. Allg. Chem.* **2008**, *634*, 441-444.
-

- [58] F. J. Feher, T. A. Budzichowski, J. W. Ziller, *Inorg. Chem.* **1992**, *31*, 5100-5105.
- [59] a) F. J. Feher, K. J. Weller, *Organometallics* **1990**, *9*, 2638-2640; b) F. J. Feher, K. J. Weller, J. W. Ziller, *J. Am. Chem. Soc.* **1992**, *114*, 9686-9688; c) G. Gerritsen, R. Duchateau, R. A. van Santen, G. P. A. Yap, *Organometallics* **2003**, *22*, 100-110.
- [60] a) D. Frąckowiak, P. Żak, G. Spólnik, M. Pyziak, B. Marciniak, *Organometallics* **2015**, *34*, 3950-3958; b) P. Żak, D. Frąckowiak, M. Grzelak, M. Bołt, M. Kubicki, B. Marciniak, *Adv. Synth. Catal.* **2016**, *358*, 3265-3276.
- [61] a) F. J. Feher, T. A. Budzichowski, *Organometallics* **1991**, *10*, 812-815, b) T. Alphazan, L. Mathey, M. Schwarzwälder, T.-H. Lin, A. J. Rossini, R. Wischert, V. Enyedi, H. Fontaine, M. Veillerot, A. Lesage, L. Emsley, L. Veyre, F. Martin, C. Thieuleux, C. Copéret, *Chem. Mater.* **2016**, *28*, 3634-3640; c) S. Marchesi, C. Bisio, F. Carniato, E. Boccaleri, *Inorganics* **2023**, *11*, 426.
- [62] a) F. J. Feher, T. A. Budzichowski, K. Rahimian, J. W. Ziller, *J. Am. Chem. Soc.* **1992**, *114*, 3859-3866; b) J. I. van der Vlugt, J. Akerstaff, T. W. Dijkstra, A. M. Mills, H. Kooijman, A. L. Spek, A. Meetsma, H. C. L. Abbenhuis, D. Vogt, *Adv. Synth. Catal.* **2004**, *346*, 399-412; c) R. Baba, A. Thakur, P. Chammingkwan, M. Terano, T. Taniike, *Dalton Trans.* **2017**, *46*, 12158-12166; d) R. Katoh, H. Imoto, K. Naka, *Polym. Chem.* **2019**, *10*, 2223-2229.
- [63] a) W. A. Herrmann, R. Anwender, V. Dufaud, W. Scherer, *Angew. Chem.* **1994**, *106*, 1338-1340; *Angew. Chem. Int. Ed. Engl.* **1994**, *33*, 1285-1286; b) V. Lorenz, S. Blaurock, C. G. Hrib, F. T. Edelmann, *Eur. J. Inorg. Chem.* **2010**, *2010*, 2605-2608; c) I. Koehne, M. Gerstel, C. Bruhn, J. P. Reithmaier, M. Benyoucef, R. Pietschnig, *Inorg. Chem.* **2021**, *60*, 5297-5309.
- [64] V. Lorenz, S. Blaurock, F. T. Edelmann, *Z. Anorg. Allg. Chem.* **2008**, *634*, 2819-2824.
- [65] a) E. Rikowski, H. C. Marsmann, *Polyhedron* **1997**, *16*, 3357-3361; b) M. Z. Asuncion, R. M. Laine, *J. Am. Chem. Soc.* **2010**, *132*, 3723-3736; c) V. Ervithayasuporn, S. Chimjarn, *Inorg. Chem.* **2013**, *52*, 13108-13112; d) M. Janeta, Ł. John, J. Ejfler, S. Szafert, *RSC Adv.* **2015**, *5*, 72340-72351; e) S. Chimjarn, R. Kunthom, P. Chancharone, R. Sodkhomkhum, P. Sangtrirutnugul,

- V. Ervithayasuporn, *Dalton Trans.* **2015**, 44, 916-919; f) J. C. Furgal, T. Goodson III, R. M. Laine, *Dalton Trans.* **2016**, 45, 1025-1039 g) K. Imai, Y. Kaneko, *Inorg. Chem.* **2017**, 56, 4133-4140.
- [66] M. Laird, N. Herrmann, N. Ramsahye, C. Totée, C. Carcel, M. Unno, J. R. Bartlett, M. Wong Chi Man, *Angew. Chem.* **2021**, 133, 3059-3064; *Angew. Chem. Int. Ed.* **2021**, 60, 3022-3027.
- [67] a) Y. Kawakami, K. Yamaguchi, T. Yokozawa, T. Serizawa, M. Hasegawa, Y. Kabe, *Chem. Lett.* **2007**, 36, 792-293; b) D. Brząkański, R. E. Przekop, B. Sztorch, P. Jakubowska, M. Jałbrzykowski, B. Marciniec, *Polymers* **2020**, 12, 2269.
- [68] K.-H. Xiang, R. Pandey, U. C. Pernisz, C. Freeman, *J. Phys. Chem. B* **1998**, 102, 8704-8711.
- [69] E. A. Quadrelli, J.-M. Basset, *Coord. Chem. Rev.* **2010**, 254, 707-728.
- [70] a) F. J. Feher, R. L. Blanski, *J. Chem. Soc. Chem. Commun.* **1990**, 1614-1616; b) F. J. Feher, J. F. Walzer, R. L. Blanski, *J. Am. Chem. Soc.* **1991**, 113, 3618-3619; c) G. Wu, Y. Chen, D.-J. Xu, J.-C. Liu, W. Sun, Z. Shen, *J. Organomet. Chem.* **2009**, 694, 1571-1574; d) M. D. Jones, C. G. Keir, A. L. Johnson, M. F. Mahon, *Polyhedron* **2010**, 29, 312-316; e) M. Mateos, J. Vinuesa, M. E. G. Mosquera, V. Taberner, T. Cuenca, G. Jiménez, *Inorg. Chim. Acta* **2020**, 501, 119275.
- [71] a) H. M. Cho, H. Weissman, S. R. Wilson, J. S. Moore, *J. Am. Chem. Soc.* **2006**, 128, 14742-14743; b) L. A. Bivona, O. Fichera, L. Fusaro, F. Giacalone, M. Buaki-Sogo, M. Gruttadauria, C. Aprile, *Catal. Sci. Technol.* **2015**, 5, 5000-5007; c) H. E. Starr, M. R. Gagné, *Organometallics* **2022**, 41, 3152-3160.
- [72] a) M. Baertsch, P. Bornhauser, G. Calzaferri, R. Imhof, *J. Phys. Chem.* **1994**, 98, 2817-2831; b) C. W. Early, *J. Phys. Chem.* **1994**, 98, 8693-9698; c) P. Bornhauser, G. Calzaferri, *J. Phys. Chem.* **1996**, 100, 2035-2044; d) Saito, H. Wada, A. Shimojima, K. Kuroda, *Inorg. Chem.* **2018**, 57, 14686-14691.
- [73] a) W. Loewenstein, *Am. Mineral.* **1954**, 39, 92-96; b) E. Fletcher, S. Ling, B. Slater, *Chem. Sci.* **2017**, 8, 7483-7491; c) M. Fant, M. Ångqvist, A. Hellman, P.

- Erhart, *Angew. Chem.* **2021**, 133, 5192-5195; *Angew. Chem. Int Ed.* **2021**, 60, 5132-5135.
- [74] a) R. Duchateau, R. J. Harmsen, H. C. L. Abbenhuis, R. A. van Santen, A. Meetsma, S. K.-H. Thiele, M. Kranenburg, *Chem. Eur. J.* **1999**, 5, 3130-3135; b) F. T. Edelmann, Y. K. Gun'ko, S. Giessmann, F. Olbrich, K. Jacob, *Inorg. Chem.* **1999**, 38, 210-211.
- [75] a) J. D. Lichtenhan, *Comments Inorg. Chem.* **1995**, 17, 115-130; b) M. G. Mohamed, T. H. Mansoure, Y. Takashi, M. M. Samy, T. Chen, S.-W. Kuo, *Microporous Mesoporous Mater.* **2021**, 328, 111505.
- [76] a) S. Sulaiman, A. Bhaskar, J. Zhang, R. Guda, T. Goodson III, R. M. Laine, *Chem. Mater.* **2008**, 20, 5563-5573; b) A. Castaldo, L. Quercia, G. Di Francia, A. Cassinese, P. D'Angelo, *J. Appl. Phys.* **2008**, 103, 054511; c) Y. Zuo, X. Wang, Y. Yang, D. Huang, F. Yang, H. Shen, D. Wu, *Polym. Chem.* **2016**, 7, 6432-6436; d) H. Narikiyo, M. Gon, K. Tanaka, Y. Chujo, *Polym. J.* **2024**, 56, 661-666.
- [77] a) V. Ervithayasuporn, J. Abe, X. Wang, T. Matsushima, H. Murata, Y. Kawakami, *Tetrahedron* **2010**, 66, 9348-9355; b) E. O. Afolayan, I. Dursun, A. Pizano, C. Lang, D. Lungwitz, M. Kondakova, M. Boroson, A. Kahn, M. Hickner, N. C. Giebink, *Adv. Optical Mater.* **2024**, 12, 2302588.
- [78] a) N. Maxim, P. C. M. M. Magusin, P. J. Kooyman, J. H. M. C. van Wolput, R. A. van Santen, H. C. L. Abbenhuis, *Chem. Mater.* **2001**, 13, 2958-2964; b) N. Maxim, A. Overweg, P. J. Kooyman, J. H. M. C. van Wolput, R. W. J. M. Hanssen, R. A. van Santen, H. C. L. Abbenhuis, *J. Phys. Chem. B* **2002**, 106, 2203-2209; c) T. Alphazan, P. Florian, C. Thieuleux, *Phys. Chem. Chem. Phys.* **2017**, 19, 8595-8601; d) T. Alphazan, A. D. Álvarez, F. Martin, H. Grampeix, V. Enyedi, E. Martinez, N. Rochat, M. Veillerot, M. Dewitte, J.-P. Nys, M. Berthe, D. Stiévenard, C. Thieuleux, B. Grandidier, *ACS Appl. Mater. Interfaces* **2017**, 9, 20179-20187.
- [79] a) S.-Y. Lu, I. Hamerton, *Prog. Polym. Sci.* **2002**, 27, 1661-1712; b) A. Fina, H. C. L. Abbenhuis, D. Tabuani, G. Camino *Polym. Degrad. Stab.* **2006**, 91, 2275-2281; c) Z. Qi, W. Zhang, X. He, R. Yang, *Compos. Sci. Technol.* **2016**, 127, 8-19.

- [80] a) M. Peuker, M. H. Lim, H. I. Smith, R. Morton, A. K. van Langen-Suurling, J. Romijn, E. W. J. M. van der Drift, F. C. M. J. M. van Delft, *Microelectron. Eng.* **2002**, 61-62, 803-809; b) A. Rathore, I. Pollentier, M. Cipriani, H. Singh, D. De Simone, O. Ingólfsson, S. De Gendt, *ACS Appl. Polym. Mater.* **2021**, 3, 1964-1972; c) L. Miao, R. Zhang, X. Lu, L. Wu, Z. Wen, H. Qiu, G.-P. Wu, *ACS Appl. Mater. Interfaces* **2024**, 16, 51554-51564.
- [81] S. Pohl, O. Janka, E. Füglein, G. Kickelbick, *Macromolecules* **2021**, 54, 3873-3885.
- [82] a) P. Muller, *Pure Appl. Chem.* **1994**, 66, 1077-1184; b) IUPAC Compendium of Chemical Terminology, 3rd ed., **2006**, 'Lewis base', International Union of Pure and Applied Chemistry, Online Version 3.0.1, **2019** (accessed: 12.15.2024), <https://doi.org/10.1351/goldbook.L03511>.
- [83] S. Konishi, T. Iwai, M. Sawamura, *Organometallics* **2018**, 37, 1876-1883.
- [84] a) A. B. Chaplin, A. S. Weller, *Organometallics* **2010**, 29, 2332-2342; b) M. Lemmerer, N. Maulide, *Chem. Eur. J.* **2023**, 29, e202302490.
- [85] a) P. H. Huy, *Eur. J. Org. Chem.* **2020**, 2020, 10-27; b) S. M. Fischer, P. Kaschnitz, C. Slugovc, *Catal. Sci. Technol.* **2022**, 12, 6204-6212.
- [86] a) M. M. Morgan, A. J. V. Marwitz, W. E. Piers, M. Parvez, *Organometallics* **2013**, 32, 317-322; b) J. M. Bayne, D. W. Stephan, *Chem. Soc. Rev.* **2016**, 45, 765-774.
- [87] a) M. North, D. L. Usanov, C. Young, *Chem. Rev.* **2008**, 108, 5146-5226; b) J. Ishihara, *Molecules* **2024**, 29, 1187.
- [88] B. L. Murphy, F. P. Gabbaï, *J. Am. Chem. Soc.* **2023**, 145, 19458-19477.
- [89] a) G. C. Welch, R. R. S. Juan, J. D. Masuda, D. W. Stephan, *Science* **2006**, 314, 1124-1126; b) G. C. Welch, D. W. Stephan, *J. Am. Chem. Soc.* **2007**, 129, 1880-1881.
- [90] a) P. Spies, G. Kehr, K. Bergander, B. Wibbeling, R. Fröhlich, G. Erker, *Dalton Trans.* **2009**, 1534-1541; b) K. V. Axenov, C. M. Mömming, G. Kehr, R. Fröhlich, G. Erker, *Chem. Eur. J.* **2010**, 16, 14069-14073; c) P. Holtkamp, F. Friedrich, E. Stratmann, A. Mix, B. Neumann, H.-G. Stämmler, N. W. Mitzel, *Angew. Chem.*

- 2019**, *131*, 5168-5172, *Angew. Chem. Int. Ed.* **2019**, *58*, 5114-5118; d) M. Siedzielnik, K. Kaniewska-Laskowska, N. Szynekiewicz, J. Chojnacki, R. Grubba, *Polyhedron* **2021**, *194*, 114930.
- [91] R. C. Neu, E. Y. Ouyang, S. J. Geier, X. Zhao, A. Ramos, D. W. Stephan, *Dalton Trans.* **2010**, *39*, 4285-4294.
- [92] a) L. L. Liu, L. L. Cao, Y. Shao, G. Ménard, D. W. Stephan, *Chem* **2017**, *3*, 259-267; b) F. Holtrop, A. R. Jupp, B. J. Kooij, N. P. van Leest, B. de Bruin, J. C. Slootweg, *Angew. Chem.* **2020**, *132*, 22394-22400; *Angew. Chem. Int. Ed.* **2020**, *59*, 22210-22216.
- [93] a) P. Erdmann, J. Leitner, J. Schwarz, L. Greb, *ChemPhysChem* **2020**, *21*, 987-994; b) P. Erdmann, L. Greb, *Angew. Chem.* **2022**, *134*, e202114550; *Angew. Chem. Int. Ed.* **2022**, *61*, e202114550; c) L. Zapf, M. Riethmann, S. A. Föhrenbacher, M. Finze, U. Radius, *Chem. Sci.* **2023**, *14*, 2275-2288; d) L. M. Sigmund, S. S. S. V., A. Albers, P. Erdmann, R. S. Paton, L. Greb, *Angew. Chem.* **2024**, *136*, e20241084; *Angew. Chem. Int. Ed.* **2024**, *63*, e202401084; e) P. Erdmann, M. Schmitt, L. M. Sigmund, F. Krämer, F. Breher, L. Greb, *Angew. Chem.* **2024**, *136*, e202403356; *Angew. Chem. Int. Ed.* **2024**, *63*, e202403356.
- [94] a) C. Laurence, J. Graton, J.-F. Gal, *J. Chem. Educ.* **2011**, *88*, 1651-1657; b) R. Szlosek, A. S. Niefanger, G. Balázs, M. Seidl, A. Y. Timoshkin, M. Scheer, *Chem. Eur. J.* **2023**, *30*, e202303603.
- [95] T. A. Rokob, A. Hamza, I. Pápai, *J. Am. Chem. Soc.* **2009**, *131*, 10701-10710.
- [96] T. Özgün, K.-Y. Ye, C. G. Daniliuc, B. Wibbeling, L. Liu, S. Grimme, G. Kehr, G. Erker, *Chem. Eur. J.* **2016**, *22*, 5988-5995.
- [97] A. Indriksons, R. West, *J. Am. Chem. Soc.* **1970**, *92*, 6704-6705.
- [98] J. Tillmann, J. H. Wender, U. Bahr, M. Bolte, H.-W. Lerner, M. C. Holthausen, M. Wagner, *Angew. Chem.* **2015**, *127*, 5519-5523; *Angew. Chem. Int. Ed.* **2015**, *54*, 5429-5433.
- [99] a) V. Quéneau, E. Todorov, S. C. Sevov, *J. Am. Chem. Soc.* **1998**, *120*, 3263-3264; b) C. Hoch, M. Wendorff, C. Röhr, *J. Alloys Compd.* **2003**, *361*, 206-221.

- [100] J. M. Goicoechea, S. C. Sevov, *J. Am. Chem. Soc.* **2004**, *126*, 6860-6861.
- [101] a) C. Lorenz, S. Gärtner, N. Korber, *Z. Anorg. Allg. Chem.* **2017**, *643*, 141-145; b) C. B. Benda, T. Henneberger, W. Klein, T. F. Fässler, *Z. Anorg. Allg. Chem.* **2017**, *643*, 146-148.
- [102] D. Scheschkewitz, *Angew. Chem.* **2005**, *117*, 3014-3016; *Angew. Chem. Int. Ed.* **2005**, *44*, 2954-2956.
- [103] a) A. Purath, R. Köppe, H. Schnöckel, *Angew. Chem.* **1999**, *111*, 3114-3116; *Angew. Chem. Int. Ed.* **1999**, *38*, 2926-2928; b) A. Schnepf, G. Stösser, H. Schnöckel, *J. Am. Chem. Soc.* **2000**, *122*, 9178-9181; c) A. Schnepf, H. Schnöckel, *Angew. Chem.* **2002**, *114*, 3682-3704; *Angew. Chem. Int. Ed.* **2002**, *41*, 3532-3554; d) H. Schnöckel, *Dalton Trans.* **2008**, 4344-4362.
- [104] A. Schnepf, *Chem. Soc. Rev.* **2007**, *36*, 745-758.
- [105] K. Abersfelder, A. Russell, H. S. Rzepa, A. J. P. White, P. R. Haycock, D. Scheschkewitz, *J. Am. Chem. Soc.* **2012**, *134*, 16008-16016.
- [106] Y. Heider, D. Scheschkewitz, *Dalton Trans.* **2018**, *47*, 7104-7112.
- [107] J. T. Lyon, P. Gruene, A. Fielicke, G. Meijer, E. Janssens, P. Claes, P. Lievens, *J. Am. Chem. Soc.* **2009**, *131*, 1115-1121.
- [108] D. Scheschkewitz, *Angew. Chem.* **2004**, *116*, 3025-3028; *Angew. Chem. Int. Ed.* **2004**, *43*, 2965-2967.
- [109] M. Weidenbruch, S. Willms, W. Saak, G. Henkel, *Angew. Chem.* **1997**, *109*, 2612-2613; *Angew. Chem. Int. Ed.* **1997**, *36*, 2503-2504.
- [110] a) G. Fischer, V. Huch, P. Mayer, S. K. Vasisht, M. Veith, N. Wiberg, *Angew. Chem.* **2005**, *117*, 8096-8099; *Angew. Chem. Int. Ed.* **2005**, *44*, 7884-7887; b) D. Nied, R. Köppe, W. Kloppe, H. Schnöckel, F. Breher, *J. Am. Chem. Soc.* **2010**, *132*, 10264-10265; c) K. Abersfelder, A. J. P. White, H. S. Rzepa, D. Scheschkewitz, *Science* **2010**, *327*, 564-566; d) K. Abersfelder, A. J. P. White, R. J. F. Berger, H. S. Rzepa, D. Scheschkewitz, *Angew. Chem.* **2011**, *123*, 8082-8086; *Angew. Chem. Int. Ed.* **2011**, *50*, 7936-7939; e) A. Tsurusaki, C. Iizuka, K. Otsuka, S. Kyushin, *J. Am. Chem. Soc.* **2013**, *135*, 16340-16343; f) T. Iwamoto, N. Akasaka, S. Ishida, *Nat. Commun.* **2014**, *5*, 5353; g) L. J.

- Schiegerl, A. J. Karttunen, W. Klein, T. F. Fässler, *Chem. Eur. J.* **2018**, *24*, 19171-19174; h) N. Akasaka, S. Ishida, T. Iwamoto, *Inorganics* **2018**, *6*, 107; i) J. Keuter, C. Schwermann, A. Hepp, K. Bergander, J. Droste, M. R. Hansen, N. L. Doltsinis, C. Mück-Lichtenfeld, F. Lips, *Chem. Sci.* **2020**, *11*, 5895-5901.
- [111] S. Marutheeswaran, P. D. Pancharatna, M. M. Balakrishnarajan, *Phys. Chem. Chem. Phys.* **2014**, *16*, 11186-11190.
- [112] a) P. Willmes, K. Leszczyńska, Y. Heider, K. Abersfelder, M. Zimmer, V. Huch, D. Scheschkewitz, *Angew. Chem.* **2016**, *128*, 2959-2963; *Angew. Chem. Int. Ed.* **2016**, *55*, 2907-2910; b) Y. Heider, N. E. Poitiers, P. Willmes, K. Leszczyńska, V. Huch, D. Scheschkewitz, *Chem. Sci.* **2019**, *10*, 4523-4530; c) Y. Heider, P. Willmes, V. Huch, M. Zimmer, D. Scheschkewitz, *J. Am. Chem. Soc.* **2019**, *141*, 19498-19504; d) K. I. Leszczyńska, V. Huch, C. Präsang, J. Schwabedissen, R. J. F. Berger, D. Scheschkewitz, *Angew. Chem.* **2019**, *131*, 5178-5182; *Angew. Chem. Int. Ed.* **2019**, *58*, 5124-5128.
- [113] a) D. Nied, P. Oña-Burgos, W. Kloppe, F. Breher, *Organometallics* **2011**, *30*, 1419-1428; b) A. Jana, V. Huch, M. Repisky, R. J. F. Berger, D. Scheschkewitz, *Angew. Chem.* **2014**, *126*, 3583-3588; *Angew. Chem. Int. Ed.* **2014**, *53*, 3514-3518.
- [114] a) N. E. Poitiers, L. Giarrana, K. I. Leszczyńska, V. Huch, M. Zimmer, D. Scheschkewitz, *Angew. Chem.* **2020**, *132*, 8610-8614; *Angew. Chem. Int. Ed.* **2020**, *59*, 8532-8536; b) N. E. Poitiers, L. Giarrana, V. Huch, M. Zimmer, D. Scheschkewitz, *Chem. Sci.* **2020**, *11*, 7782-7788; c) N. E. Poitiers, V. Huch, M. Zimmer, D. Scheschkewitz, *Chem. Eur. J.* **2020**, *26*, 16599-16602; d) N. E. Poitiers, V. Huch, M. Zimmer, D. Scheschkewitz, *Chem. Commun.* **2020**, *56*, 10898-10901; e) N. E. Poitiers, V. Huch, B. Morgenstern, M. Zimmer, D. Scheschkewitz, *Angew. Chem.* **2022**, *134*, e202205399; *Angew. Chem. Int. Ed.* **2022**, *61*, e202205399; f) L. Giarrana, M. Zimmer, B. Morgenstern, D. Scheschkewitz, *Inorg. Chem.* **2024**, *63*, 20083-20087.
- [115] a) M. I. Kay, *Acta Cryst.* **1961**, *14*, 80-81; b) F. Izumi, *J. Solid State Chem.* **1981**, *38*, 381-385; c) D. U. Wiechert, S. P. Grabowski, M. Simon, *Thin Solid Films* **2005**, *484*, 73-82; d) H. Giefers, F. Porsch, G. Wortmann, *Phys. B* **2006**, *373*,

- 76-81; e) K. Li, J. Wang, V. A. Blatov, Y. Gong, N. Umezawa, T. Tada, H. Hosono, A. R. Oganov, *J. Adv. Ceram.* **2021**, *10*, 565-577.
- [116] K. N. Astankova, V. A. Volodin, I. A. Azarov, *Semiconductors* **2020**, *54*, 1555-1560.
- [117] G. Hass, *J. Am. Ceram. Soc.* **1950**, *33*, 353-360.
- [118] J. S. Anderson, J. S. Ogden, *J. Chem. Phys.* **1969**, *51*, 4189-4196.
- [119] E.-G. Lee, J.-H. Kim, H. Ko, C.-Y. Kim, *J. Comput. Theor. Nanosci.* **2015**, *12*, 871-874.
- [120] a) J.-H. Kim C.-M. Park, H. Kim, Y.-J. Kim, H.-J. Sohn, *J. Electroanal. Chem.* **2010**, *661*, 245-249; b) T. Mae, K. Kaneko, H. Sakurai, S. Noda, *Carbon* **2024**, *218*, 118663.
- [121] a) S.-W. Cheng, H.-F. Cheung, *J. Appl. Phys.* **2003**, *94*, 1190-1194; b) Y.-W. Chen, Y.-H. Tang, L.-Z. Pei, C. Guo, *Adv. Mater.* **2005**, *17*, 564-567; c) S. Zeng, X. Zeng, L. Huang, H. Wu, Y. Yao, X. Zheng, J. Zou, *RSC Adv.* **2017**, *7*, 7990-7995.
- [122] a) G. W. Brady, *J. Phys. Chem.* **1959**, *63*, 1119-1120; b) B. Friede, M. Jansen, *J. Non-Cryst. Solids* **1996**, *204*, 202-203; c) F. T. Ferguson, J. A. Nuth III, *J. Chem. Eng. Data* **2012**, *57*, 721-728.
- [123] a) J. A. Yasaitis, R. Kaplow, *J. Appl. Phys.* **1972**, *43*, 995-1000; b) M. T. Costa Lima, C. Senemaud, *Chem. Phys. Lett.* **1976**, *40*, 157-159; c) M. Nagamori, J.-A. Boivin, A. Claveau, *J. Non-Cryst. Solids* **1995**, *189*, 270-276; d) D. C. Gunduz, A. Tankut, S. Sedani, M. Karaman, R. Turan, *Phys. Status Solidi C* **2015**, *12*, 1229-1235.
- [124] M. Hoch, H. L. Johnston, *J. Am. Chem. Soc.* **1953**, *75*, 5224-5225.
- [125] a) S. Geller, C. D. Thurmond, *J. Am. Chem. Soc.* **1955**, *77*, 5285-5287; b) S. M. Schnurre, J. Gröbner, R. Schmid-Fetzer, *J. Non-Cryst. Solids* **2004**, *336*, 1-25.
- [126] K. AlKaabi, D. L. V. K. Prasad, P. Kroll, N. W. Ashcroft, R. Hoffmann, *J. Am. Chem. Soc.* **2014**, *136*, 3410-3423.

- [127] M. Mamiya, H. Takei, M. Kikuchi, C. Uyeda, *J. Cryst. Growth* **2001**, 229, 457-461.
 - [128] R. J. Temkin, *J. Non-Cryst. Solids* **1975**, 17, 215-230.
 - [129] a) H. R. Philipp, *J. Phys. Chem. Solids* **1971**, 32, 1935-1945; b) H. R. Philipp, *J. Non-Cryst. Solids* **1972**, 8-10, 627-632.
 - [130] K. Schulmeister, W. Mader *J. Non-Cryst. Solids* **2003**, 320, 143-150.
 - [131] A. Hohl, T. Wieder, P. A. van Aken, T. E. Weirich, G. Denninger, M. Vidal, S. Oswald, C. Deneke, J. Mayer, H. Fuess, *J. Non-Cryst. Solids* **2003**, 320, 255-280.
 - [132] A. Hirata, S. Kohara, T. Asada, M. Arao, C. Yogi, H. Imai, Y. Tan, T. Fujita, M. Chen, *Nat. Commun.* **2016**, 7, 11591.
 - [133] L. C. Erhard, J. Rohrer, K. Albe, V. L. Deringer, *Nat. Commun.* **2024**, 15, 1927.
 - [134] a) A. C. Filippou, B. Baars, O. Chernov, Y. N. Lebedev, G. Schnakenburg, *Angew. Chem.* **2014**, 126, 576-581; *Angew. Chem. Int. Ed.* **2014**, 53, 565-570; b) R. Kobayashi, S. Ishida, T. Iwamoto, *Angew. Chem.* **2019**, 131, 9525-9528; *Angew. Chem. Int. Ed.* **2019**, 58, 9425-9428; c) T. Muraoka, T. Ishita, K. Kawachi, T. Nishio, H. Ishihara, K. Ueno, *Dalton Trans.* **2024**, 53, 7105-7114.
 - [135] S. Hoffmann, T. F. Fässler, C. Hoch, C. Röhr, *Angew. Chem.* **2001**, 113, 4527-4529; *Angew. Chem. Int. Ed.* **2001**, 40, 4398-4400.
 - [136] a) S. U. Ahmad, T. Szilvási, E. Irran, S. Inoue, *J. Am. Chem. Soc.* **2015**, 137, 5828-5836; b) Y. Wang, M. Chen, Y. Xie, P. Wei, H. F. Schaefer III, P. von R. Schleyer, G. H. Robinson, *Nat. Chem.* **2015**, 7, 509-513.
 - [137] S. Tateyama, Y. Kakihana, Y. Kawakami, *J. Organomet. Chem.* **2010**, 695, 898-902.
 - [138] S. Spirk, M. Nieger, F. Belaj, R. Pietschnig, *Dalton Trans.* **2009**, 163-167.
 - [139] C. A. Tolman, *Chem. Rev.* **1977**, 77, 313-348.
 - [140] J. I. van der Vlugt, M. M. P. Grutters, J. Ackerstaff, R. W. J. M. Hanssen, H. C. L. Abbenhuis, D. Vogt, *Tetrahedron Lett.* **2003**, 44, 8301-8305.
 - [141] T. E. Müller, D. M. P. Mingos, *Transition Met. Chem.* **1995**, 20, 533-539.
-

- [142] H. Clavier, S. P. Nolan, *Chem. Commun.* **2010**, 46, 841-861.
- [143] a) P. Jeleń, M. Szumera, M. Gawęda, E. Długon, M. Sitarz, *J. Therm. Anal. Calorim.* **2017**, 130, 103-111; b) B. Krüner, C. Odenwald, N. Jäckel, A. Tolosa, G. Kickelbick, V. Presser, *ACS Appl. Energy Mater.* **2018**, 1, 2961-2970.
- [144] a) D.-L. Zhou, J.-H. Li, Q.-Y. Guo, X. Lin, Q. Zhang, F. Chen, D. Han, Q. Fu, *Adv. Funct. Mater.* **2021**, 31, 2102074; b) X. Lin, Y.-Y. Deng, Q. Zhang, D. Han, Q. Fu, *Macromolecules* **2023**, 56, 1243-1252.
- [145] J. I. van der Vlugt, M. Fioroni, J. Ackerstaff, R. W. J. M. Hanssen, A. M. Mills, A. L. Spek, A. Meetsma, H. C. L. Abbenhuis, D. Vogt, *Organometallics* **2003**, 22, 5297-5306.
- [146] T. C. Johnstone, G. N. J. H. Wee, D. W. Stephan, *Angew. Chem.* **2018**, 130, 5983-5986; *Angew. Chem. Int. Ed.* **2018**, 57, 5881-5884.

6 Supporting Information

6.1 Interlinkage of a siliconoid with a silsesquioxane: en route to a molecular model system for silicon monoxide

Zeitschrift für anorganische und allgemeine Chemie

Supporting Information

Interlinkage of a siliconoid with a silsesquioxane: en route to a molecular model system for silicon monoxide

Marc Hunsicker, Nadine E. Poitiers, Volker Huch, Bernd Morgenstern, Michael Zimmer, and
David Scheschkewitz*

Zeitschrift für anorganische und allgemeine Chemie

Supporting Information

Interlinkage of a siliconoid with a silsesquioxane: en route to a molecular model system for silicon monoxide

Marc Hunsicker, Nadine E. Poitiers, Volker Huch, Bernd Morgenstern, Michael Zimmer,
David Scheschkewitz^[a]

Supporting Information for

Interlinkage of a siliconoid with a silsesquioxane: en route to a molecular model system for silicon monoxide

Marc Hunsicker, Nadine E. Poitiers, Volker Huch, Bernd Morgenstern, Michael Zimmer,
David Scheschkewitz^[a]

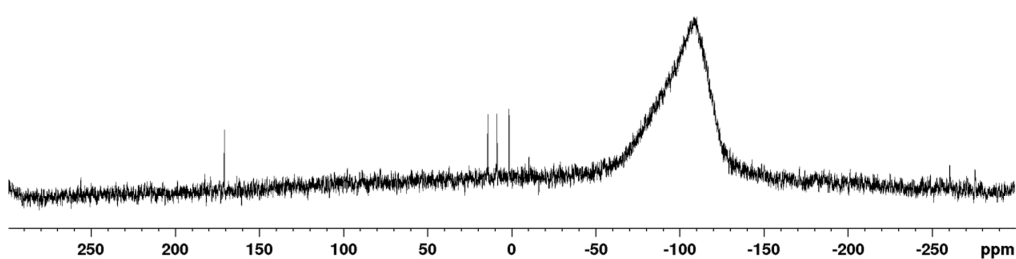
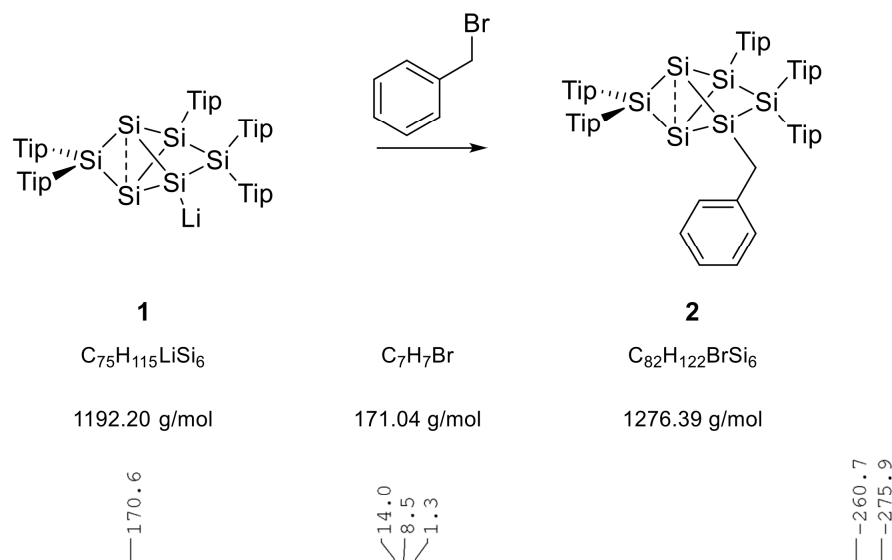
Table of Contents

| | | |
|---|--------------------------|-----|
| 1 | Plots of NMR Spectra | S3 |
| 2 | Plots of UV/vis Spectra | S27 |
| 3 | Crystallographic details | S33 |

[a] M. Sc. M. Hunsicker, Dr. N. E. Poitiers, Dr. V. Huch, Dr. B.
Morgenstern Dr. M. Zimmer,
Prof. Dr. D. Scheschkewitz
Krupp-Chair of Inorganic and General Chemistry
Saarland University
66123 Saarbrücken (Germany)
E-mail: scheschkewitz@mx.uni-saarland.de

Supporting information for this article is given via a link at the end of
the document.

1 Plots of NMR Spectra

Preparation of the benzyl-functionalized siliconoid **2**Figure S1. ^{29}Si NMR of benzyl-functionalized siliconoid **2** in benzene- D_6 at 300 K.

Deprotonation of Heptaphenyl trisilanol silsesquioxane with sodium hydride

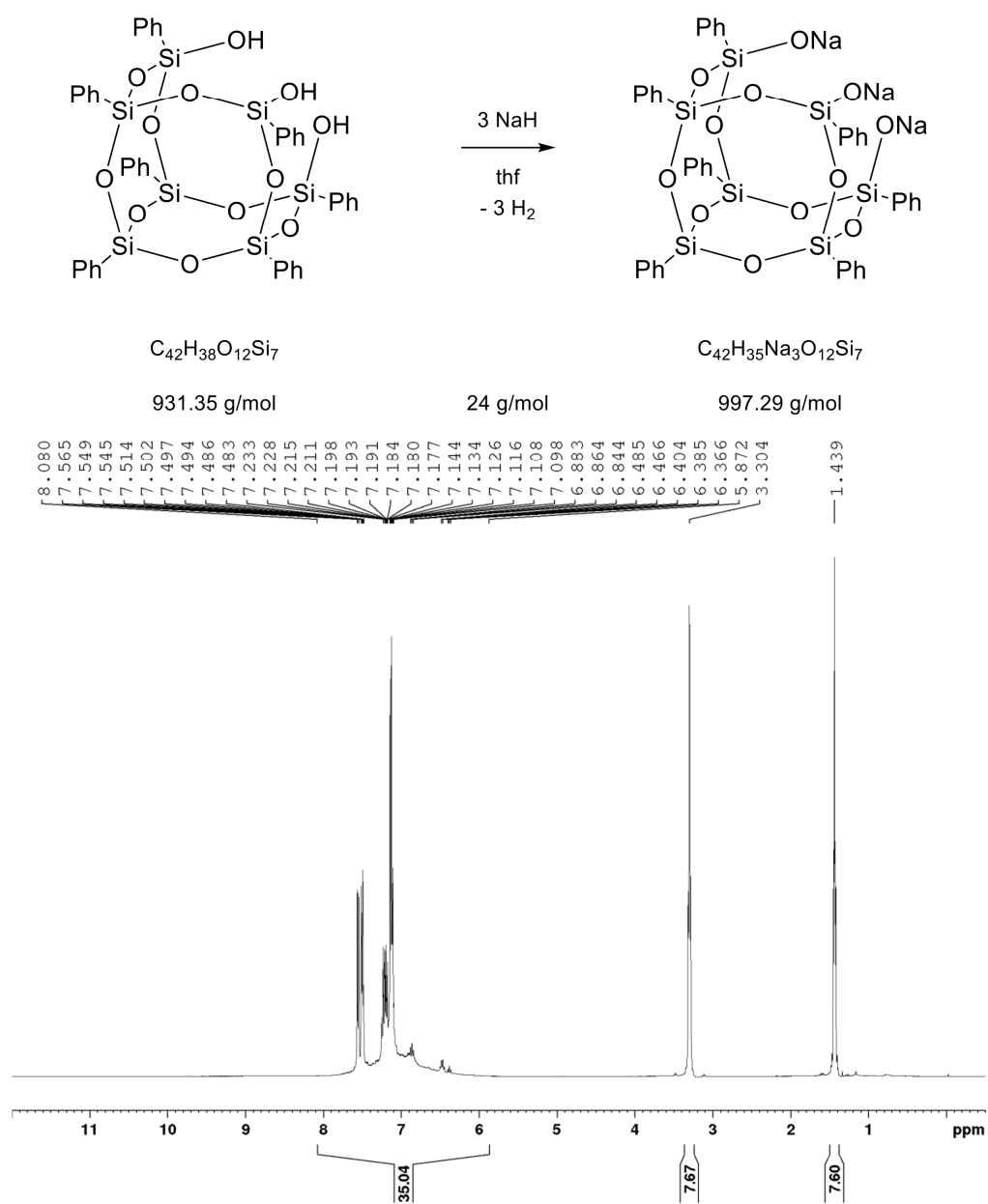
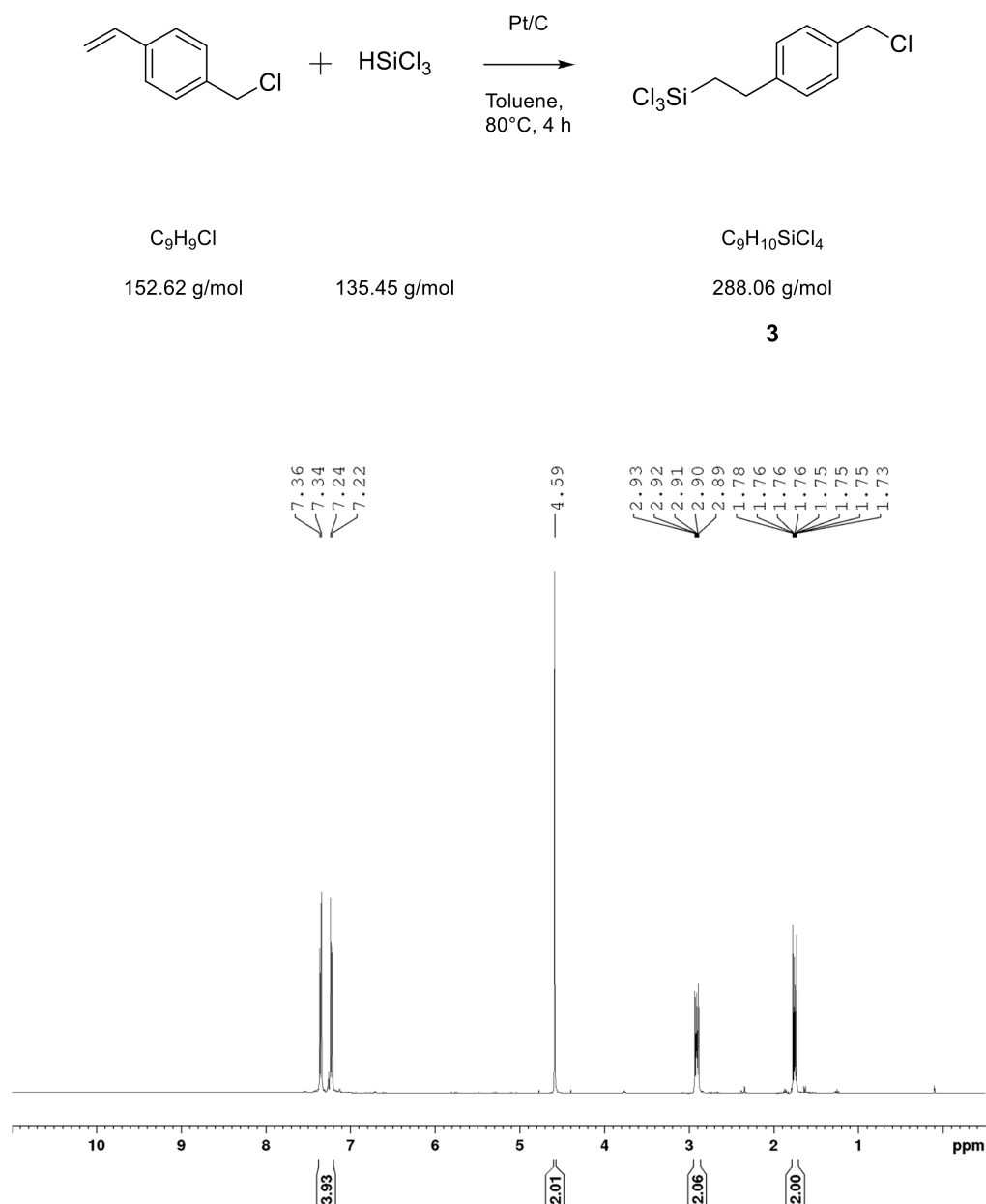


Figure S2. ¹H NMR of $\text{Ph}_7\text{T}_7(\text{ONa})_3$ in CDCl_3 at 300 K.

4-(Chloromethyl)phenethyltrichlorosilane **3**Figure S3. ^1H NMR of trichlorosilane **3** in CDCl_3 at 300 K.

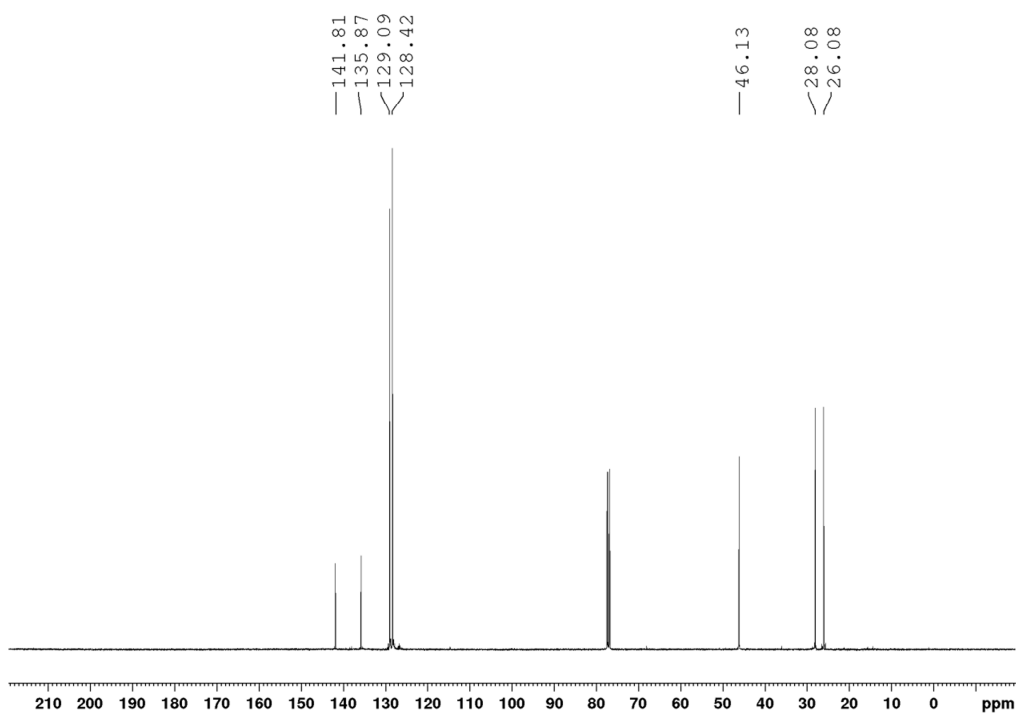


Figure S4. ^{13}C NMR of trichlorosilane **3** in CDCl_3 at 300 K.

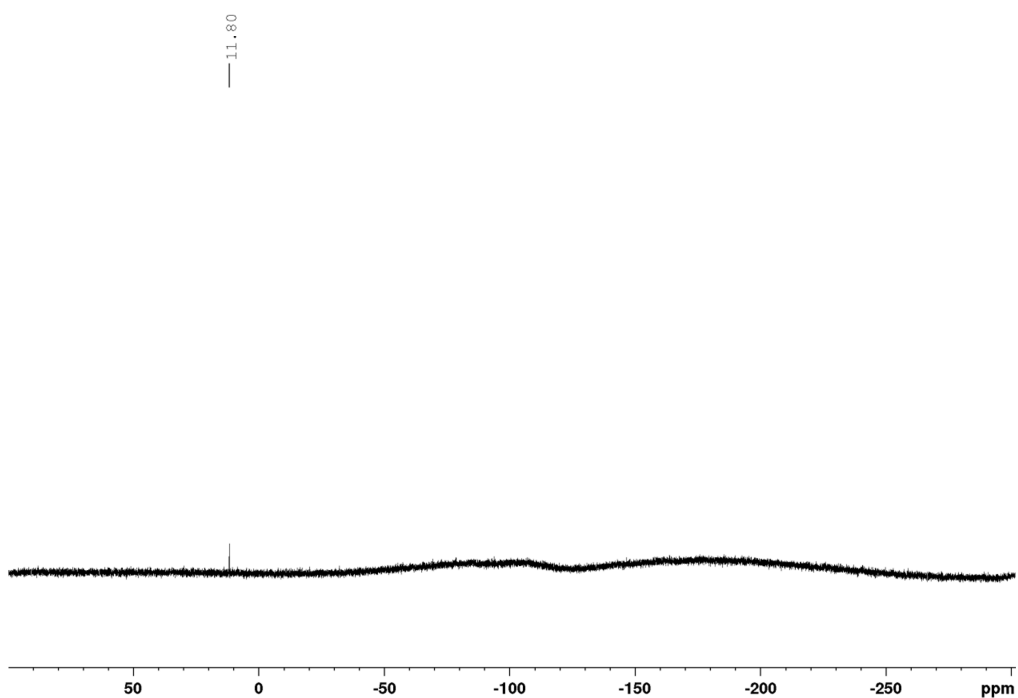
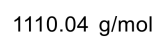
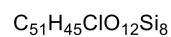


Figure S5. ^{29}Si NMR of trichlorosilane **3** in CDCl_3 at 300 K.



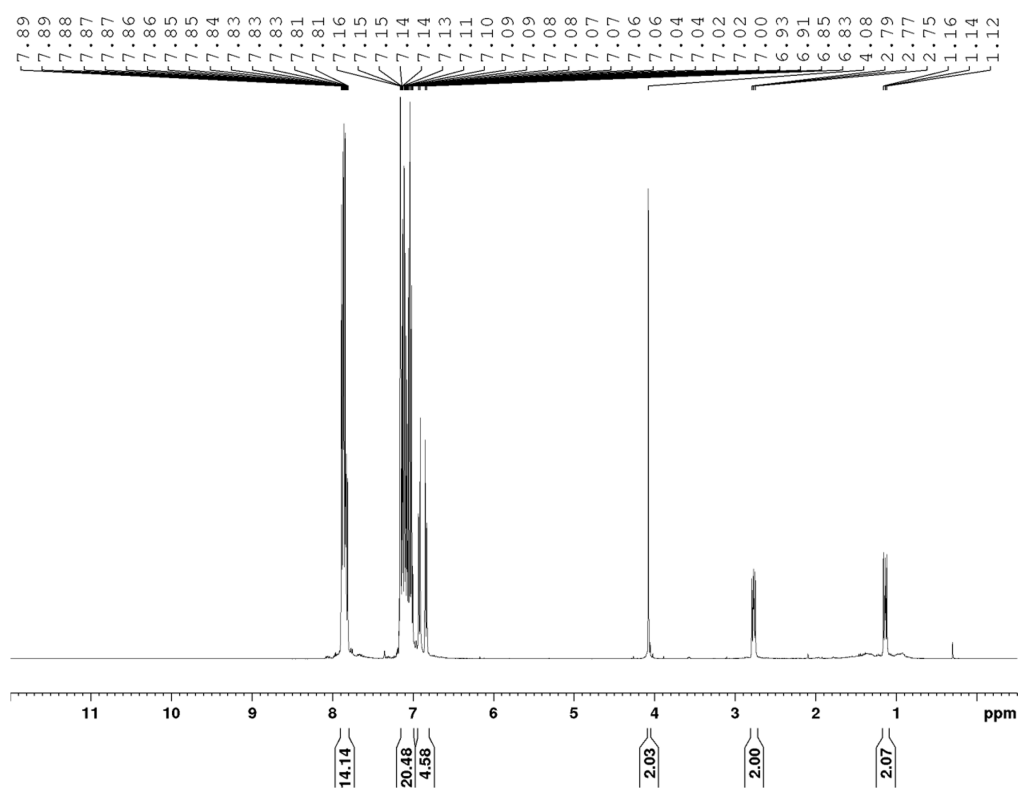


Figure S6. ^1H NMR of silsesquioxane **4** in benzene- D_6 at 300 K.

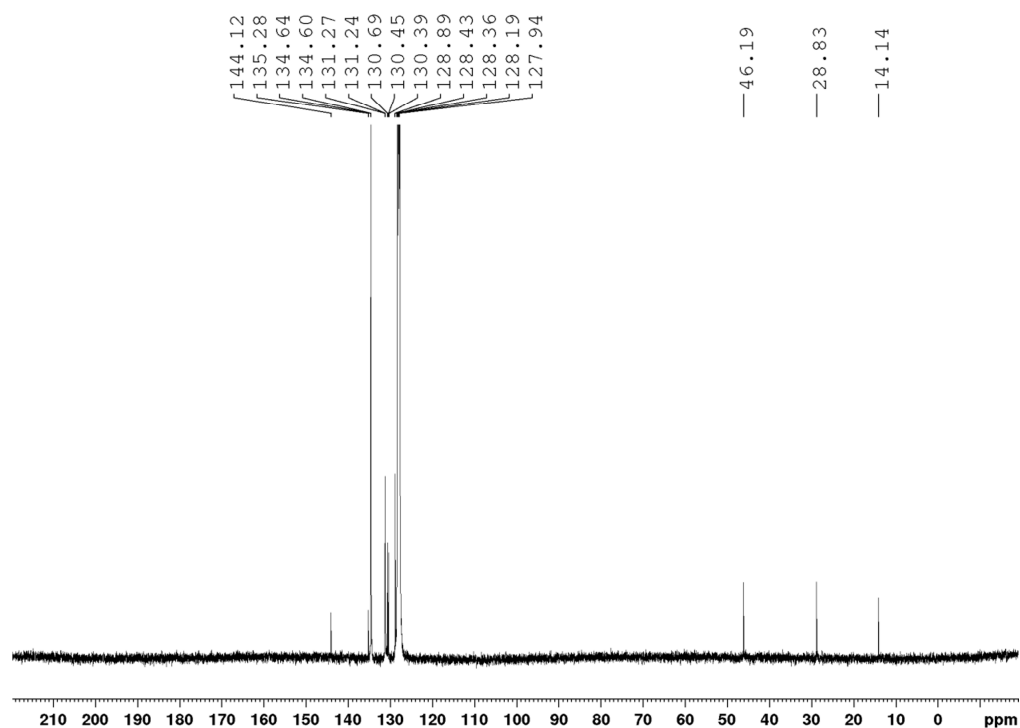


Figure S7. ¹³C NMR of silsesquioxane **4** in benzene-D₆ at 300 K.

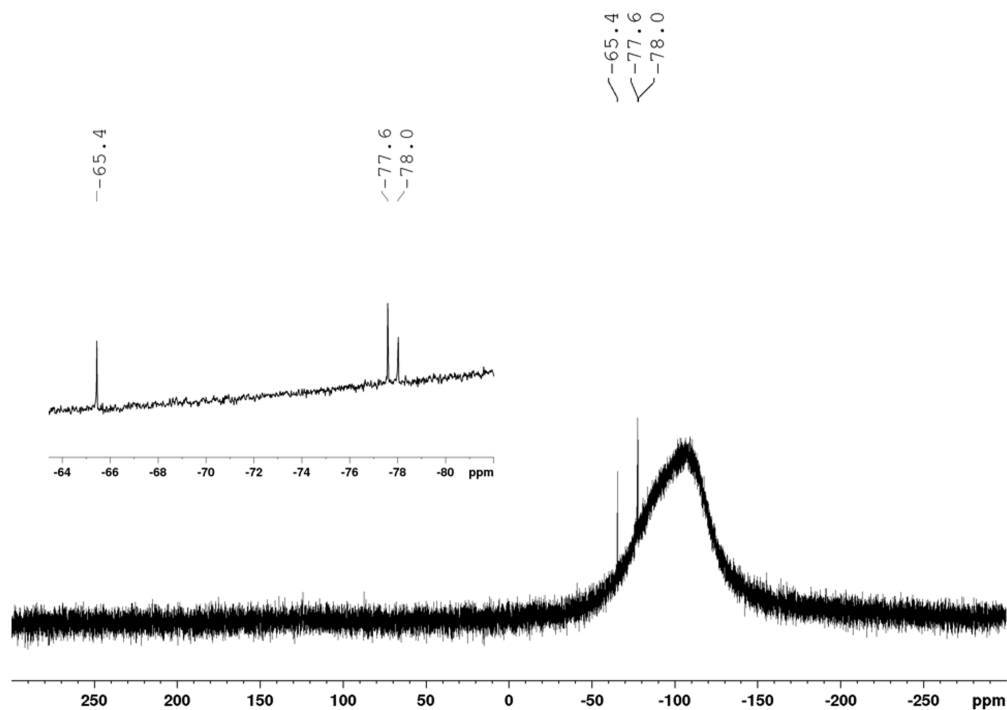


Figure S8. ²⁹Si NMR of silsesquioxane **4** in benzene-D₆ at 300 K.

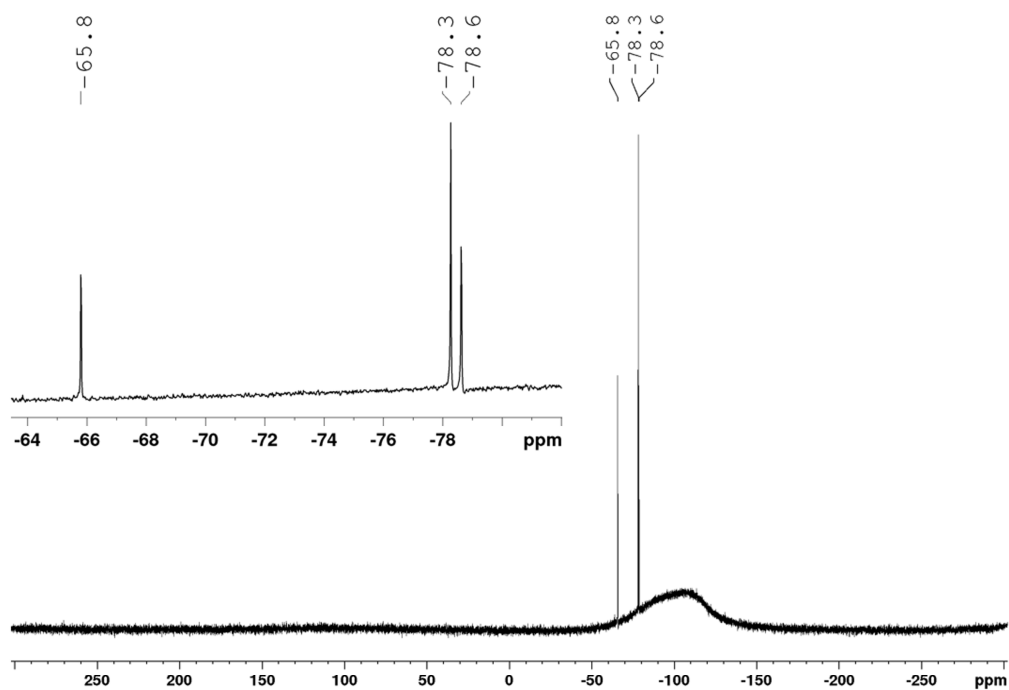


Figure S9. ^{29}Si NMR silsesquioxane **4** in CDCl_3 at 300 K.

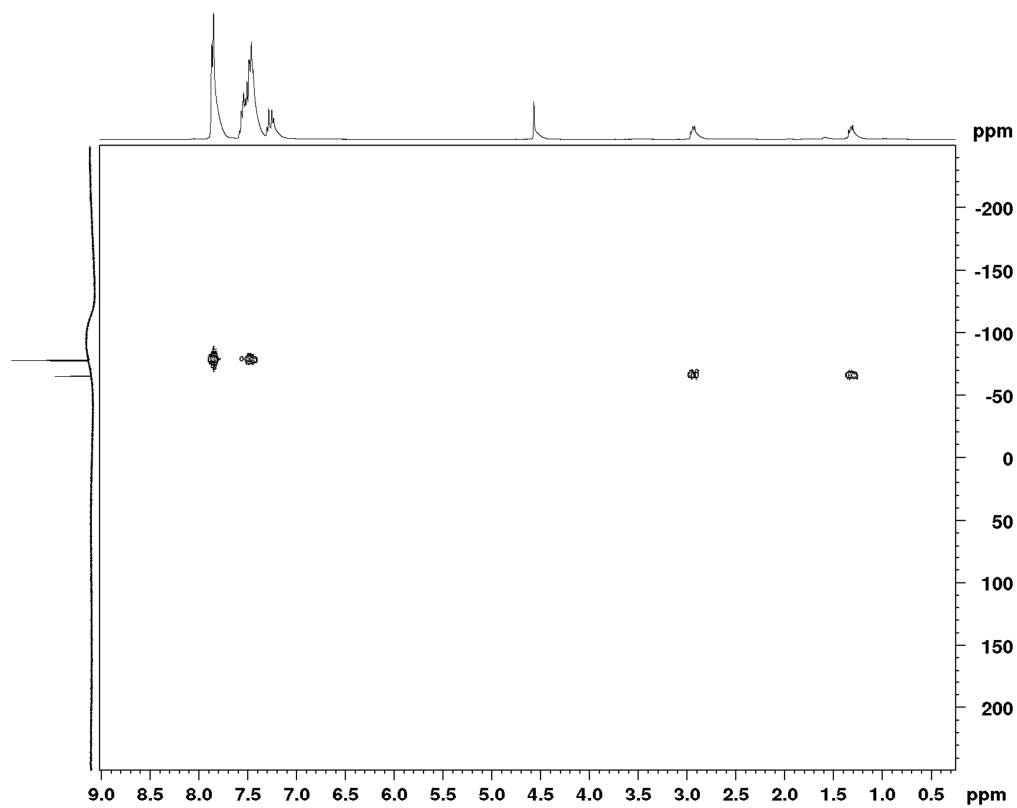
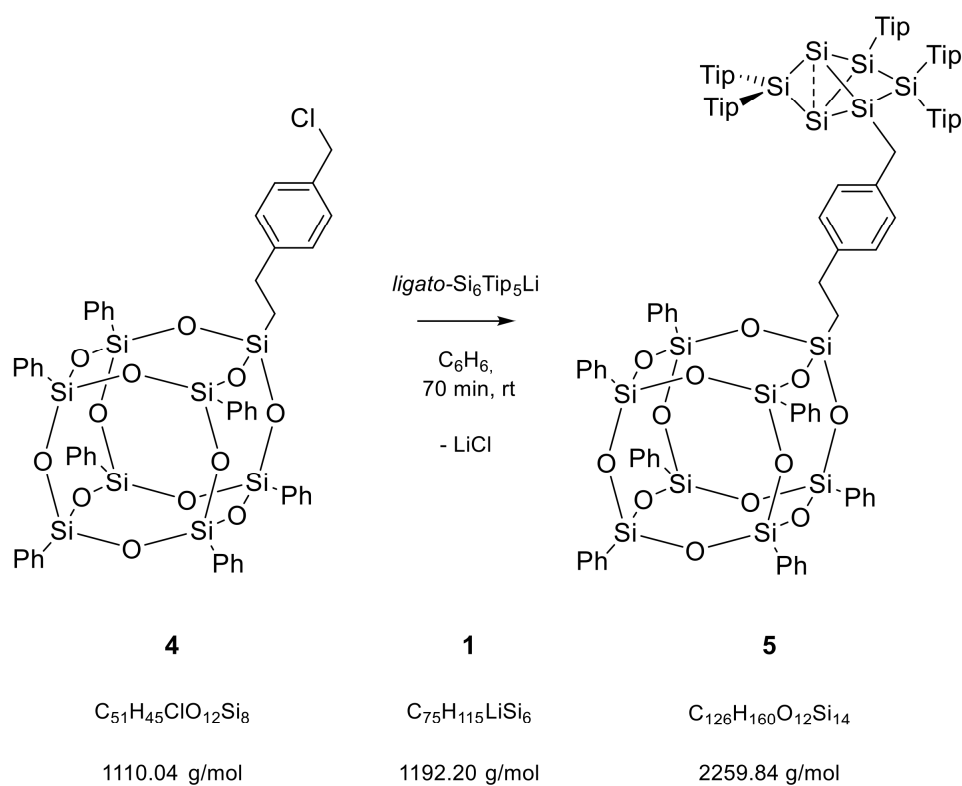


Figure S10. ^1H ^{29}Si correlation NMR experiment of silsesquioxane **4** in benzene- D_6 at 300 K.

Preparation of hybrid model system **5**



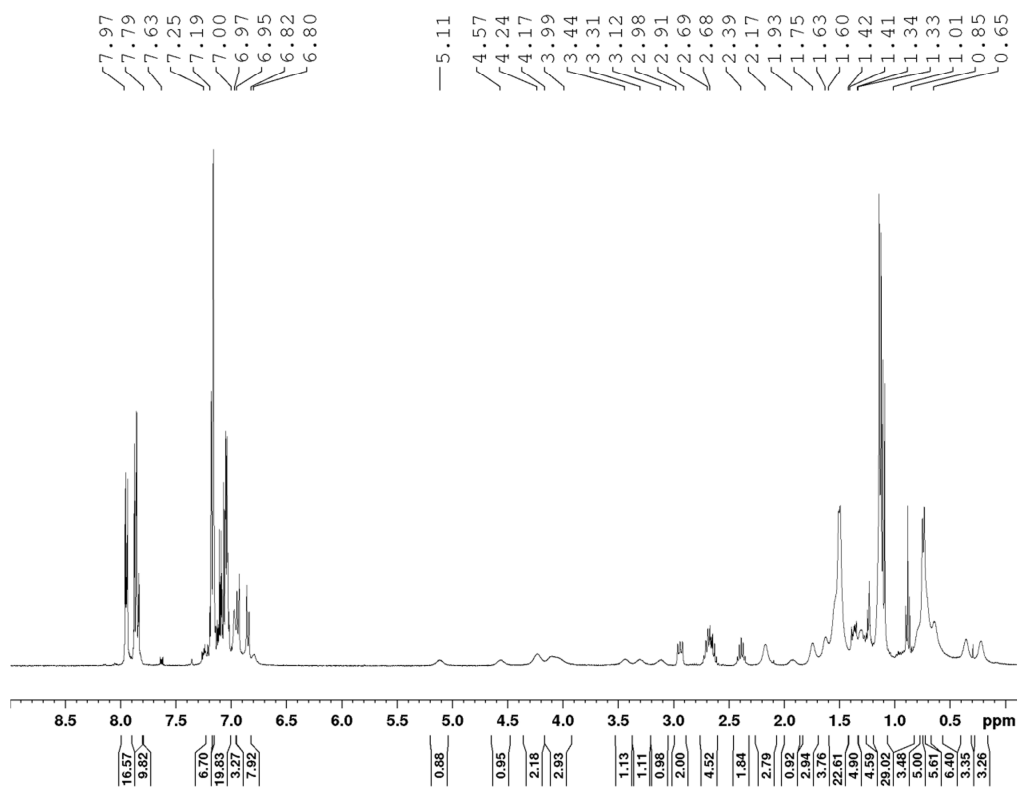


Figure S11. ¹H NMR of potential SiO model system 5 in benzene-D₆ at 300 K.

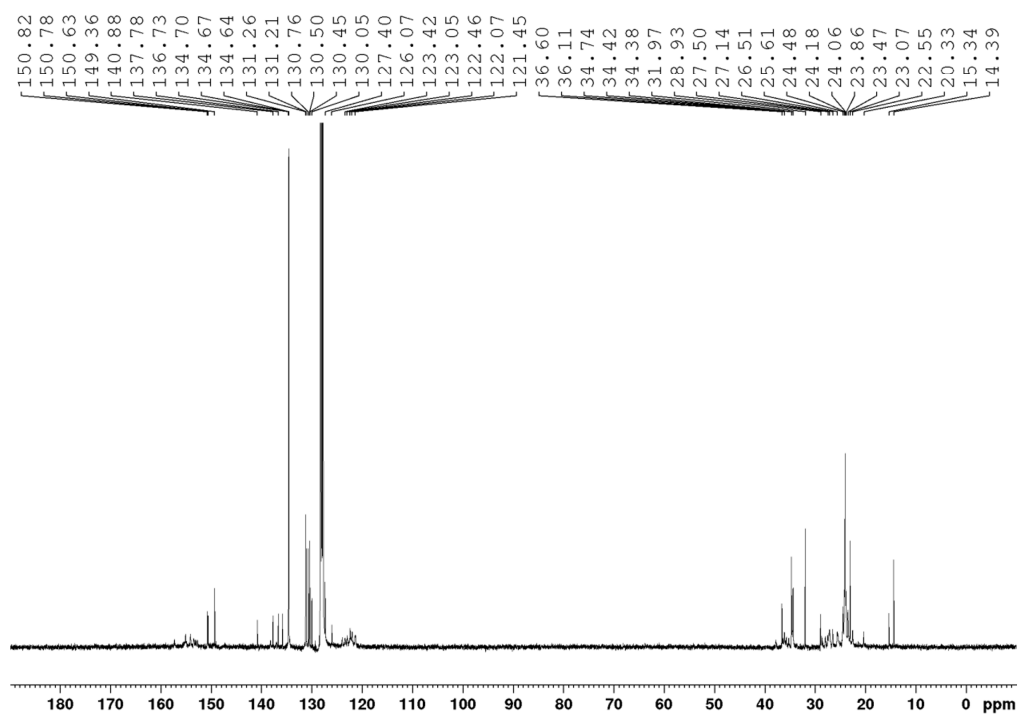


Figure S12. ^{13}C NMR of potential SiO model system 5 in benzene- D_6 at 300 K.

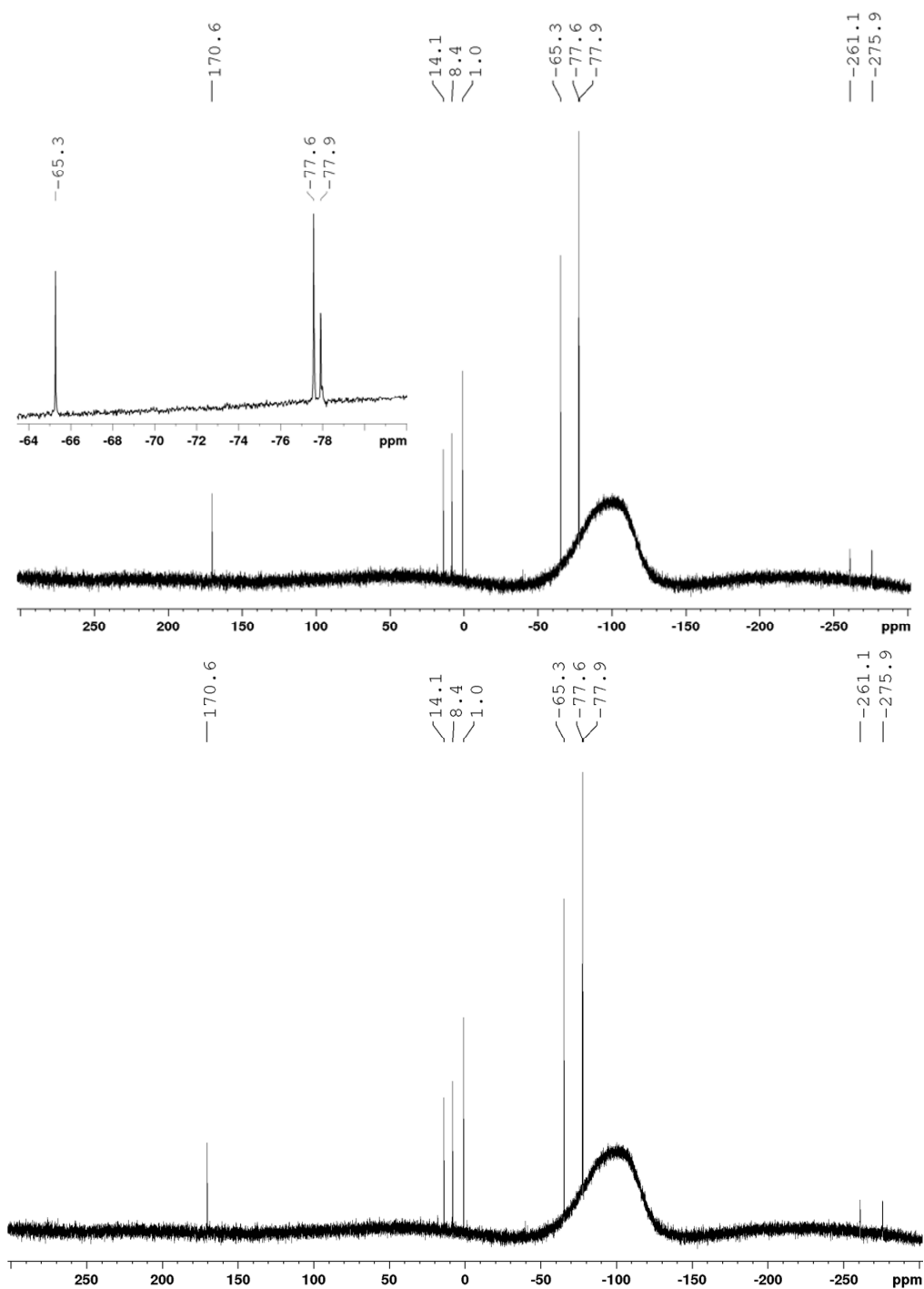


Figure S13. ^{29}Si NMR of potential SiO model system 5 in benzene- D_6 at 300 K.

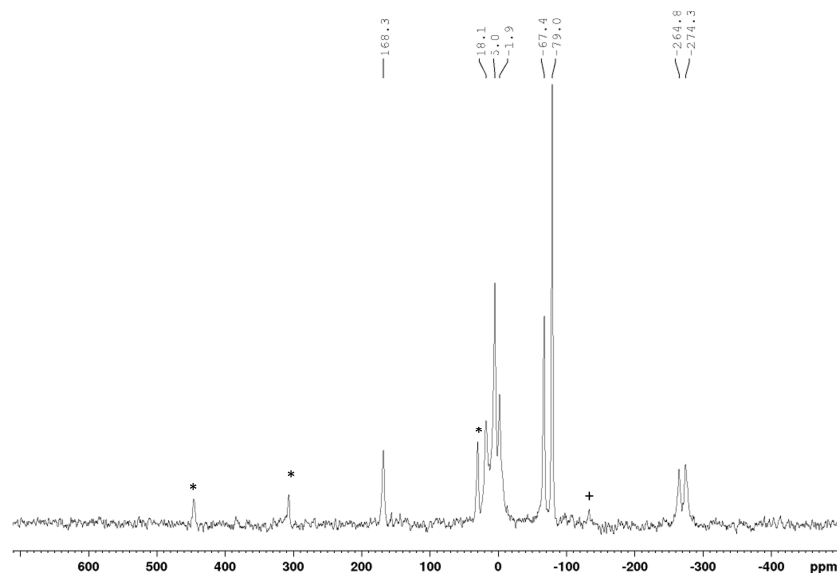
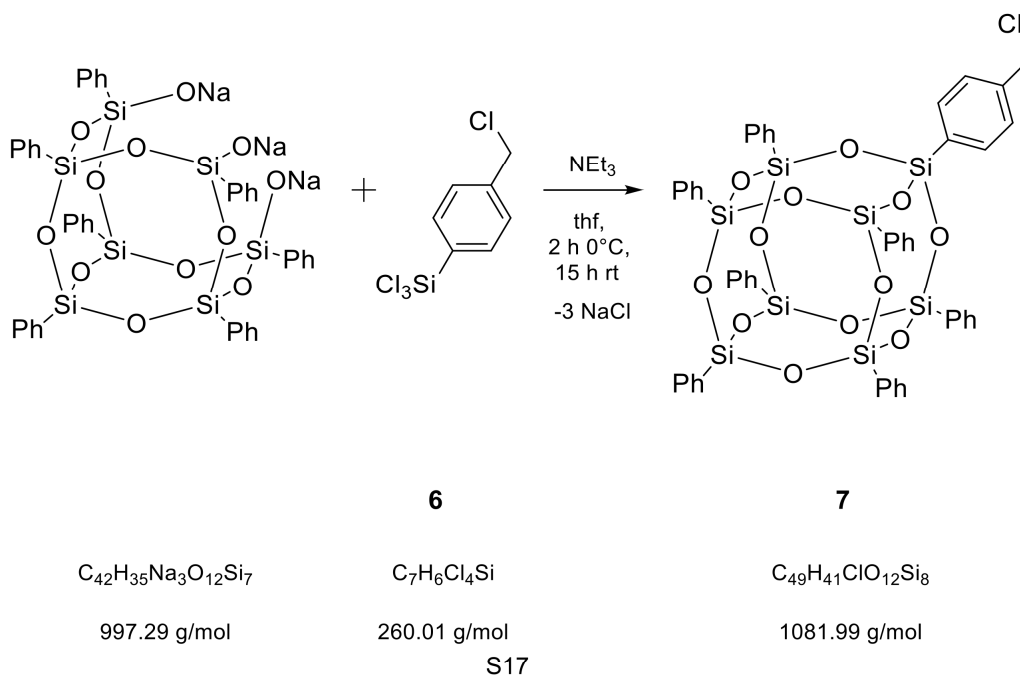


Figure S14. ^{29}Si /CP-MAS spectrum of compound potential SiO model system **5**. * side spinning bands of *privo*-SiTip₂ (168.3 ppm). + side spinning band of RSi₃Si (5.0 ppm).

Corner-capping reaction of T₇(ONa)₃ with 4-((chloromethyl)-phenyl)-trichlorosilane. Preparation of **7.**



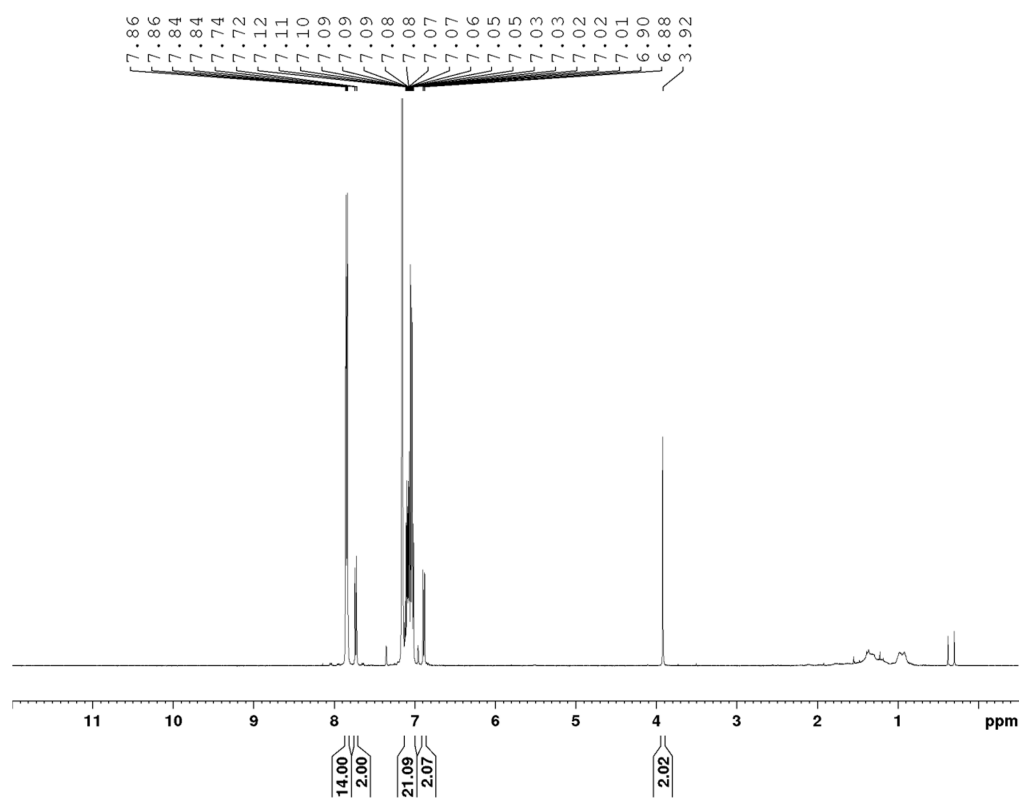


Figure S15 ^1H NMR of silsesquioxane **7** in benzene- D_6 at 300 K.

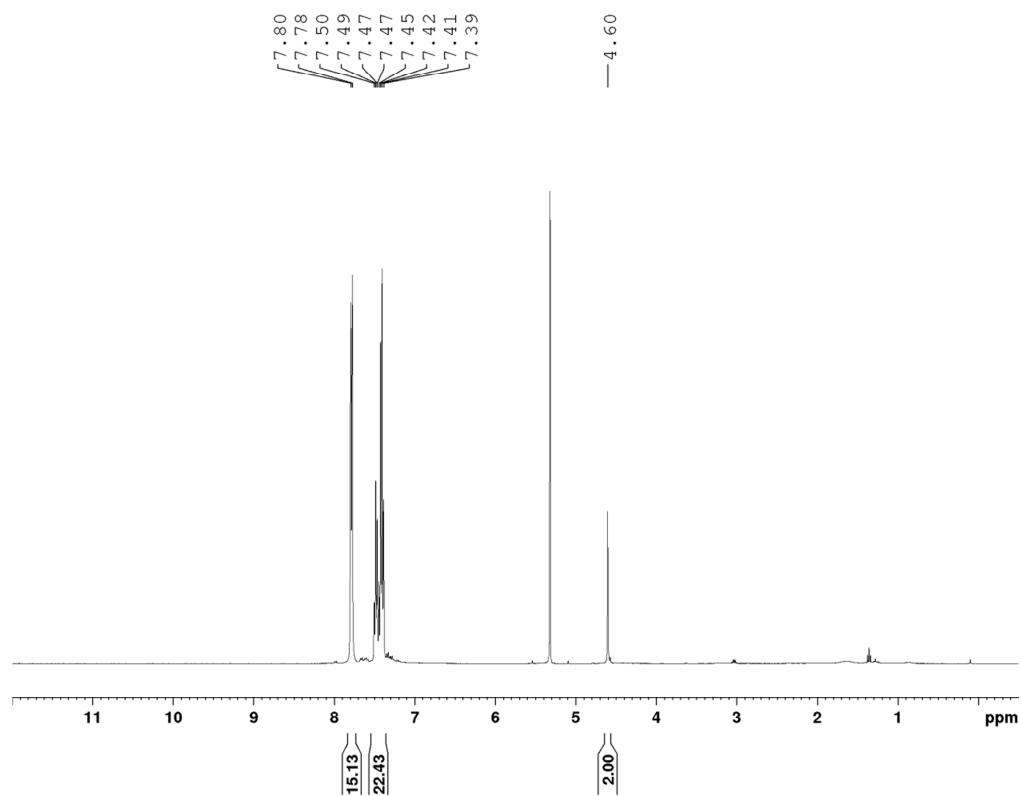


Figure S16. ^1H NMR of silsesquioxane **7** in CD_2Cl_2 at 300 K.

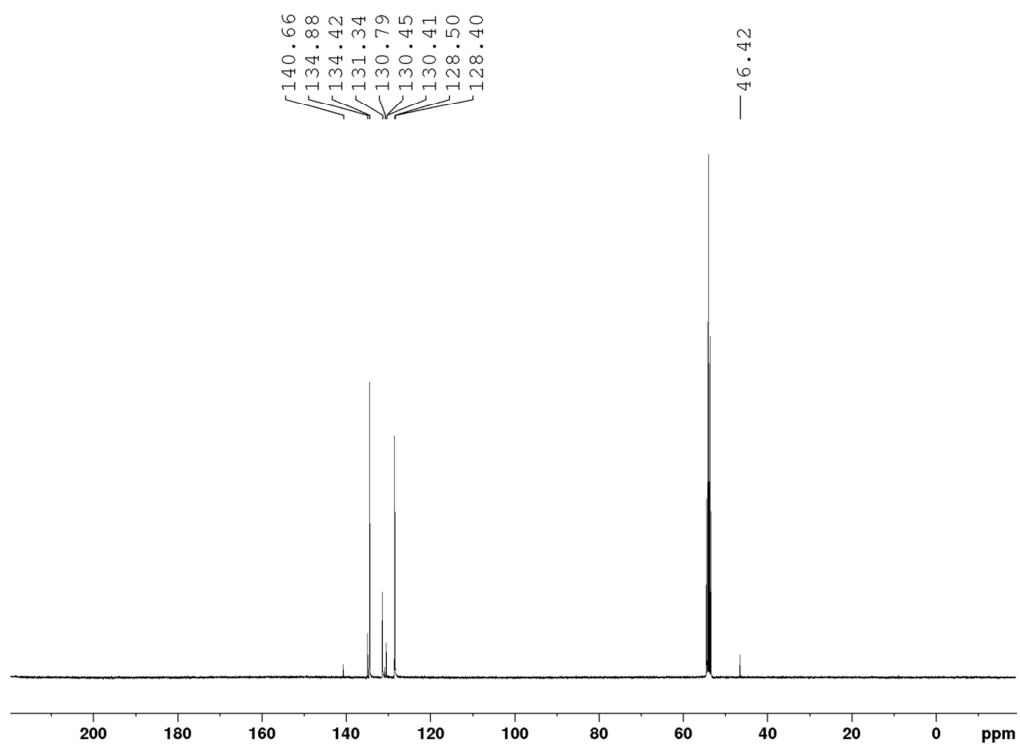


Figure S17. ^{13}C NMR of silsesquioxane **7** in CD_2Cl_2 at 300 K.

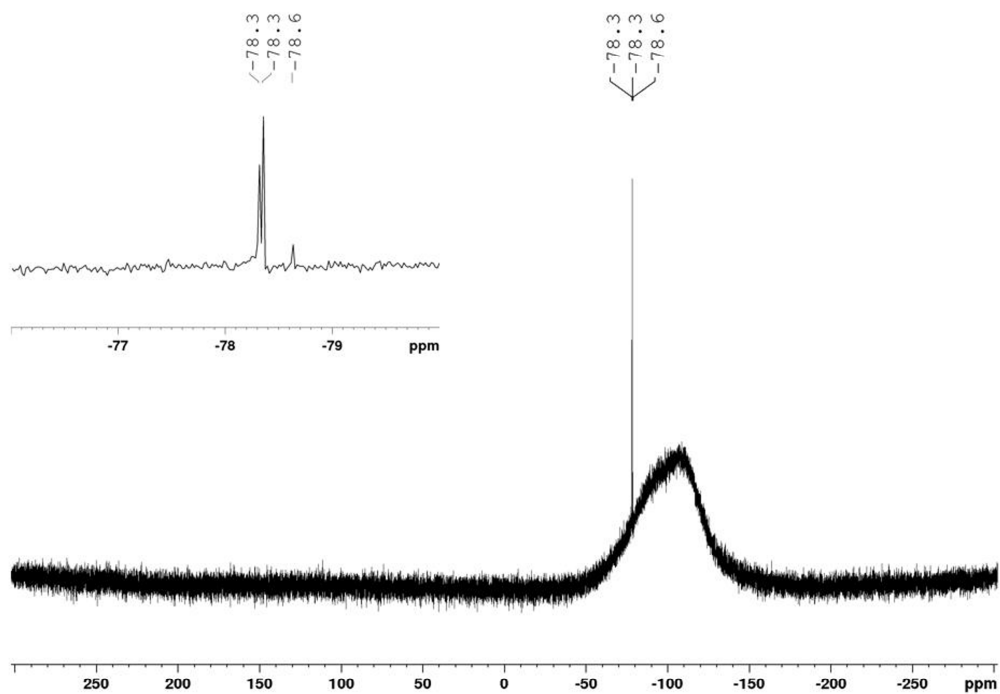


Figure S18. ^{29}Si NMR of silsesquioxane 7 in CD_2Cl_2 at 300 K.

Preparation of hybrid model system 8

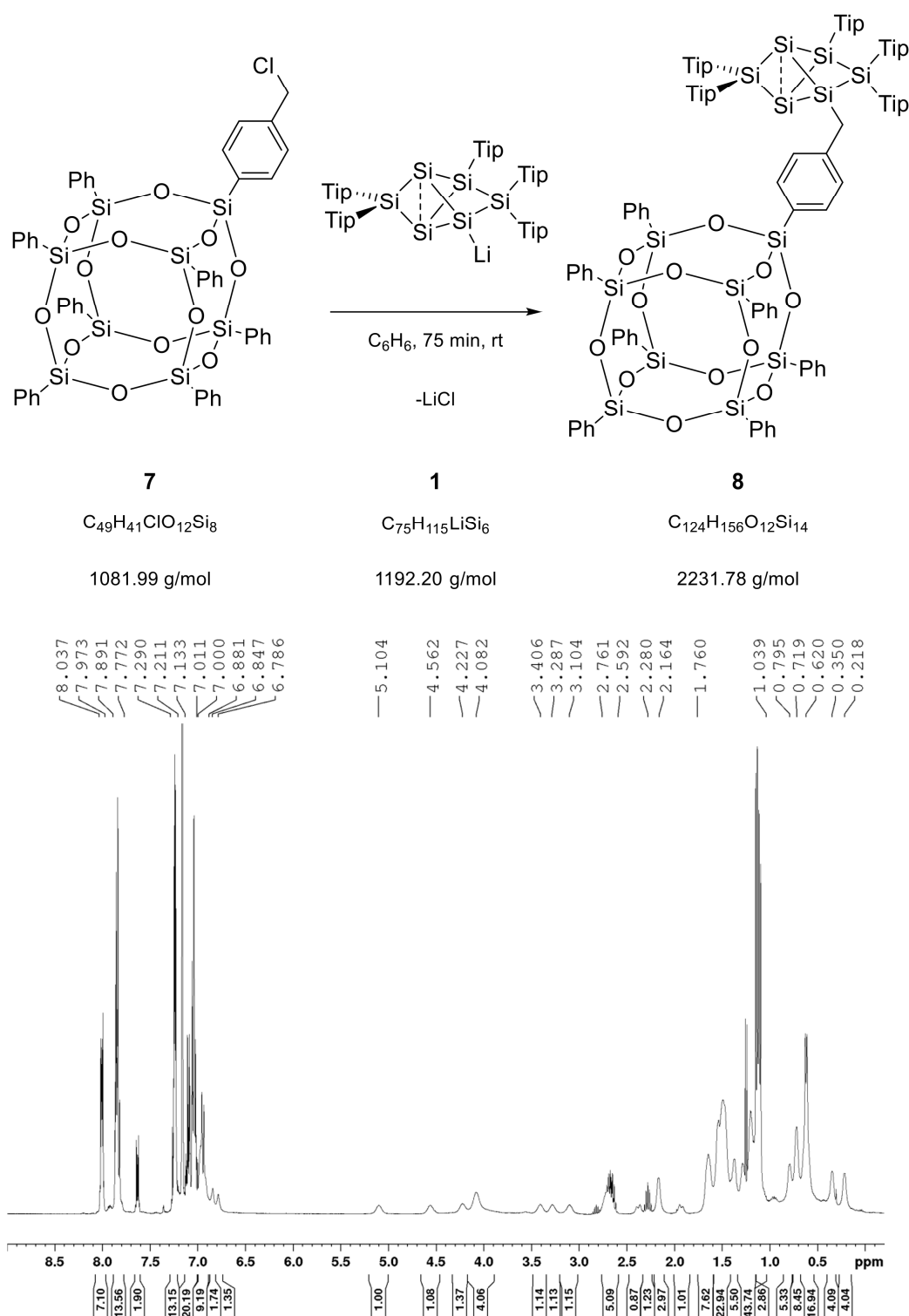


Figure S19. ¹H NMR of potential SiO model system **8** in benzene-D₆ at 300 K.

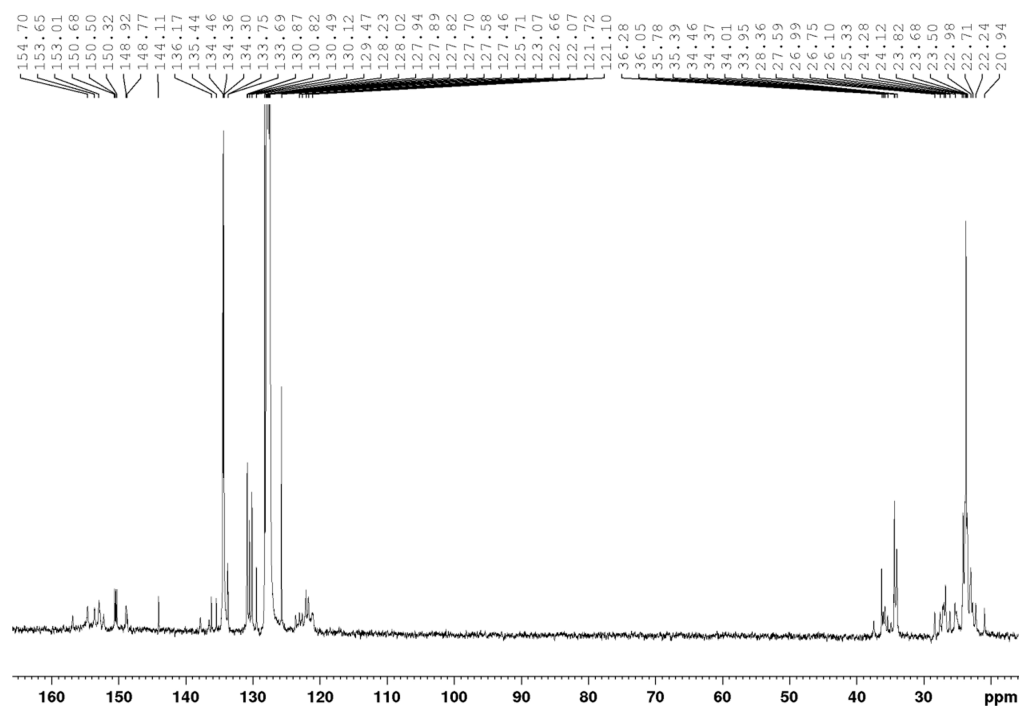


Figure S20. ^{13}C NMR of potential SiO model system **8** in benzene- D_6 at 300 K.

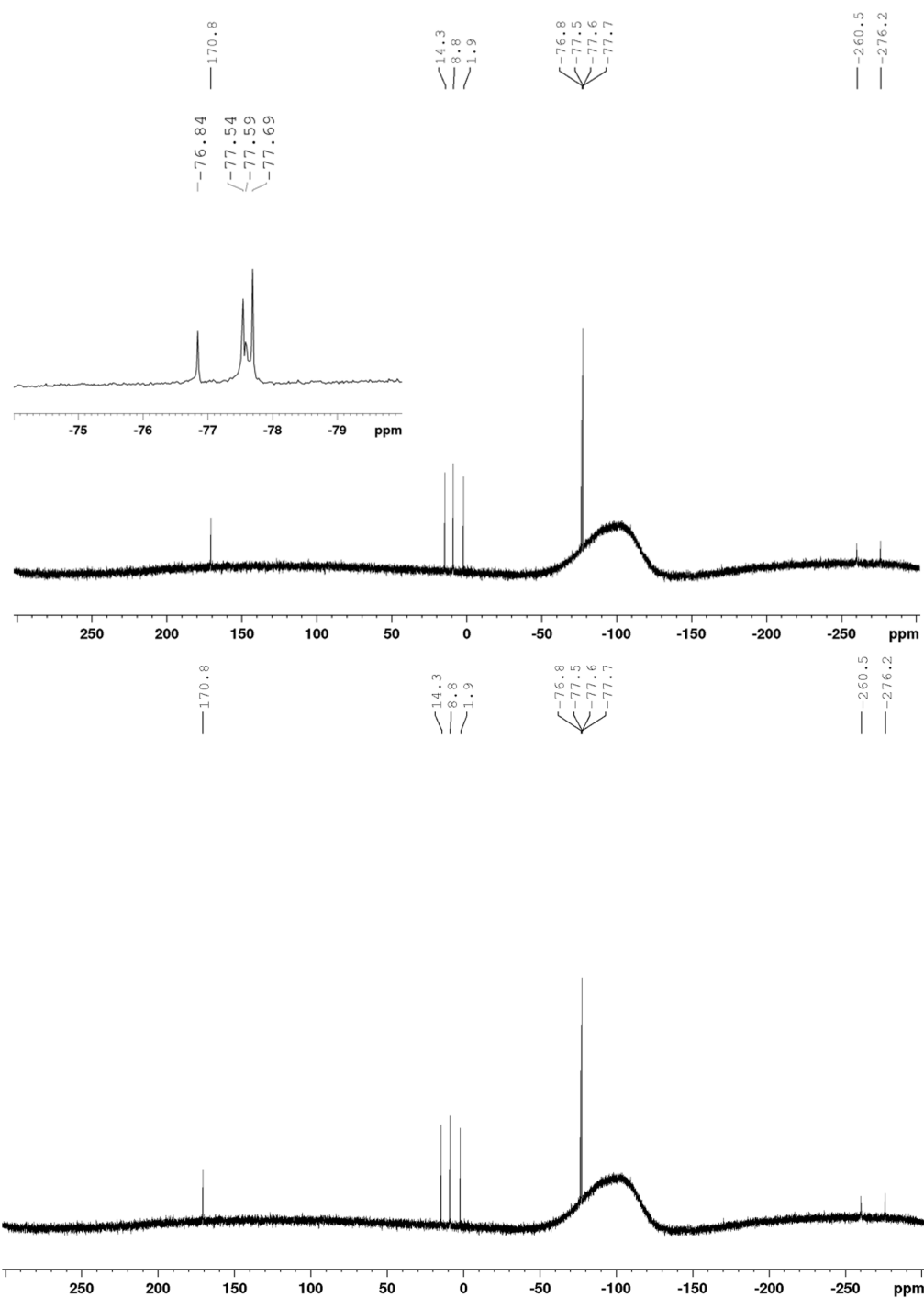


Figure S21. ^{29}Si NMR of potential SiO model system **8** in benzene- D_6 at 300 K.

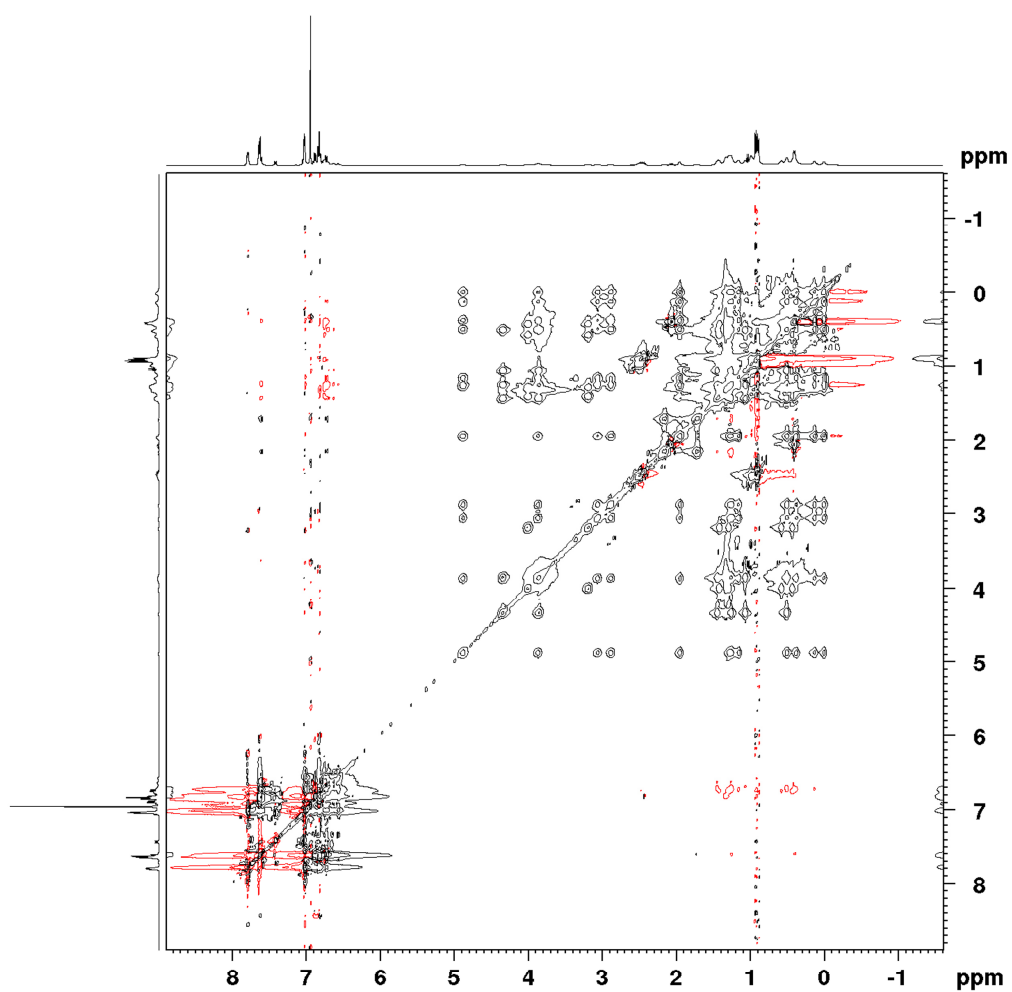


Figure S22. Total correlation experiment potential SiO model system **8** in benzene- D_6 at 300 K.

2 Plots of UV/vis spectra

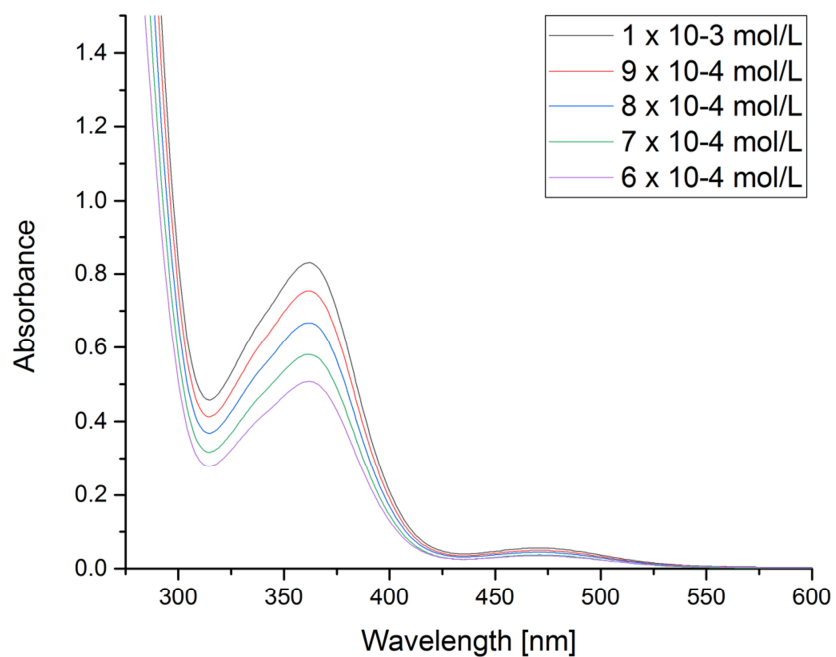


Figure S23. UV/vis spectra of potential SiO model system **5** in hexane at different concentrations

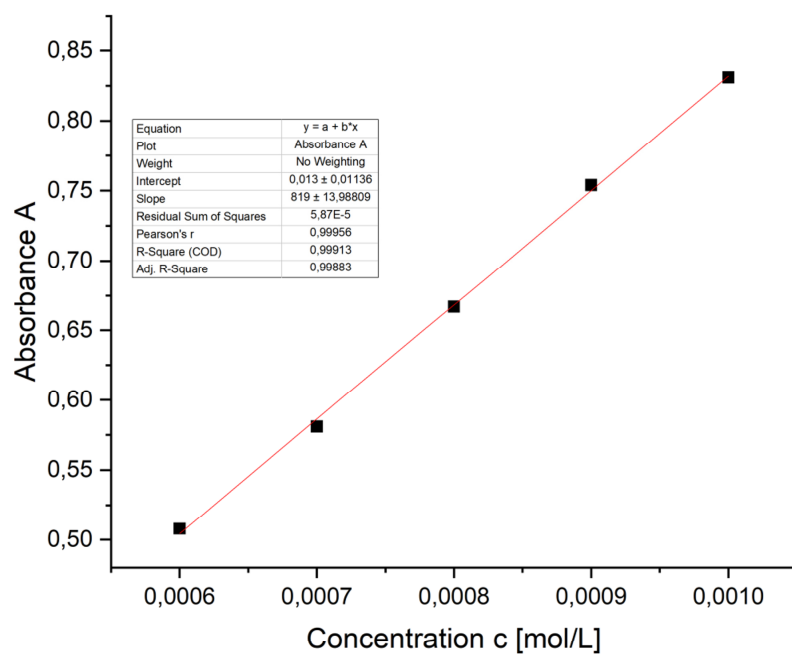


Figure S24. Determination of ϵ ($8190 \text{ M}^{-1}\text{cm}^{-1}$) by linear regression of absorptions (375 nm) of potential SiO model system **5** against concentration.

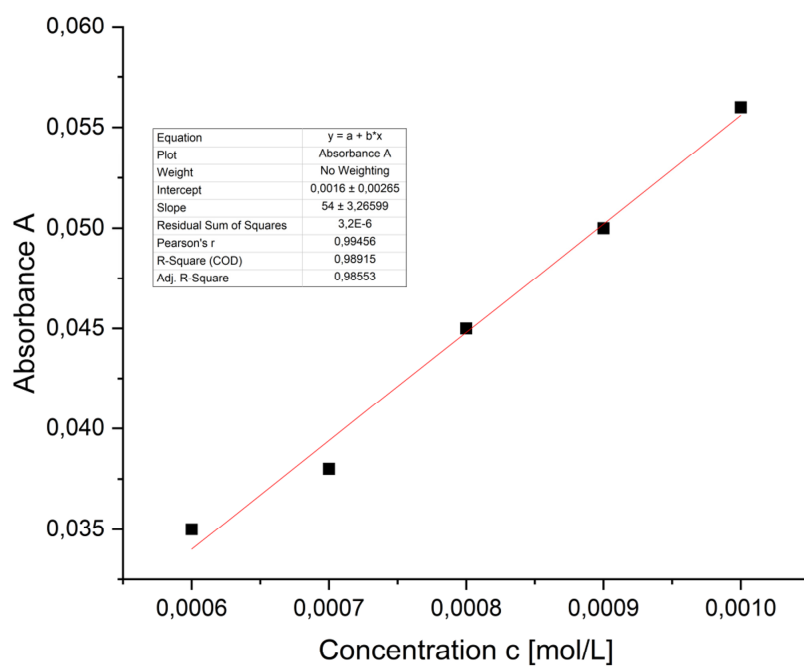


Figure S25. Determination of ϵ ($540 \text{ M}^{-1}\text{cm}^{-1}$) by linear regression of absorptions (470 nm) of potential SiO model system **5** against concentration.

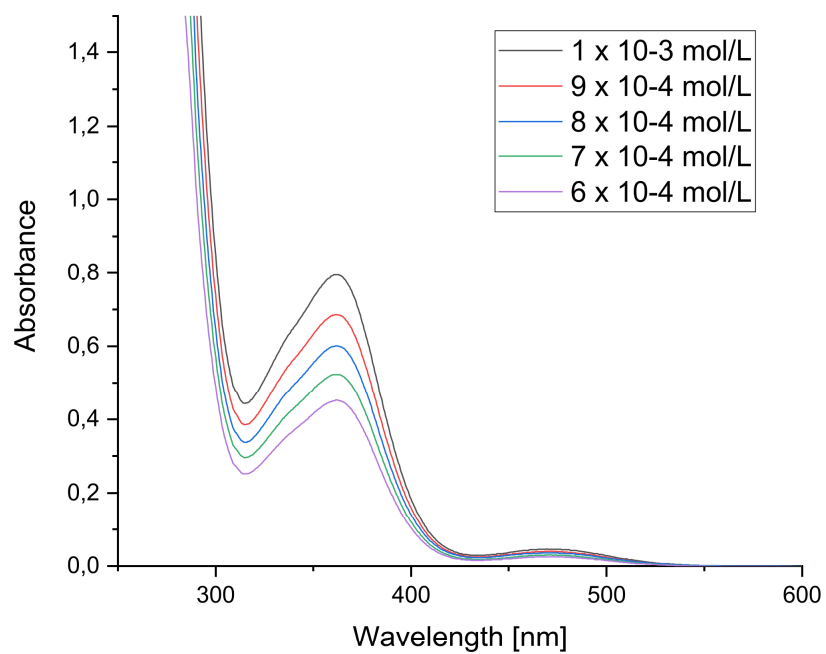


Figure S26. UV/VIS spectra of potential SiO model system **8** in hexane at different concentrations

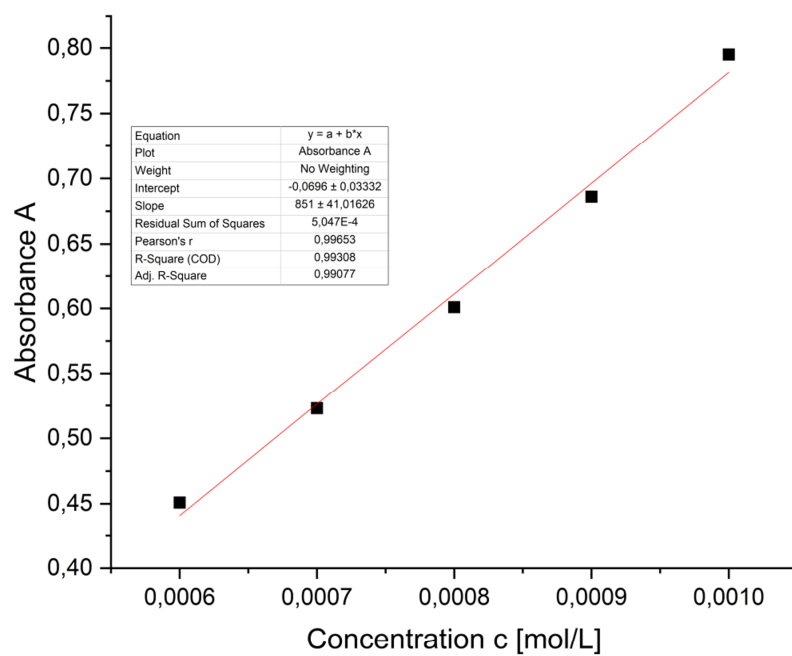


Figure S27. Determination of ϵ ($8510 \text{ M}^{-1}\text{cm}^{-1}$) by linear regression of absorptions (362 nm) of potential SiO model system **8** against concentration.

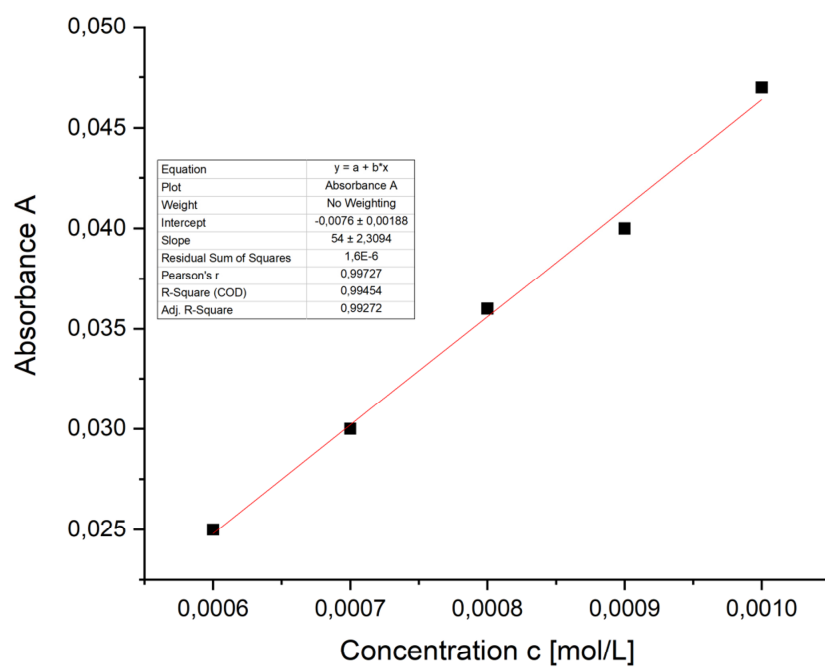


Figure S28. Determination of ϵ ($540 \text{ M}^{-1}\text{cm}^{-1}$) by linear regression of absorptions (470 nm) of potential SiO model system **8** against concentration.

3 Crystallographic data

Table 1. Crystal data and structure refinement for sh3725.

| | | |
|-----------------------------------|--|--------------------------------|
| Identification code | sh3725 | |
| Empirical formula | C ₁₇₉ H ₂₈₀ Si ₁₂ | |
| Formula weight | 2769.09 | |
| Temperature | 122(2) K | |
| Wavelength | 0.71073 Å | |
| Crystal system | Monoclinic | |
| Space group | P2 ₁ /c | |
| Unit cell dimensions | a = 24.8143(9) Å | $\alpha = 90^\circ$. |
| | b = 13.7674(5) Å | $\beta = 102.7690(10)^\circ$. |
| | c = 26.2617(9) Å | $\gamma = 90^\circ$. |
| Volume | 8749.9(5) Å ³ | |
| Z | 2 | |
| Density (calculated) | 1.051 Mg/m ³ | |
| Absorption coefficient | 0.136 mm ⁻¹ | |
| F(000) | 3044 | |
| Crystal size | 0.358 x 0.202 x 0.112 mm ³ | |
| Theta range for data collection | 1.590 to 28.785°. | |
| Index ranges | -33 ≤ h ≤ 33, -16 ≤ k ≤ 18, -35 ≤ l ≤ 27 | |
| Reflections collected | 92580 | |
| Independent reflections | 22663 [R(int) = 0.0690] | |
| Completeness to theta = 25.242° | 100.0 % | |
| Absorption correction | Semi-empirical from equivalents | |
| Max. and min. transmission | 0.7458 and 0.6953 | |
| Refinement method | Full-matrix least-squares on F ² | |
| Data / restraints / parameters | 22663 / 799 / 982 | |
| Goodness-of-fit on F ² | 1.029 | |
| Final R indices [I > 2σ(I)] | R1 = 0.0538, wR2 = 0.1205 | |
| R indices (all data) | R1 = 0.1013, wR2 = 0.1403 | |
| Extinction coefficient | n/a | |
| Largest diff. peak and hole | 0.682 and -0.395 e.Å ⁻³ | |

Refinement details for sh3725:

All non H-atoms were located in the electron density maps and refined anisotropically. C-bound H atoms were placed in positions of optimized geometry and treated as riding atoms. Their isotropic displacement parameters were coupled to the corresponding carrier atoms by a factor of 1.2 (CH, CH₂) or 1.5 (CH₃). One isopropyl-group and one n-pentane solvent molecules were split over two positions. Their occupancy factors refined to 0.44 and 0.70, respectively. One n-pentane solvent was split over a center of inversion using PART -1. Its occupancy factors were set to 10.5.

Table 2. Crystal data and structure refinement for sh4243a_sq.

| | | |
|-----------------------------------|--|---|
| Identification code | sh4243a_sq | |
| Empirical formula | C142.50 H186 O12 Si14 | |
| Formula weight | 2484.16 | |
| Temperature | 130(2) K | |
| Wavelength | 0.71073 Å | |
| Crystal system | Triclinic | |
| Space group | P-1 | |
| Unit cell dimensions | a = 15.5337(5) Å b = 21.1596(7) Å c = 24.3408(8) Å | $\alpha = 71.4690(10)^\circ$ $\beta = 82.8310(10)^\circ$ $\gamma = 69.1110(10)^\circ$ |
| Volume | 7086.5(4) Å ³ | |
| Z | 2 | |
| Density (calculated) | 1.164 Mg/m ³ | |
| Absorption coefficient | 0.183 mm ⁻¹ | |
| F(000) | 2666 | |
| Crystal size | 0.283 x 0.194 x 0.076 mm ³ | |
| Theta range for data collection | 2.010 to 25.681° | |
| Index ranges | -18 ≤ h ≤ 18, -25 ≤ k ≤ 25, -29 ≤ l ≤ 29 | |
| Reflections collected | 126353 | |
| Independent reflections | 26889 [R(int) = 0.0824] | |
| Completeness to theta = 25.242° | 99.9 % | |
| Absorption correction | Semi-empirical from equivalents | |
| Max. and min. transmission | 0.7454 and 0.7022 | |
| Refinement method | Full-matrix least-squares on F ² | |
| Data / restraints / parameters | 26889 / 714 / 1546 | |
| Goodness-of-fit on F ² | 1.044 | |
| Final R indices [I > 2σ(I)] | R1 = 0.0532, wR2 = 0.1314 | |
| R indices (all data) | R1 = 0.0850, wR2 = 0.1502 | |
| Extinction coefficient | n/a | |
| Largest diff. peak and hole | 0.667 and -0.552 e.Å ⁻³ | |

Refinement details for sh4243a_sq:

All non H-atoms were located in the electron density maps and refined anisotropically. C-bound H atoms were placed in positions of optimized geometry and treated as riding atoms. Their isotropic displacement parameters were coupled to the corresponding carrier atoms by a factor of 1.2 (CH, CH₂) or 1.5 (CH₃). The structure was first refined using isotropic displacement parameters for two toluene and one n-hexane solvent molecules in the asymmetric unit. The occupancy factors of these solvent molecules refine to a value of approximately 1.5 toluene and one hexane. The solvent molecules have been treated as a diffuse contribution to the overall scattering without specific atom positions by SQUEEZE/PLATON. In a final refinement procedure SQUEEZE found 246e (V = 1281 Å³), which is in good agreement with the suggested solvent (calcd: 250e)

6.2 Polyhedral Oligomeric Silsesquioxane D_{3h} -(RsiO_{1.5})₁₄

Chemistry–A European Journal

Supporting Information

Polyhedral Oligomeric Silsesquioxane D_{3h} -(RSiO_{1.5})₁₄

Marc Hunsicker, Ankur, Bernd Morgenstern, Michael Zimmer, and David Scheschkewitz*

SUPPORTING INFORMATION

Table of Contents

| | |
|--|----|
| 1. NMR and IR spectra..... | 1 |
| 2. Thermal Analysis..... | 6 |
| 3. Crystallographic data..... | 8 |
| 3.1 Refinement Details for $T_{14}Ph_{14}$ | 8 |
| 3.2 Refinement Details for $T_7Ph_7(OTf)_3$ | 9 |
| 3.3 Overlap of the $T_{14}Ph_{14}$ units in the asymmetric unit..... | 10 |
| 4. Computational details..... | 11 |

1. NMR and IR spectra

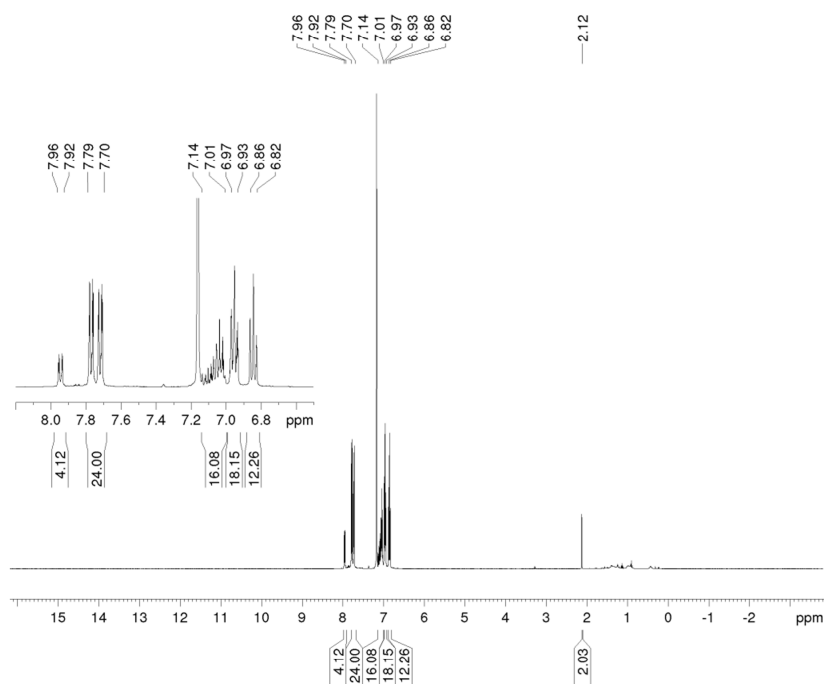
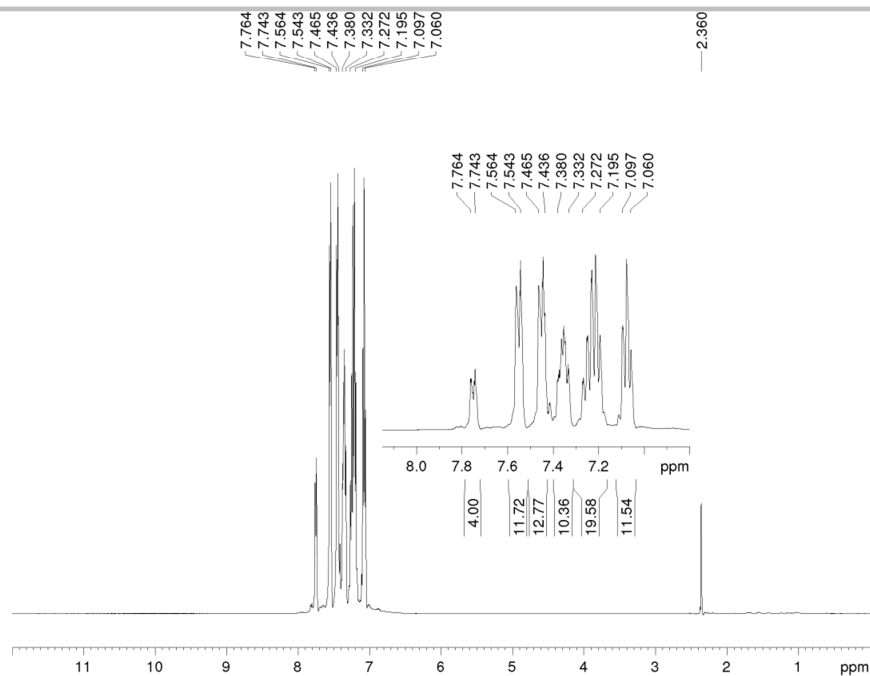
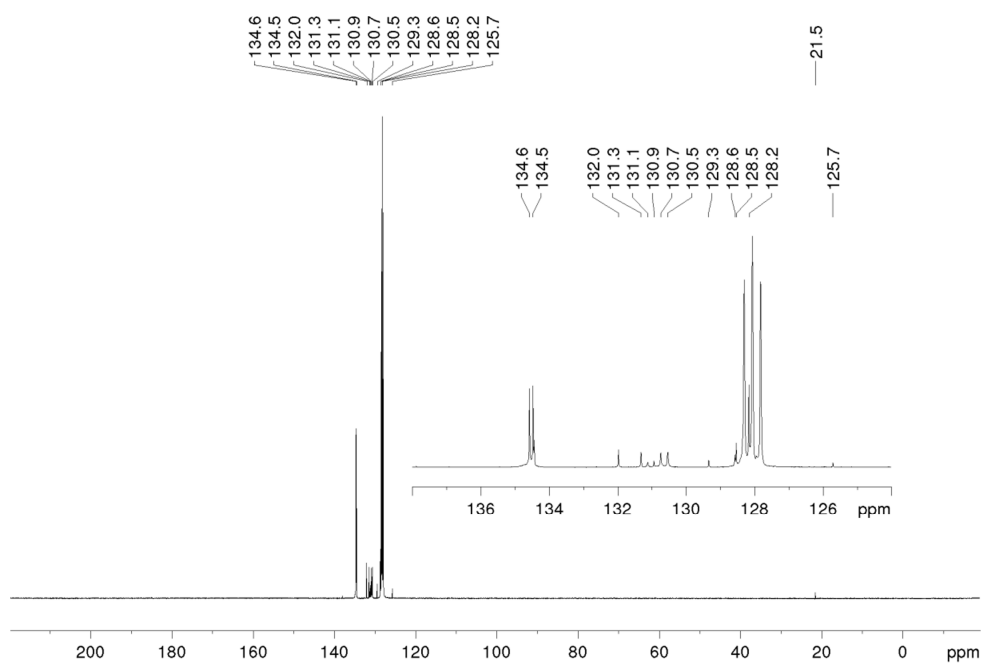


Figure S1. 1H NMR spectrum of $T_{14}Ph_{14}$ measured in benzene- d_6 at 300 K.

SUPPORTING INFORMATION

Figure S2. ¹H NMR of T₁₄Ph₁₄ in chloroform-d at 300 K.Figure S3. ¹³C NMR of T₁₄Ph₁₄ in benzene-d₆ at 300 K.

SUPPORTING INFORMATION

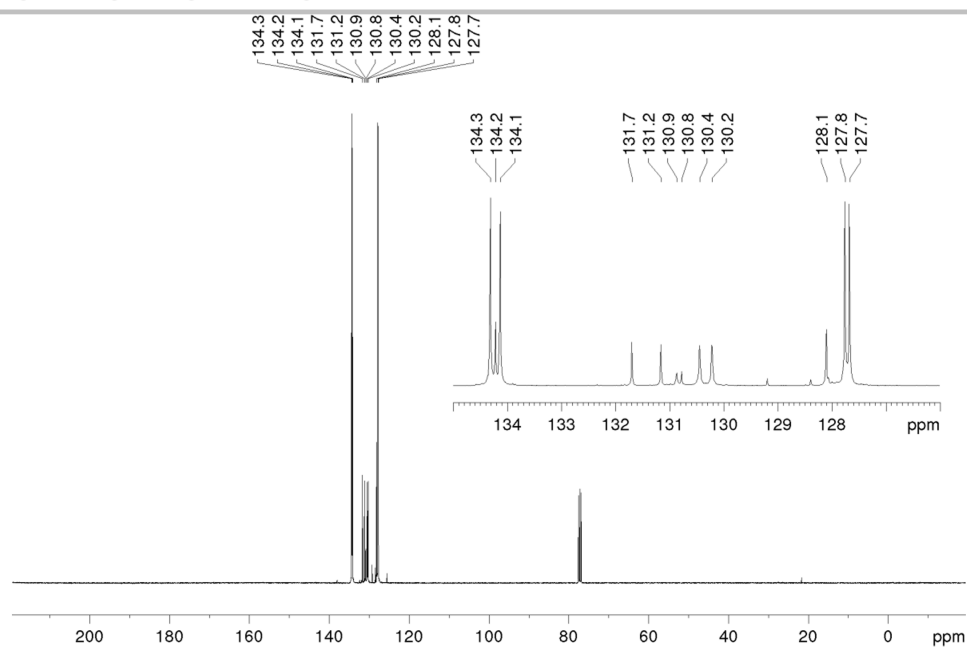


Figure S4. ^{13}C NMR of $\text{T}_{14}\text{Ph}_{14}$ in chloroform- d at 300 K.

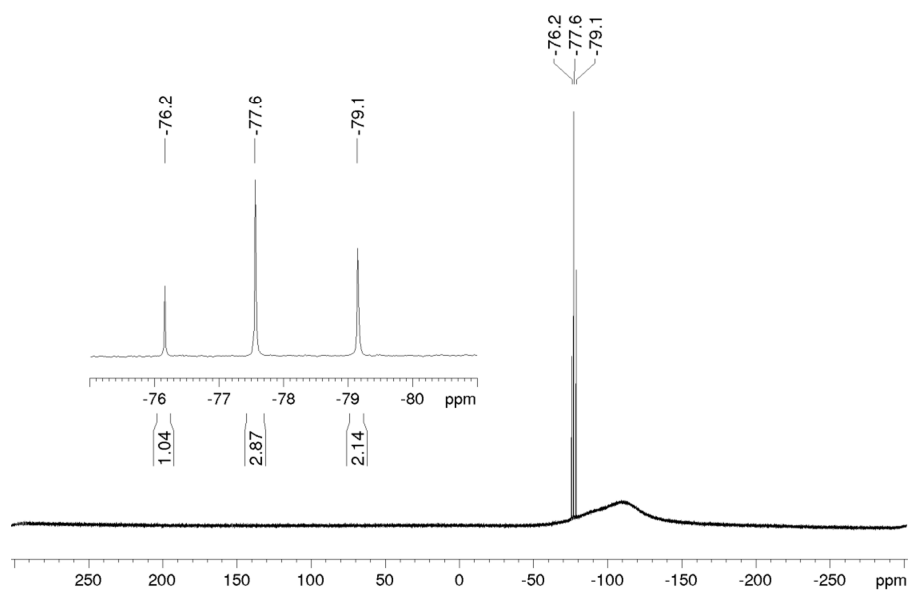


Figure S5. ^{29}Si NMR spectrum of $\text{T}_{14}\text{Ph}_{14}$ in benzene- d_6 at 300 K.

SUPPORTING INFORMATION

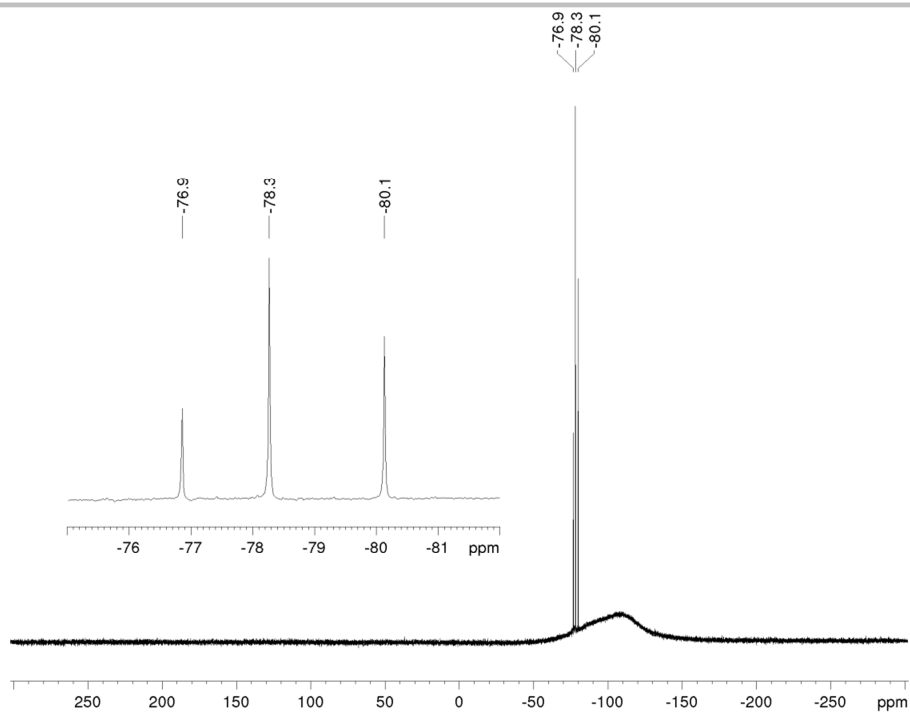


Figure S6. ^{29}Si NMR of $\text{T}_{14}\text{Ph}_{14}$ in chloroform-d at 300 K.

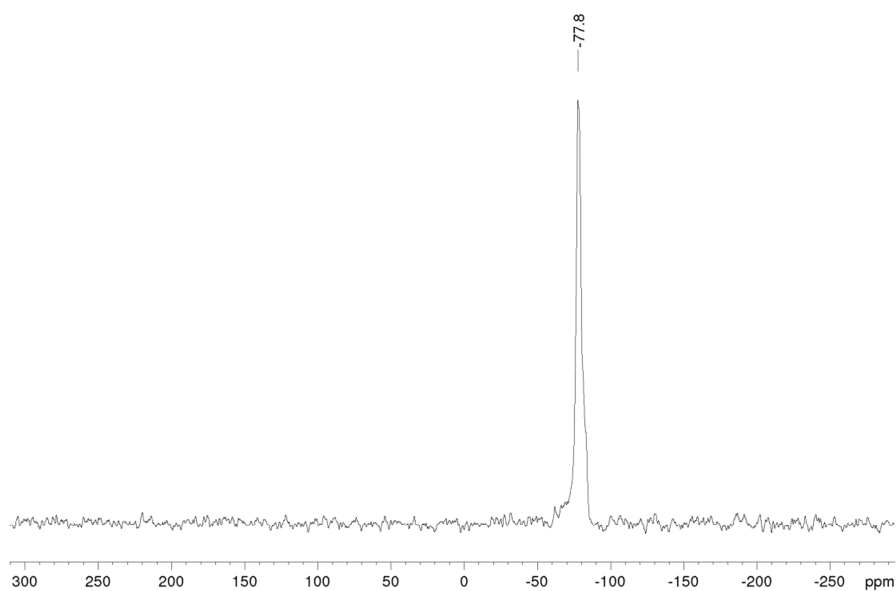


Figure S7. $^{29}\text{Si}/\text{CP-MAS}$ spectrum of $\text{T}_{14}\text{Ph}_{14}$.

SUPPORTING INFORMATION

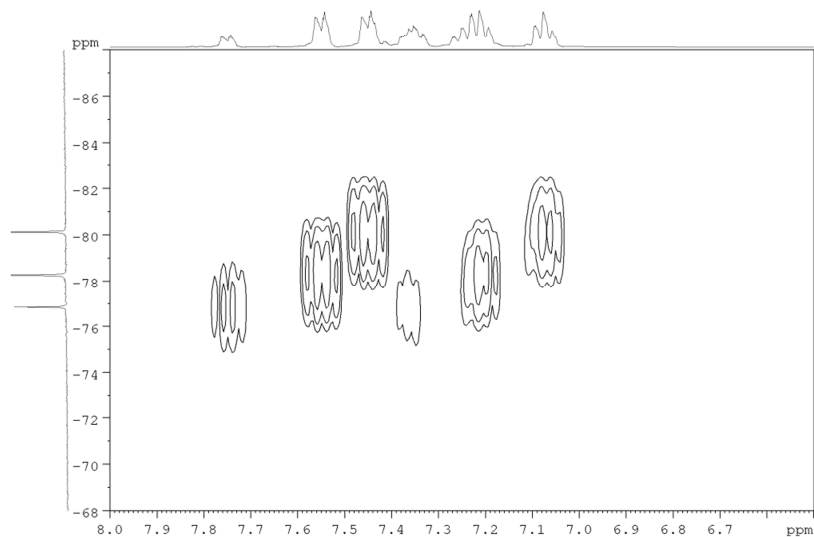


Figure S8. ^1H - ^{29}Si correlation NMR of $\text{T}_{14}\text{Ph}_{14}$ in chloroform- d at room temperature.

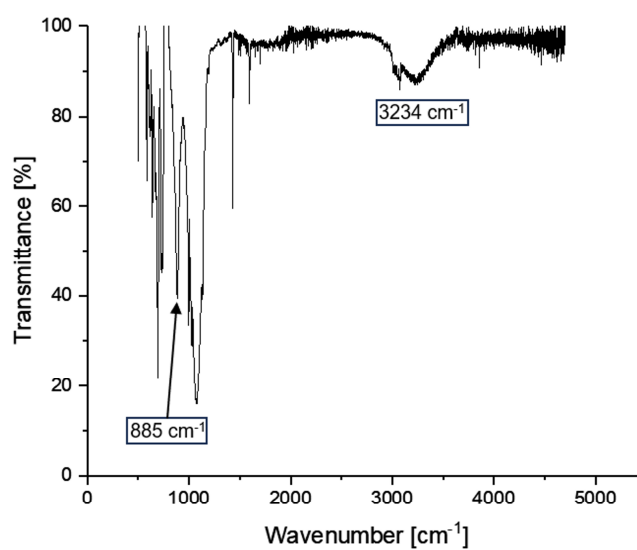


Figure S9. IR Spectrum (ATR) of the $\text{T}_7\text{Ph}_7(\text{OH})_3$ precursor.

SUPPORTING INFORMATION

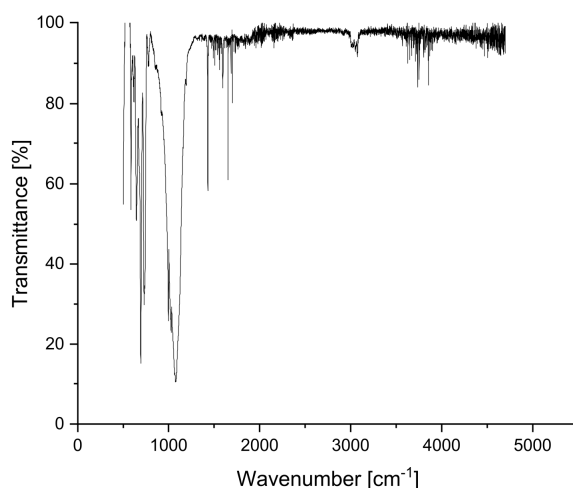


Figure S10. IR spectrum (ATR) of T14Ph14.

2. Thermal Analysis

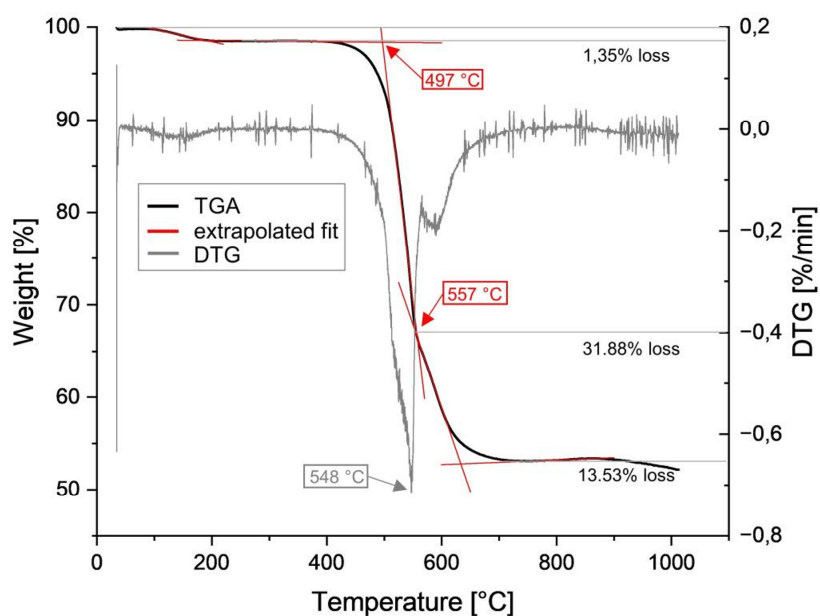


Figure S11. Thermogravimetric Analysis (TGA) of T14Ph14. The first mass loss of 1.35% is attributed to residual toluene.

Thermogravimetric analysis (TGA) of **2** reveals the decomposition onset at about 428 °C, and the extrapolated onset at 496 °C as displayed in Figure S11. This is slightly higher than in the case of known T₈Ph₈ (N₂) and T₁₀Ph₁₀ (air) cases, where the onset had been observed at 472 °C and 490 °C, respectively.^[14, 21] In contrast, the T₁₂Ph₁₂ silsesquioxane is reported to decompose at a relatively low temperature of 342 °C, although no significant decrease of the residual mass happened at temperatures below approximately 400 °C.^[22] The small decrease in mass of the T₁₄Ph₁₄ sample at 90 °C is attributed to the loss of residual toluene. After the initial decomposition onset of T₁₄Ph₁₄, a small saddle point with a second decomposition step can be observed at 557 °C (33% total weight loss), which had similarly been described in the T₈Ph₈ and T₁₂Ph₁₂ cases. The first derivative reveals the peak temperature to be at 548 °C, which corresponds to the first decomposition event. The total weight loss until 1000 °C is about 47%, just slightly more than the organic components of the entire T₁₄Ph₁₄. This is in accord with the behavior of other reported silsesquioxane species.^[14]

SUPPORTING INFORMATION

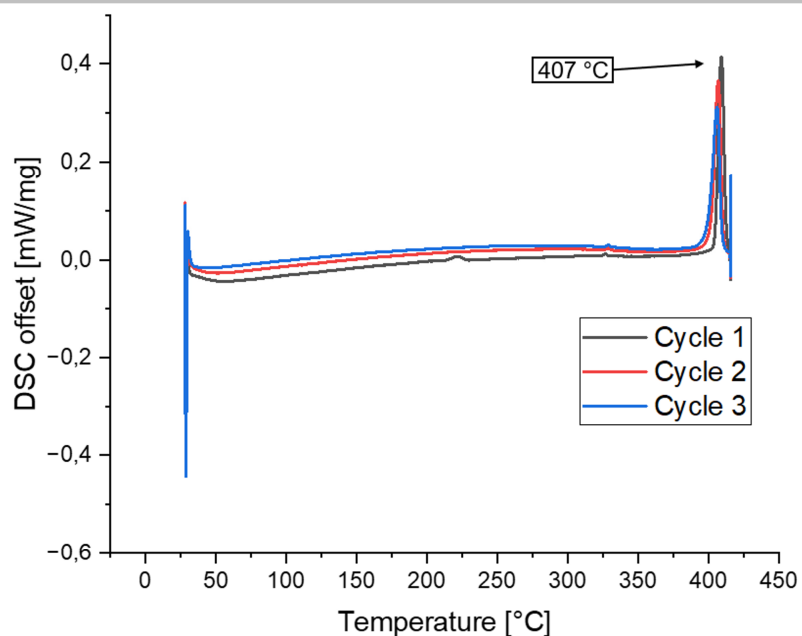


Figure S12. Differential Scanning Calorimetric analysis of T₁₄Ph₁₄ upon heating.

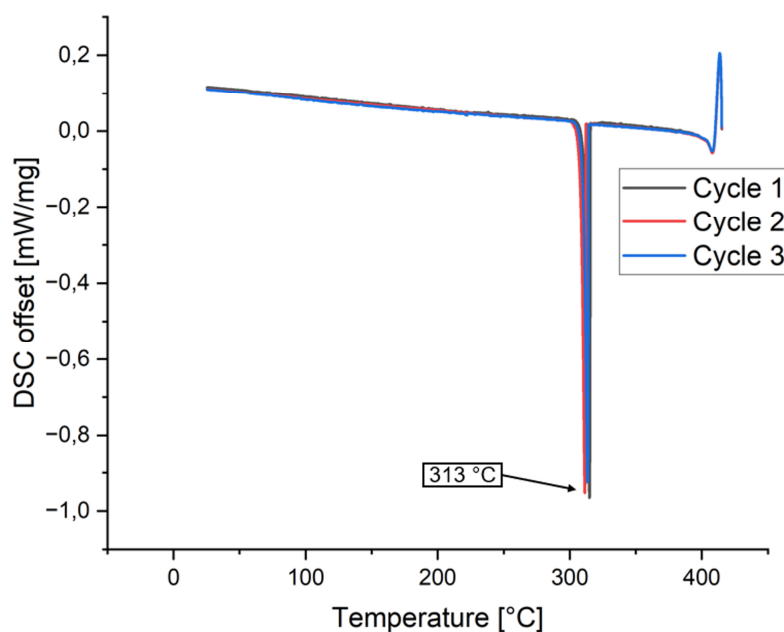


Figure S13. Differential Scanning Calorimetric analysis of T₁₄Ph₁₄ upon cooling of the hot sample.

Differential scanning calorimetric (DSC, see Figures S12 and S13) analysis gives rise to a peak at 407 °C upon heating, which can be assigned to the melting point of the silsesquioxane. It was reproduced well in the second and third cycle of the DSC analysis. A small endothermic event was observed in the first cycle at 225.5 °C, which is not present in the following cycles. Upon cooling the hot sample, one exothermic event in each cycle can be observed at 313 °C.

SUPPORTING INFORMATION

3. Crystallographic data

The data set was collected using a Bruker D8 Venture diffractometer with a microfocus sealed tube and a Photon II detector. Monochromated MoK α radiation ($\lambda = 0.71073 \text{ \AA}$) was used. Data were collected at 133(2) K and corrected for absorption effects using the multi-scan method. The structure was solved by direct methods using SHELXT^[23] and was refined by full matrix least squares calculations on F^2 (SHELXL2018^[24]) in the graphical user interface Shelxle.^[25]

Acknowledgments. Instrumentation and technical assistance for this work were provided by the Service Center X-ray Diffraction, with financial support from Saarland University and German Science Foundation (project number INST 256/506-1).

3.1 Refinement Details for T₁₄Ph₁₄

Refinement: All non H-atoms were located in the electron density maps and refined anisotropically. C-bound H atoms were placed in positions of optimized geometry and treated as riding atoms. Their isotropic displacement parameters were coupled to the corresponding carrier atoms by a factor of 1.2 (CH) or 1.5 (CH₃). Disorder: 20 of the 42 phenyl groups were treated as a disorder over two layers. One of the two toluene solvent molecules was 62% occupied (C133-C138; A: 62%), as it would otherwise have collided with the second layer of a disordered phenyl ring (C333-C338; B: 38 %).

Table S1. Crystal data and structure refinement for sh4622_a.

| | | |
|-----------------------------------|---|-------------------|
| Identification code | sh4622_a | |
| Empirical formula | C87.76 H74.30 O21 Si14 | |
| Formula weight | 1858.18 | |
| Temperature | 133(2) K | |
| Wavelength | 0.71073 \AA | |
| Crystal system | Monoclinic | |
| Space group | Pn | |
| Unit cell dimensions | a = 16.8254(4) \AA | a = 90°. |
| | b = 19.6600(5) \AA | b = 97.2230(10)°. |
| | c = 41.3867(12) \AA | g = 90°. |
| Volume | 13581.6(6) \AA ³ | |
| Z | 6 | |
| Density (calculated) | 1.363 Mg/m ³ | |
| Absorption coefficient | 0.269 mm ⁻¹ | |
| F(000) | 5789 | |
| Crystal size | 0.289 x 0.178 x 0.131 mm ³ | |
| Theta range for data collection | 1.962 to 25.681°. | |
| Index ranges | -20 ≤ h ≤ 20, -21 ≤ k ≤ 23, -50 ≤ l ≤ 50 | |
| Reflections collected | 211626 | |
| Independent reflections | 50301 [R(int) = 0.0702] | |
| Completeness to theta = 25.242° | 100.0 % | |
| Absorption correction | Semi-empirical from equivalents | |
| Max. and min. transmission | 0.7455 and 0.6955 | |
| Refinement method | Full-matrix least-squares on F ² | |
| Data / restraints / parameters | 50301 / 5974 / 4456 | |
| Goodness-of-fit on F ² | 1.040 | |
| Final R indices [I > 2σ(I)] | R1 = 0.0591, wR2 = 0.1367 | |
| R indices (all data) | R1 = 0.0846, wR2 = 0.1529 | |
| Absolute structure parameter | 0.40(9) | |
| Extinction coefficient | n/a | |
| Largest diff. peak and hole | 0.707 and -0.377 e.\AA ⁻³ | |

SUPPORTING INFORMATION

3.2 Refinement Details for T₇Ph₇(OTf)₃

Refinement: All non H-atoms were located in the electron density maps and refined anisotropically. C-bound H atoms were placed in positions of optimized geometry and treated as riding atoms. Their isotropic displacement parameters were coupled to the corresponding carrier atoms by a factor of 1.2 (CH). Disorder: The structure is highly disordered. The phenyl groups on Si1, Si2, Si3, Si5 and Si6 are split over two positions (fvar 2: 0.60/0.40, fvar 3: 0.44/0.56, fvar 4: 0.53/0.47, fvar 5: 0.68/0.32 and fvar 6: 0.69/0.31) as well as the trifluoromethanesulfonates on Si5 and Si7 (fvar 7: 0.48/0.52 and fvar 8: 0.57/0.43). For the refinement of the disorder SIMU, DELU, FLAT and SADI restraints were applied.

Table S2. Crystal data and structure refinement for sh4765_a.

| | | |
|-----------------------------------|---|------------------|
| Identification code | sh4765_a | |
| Empirical formula | C45 H35 F9 O18 S3 Si7 | |
| Formula weight | 1327.54 | |
| Temperature | 133(2) K | |
| Wavelength | 0.71073 Å | |
| Crystal system | Monoclinic | |
| Space group | P2 ₁ | |
| Unit cell dimensions | a = 11.7970(6) Å | a = 90°. |
| | b = 19.5273(10) Å | b = 108.180(2)°. |
| | c = 12.8813(6) Å | g = 90°. |
| Volume | 2819.3(2) Å ³ | |
| Z | 2 | |
| Density (calculated) | 1.564 Mg/m ³ | |
| Absorption coefficient | 0.380 mm ⁻¹ | |
| F(000) | 1352 | |
| Crystal size | 0.257 x 0.192 x 0.108 mm ³ | |
| Theta range for data collection | 1.964 to 25.026°. | |
| Index ranges | -14 ≤ h ≤ 14, -23 ≤ k ≤ 23, -15 ≤ l ≤ 15 | |
| Reflections collected | 37812 | |
| Independent reflections | 9928 [R(int) = 0.0620] | |
| Completeness to theta = 25.026° | 100.0 % | |
| Absorption correction | Semi-empirical from equivalents | |
| Max. and min. transmission | 0.7456 and 0.6780 | |
| Refinement method | Full-matrix least-squares on F ² | |
| Data / restraints / parameters | 9928 / 2065 / 1160 | |
| Goodness-of-fit on F ² | 1.047 | |
| Final R indices [I > 2σ(I)] | R1 = 0.0694, wR2 = 0.1807 | |
| R indices (all data) | R1 = 0.0952, wR2 = 0.2052 | |
| Absolute structure parameter | 0.00(5) | |
| Extinction coefficient | n/a | |
| Largest diff. peak and hole | 0.451 and -0.468 e.Å ⁻³ | |

SUPPORTING INFORMATION

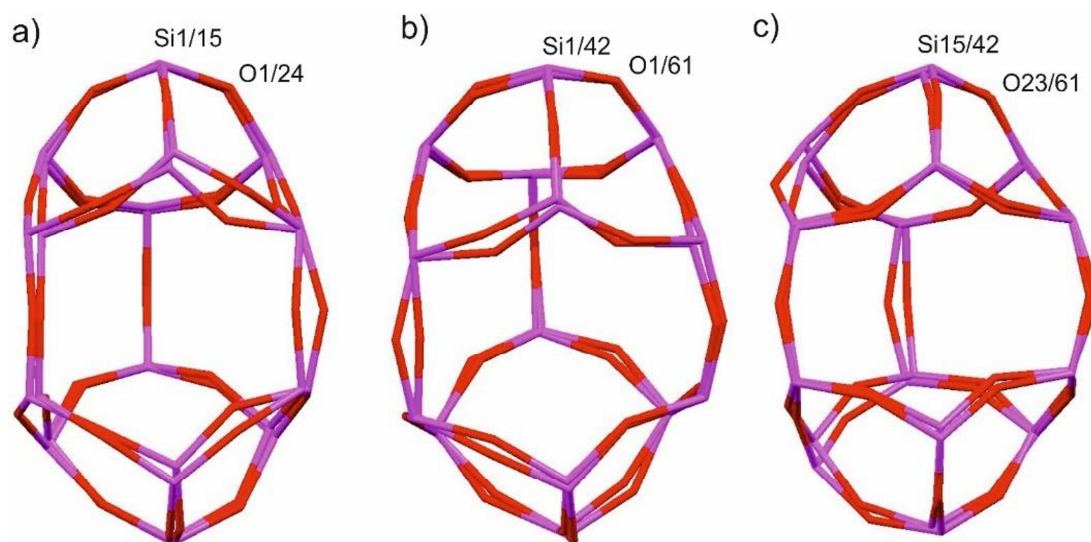
3.3 Overlap of the $T_{14}Ph_{14}$ units in the asymmetric unit

Figure S14. Overlay of the three crystallographically independent T_{14} units in the solid state structure of **2**. a) Overlay of Unit 1 with 2; b) overlay of 1 with 3; c) overlay of 2 with 3.

SUPPORTING INFORMATION

4 Computational details

Geometry optimizations were performed using Gaussian16 suite of programs^[26] using the B3LYP^[27] functional. The 6-311G^[28] basis set was used for all the atoms. All stationary points have been identified for minimum.

4.1 Atomic coordinates

Table S3. Atomic coordinates for the optimized structure of the D_{3h} ($6^{\circ}54^{\circ}$) isomer of the $T_{14}Ph_{14}$ System.

| | | | |
|----------------------|-------------|-------------|-------------|
| NImag = 0 | | | |
| -8877.855176 Hartree | | | |
| Si | 2.36195200 | -1.94984100 | -2.33283700 |
| O | 3.35448400 | -1.02356600 | -1.36933200 |
| O | 1.20121300 | -0.97616800 | -3.01762500 |
| O | 1.61039500 | -3.09842700 | -1.38888800 |
| Si | 0.02295600 | 0.05831300 | -3.55926200 |
| Si | 3.99595700 | -0.31333900 | -0.00046600 |
| O | 3.35765600 | -1.10292300 | 1.31867000 |
| O | 3.56131500 | 1.28792800 | 0.00210800 |
| O | -1.45987000 | -0.48121100 | -3.02719900 |
| O | 0.26410600 | 1.58828700 | -2.95966600 |
| Si | 0.50557900 | 3.07642600 | -2.26440200 |
| O | 1.87645900 | 2.99628800 | -1.31528000 |
| O | -0.77682900 | 3.47641800 | -1.28263900 |
| Si | 2.87179000 | 2.79708400 | 0.00404100 |
| O | 0.29706900 | 1.51807500 | 3.01836300 |
| Si | -1.74684300 | 3.60351200 | 0.07113400 |
| O | -0.74404700 | 3.41158800 | 1.38920000 |
| Si | -2.87630600 | -1.00603900 | -2.34587500 |
| Si | -2.85730300 | -1.06443700 | 2.34381900 |
| O | -2.59147200 | -2.33617100 | -1.37788900 |
| Si | 0.96104900 | -3.88664800 | -0.07089500 |
| O | -1.43307200 | -0.56276800 | 3.02647200 |
| O | 1.62500500 | -3.16927500 | 1.28354300 |
| O | -0.68469600 | -3.70991200 | -0.03754500 |
| O | -2.58896500 | -2.36946500 | 1.33835600 |
| Si | -2.28618900 | -3.26623100 | -0.03153300 |
| O | -2.90039100 | 2.41633800 | 0.03689000 |
| Si | -3.84765300 | 1.05100700 | 0.02933500 |
| O | -3.50587900 | 0.16863300 | -1.34081700 |
| O | -3.48874000 | 0.14062300 | 1.37603400 |
| Si | 0.05197600 | -0.03067800 | 3.55977800 |
| O | 1.21592600 | -1.05329300 | 2.96145000 |
| Si | 2.35426300 | -2.04197600 | 2.26631100 |
| O | 1.92390700 | 2.93273100 | 1.37268400 |
| Si | 0.56725500 | 3.00927600 | 2.33458300 |
| C | 1.39578800 | -5.70573400 | -0.12473800 |
| C | 0.43230600 | -6.69224300 | 0.14114100 |
| C | 2.71079300 | -6.11327800 | -0.41087500 |
| C | 0.77209300 | -8.04795300 | 0.12287000 |
| H | -0.58739100 | -6.40082000 | 0.35384900 |
| C | 3.05358900 | -7.46680600 | -0.42966700 |
| H | 3.47001000 | -5.37373400 | -0.63219900 |
| C | 2.08336300 | -8.43696000 | -0.16102600 |
| H | 0.01554900 | -8.79435600 | 0.32633300 |
| H | 4.06964500 | -7.76247400 | -0.65599300 |
| H | 2.34719300 | -9.48649300 | -0.17665700 |
| C | -3.37188900 | -4.78996500 | -0.04464300 |
| C | -3.76368900 | -5.40218900 | 1.15823700 |
| C | -3.77751200 | -5.37274600 | -1.25717700 |
| C | -4.53872900 | -6.56485300 | 1.15015300 |
| H | -3.47469700 | -4.96035000 | 2.10296300 |
| C | -4.55274600 | -6.53498700 | -1.26841500 |
| H | -3.49732800 | -4.90939100 | -2.19408700 |
| C | -4.93247100 | -7.13406100 | -0.06414100 |
| H | -4.83623600 | -7.02043100 | 2.08559100 |
| H | -4.86036000 | -6.96803400 | -2.21119400 |
| H | -5.53383500 | -8.03389500 | -0.07176800 |
| C | -4.07649500 | -1.52227900 | 3.68789700 |

SUPPORTING INFORMATION

| | | | |
|---|-------------|-------------|-------------|
| C | -3.75955400 | -1.37320300 | 5.04748200 |
| C | -5.34575400 | -2.02289700 | 3.34706200 |
| C | -4.68333400 | -1.71474100 | 6.03971000 |
| H | -2.78877700 | -0.99171400 | 5.33279100 |
| C | -6.27052900 | -2.36509700 | 4.33540900 |
| H | -5.61624400 | -2.14944800 | 2.30632300 |
| C | -5.93981900 | -2.21086500 | 5.68525300 |
| H | -4.42030200 | -1.59369700 | 7.08229100 |
| H | -7.24239500 | -2.74940400 | 4.05454700 |
| H | -6.65570100 | -2.47569400 | 6.45259100 |
| C | 0.09370700 | -0.05429400 | 5.43346600 |
| C | 0.28193800 | -1.26353200 | 6.12585800 |
| C | -0.09939600 | 1.11956200 | 6.18045300 |
| C | 0.27672600 | -1.29935300 | 7.52206300 |
| H | 0.44771000 | -2.18033400 | 5.57476400 |
| C | -0.10473000 | 1.08778100 | 7.57771300 |
| H | -0.23278400 | 2.06422500 | 5.67058300 |
| C | 0.08118700 | -0.12238800 | 8.25067000 |
| H | 0.42950900 | -2.23862300 | 8.03720700 |
| H | -0.24905100 | 2.00379100 | 8.13539400 |
| H | 0.07906600 | -0.14810300 | 9.33270100 |
| C | -5.65729700 | 1.52620700 | 0.04097500 |
| C | -6.34232300 | 1.71682800 | 1.25293300 |
| C | -6.35044800 | 1.74114000 | -1.16260600 |
| C | -7.68246200 | 2.11159100 | 1.26290000 |
| H | -5.83040600 | 1.54328700 | 2.19041200 |
| C | -7.69071700 | 2.13638300 | -1.15578100 |
| H | -5.84535700 | 1.58424100 | -2.10681100 |
| C | -8.35790100 | 2.32426400 | 0.05792800 |
| H | -8.19631100 | 2.24925000 | 2.20523600 |
| H | -8.21109500 | 2.29232100 | -2.09172700 |
| H | -9.39637500 | 2.62909400 | 0.06460300 |
| C | -2.57528800 | 5.28042300 | 0.12402400 |
| C | -1.82504400 | 6.43462600 | 0.41051800 |
| C | -3.94655000 | 5.42285100 | -0.14354200 |
| C | -2.42687200 | 7.69453400 | 0.42812400 |
| H | -0.76869900 | 6.35151800 | 0.63304600 |
| C | -4.55209500 | 6.68249200 | -0.12646400 |
| H | -4.54384900 | 4.54666200 | -0.35669900 |
| C | -3.79283600 | 7.82008200 | 0.15786400 |
| H | -1.83490000 | 8.57157900 | 0.65477000 |
| H | -5.61077800 | 6.77263700 | -0.33123900 |
| H | -4.26097800 | 8.79578500 | 0.17252400 |
| C | 0.79876900 | 4.30013000 | 3.66924300 |
| C | -0.31266400 | 4.93764600 | 4.24729400 |
| C | 2.07994600 | 4.62580000 | 4.14418200 |
| C | -0.14875100 | 5.87246600 | 5.27266000 |
| H | -1.30750200 | 4.71551100 | 3.88331100 |
| C | 2.24740100 | 5.56055400 | 5.16890800 |
| H | 2.94905000 | 4.15761000 | 3.70133000 |
| C | 1.13261600 | 6.18324300 | 5.73663600 |
| H | -1.01491600 | 6.35860800 | 5.70222100 |
| H | 3.24199900 | 5.80363200 | 5.51912700 |
| H | 1.26135300 | 6.90850400 | 6.52957600 |
| C | 3.34897100 | -2.92461900 | 3.58303400 |
| C | 3.39004500 | -4.32742500 | 3.63930300 |
| C | 4.07604300 | -2.19346400 | 4.53905200 |
| C | 4.13685300 | -4.98267100 | 4.62293200 |
| H | 2.83562100 | -4.90565500 | 2.91251600 |
| C | 4.82313300 | -2.84496200 | 5.52222500 |
| H | 4.05901500 | -1.11110500 | 4.51956800 |
| C | 4.85443100 | -4.24226100 | 5.56527600 |
| H | 4.15705600 | -6.06424300 | 4.65150000 |
| H | 5.37538900 | -2.26669800 | 6.25130200 |
| H | 5.43267800 | -4.74822700 | 6.32752600 |
| C | 3.36692300 | -2.79317900 | -3.66708100 |
| C | 2.92309400 | -3.99620000 | -4.24296600 |
| C | 4.55769900 | -2.22113200 | -4.14434900 |
| C | 3.64740700 | -4.60901900 | -5.26864300 |
| H | 2.01805500 | -4.46373600 | -3.87715900 |
| C | 5.28476600 | -2.83169000 | -5.16926000 |

SUPPORTING INFORMATION

| | | | |
|---|-------------|-------------|-------------|
| H | 4.92406000 | -1.30354500 | -3.70334400 |
| C | 4.82879700 | -4.02538400 | -5.73494300 |
| H | 3.29462400 | -5.53821500 | -5.69670400 |
| H | 6.20297200 | -2.38010700 | -5.52129700 |
| H | 5.39194100 | -4.49982800 | -6.52810500 |
| C | 5.86110000 | -0.46017400 | 0.01665400 |
| C | 6.50208300 | -1.43017700 | 0.80453200 |
| C | 6.65186000 | 0.37995700 | -0.78651600 |
| C | 7.89354400 | -1.55959500 | 0.78971500 |
| H | 5.91292800 | -2.07759100 | 1.44027000 |
| C | 8.04252700 | 0.25258600 | -0.80445200 |
| H | 6.18278600 | 1.14639300 | -1.39021200 |
| C | 8.66554000 | -0.71982200 | -0.01674700 |
| H | 8.37065500 | -2.31003000 | 1.40630200 |
| H | 8.63607600 | 0.91056300 | -1.42562600 |
| H | 9.74319200 | -0.81909200 | -0.02904900 |
| C | 4.21270800 | 4.10174300 | -0.01332200 |
| C | 5.36302800 | 3.95523700 | 0.78124700 |
| C | 4.08092800 | 5.26270400 | -0.79269400 |
| C | 6.35151600 | 4.94168700 | 0.79949200 |
| H | 5.49595400 | 3.06142100 | 1.37730100 |
| C | 5.06863800 | 6.25126200 | -0.77749800 |
| H | 3.21021800 | 5.38834900 | -1.42242900 |
| C | 6.20423400 | 6.09317000 | 0.02068900 |
| H | 7.23259500 | 4.81054000 | 1.41397300 |
| H | 4.95232500 | 7.13745200 | -1.38750400 |
| H | 6.96983400 | 6.85805300 | 0.03321100 |
| C | 0.70588000 | 4.39117400 | -3.58107500 |
| C | -0.16588800 | 5.49063700 | -3.64351000 |
| C | 1.73821100 | 4.29901200 | -4.53134800 |
| C | -0.01131500 | 6.47160400 | -4.62758400 |
| H | -0.96645900 | 5.57675800 | -2.92128000 |
| C | 1.89556300 | 5.27740900 | -5.51481100 |
| H | 2.42229400 | 3.46019900 | -4.50701300 |
| C | 1.01975600 | 6.36635300 | -5.56404400 |
| H | -0.69235800 | 7.31189200 | -4.66098300 |
| H | 2.69460300 | 5.19001300 | -6.23926200 |
| H | 1.14048700 | 7.12496900 | -6.32648700 |
| C | -4.10533300 | -1.43478500 | -3.69066800 |
| C | -5.40360100 | -1.85501400 | -3.35036600 |
| C | -3.76310800 | -1.35557900 | -5.04998900 |
| C | -6.33209900 | -2.18641100 | -4.33889900 |
| H | -5.69533500 | -1.92317900 | -2.30991400 |
| C | -4.69054300 | -1.68647000 | -6.04241200 |
| H | -2.77116500 | -1.03289500 | -5.33512000 |
| C | -5.97588100 | -2.10256200 | -5.68846400 |
| H | -7.32671500 | -2.50756000 | -4.05836700 |
| H | -4.40831100 | -1.61815300 | -7.08476100 |
| H | -6.69465200 | -2.35898900 | -6.45595100 |
| C | 0.04197600 | 0.10259500 | -5.43293300 |
| C | -0.59225000 | 1.14818000 | -6.12691100 |
| C | 0.65225400 | -0.91966500 | -6.17848100 |
| C | -0.61669400 | 1.17172800 | -7.52316500 |
| H | -1.05779000 | 1.95613200 | -5.57717200 |
| C | 0.63012300 | -0.89939000 | -7.57580300 |
| H | 1.15799500 | -1.72782600 | -5.66740300 |
| C | -0.00639700 | 0.14548800 | -8.25031300 |
| H | -1.10422200 | 1.98823100 | -8.03948300 |
| H | 1.11103000 | -1.69311600 | -8.13226100 |
| H | -0.02262200 | 0.16339800 | -9.33238000 |

Table S4. Atomic coordinates for the optimized structure of the C_{2v} (6'5'4') isomer of the T₁₄Ph₁₄ system.

Nimag = 0

-8877.846934 Hartree

| | | | |
|----|-------------|------------|-------------|
| Si | -0.02687600 | 1.69758400 | 3.01921900 |
| O | -1.35944700 | 2.22746200 | 2.17975900 |
| O | 1.32929700 | 2.23473300 | 2.21674100 |
| O | 2.10557600 | 2.94706800 | -0.30682200 |
| O | 0.03414700 | 2.73451700 | -2.03002100 |

SUPPORTING INFORMATION

| | | | |
|----|--------------|-------------|-------------|
| O | -2.09461700 | 2.95961700 | -0.34883800 |
| O | 0.00338800 | 0.04122300 | 3.09277700 |
| Si | 0.00569900 | -1.62282300 | 3.05715400 |
| O | -2.08783600 | -2.97374300 | -0.20790800 |
| O | -0.01907600 | -2.81750800 | -1.94280900 |
| O | 2.08763800 | -2.97013700 | -0.21031000 |
| O | 1.36358700 | -2.16486100 | 2.27229700 |
| O | -1.35204600 | -2.12437200 | 2.24308900 |
| Si | -2.64517400 | -2.60173700 | 1.32079700 |
| Si | -2.62589200 | 2.66157900 | 1.19868800 |
| Si | 2.61040600 | 2.66304500 | 1.25813400 |
| Si | 2.64899800 | -2.60453900 | 1.31451900 |
| Si | 1.63034500 | -2.86568400 | -1.81168500 |
| Si | 1.69010600 | 2.73473600 | -1.90598500 |
| Si | -1.67492900 | -2.82813300 | -1.81535500 |
| Si | -1.61809400 | 2.76782900 | -1.93934500 |
| O | -3.74147800 | -1.35342500 | 1.17807500 |
| O | -3.70084300 | 1.38280700 | 1.13927700 |
| O | -2.28446800 | -1.39827900 | -2.41304000 |
| O | -2.27253400 | 1.32360900 | -2.45458900 |
| Si | -3.23686300 | -0.03165900 | -2.48132300 |
| Si | -4.44770500 | 0.01945200 | 0.54507800 |
| O | -4.19740600 | -0.03297100 | -1.11021400 |
| O | 3.70969900 | -1.32418300 | 1.20908200 |
| O | 3.69247200 | 1.39268600 | 1.17354000 |
| O | 2.29359100 | -1.45108200 | -2.40214200 |
| O | 2.30114000 | 1.28343800 | -2.44617700 |
| Si | 4.43790800 | 0.03437300 | 0.56815300 |
| Si | 3.24786200 | -0.09108200 | -2.46560100 |
| O | 4.19732400 | -0.03128500 | -1.08723800 |
| C | -6.27219200 | 0.06047300 | 0.94573000 |
| C | -6.84015400 | 1.15011200 | 1.62450300 |
| C | -7.10907600 | -1.00278700 | 0.56312200 |
| C | -8.20745900 | 1.17808000 | 1.91391100 |
| H | -6.21100300 | 1.97684500 | 1.92537600 |
| C | -8.47528700 | -0.97736700 | 0.85047500 |
| H | -6.69568900 | -1.85508300 | 0.03802700 |
| C | -9.02651500 | 0.11481700 | 1.52749500 |
| H | -8.62912800 | 2.02609600 | 2.43728300 |
| H | -9.10586800 | -1.80325300 | 0.54821100 |
| H | -10.08524600 | 0.13589600 | 1.75064700 |
| C | 6.26200700 | 0.07629800 | 0.96513100 |
| C | 6.74761300 | 0.84954200 | 2.03246100 |
| C | 7.17418400 | -0.68980000 | 0.21951100 |
| C | 8.10879800 | 0.85562400 | 2.34834000 |
| H | 6.06106700 | 1.45625200 | 2.60770700 |
| C | 8.53512100 | -0.68487700 | 0.53269100 |
| H | 6.82264900 | -1.28093100 | -0.61631800 |
| C | 9.00384800 | 0.08689500 | 1.59984900 |
| H | 8.46784300 | 1.45990700 | 3.17105900 |
| H | 9.22549900 | -1.27719000 | -0.05347300 |
| H | 10.05846200 | 0.09196800 | 1.84294900 |
| C | -0.05248500 | 2.40907600 | 4.75292300 |
| C | 0.42706000 | 1.67043600 | 5.84737800 |
| C | -0.51067200 | 3.71887600 | 4.97994900 |
| C | 0.44709500 | 2.22185200 | 7.13139000 |
| H | 0.77371900 | 0.65635200 | 5.70045100 |
| C | -0.49175100 | 4.27351500 | 6.26206500 |
| H | -0.89720500 | 4.30495100 | 4.15619500 |
| C | -0.01061300 | 3.52524900 | 7.34040000 |
| H | 0.81442600 | 1.63450700 | 7.96259400 |
| H | -0.85407000 | 5.28129400 | 6.41787200 |
| H | 0.00326900 | 3.95284600 | 8.33459700 |
| C | 3.44727400 | 4.18243300 | 1.95914800 |
| C | 3.14584700 | 4.65069800 | 3.24820100 |
| C | 4.41945200 | 4.86635400 | 1.20806300 |
| C | 3.79571500 | 5.77170700 | 3.77265800 |
| H | 2.39895600 | 4.14186300 | 3.84235600 |
| C | 5.07006800 | 5.98667000 | 1.72891600 |
| H | 4.66641000 | 4.52963200 | 0.20918100 |
| C | 4.75888200 | 6.44092000 | 3.01407800 |

SUPPORTING INFORMATION

| | | | |
|---|-------------|-------------|-------------|
| H | 3.54856100 | 6.11922300 | 4.76715300 |
| H | 5.81446900 | 6.50183800 | 1.13596700 |
| H | 5.26225300 | 7.30929800 | 3.41896900 |
| C | -3.47860100 | 4.18389700 | 1.87589500 |
| C | -3.56887700 | 5.36201600 | 1.11724100 |
| C | -4.04718000 | 4.16940300 | 3.16226100 |
| C | -4.20931500 | 6.49499400 | 1.62787200 |
| H | -3.13727600 | 5.39152000 | 0.12597200 |
| C | -4.68831700 | 5.29932000 | 3.67469900 |
| H | -3.98647200 | 3.27547100 | 3.77029800 |
| C | -4.77028900 | 6.46502600 | 2.90664200 |
| H | -4.26939700 | 7.39420500 | 1.02899000 |
| H | -5.11934300 | 5.27119500 | 4.66695600 |
| H | -5.26661400 | 7.34144000 | 3.30270200 |
| C | 2.39769300 | 4.13436000 | -2.93052600 |
| C | 2.50621800 | 5.43016500 | -2.39632700 |
| C | 2.79137800 | 3.92445300 | -4.26293200 |
| C | 2.99432000 | 6.48590400 | -3.17054500 |
| H | 2.22019900 | 5.61211300 | -1.36842000 |
| C | 3.28011500 | 4.97807000 | -5.03996400 |
| H | 2.72720600 | 2.93246700 | -4.69031800 |
| C | 3.38025700 | 6.26112000 | -4.49519900 |
| H | 3.07502700 | 7.47614000 | -2.74155700 |
| H | 3.58397000 | 4.79664400 | -6.06252800 |
| H | 3.75991000 | 7.07761300 | -5.09568000 |
| C | -2.28116200 | 4.18283700 | -2.97236700 |
| C | -1.42681000 | 5.06094200 | -3.65793800 |
| C | -3.66929800 | 4.38681600 | -3.07236800 |
| C | -1.94249900 | 6.11324000 | -4.42042200 |
| H | -0.35597900 | 4.92363800 | -3.59877000 |
| C | -4.18785500 | 5.43650200 | -3.83263500 |
| H | -4.35353400 | 3.72199500 | -2.55977700 |
| C | -3.32328800 | 6.30284900 | -4.50858300 |
| H | -1.26728200 | 6.77876100 | -4.94193200 |
| H | -5.25887600 | 5.57541800 | -3.90000200 |
| H | -3.72362500 | 7.11636300 | -5.09961000 |
| C | 4.32494900 | -0.13651700 | -3.99215300 |
| C | 5.53605400 | 0.57529500 | -4.03204600 |
| C | 3.92830100 | -0.85178900 | -5.13408800 |
| C | 6.32907200 | 0.57326900 | -5.18179000 |
| H | 5.86681500 | 1.12135600 | -3.15807200 |
| C | 4.71910800 | -0.85482500 | -6.28600800 |
| H | 3.00627500 | -1.41745500 | -5.11704500 |
| C | 5.91988900 | -0.14066700 | -6.31173900 |
| H | 7.26102300 | 1.12313600 | -5.19469400 |
| H | 4.40172600 | -1.41521600 | -7.15557100 |
| H | 6.53409900 | -0.14399500 | -7.20286400 |
| C | 3.52828300 | -4.08312600 | 2.04979400 |
| C | 4.63887000 | -3.91120100 | 2.89324500 |
| C | 3.06989600 | -5.38819200 | 1.80219600 |
| C | 5.27259400 | -5.01236400 | 3.47538000 |
| H | 5.01717700 | -2.91500600 | 3.08139900 |
| C | 3.70155900 | -6.49085100 | 2.38188100 |
| H | 2.22627300 | -5.54427500 | 1.14232500 |
| C | 4.80287300 | -6.30385100 | 3.22201300 |
| H | 6.13031500 | -4.86264800 | 4.11802500 |
| H | 3.33905700 | -7.48951300 | 2.17626700 |
| H | 5.29370600 | -7.15760600 | 3.67089700 |
| C | 2.28812300 | -4.34116000 | -2.75923800 |
| C | 3.60657300 | -4.78407900 | -2.55421800 |
| C | 1.49755300 | -5.01368500 | -3.70527900 |
| C | 4.12045500 | -5.86534800 | -3.27251800 |
| H | 4.23422600 | -4.29152700 | -1.82233700 |
| C | 2.00840400 | -6.09672600 | -4.42625800 |
| H | 0.47607400 | -4.69959500 | -3.87146400 |
| C | 3.32115700 | -6.52307800 | -4.21207000 |
| H | 5.13666000 | -6.19404200 | -3.09850900 |
| H | 1.38178000 | -6.60541000 | -5.14700300 |
| H | 3.71767300 | -7.36213000 | -4.76900000 |
| C | -4.30623500 | -0.03338100 | -4.01375300 |
| C | -3.77344300 | 0.34611600 | -5.25772700 |

SUPPORTING INFORMATION

| | | | |
|---|-------------|-------------|-------------|
| C | -5.64930800 | -0.43935000 | -3.95409000 |
| C | -4.56024400 | 0.31671600 | -6.41115500 |
| H | -2.74543300 | 0.67845900 | -5.32375100 |
| C | -6.43939700 | -0.46810100 | -5.10621300 |
| H | -6.07939600 | -0.72006300 | -3.00190500 |
| C | -5.89482900 | -0.09254000 | -6.33679900 |
| H | -4.13640400 | 0.61669500 | -7.36056400 |
| H | -7.47390900 | -0.77921800 | -5.04250600 |
| H | -6.50604500 | -0.11353600 | -7.22973300 |
| C | -2.37915300 | -4.26682000 | -2.78532200 |
| C | -2.64602800 | -4.14171700 | -4.15965600 |
| C | -2.61697600 | -5.50588300 | -2.16764800 |
| C | -3.13465400 | -5.22381100 | -4.89610100 |
| H | -2.48823700 | -3.19111100 | -4.65258600 |
| C | -3.10615000 | -6.58994600 | -2.90072800 |
| H | -2.43325800 | -5.61906700 | -1.10727000 |
| C | -3.36307400 | -6.45104300 | -4.26729000 |
| H | -3.34172900 | -5.10734000 | -5.95185600 |
| H | -3.28892500 | -7.53545100 | -2.40712800 |
| H | -3.74381200 | -7.28953900 | -4.83592800 |
| C | -3.48636800 | -4.08303900 | 2.09422600 |
| C | -2.76825000 | -5.27015200 | 2.32162300 |
| C | -4.83993900 | -4.03866000 | 2.46401600 |
| C | -3.38590800 | -6.38214800 | 2.89703800 |
| H | -1.72002900 | -5.32759100 | 2.05541300 |
| C | -5.46131200 | -5.14982100 | 3.04149200 |
| H | -5.40544900 | -3.13058400 | 2.30390300 |
| C | -4.73557000 | -6.32338800 | 3.25736500 |
| H | -2.81745900 | -7.28696900 | 3.06793700 |
| H | -6.50512200 | -5.09728400 | 3.32225800 |
| H | -5.21503700 | -7.18406900 | 3.70524600 |
| C | -0.00876100 | -2.29457900 | 4.80627100 |
| C | 1.09691600 | -2.97891100 | 5.33638600 |
| C | -1.13566700 | -2.10862400 | 5.62656900 |
| C | 1.07973900 | -3.46241000 | 6.64802600 |
| H | 1.97037100 | -3.14306300 | 4.71998200 |
| C | -1.15655700 | -2.58961500 | 6.93695500 |
| H | -2.00509500 | -1.59101200 | 5.24119400 |
| C | -0.04664500 | -3.26727400 | 7.45055000 |
| H | 1.94003000 | -3.99099100 | 7.03730000 |
| H | -2.03385900 | -2.43945100 | 7.55237200 |
| H | -0.06220500 | -3.64245900 | 8.46564900 |

Table S5. Atomic coordinates for the optimized structure of the C_{2v} ($6^25^24^5$) isomer of the $T_{14}Ph_{14}$ System.

NImag = 0

-8877.838906 Hartree

| | | | |
|----|-------------|-------------|-------------|
| Si | -3.48260400 | -1.70011900 | -1.60691700 |
| Si | -3.52689800 | 1.56429700 | -1.66012200 |
| Si | -0.67611000 | 3.16392700 | -1.73389200 |
| Si | 2.09104300 | 1.59268100 | -2.62566000 |
| Si | 2.11980400 | -1.69632300 | -2.56373000 |
| Si | -0.61124500 | -3.26599000 | -1.56616700 |
| Si | -3.52652000 | -1.56417400 | 1.66039700 |
| Si | -3.48256900 | 1.70022300 | 1.60717100 |
| Si | -0.61105800 | 3.26585400 | 1.56621600 |
| Si | 2.12000000 | 1.69620700 | 2.56374500 |
| Si | 2.09153500 | -1.59279100 | 2.62553000 |
| Si | -0.67581800 | -3.16388500 | 1.73392200 |
| Si | 4.11742900 | -1.61879500 | 0.03349400 |
| Si | 4.11721300 | 1.61887300 | -0.03380400 |
| O | 1.88607600 | 0.05925500 | 2.73510200 |
| O | 3.20497800 | 1.95643900 | 1.31948600 |
| O | 4.54986000 | 0.00006400 | -0.00028200 |
| O | 3.18562700 | -1.85860800 | 1.39299400 |
| O | 0.68007000 | -2.42577100 | -2.17569400 |
| O | -2.02083400 | -2.43413000 | -1.90254800 |
| O | -3.41567400 | -0.06961800 | -1.95828700 |
| O | -2.07708400 | 2.30903200 | -2.01398900 |
| O | 0.63980200 | 2.30853300 | -2.27152300 |

SUPPORTING INFORMATION

| | | | |
|---|-------------|-------------|-------------|
| O | 1.88565100 | -0.05939900 | -2.73495900 |
| O | -3.81414400 | -1.80895600 | 0.03159000 |
| O | -3.81442700 | 1.80905200 | -0.03127900 |
| O | -2.02080700 | 2.43432600 | 1.90267200 |
| O | -2.07657300 | -2.30869200 | 2.01419900 |
| O | -0.51357500 | -3.39884200 | 0.09087700 |
| O | 3.20486500 | -1.95650800 | -1.31952900 |
| O | 3.18487100 | 1.85862300 | -1.39293000 |
| O | 0.68012300 | 2.42542900 | 2.17578000 |
| O | 0.64032300 | -2.30852900 | 2.27102300 |
| O | -0.51338700 | 3.39847400 | -0.09085000 |
| O | -3.41528800 | 0.06974600 | 1.95854700 |
| C | -0.78048200 | -4.81540500 | 2.61097300 |
| C | 0.17780100 | -5.81441800 | 2.36480900 |
| C | -1.79883800 | -5.08051700 | 3.54120700 |
| C | 0.12000600 | -7.04204200 | 3.02719000 |
| H | 0.97026300 | -5.63740700 | 1.64860900 |
| C | -1.85964900 | -6.30862800 | 4.20631100 |
| H | -2.54862000 | -4.32692200 | 3.74126400 |
| C | -0.89981600 | -7.29060500 | 3.95072000 |
| H | 0.86588000 | -7.79950000 | 2.82492500 |
| H | -2.65340800 | -6.49617100 | 4.91751300 |
| H | -0.94533100 | -8.24168900 | 4.46526300 |
| C | -0.66631600 | 4.97228900 | 2.33638200 |
| C | -1.24958600 | 6.04941700 | 1.64753600 |
| C | -0.16390700 | 5.19873300 | 3.62905300 |
| C | -1.32896200 | 7.31574900 | 2.23180400 |
| H | -1.62924000 | 5.90377000 | 0.64462500 |
| C | -0.24240900 | 6.46399600 | 4.21690100 |
| H | 0.30387400 | 4.38951000 | 4.17421700 |
| C | -0.82702800 | 7.52432600 | 3.51933500 |
| H | -1.77674600 | 8.13434200 | 1.68371100 |
| H | 0.15576800 | 6.62050100 | 5.21084900 |
| H | -0.88682800 | 8.50526100 | 3.97281700 |
| C | -4.82056300 | 2.53819300 | 2.60827300 |
| C | -4.50009600 | 3.44506400 | 3.63129300 |
| C | -6.17548600 | 2.25630000 | 2.36118800 |
| C | -5.50529600 | 4.05432500 | 4.38762500 |
| H | -3.46333500 | 3.68043000 | 3.82974800 |
| C | -7.18183800 | 2.86353600 | 3.11460500 |
| H | -6.44869100 | 1.56615000 | 1.57303000 |
| C | -6.84718700 | 3.76352700 | 4.13092600 |
| H | -5.24064900 | 4.75381700 | 5.16964500 |
| H | -8.21996700 | 2.63657000 | 2.91019600 |
| H | -7.62644100 | 4.23527400 | 4.71539000 |
| C | -4.91126100 | -2.30419500 | 2.67556800 |
| C | -5.23043200 | -1.78700200 | 3.94249300 |
| C | -5.63051000 | -3.41488900 | 2.20273600 |
| C | -6.23923900 | -2.36500900 | 4.71712600 |
| H | -4.69880100 | -0.92244200 | 4.31773900 |
| C | -6.64051700 | -3.99423700 | 2.97476200 |
| H | -5.40988200 | -3.81770000 | 1.22285100 |
| C | -6.94433900 | -3.47113400 | 4.23470800 |
| H | -6.47619600 | -1.95135200 | 5.68855600 |
| H | -7.18818600 | -4.84630600 | 2.59386500 |
| H | -7.72722800 | -3.91849800 | 4.83330800 |
| C | 2.75996200 | -2.28889500 | 4.22885700 |
| C | 1.88883000 | -2.66201100 | 5.26627600 |
| C | 4.14283700 | -2.41612900 | 4.43922200 |
| C | 2.38419700 | -3.14688800 | 6.47880500 |
| H | 0.81880200 | -2.58727800 | 5.12242800 |
| C | 4.64221500 | -2.90156200 | 5.65012400 |
| H | 4.83253900 | -2.14911500 | 3.64934400 |
| C | 3.76292600 | -3.26577800 | 6.67302700 |
| H | 1.69803400 | -3.43538400 | 7.26428600 |
| H | 5.71066900 | -2.99742300 | 5.79246200 |
| H | 4.14833000 | -3.64322400 | 7.61131500 |
| C | 2.79670600 | 2.42351400 | 4.15078900 |
| C | 2.21886400 | 2.08795300 | 5.38787100 |
| C | 3.86743700 | 3.33168700 | 4.13751700 |
| C | 2.69498600 | 2.64618700 | 6.57610700 |

SUPPORTING INFORMATION

| | | | |
|---|-------------|-------------|-------------|
| H | 1.40326400 | 1.37708300 | 5.42645200 |
| C | 4.34741000 | 3.89155600 | 5.32474200 |
| H | 4.33351500 | 3.59256400 | 3.19685100 |
| C | 3.76005000 | 3.55136400 | 6.54568100 |
| H | 2.24249100 | 2.37154500 | 7.51992900 |
| H | 5.17665700 | 4.58626500 | 5.29583300 |
| H | 4.13184800 | 3.98257200 | 7.46609100 |
| C | -0.78080600 | 4.81558300 | -2.61068000 |
| C | 0.17739900 | 5.81462500 | -2.36432300 |
| C | -1.79910300 | 5.08074000 | -3.54096800 |
| C | 0.11959300 | 7.04231600 | -3.02657600 |
| H | 0.96980400 | 5.63758100 | -1.64806800 |
| C | -1.85992500 | 6.30892300 | -4.20594100 |
| H | -2.54883400 | 4.32713000 | -3.74115300 |
| C | -0.90016400 | 7.29092100 | -3.95016900 |
| H | 0.86540500 | 7.79979600 | -2.82416200 |
| H | -2.65363800 | 6.49650200 | -4.91718600 |
| H | -0.94568800 | 8.24205900 | -4.46461200 |
| C | -4.91177300 | 2.30416900 | -2.67522700 |
| C | -5.63049200 | 3.41538300 | -2.20281700 |
| C | -5.23158500 | 1.78628900 | -3.94171300 |
| C | -6.64061400 | 3.99456800 | -2.97481400 |
| H | -5.40937100 | 3.81874700 | -1.22326800 |
| C | -6.24050900 | 2.36413200 | -4.71631900 |
| H | -4.70035000 | 0.92134300 | -4.31662300 |
| C | -6.94508300 | 3.47077500 | -4.23431800 |
| H | -7.18786900 | 4.84704500 | -2.59423700 |
| H | -6.47796100 | 1.94995100 | -5.68740500 |
| H | -7.72806300 | 3.91800800 | -4.83289500 |
| C | -4.82066500 | -2.53815100 | -2.60788000 |
| C | -6.17552400 | -2.25521300 | -2.36160500 |
| C | -4.50033300 | -3.44618200 | -3.62990900 |
| C | -7.18193600 | -2.86257300 | -3.11483900 |
| H | -6.44863200 | -1.56410000 | -1.57425800 |
| C | -5.50559800 | -4.05557400 | -4.38605400 |
| H | -3.46363500 | -3.68232500 | -3.82777100 |
| C | -6.84741500 | -3.76374400 | -4.13015900 |
| H | -8.22001100 | -2.63478900 | -2.91106700 |
| H | -5.24105000 | -4.75595500 | -5.16731300 |
| H | -7.62672000 | -4.23558500 | -4.71448000 |
| C | -0.66694800 | -4.97231200 | -2.33654600 |
| C | -1.25016400 | -6.04947800 | -1.64772100 |
| C | -0.16494100 | -5.19859300 | -3.62940700 |
| C | -1.32989000 | -7.31569500 | -2.23219500 |
| H | -1.62950300 | -5.90394700 | -0.64467300 |
| C | -0.24379200 | -6.46374000 | -4.21745700 |
| H | 0.30278900 | -4.38933400 | -4.17456200 |
| C | -0.82836000 | -7.52411200 | -3.51990800 |
| H | -1.77762800 | -8.13432300 | -1.68411700 |
| H | 0.15407300 | -6.62012800 | -5.21154800 |
| H | -0.88843000 | -8.50495800 | -3.97354700 |
| C | 2.79646300 | -2.42340200 | -4.15089700 |
| C | 2.21913700 | -2.08691800 | -5.38797500 |
| C | 3.86654500 | -3.33233600 | -4.13776200 |
| C | 2.69514800 | -2.64498400 | -6.57633300 |
| H | 1.40405200 | -1.37545700 | -5.42643400 |
| C | 4.34640800 | -3.89204000 | -5.32511000 |
| H | 4.33225500 | -3.59391700 | -3.19710900 |
| C | 3.75957300 | -3.55091800 | -6.54604200 |
| H | 2.24306900 | -2.36962400 | -7.52014500 |
| H | 5.17516600 | -4.58733600 | -5.29629900 |
| H | 4.13128700 | -3.98199300 | -7.46654900 |
| C | 2.75962500 | 2.28851200 | -4.22904100 |
| C | 1.88844900 | 2.66306400 | -5.26591200 |
| C | 4.14255100 | 2.41409000 | -4.44004300 |
| C | 2.38383600 | 3.14772800 | -6.47852200 |
| H | 0.81840600 | 2.58964900 | -5.12153900 |
| C | 4.64194900 | 2.89929900 | -5.65102200 |
| H | 4.83232800 | 2.14592500 | -3.65061500 |
| C | 3.76261700 | 3.26496000 | -6.67337500 |
| H | 1.69765200 | 3.43734800 | -7.26357100 |

SUPPORTING INFORMATION

| | | | |
|---|------------|-------------|-------------|
| H | 5.71045300 | 2.99387000 | -5.79384800 |
| H | 4.14803900 | 3.64223700 | -7.61172300 |
| C | 5.64887000 | 2.68790300 | -0.07921300 |
| C | 5.57945600 | 4.05249400 | 0.24975600 |
| C | 6.88579600 | 2.15651900 | -0.47969000 |
| C | 6.71491400 | 4.86291100 | 0.18373800 |
| H | 4.63615400 | 4.48429100 | 0.55919200 |
| C | 8.02394200 | 2.96502500 | -0.54641100 |
| H | 6.95741200 | 1.10734100 | -0.73413700 |
| C | 7.93963200 | 4.31945200 | -0.21471900 |
| H | 6.64462600 | 5.91166000 | 0.44075700 |
| H | 8.96995900 | 2.53969200 | -0.85491200 |
| H | 8.82001600 | 4.94658900 | -0.26601200 |
| C | 5.64918000 | -2.68770600 | 0.07865500 |
| C | 5.57994900 | -4.05218300 | -0.25080600 |
| C | 6.88598800 | -2.15635900 | 0.47955600 |
| C | 6.71546500 | -4.86252800 | -0.18486200 |
| H | 4.63673700 | -4.48394900 | -0.56056100 |
| C | 8.02419100 | -2.96478900 | 0.54620600 |
| H | 6.95748100 | -1.10726300 | 0.73437900 |
| C | 7.94006000 | -4.31910800 | 0.21401800 |
| H | 6.64531300 | -5.91119200 | -0.44226400 |
| H | 8.97011500 | -2.53948400 | 0.85503300 |
| H | 8.82048900 | -4.94618600 | 0.26525500 |

Table S6. Atomic coordinates for the optimized structure of the D_{3h} ($6^35^46^4$) isomer of the $T_{14}Ph_{14}$ System.

NImag = 0

-8877.833986 Hartree

| | | | |
|----|-------------|-------------|-------------|
| Si | -5.00335700 | -0.07109100 | 0.01819600 |
| Si | -3.13990000 | 0.95945600 | -2.43551600 |
| Si | -3.14808200 | 1.58401400 | 2.10127500 |
| Si | -3.06700600 | -2.65851800 | 0.36478600 |
| Si | -1.62809200 | -1.95439300 | -2.50914700 |
| Si | -1.70558100 | 3.10360400 | -0.41749800 |
| Si | -1.61746100 | -1.19926400 | 2.93360700 |
| Si | 1.69324900 | -1.16359000 | 2.90332700 |
| Si | 1.68247600 | -1.91437700 | -2.49587300 |
| Si | 1.60531000 | 3.17166500 | -0.44440100 |
| Si | 3.10384600 | 1.68064500 | 2.07155700 |
| Si | 3.16869000 | -2.59037800 | 0.34435400 |
| Si | 3.10363700 | 1.03741300 | -2.44519900 |
| Si | 5.00966800 | 0.05144100 | -0.00343300 |
| O | -4.42473800 | 0.91563200 | 1.24443500 |
| O | -4.37216300 | -1.60363700 | 0.22213500 |
| O | -4.41058600 | 0.55831000 | -1.41821100 |
| O | -2.23662600 | 2.48535000 | 1.03560000 |
| O | -2.22400100 | 0.33552000 | 2.69706600 |
| O | -2.19046400 | -2.14217900 | 1.68048400 |
| O | -2.20635800 | -2.52983000 | -1.05293100 |
| O | -2.21375200 | -0.40110500 | -2.67671600 |
| O | -2.23040000 | 2.12032300 | -1.65573300 |
| O | -0.04786800 | 3.16223400 | -0.42038600 |
| O | 0.03683700 | -1.18997200 | 2.92222900 |
| O | 0.02593600 | -1.96181300 | -2.51144400 |
| O | 2.20825900 | 2.57861800 | 0.99720600 |
| O | 2.22406800 | 0.40064100 | 2.67732100 |
| O | 2.25892500 | -2.11028600 | 1.65472700 |
| O | 2.24184800 | -2.49368500 | -1.03579000 |
| O | 2.19773000 | -0.34182900 | -2.68925600 |
| O | 2.18804100 | 2.17543000 | -1.64889200 |
| O | 4.44413400 | -1.51501200 | 0.19080900 |
| O | 4.38447100 | 1.00242400 | 1.21981600 |
| O | 4.38820600 | 0.60647500 | -1.45717400 |
| C | -6.86716400 | -0.12800100 | 0.02200300 |
| C | -7.62018200 | 1.05350200 | -0.09257600 |
| H | -7.11778600 | 2.00892900 | -0.17919400 |
| C | -9.01577400 | 1.01261600 | -0.09406200 |
| H | -9.58258900 | 1.93016100 | -0.18282400 |
| C | -9.67899600 | -0.21316400 | 0.01947000 |

SUPPORTING INFORMATION

| | | | |
|---|--------------|-------------|-------------|
| H | -10.76071900 | -0.24570900 | 0.01841300 |
| C | -8.94285000 | -1.39464800 | 0.13483300 |
| H | -9.45213900 | -2.34517900 | 0.22396400 |
| C | -7.54575100 | -1.35173600 | 0.13598700 |
| H | -6.97727400 | -2.26733400 | 0.22712200 |
| C | -3.80307200 | 2.65251500 | 3.48607900 |
| C | -2.92221000 | 3.25486700 | 4.40133000 |
| H | -1.85572600 | 3.09003000 | 4.31359700 |
| C | -3.40650100 | 4.06126600 | 5.43312500 |
| H | -2.71606400 | 4.51588000 | 6.13139300 |
| C | -4.78173500 | 4.27648400 | 5.56579600 |
| H | -5.15780700 | 4.90004100 | 6.36645700 |
| C | -5.66870900 | 3.68217300 | 4.66513600 |
| H | -6.73406700 | 3.84338400 | 4.76589000 |
| C | -5.18159200 | 2.87594400 | 3.63240500 |
| H | -5.87084800 | 2.41380000 | 2.93847700 |
| C | -2.26842600 | -3.02801400 | -3.90605000 |
| C | -3.63328300 | -2.99523800 | -4.24454100 |
| H | -4.30532600 | -2.32704700 | -3.72014500 |
| C | -4.14109000 | -3.80548000 | -5.26194400 |
| H | -5.19330500 | -3.76223500 | -5.51086400 |
| C | -3.28876700 | -4.66598400 | -5.96032600 |
| H | -3.68000100 | -5.29328000 | -6.75079200 |
| C | -1.93060400 | -4.70935500 | -5.63758400 |
| H | -1.26379500 | -5.36896200 | -6.17712300 |
| C | -1.42624700 | -3.89694900 | -4.61780700 |
| H | -0.37135400 | -3.93494700 | -4.38338800 |
| C | -2.39616200 | 4.83016900 | -0.64927700 |
| C | -2.61703200 | 5.34931500 | -1.93640600 |
| H | -2.42586700 | 4.73127400 | -2.80406600 |
| C | -3.09664300 | 6.64961200 | -2.11229500 |
| H | -3.26600600 | 7.03066600 | -3.11083200 |
| C | -3.36126000 | 7.45374500 | -1.00011500 |
| H | -3.73482600 | 8.46055800 | -1.13497300 |
| C | -3.14903500 | 6.95146400 | 0.28678300 |
| H | -3.36013800 | 7.56635700 | 1.15188000 |
| C | -2.66941800 | 5.65030100 | 0.45883800 |
| H | -2.52048100 | 5.26628900 | 1.45968900 |
| C | 2.35825900 | -2.97600300 | -3.88434700 |
| C | 2.68495000 | -4.32546300 | -3.66747700 |
| H | 2.58598000 | -4.74830300 | -2.67620000 |
| C | 3.15298300 | -5.12676800 | -4.71239100 |
| H | 3.40526700 | -6.16235400 | -4.52535000 |
| C | 3.29968500 | -4.58896100 | -5.99394000 |
| H | 3.66368200 | -5.20775300 | -6.80387300 |
| C | 2.98108500 | -3.24780100 | -6.22527800 |
| H | 3.09874500 | -2.82423500 | -7.21405300 |
| C | 2.51345100 | -2.44993400 | -5.17835200 |
| H | 2.27957900 | -1.41011000 | -5.36663500 |
| C | 6.87323700 | 0.09727900 | 0.01807100 |
| C | 7.61893600 | -0.75057500 | -0.81913200 |
| H | 7.11074700 | -1.44969900 | -1.47137600 |
| C | 9.01446400 | -0.70812300 | -0.81652400 |
| H | 9.57561000 | -1.36730300 | -1.46582400 |
| C | 9.68486000 | 0.18461600 | 0.02525300 |
| H | 10.76653800 | 0.21807100 | 0.02788700 |
| C | 8.95597100 | 1.03136600 | 0.86369500 |
| H | 9.47093000 | 1.72185800 | 1.51856900 |
| C | 7.55903500 | 0.98765200 | 0.85948900 |
| H | 6.99715200 | 1.64086900 | 1.51334200 |
| C | -2.24029400 | -1.88108600 | 4.56491300 |
| C | -1.41727000 | -2.64612700 | 5.40695000 |
| C | -3.57498200 | -1.66630100 | 4.95231400 |
| C | -1.91078100 | -3.18018300 | 6.60064800 |
| H | -0.38375700 | -2.81726400 | 5.13865200 |
| C | -4.07227400 | -2.19868800 | 6.14362900 |
| H | -4.22928000 | -1.07008700 | 4.32865100 |
| C | -3.23953700 | -2.95872900 | 6.97012000 |
| H | -1.25835000 | -3.76194800 | 7.23837200 |
| H | -5.10081400 | -2.01741700 | 6.42689700 |
| H | -3.62229400 | -3.37017500 | 7.89511800 |

SUPPORTING INFORMATION

| | | | |
|---|-------------|-------------|-------------|
| C | 3.72588100 | 2.77370400 | 3.45275200 |
| C | 3.44471900 | 4.14912100 | 3.46891500 |
| C | 4.49693600 | 2.23250300 | 4.49659500 |
| C | 3.92012000 | 4.96360900 | 4.50062400 |
| H | 2.85439200 | 4.58163200 | 2.67274100 |
| C | 4.97373700 | 3.04412000 | 5.52785700 |
| H | 4.72511600 | 1.17420000 | 4.50907700 |
| C | 4.68519500 | 4.41230800 | 5.53099600 |
| H | 3.69485900 | 6.02195600 | 4.49748500 |
| H | 5.56580700 | 2.61197500 | 6.32395800 |
| H | 5.05422800 | 5.04217800 | 6.33000500 |
| C | -3.79649300 | 1.60329600 | -4.06113200 |
| C | -2.96067000 | 1.68209600 | -5.18831600 |
| C | -5.12596300 | 2.04034200 | -4.17789100 |
| C | -3.43959600 | 2.18831000 | -6.39843200 |
| H | -1.93685600 | 1.33651000 | -5.12442500 |
| C | -5.60809400 | 2.54592600 | -5.38816800 |
| H | -5.78569500 | 1.97228100 | -3.32324000 |
| C | -4.76460900 | 2.62261300 | -6.49926000 |
| H | -2.78502600 | 2.23849300 | -7.25867400 |
| H | -6.63640900 | 2.87454100 | -5.46339000 |
| H | -5.13725000 | 3.01267700 | -7.43751200 |
| C | 2.22506700 | 4.92060300 | -0.70893500 |
| C | 3.59440500 | 5.14958700 | -0.93477100 |
| C | 1.36178700 | 6.02717500 | -0.66970100 |
| C | 4.08617400 | 6.44341000 | -1.11554200 |
| H | 4.28346900 | 4.31504500 | -0.97743500 |
| C | 1.85057800 | 7.32455600 | -0.85049000 |
| H | 0.30349800 | 5.87819100 | -0.50570600 |
| C | 3.21322900 | 7.53467800 | -1.07275700 |
| H | 5.14247600 | 6.59880400 | -1.29149800 |
| H | 1.16808300 | 8.16366700 | -0.82029200 |
| H | 3.59249900 | 8.53843500 | -1.21424900 |
| C | 3.81391300 | -4.32622800 | 0.58871000 |
| C | 2.92686000 | -5.41655400 | 0.63485200 |
| C | 5.18818900 | -4.56949600 | 0.74264700 |
| C | 3.40202000 | -6.71544100 | 0.82877100 |
| H | 1.86259100 | -5.25336000 | 0.51922100 |
| C | 5.66576300 | -5.86884200 | 0.93635000 |
| H | 5.88126900 | -3.73964300 | 0.70912700 |
| C | 4.77352600 | -6.94287200 | 0.97969300 |
| H | 2.70706500 | -7.54419400 | 0.86221200 |
| H | 6.72783400 | -6.04039000 | 1.05283200 |
| H | 5.14245500 | -7.94916700 | 1.12972000 |
| C | -3.64134200 | -4.41773300 | 0.61569300 |
| C | -3.86729000 | -5.26238900 | -0.48410700 |
| C | -3.88812300 | -4.91400000 | 1.90683400 |
| C | -4.32909700 | -6.56779700 | -0.29916800 |
| H | -3.67048400 | -4.90455600 | -1.48622600 |
| C | -4.34998400 | -6.21895000 | 2.09416800 |
| H | -3.70761700 | -4.28518400 | 2.76885800 |
| C | -4.57261900 | -7.04724100 | 0.99074200 |
| H | -4.49401500 | -7.20680200 | -1.15677900 |
| H | -4.53093000 | -6.58705800 | 3.09553000 |
| H | -4.92902600 | -8.05899800 | 1.13512700 |
| C | 3.73086500 | 1.72583700 | -4.06378700 |
| C | 4.98355000 | 1.34165600 | -4.57002300 |
| C | 2.94494700 | 2.61464500 | -4.81644000 |
| C | 5.43868600 | 1.83052000 | -5.79702700 |
| H | 5.60925500 | 0.67122500 | -3.99584700 |
| C | 3.39705000 | 3.10392900 | -6.04408900 |
| H | 1.98395200 | 2.93507400 | -4.43574500 |
| C | 4.64442800 | 2.71064900 | -6.53686500 |
| H | 6.40846500 | 1.52924000 | -6.17090700 |
| H | 2.78229400 | 3.79195700 | -6.60947400 |
| H | 4.99673500 | 3.09125600 | -7.48678200 |
| C | 2.35123800 | -1.82679800 | 4.52828600 |
| C | 2.36006700 | -1.01951400 | 5.67934300 |
| C | 2.81053500 | -3.15009200 | 4.63656700 |
| C | 2.81563900 | -1.51857400 | 6.90174000 |
| H | 2.01760700 | 0.00569600 | 5.62032400 |

SUPPORTING INFORMATION

| | | | |
|---|------------|-------------|------------|
| C | 3.26703700 | -3.65303100 | 5.85833500 |
| H | 2.81977700 | -3.78662400 | 3.76164400 |
| C | 3.26892500 | -2.83797400 | 6.99314700 |
| H | 2.81672800 | -0.88201100 | 7.77685000 |
| H | 3.62184100 | -4.67338300 | 5.92129200 |
| H | 3.62307100 | -3.22561900 | 7.93954300 |

References

- [21] C. Pakjamsai, Y. Kawakami, *Des. Monomers Polym.* **2005**, *8*, 423-435.
- [22] P. J. Jones, R. D. Cook, C. N. McWright, R. J. Nalty, V. Choudhary, S. E. Morgan, *Appl. Polym. Sci.* **2011**, *121*, 2945-2956.
- [23] G. M. Sheldrick, *Acta Cryst.* **2015**, *A71*, 3-8.
- [24] G. M. Sheldrick, *Acta Cryst.* **2015**, *C71*, 3-8.
- [25] C. B. Hübschle, G. M. Sheldrick, B. Dittrich, *J. Appl. Crystallogr.* **2011**, *44*, 1281-1284.
- [26] Gaussian 16, Revision C.01, M. J. Frisch, G. W. Trucks, H. B. Schlegel, G. E. Scuseria, M. A. Robb, J. R. Cheeseman, G. Scalmani, V. Barone, G. A. Petersson, H. Nakatsuji, X. Li, M. Caricato, A. V. Marenich, J. Bloino, B. G. Janesko, R. Gomperts, B. Mennucci, H. P. Hratchian, J. V. Ortiz, A. F. Izmaylov, J. L. Sonnenberg, D. Williams-Young, F. Ding, F. Lipparini, F. Egidi, J. Goings, B. Peng, A. Petrone, T. Henderson, D. Ranasinghe, V. G. Zakrzewski, J. Gao, N. Rega, G. Zheng, W. Liang, M. Hada, M. Ehara, K. Toyota, R. Fukuda, J. Hasegawa, M. Ishida, T. Nakajima, Y. Honda, O. Kitao, H. Nakai, T. Vreven, K. Throssell, J. A. Montgomery, Jr., J. E. Peralta, F. Ogliaro, M. J. Bearpark, J. J. Heyd, E. N. Brothers, K. N. Kudin, V. N. Staroverov, T. A. Keith, R. Kobayashi, J. Normand, K. Raghavachari, A. P. Rendell, J. C. Burant, S. S. Iyengar, J. Tomasi, M. Cossi, J. M. Millam, M. Klene, C. Adamo, R. Cammi, J. W. Ochterski, R. L. Martin, K. Morokuma, O. Farkas, J. B. Foresman, and D. J. Fox, Gaussian, Inc., Wallingford CT, 2019.
- [27] (a) A. D. Becke, *J. Chem. Phys.* **1993**, *98*, 5648-5652. (b) C. Lee, W. Yang, R. G. Parr, *Phys. Rev. B* **1988**, *37*, 785-789. (c) A. D. Becke, *Phys. Rev. A* **1988**, *38*, 3098-3100.
- [28] (a) R. Krishnan, J. S. Binkley, R. Seeger, J. A. Pople, *J. Chem. Phys.* **1980**, *72*, 650-654. (b) A. D. McLean, G. S. Chandler, *J. Chem. Phys.* **1980**, *72*, 5639-5648.

6.3 Synthesis and Ligand Properties of Silsesquioxane-Caged Phosphite T₇Ph₇P

Zeitschrift für anorganische und allgemeine Chemie

Supporting Information

Synthesis and Ligand Properties of Silsesquioxane-Caged Phosphite T_7Ph_7P

Marc Hunsicker, Johannes Krebs, Michael Zimmer, Bernd Morgenstern, Volker Huch, and
David Scheschkewitz*

Zeitschrift für anorganische und allgemeine Chemie

Supporting Information

Synthesis and Ligand properties of silsesquioxane-caged phosphite T₇Ph₇P

Marc Hunsicker, Johannes Krebs, Michael Zimmer, Bernd Morgenstern, Volker Huch, David Scheschkewitz^{*[a]}

Supporting Information

for

**Synthesis and Ligand properties of silsesquioxane-caged
phosphite T₇Ph₇P**

Marc Hunsicker,^[a] Johannes Krebs,^[a] Michael Zimmer,^[a] Bernd Morgenstern,^[b] Volker Huch,
David Scheschkewitz^[a]

Table of Contents

| | | |
|-----|--|----|
| 1 | Plots of NMR and IR Spectra..... | 3 |
| 2 | Crystallographic data..... | 20 |
| 2.1 | Refinement Details for T ₇ Ph ₇ P-BPh ₃ | 20 |
| 2.2 | Refinement Details for T ₇ Ph ₇ P-B(C ₆ F ₅) ₃ | 21 |

[a] M. Sc. M. Hunsicker, M.Sc. J. Krebs, Dr. M. Zimmer,
Prof. Dr. D. Scheschkewitz
Krupp-Chair of Inorganic and General Chemistry
Saarland University
66123 Saarbrücken (Germany)
E-mail: scheschkewitz@mx.uni-saarland.de

[b] Dr. B. Morgenstern
Service Center X-Ray Diffraction
Saarland University
66123 Saarbrücken (Germany)

1 Plots of NMR and IR Spectra

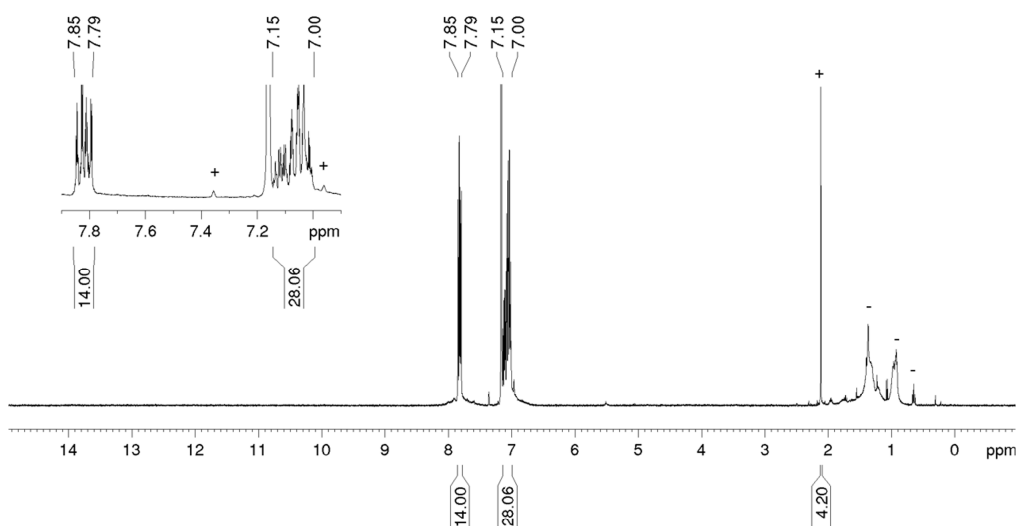


Figure S1. ^1H NMR (400.13 MHz) spectrum of $\text{T}_7\text{Ph}_7\text{P}$ **1** measured in benzene-d_6 at 300 K. Residual solvent signals of toluene and satellites of benzene-d_6 are marked with a plus sign + and remaining impurities with a minus sign –.

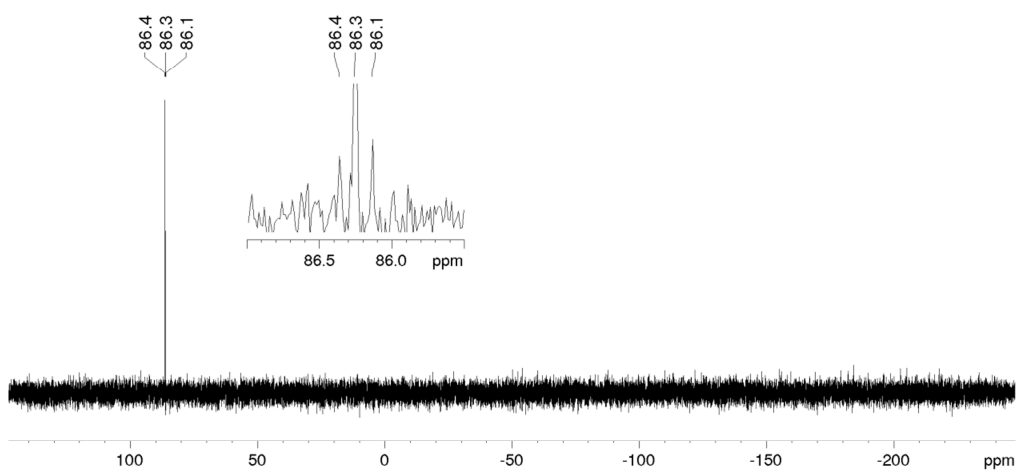


Figure S2. ^{31}P NMR (161.98 MHz) spectrum of $\text{T}_7\text{Ph}_7\text{P}$ **1** measured in benzene-d_6 at 300 K.

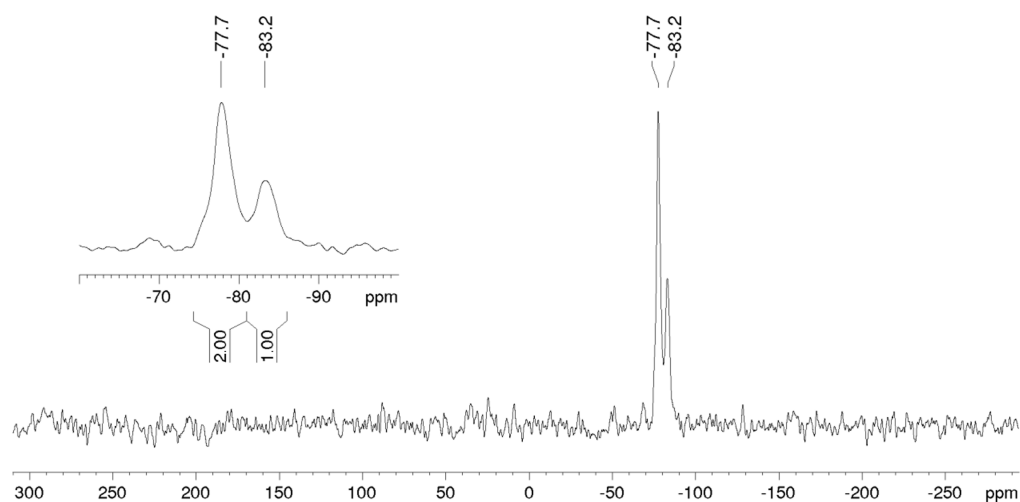


Figure S3. ^{29}Si CP/MAS NMR (79.49 MHz) spectrum of $\text{T}_7\text{Ph}_7\text{P}$ **1** at a spinning rate of 13 kHz.

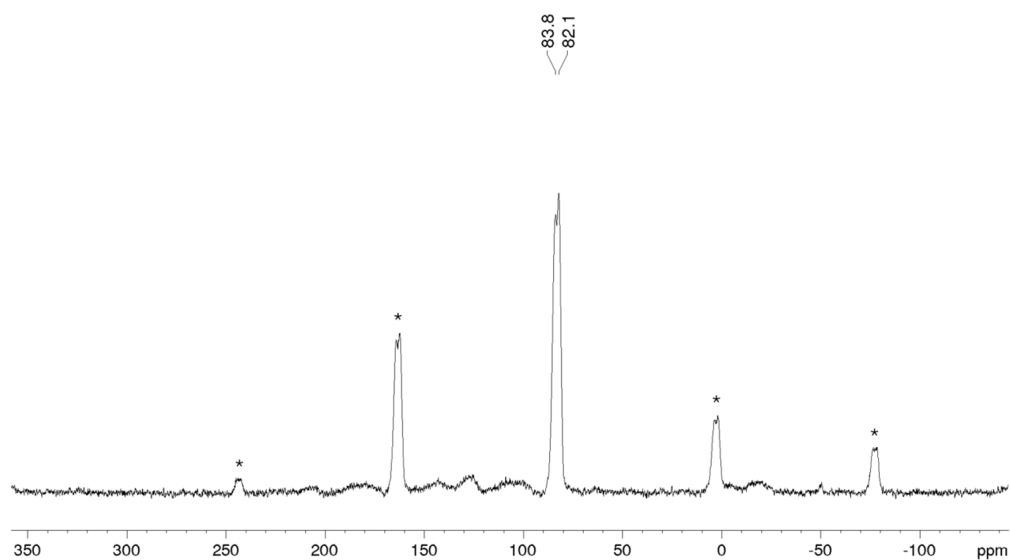


Figure S4. ^{31}P CP/MAS NMR (161.98 MHz) spectrum of $\text{T}_7\text{Ph}_7\text{P}$ **1** at a spinning rate of 13 kHz. Spinning sidebands are marked with an asterisk *.

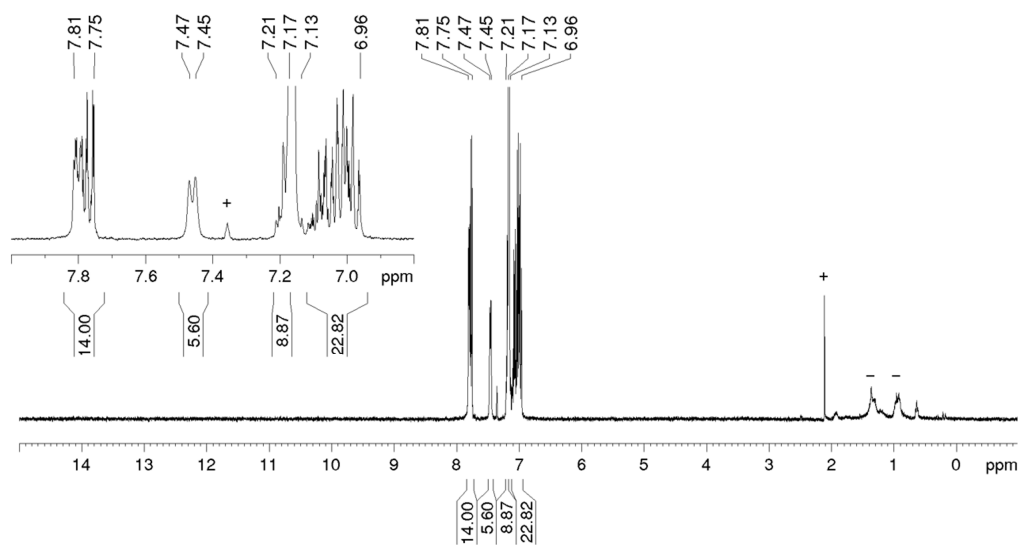


Figure S5. ^1H NMR (400.13 MHz) spectrum of $\text{T}_7\text{Ph}_7\text{P-BPh}_3$ **2** measured in benzene- d_6 at 300 K. Residual solvent signals of toluene and satellites of benzene- d_6 are marked with a plus sign + and remaining impurities with a minus sign -.

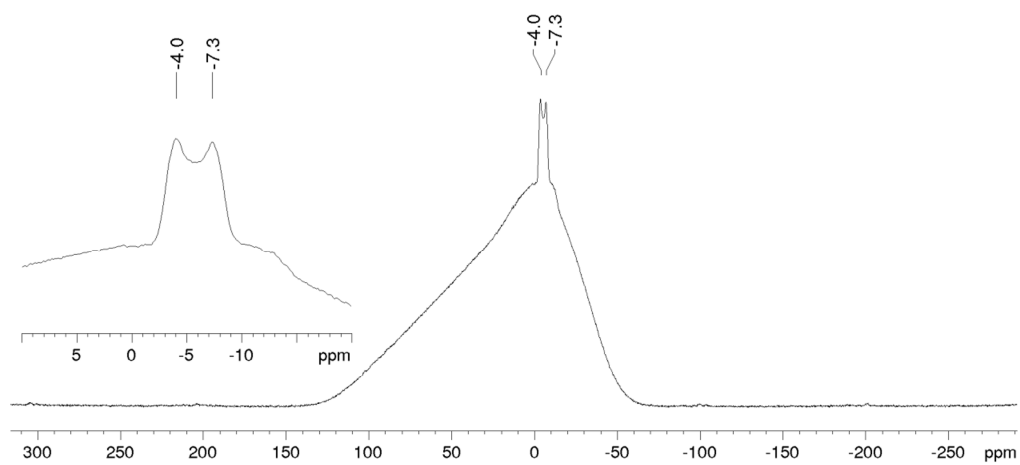


Figure S6. ^{11}B CP/MAS NMR (128.38 MHz) spectrum of $\text{T}_7\text{Ph}_7\text{P-BPh}_3$ **2** at a spinning rate of 13 kHz.

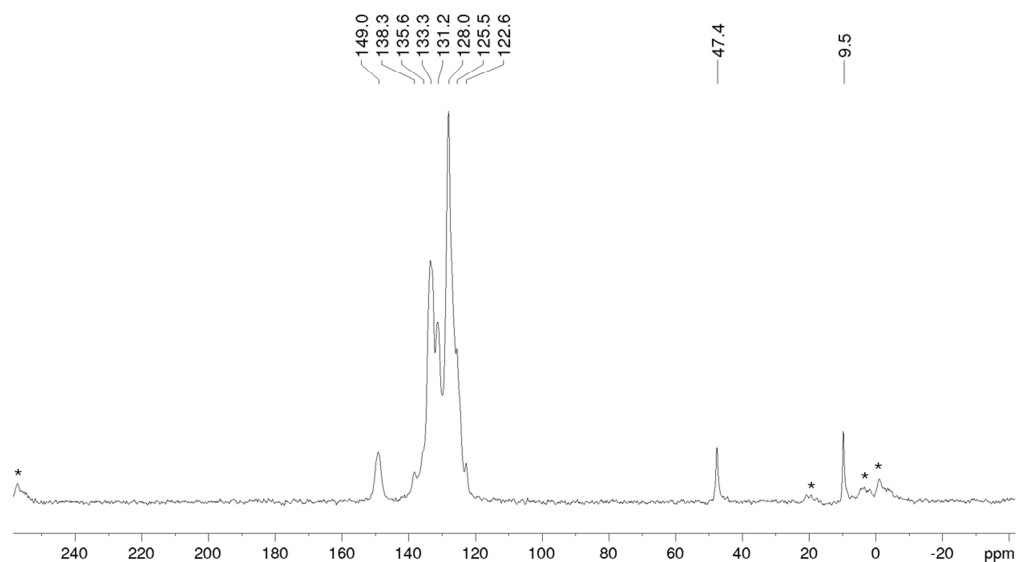


Figure S7. ^{13}C CP/MAS NMR (100.61 MHz) spectrum of $\text{T}_7\text{Ph}_7\text{P-BPh}_3$ **2** at a spinning rate of 13 kHz. Spinning side bands are marked with an asterisk *.

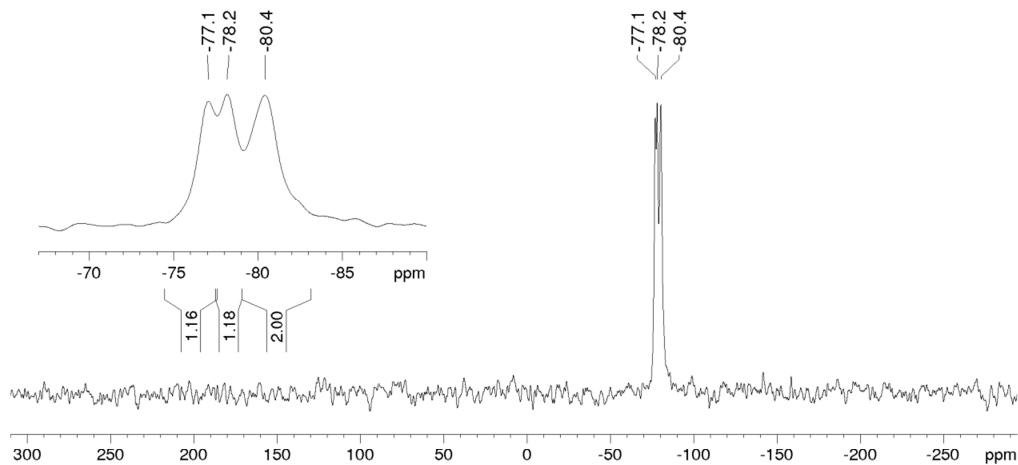


Figure S8. ^{29}Si CP/MAS NMR (79.49 MHz) spectrum of $\text{T}_7\text{Ph}_7\text{P-BPh}_3$ **2** at a spinning rate of 13 kHz.

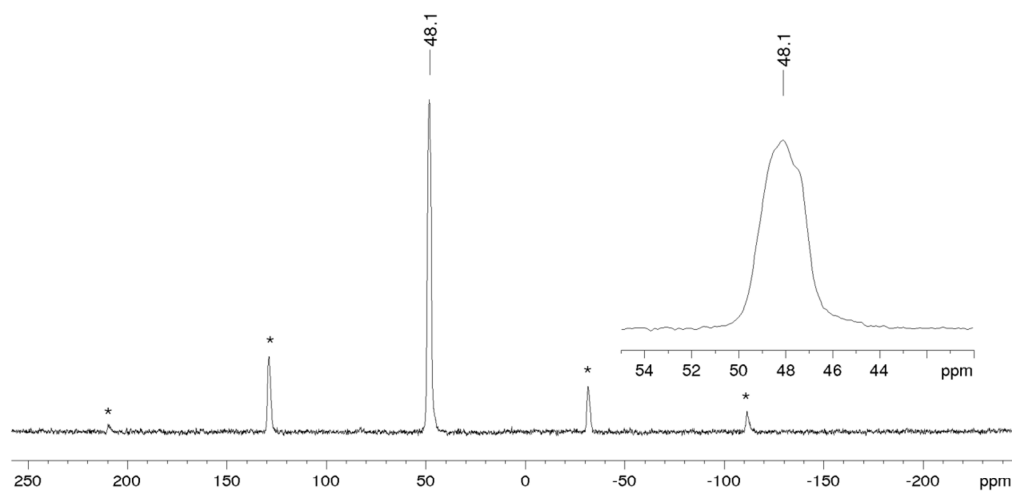


Figure S9. ^{31}P CP/MAS NMR (161.98 MHz) spectrum of $\text{T}_7\text{Ph}_7\text{P-BPh}_3$ **2** at a spinning rate of 13 kHz. Spinning sidebands are marked with an asterisk *.

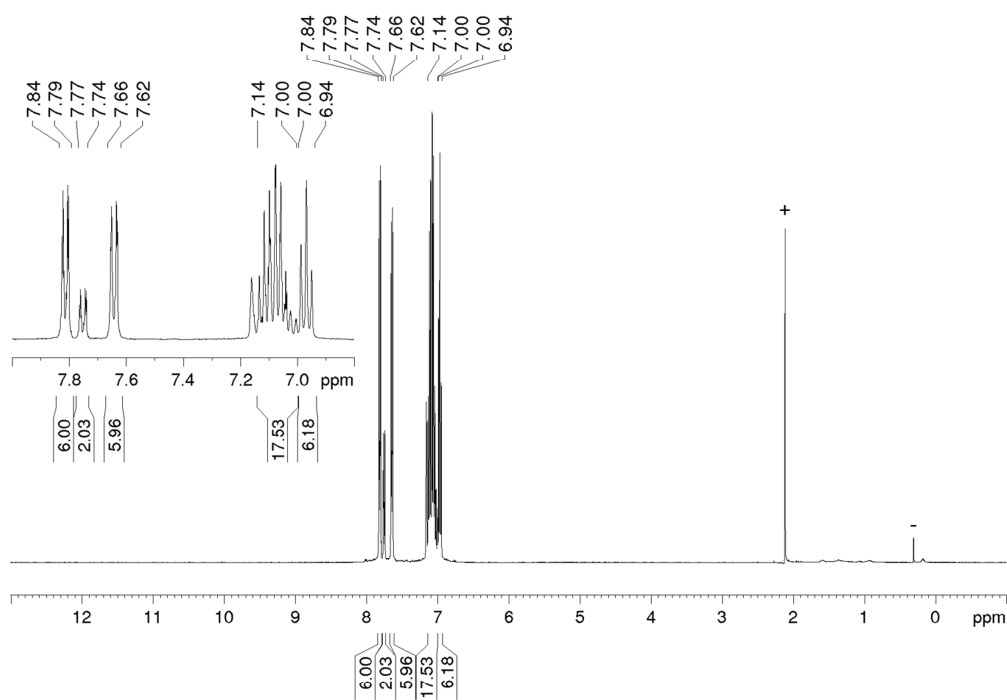


Figure S10. ^1H NMR (400.13 MHz) spectrum of $\text{T}_7\text{Ph}_7\text{P-B(C}_6\text{F}_5)_3$ **3** measured in benzene- d_6 at 300 K. Residual solvent signals of toluene are marked with a plus sign + and remaining impurities with a minus sign -.

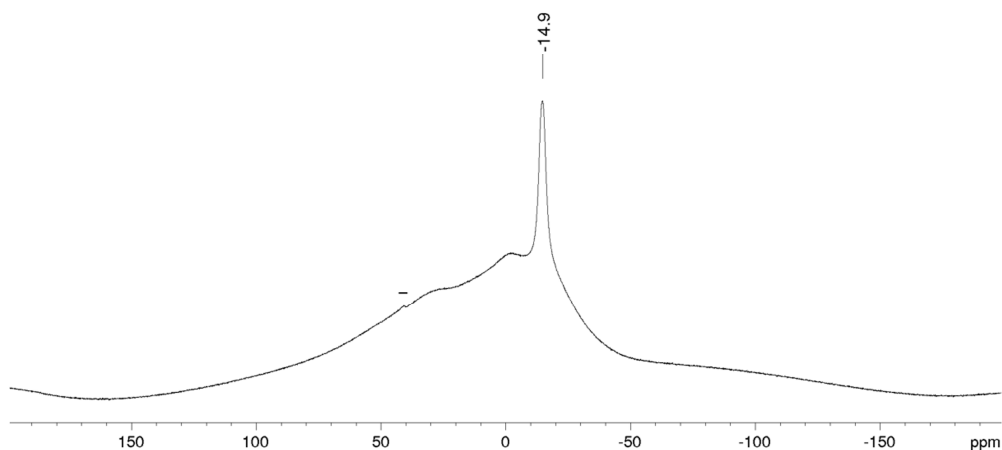


Figure S11. ^{11}B NMR (128.38 MHz) spectrum of $\text{T}_7\text{Ph}_7\text{P-B}(\text{C}_6\text{F}_5)_3$ **3** measured in benzene- d_6 at 300 K. Remaining impurities are marked with a minus sign -.

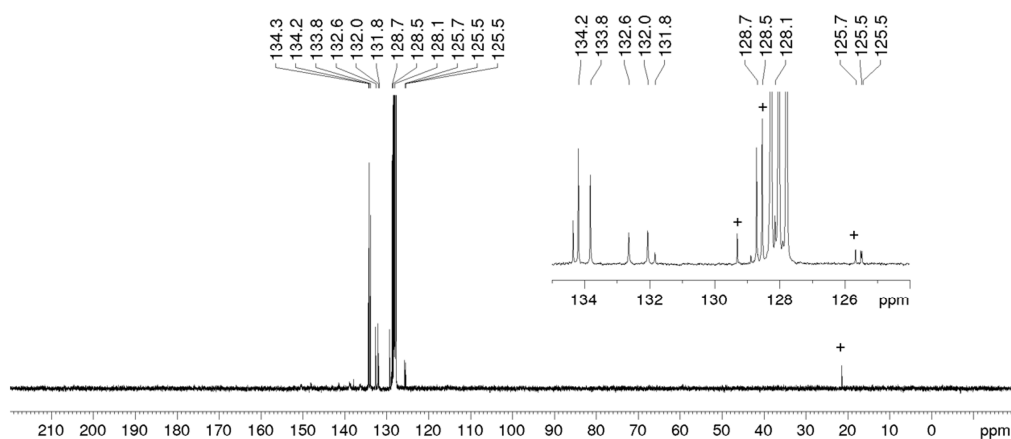


Figure S12. ^{13}C NMR (100.61 MHz) spectrum of $\text{T}_7\text{Ph}_7\text{P-B}(\text{C}_6\text{F}_5)_3$ **3** measured in benzene- d_6 at 300 K. Residual solvent signals of toluene are marked with a plus sign +.

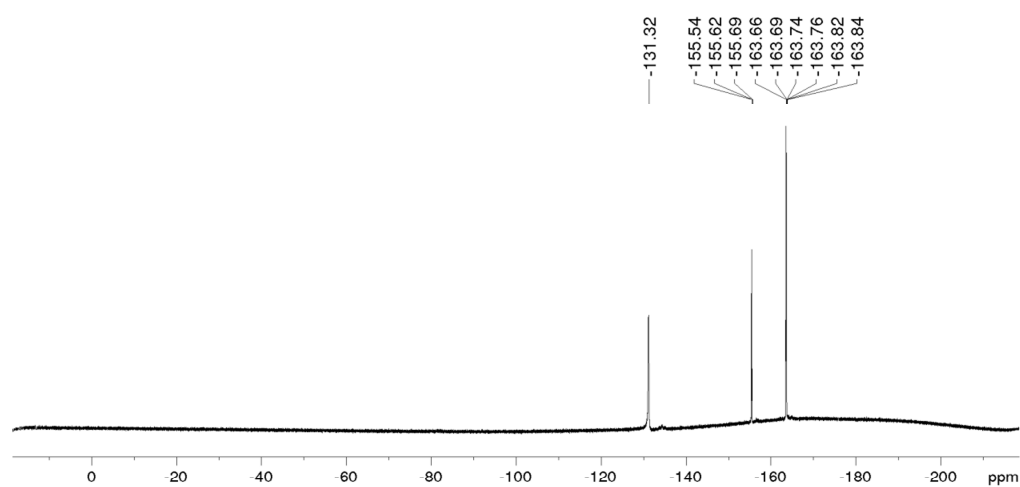


Figure 13. ^{19}F NMR (282.40 MHz) spectrum of $\text{T}_7\text{Ph}_7\text{P-B}(\text{C}_6\text{F}_5)_3$ **3** measured in benzene- d_6 at 300 K.

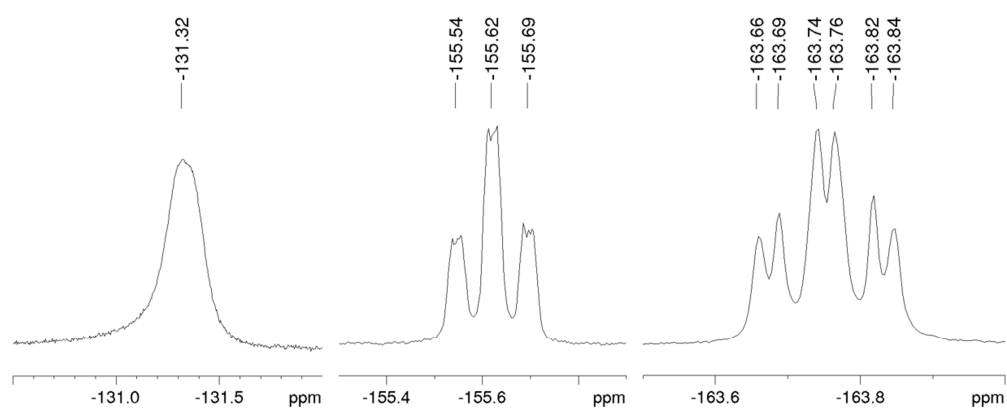


Figure S14. Magnification of the three ^{19}F NMR signals of $\text{T}_7\text{Ph}_7\text{P-B}(\text{C}_6\text{F}_5)_3$ **3** measured in benzene- d_6 at 300 K.

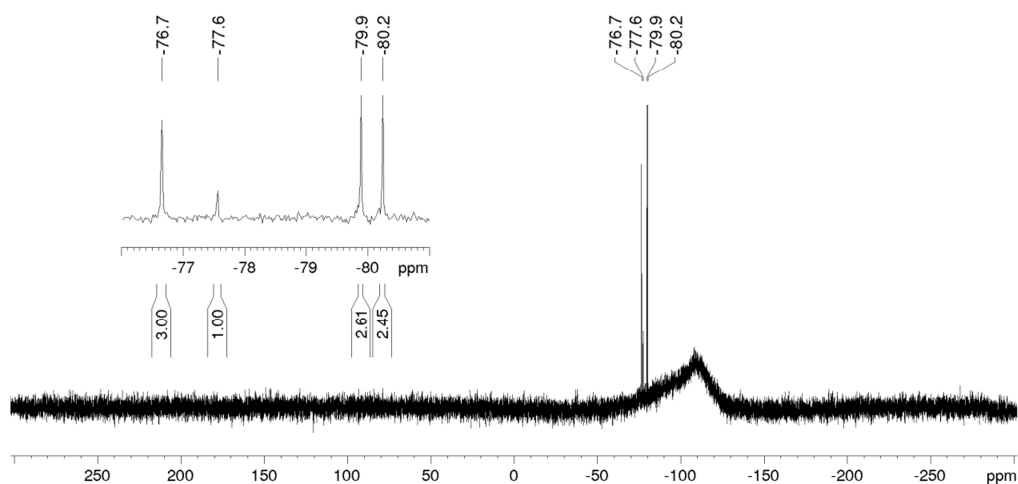


Figure S15. ^{29}Si NMR (79.49 MHz) spectrum of $\text{T}_7\text{Ph}_7\text{P-B(C}_6\text{F}_5)_3$ **3** measured in C_6D_6 at 300 K.

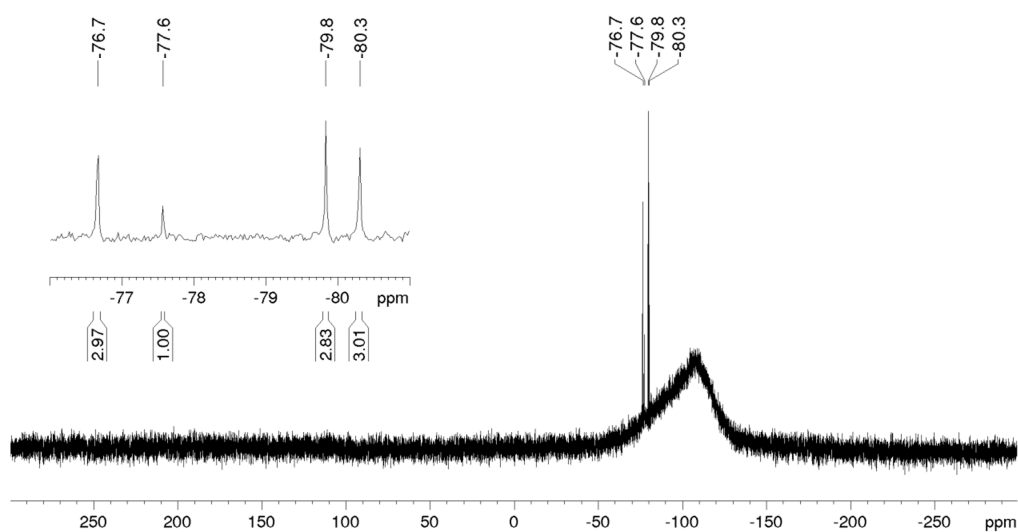


Figure S16. ^{29}Si NMR (59.63 MHz) spectrum of $\text{T}_7\text{Ph}_7\text{P-B(C}_6\text{F}_5)_3$ **3** measured in C_6D_6 at 300 K.

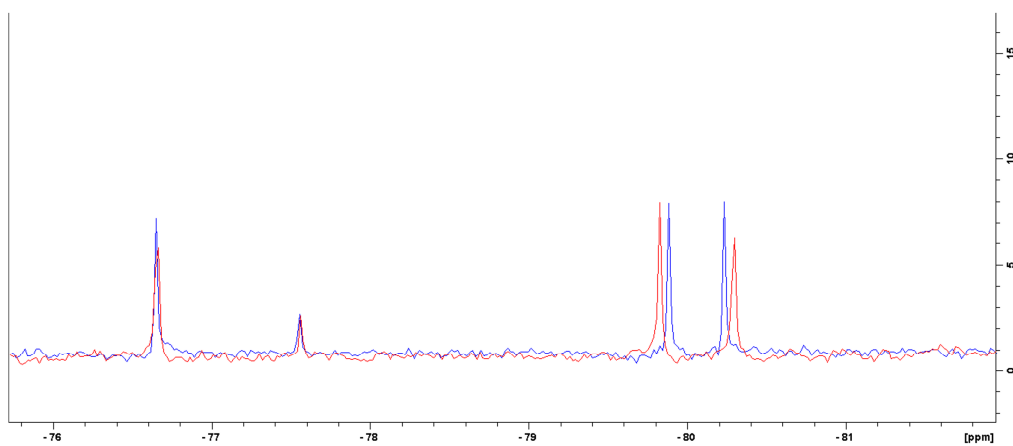


Figure S17. Overlay of the two ^{29}Si NMR spectra of $\text{T}_7\text{Ph}_7\text{P-B}(\text{C}_6\text{F}_5)_3$ **3** at 79.49 MHz (blue, from Figure S15) and 59.63 MHz (red, from Figure S16) in benzene- d_6 at 300 K.

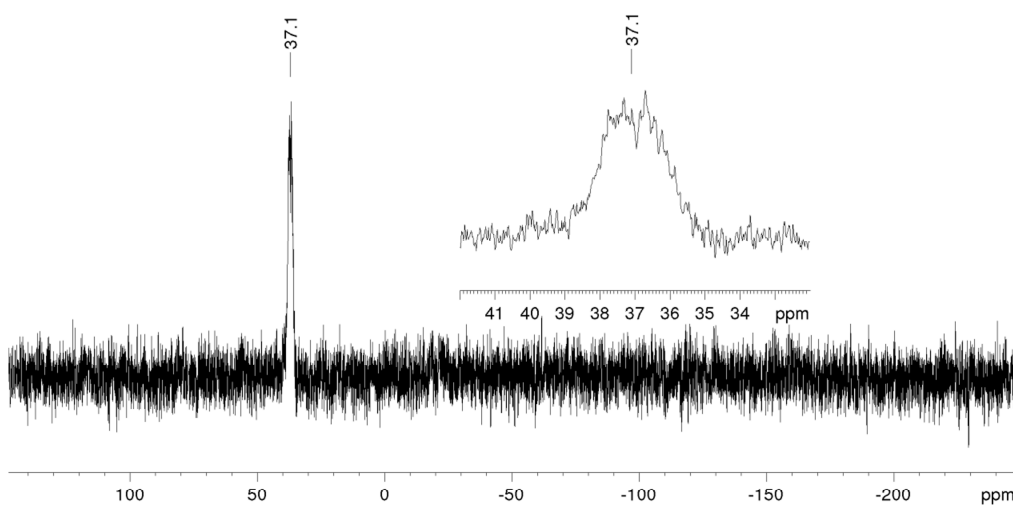


Figure S18. ^{31}P NMR (161.98 MHz) spectrum of $\text{T}_7\text{Ph}_7\text{P-B}(\text{C}_6\text{F}_5)_3$ **3** measured in benzene d_6 at 300 K.

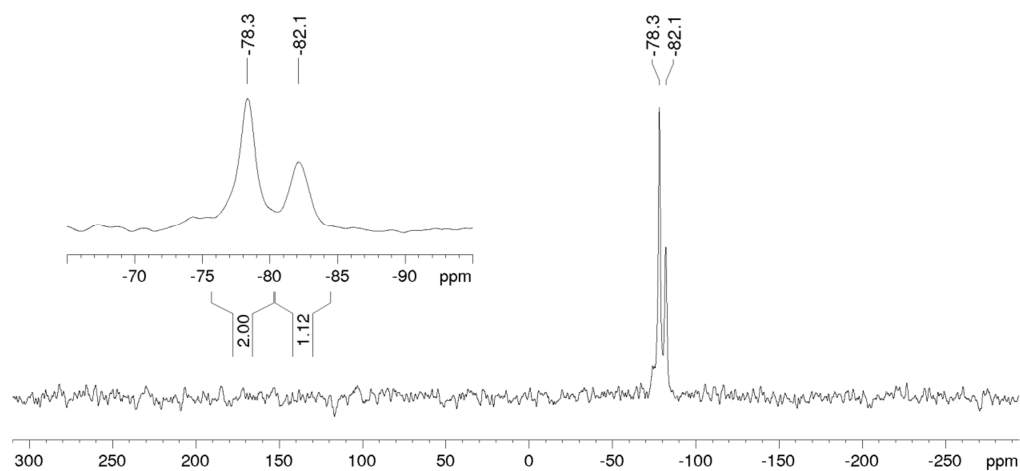


Figure S19. ^{29}Si CP/MAS NMR (79.49 MHz) spectrum of $\text{T}_7\text{Ph}_7\text{P-B(C}_6\text{F}_5)_3$ **3** at a spinning rate of 13 kHz.

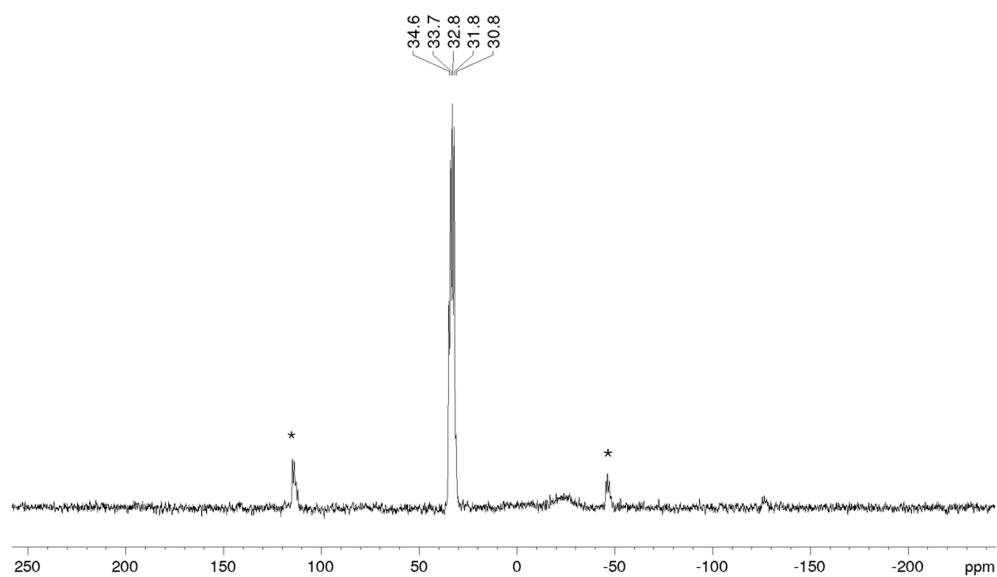


Figure S20. ^{31}P CP/MAS NMR (161.98 MHz) spectrum of $\text{T}_7\text{Ph}_7\text{P-B(C}_6\text{F}_5)_3$ **3** at a spinning rate of 13 kHz. Spinning sidebands are marked with an asterisk *.

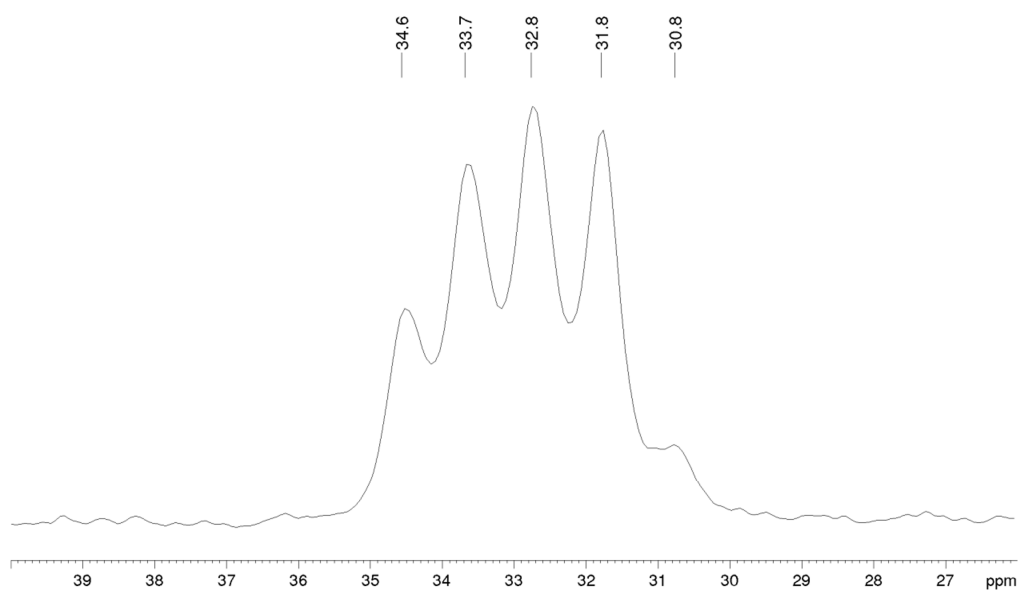


Figure S21. Magnification of the isotropic shift in the ^{31}P CP/MAS NMR (161.98 MHz) spectrum of $\text{T}_7\text{Ph}_7\text{P-B(C}_6\text{F}_5)_3$ **3** at a spinning rate of 13 kHz.

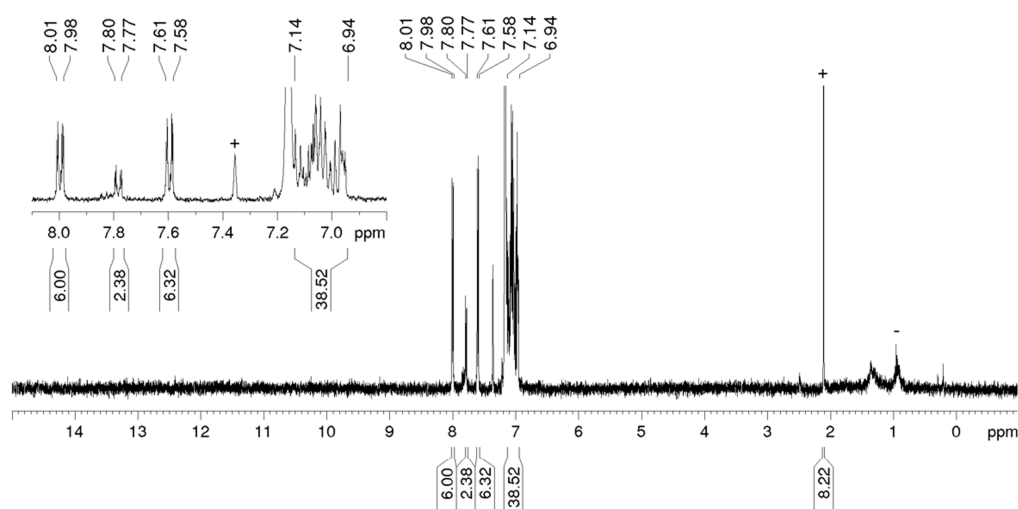


Figure 22. ^1H NMR (400.13 MHz) spectrum of $\text{T}_7\text{Ph}_7\text{P-BCl}_3$ **4** measured in benzene- d_6 at 300 K. Residual solvent signals of toluene and satellites of benzene- d_6 are marked with a plus sign +, and remaining impurities with a minus sign -.

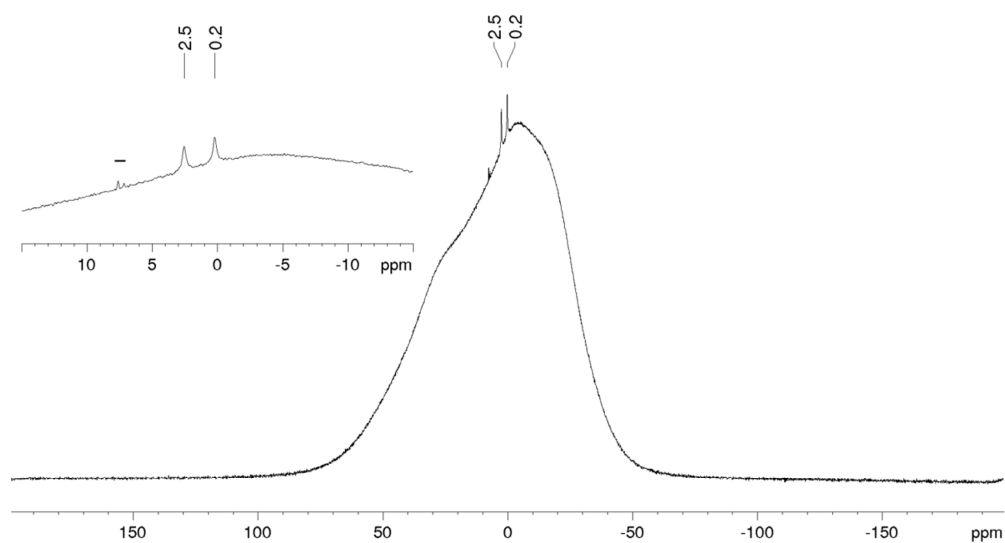


Figure S23. ^{11}B NMR (128.38 MHz) spectrum of $\text{T}_7\text{Ph}_7\text{P-BCl}_3$ **4** measured in benzene- d_6 at 300 K. Remaining impurities are marked with a minus sign $-$.

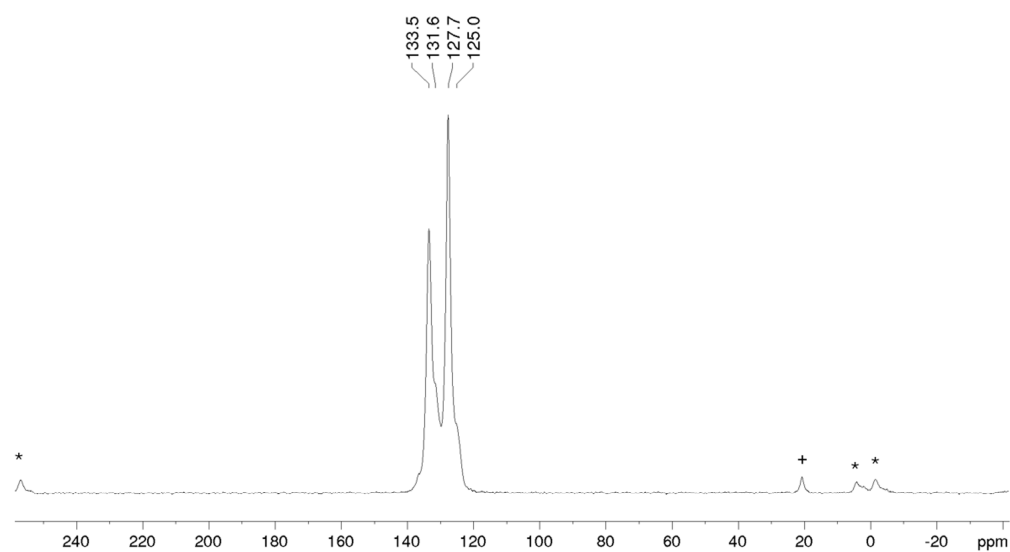


Figure S24. ^{13}C CP/MAS NMR (100.61 MHz) spectrum of $\text{T}_7\text{Ph}_7\text{P-BCl}_3$ **4** at a spinning rate of 13 kHz. Residual toluene signals are marked with a plus sign $+$, spinning side bands are marked with an asterisk $*$.

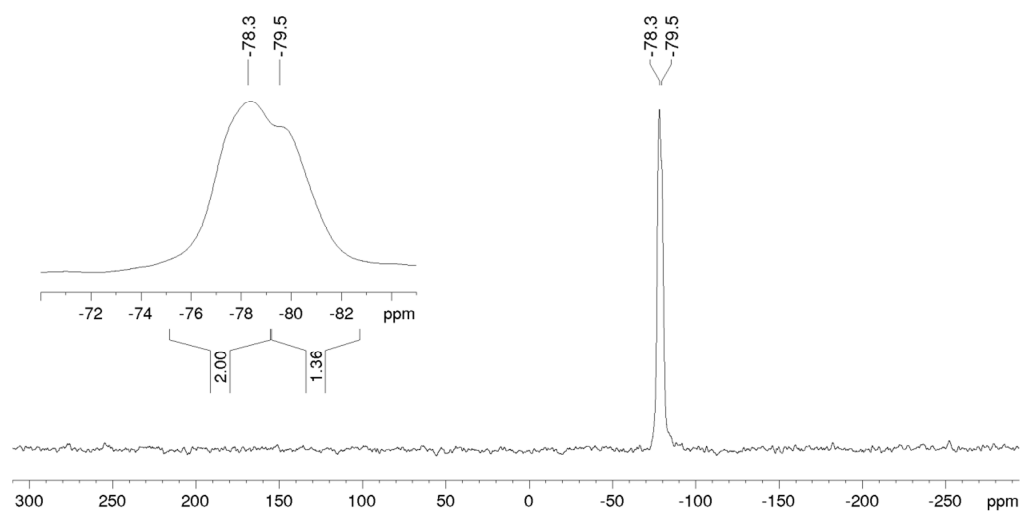


Figure S25. ^{29}Si CP/MAS NMR (79.49 MHz) spectrum of $\text{T}_7\text{Ph}_7\text{P-BCl}_3$ **4** at a spinning rate of 13 kHz.

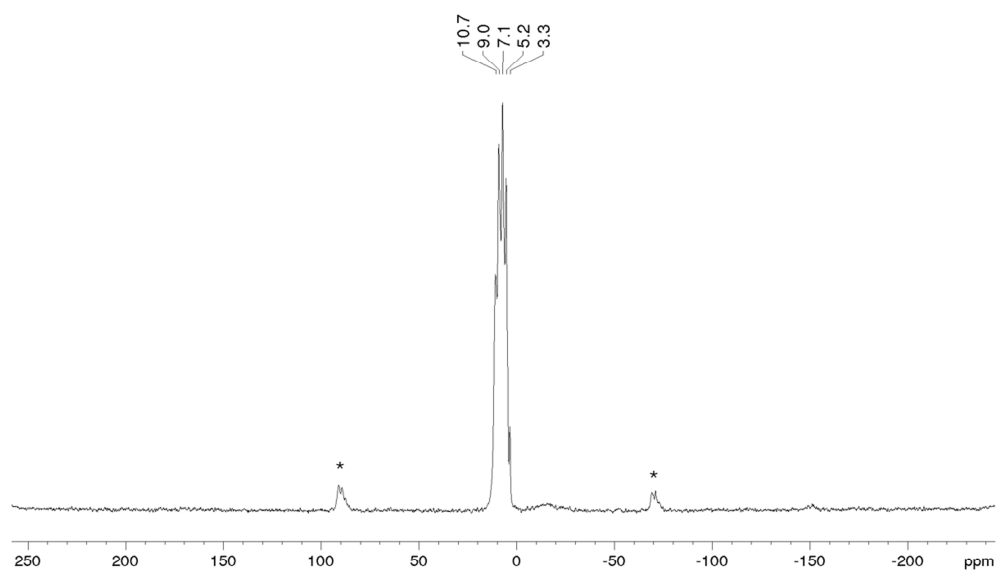


Figure S26. ^{31}P CP/MAS (161.98 MHz) NMR spectrum of $\text{T}_7\text{Ph}_7\text{P-BCl}_3$ **4** at a spinning rate of 13 kHz. Spinning side bands are marked with an asterisk *.

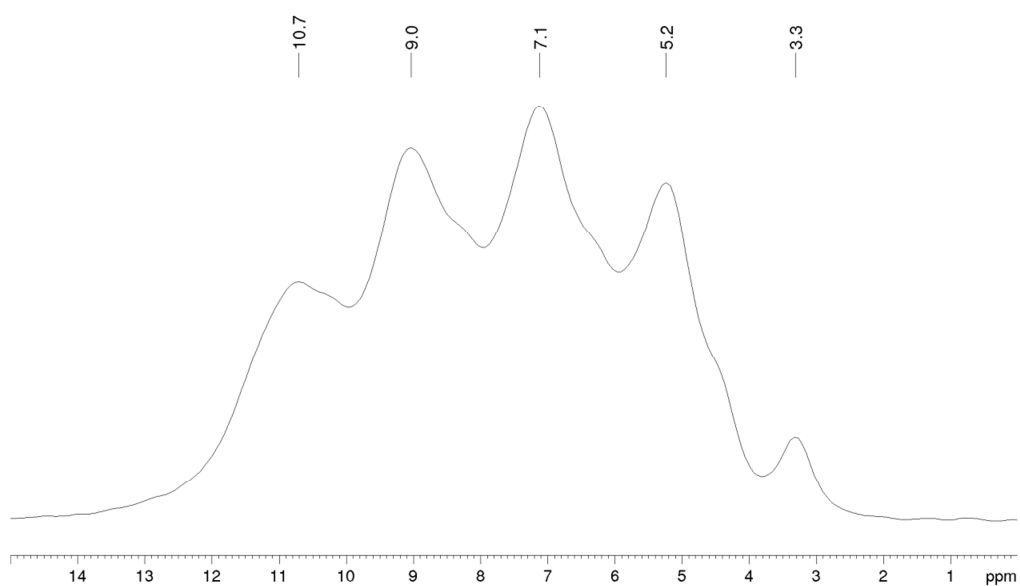


Figure S27. Magnification of the isotropic shift in the ^{31}P CP/MAS NMR spectrum of $\text{T}_7\text{Ph}_7\text{P-BCl}_3$ 4.

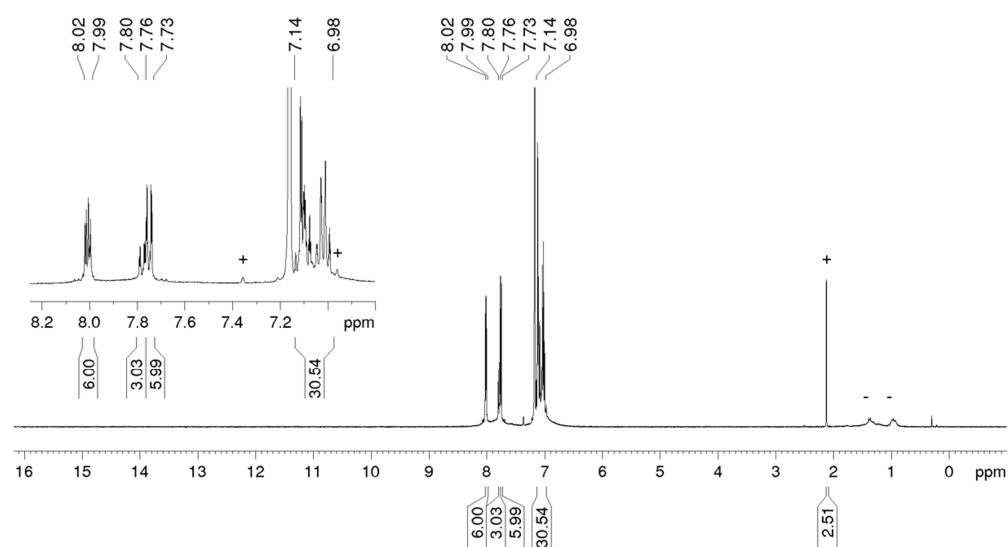


Figure S28. ^1H NMR (400.13 MHz) spectrum of $\text{T}_7\text{Ph}_7\text{P-Fe(CO)}_4$ 5 measured in benzene- d_6 at 300 K. Residual solvent signals of toluene and satellites of benzene- d_6 are marked with a plus sign + and remaining impurities with a minus sign -.

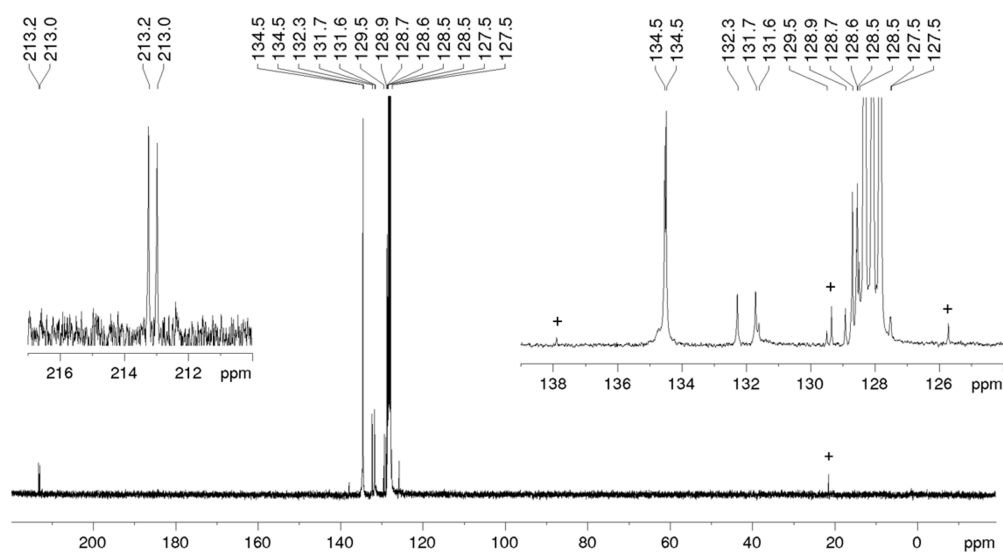


Figure S29. ^{13}C NMR (100.61 MHz) spectrum of $\text{T}_7\text{Ph}_7\text{P-Fe(CO)}_4$ **5** measured in benzene- d_6 at 300 K. Residual toluene signals are marked with a plus sign +.

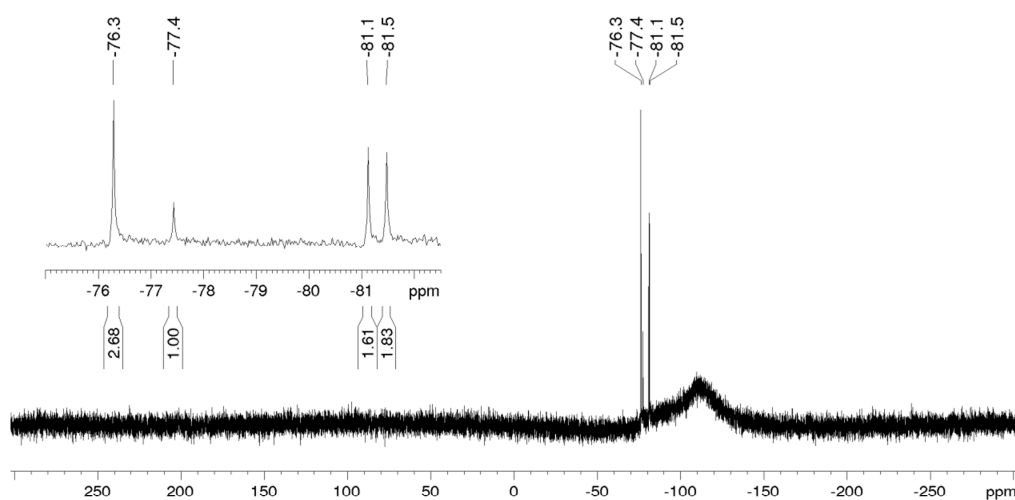


Figure S30. ^{29}Si NMR (79.49 MHz) spectrum of $\text{T}_7\text{Ph}_7\text{P-Fe(CO)}_4$ **5** measured in benzene- d_6 at 300 K.

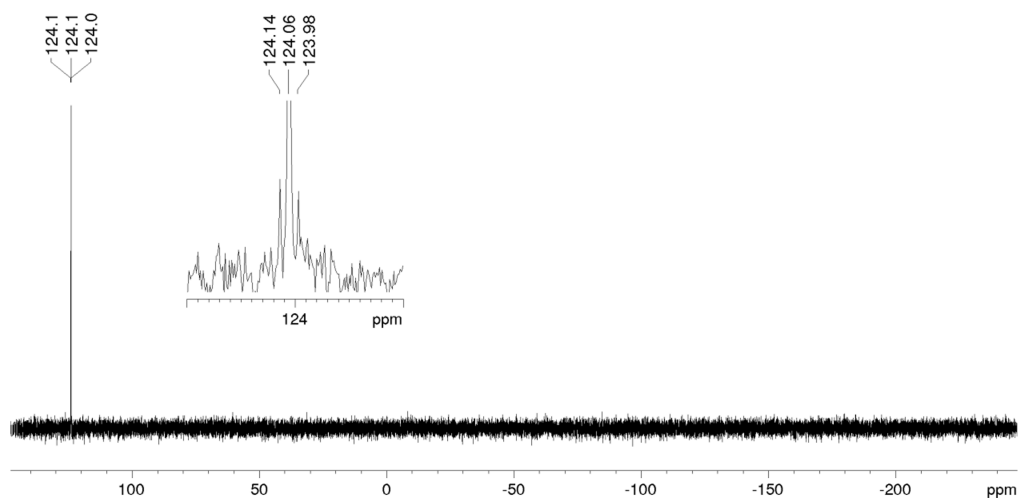


Figure S31. ^{31}P NMR (161.98 MHz) spectrum of $\text{T}_7\text{Ph}_7\text{P-Fe(CO)}_4$ **5** measured in benzene- d_6 at 300 K.

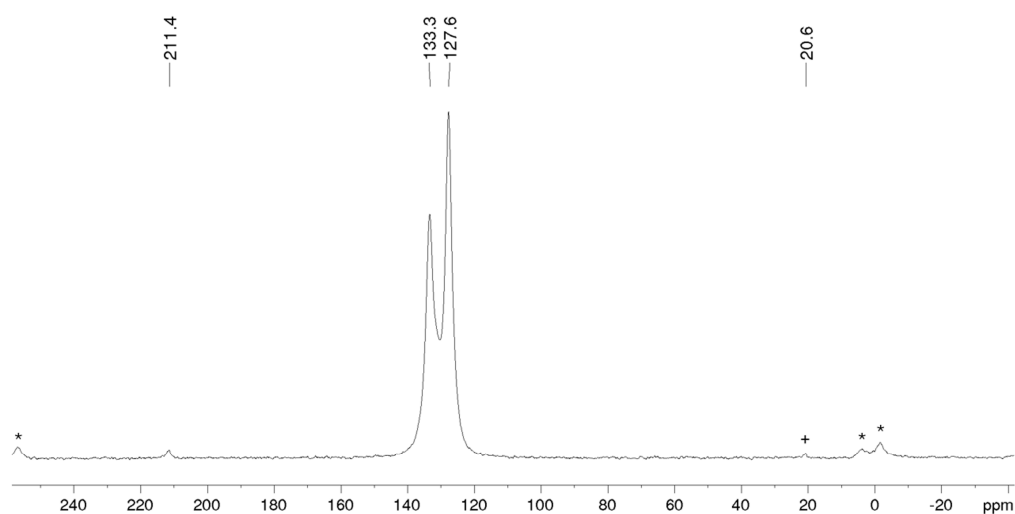


Figure 32. ^{13}C CP/MAS NMR (100.61 MHz) spectrum of $\text{T}_7\text{Ph}_7\text{P-Fe(CO)}_4$ **5** at a spinning rate of 13 kHz. Residual solvent signals of toluene are marked with a plus sign + and spinning side bands with an asterisk *.

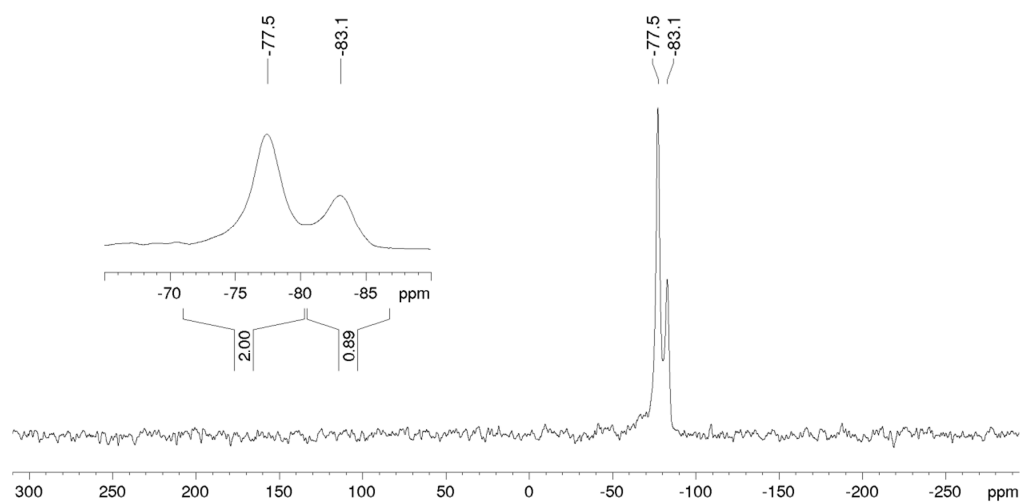


Figure S33. ^{29}Si CP/MAS NMR (79.49 MHz) spectrum of $\text{T}_7\text{Ph}_7\text{P-Fe(CO)}_4$ **5** at a spinning rate of 13 kHz.

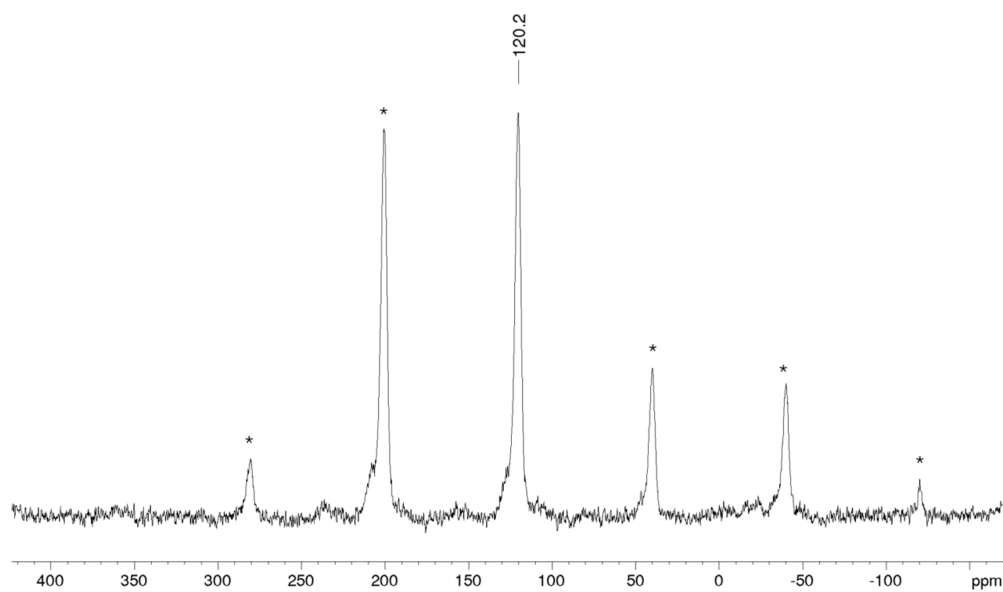


Figure S34. ^{31}P CP/MAS NMR (161.98 MHz) spectrum of $\text{T}_7\text{Ph}_7\text{P-Fe(CO)}_4$ **5** at a spinning rate 13 kHz. Spinning sidebands are marked with an asterisk *.

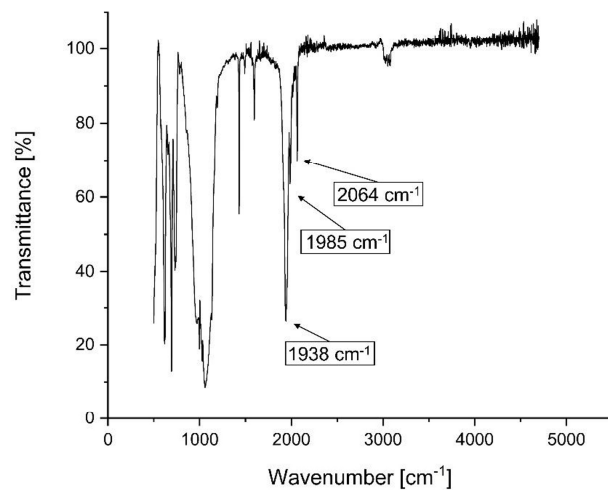


Figure S35. IR spectrum (ATR) of $T_7Ph_7P-Fe(CO)_4$ 5.

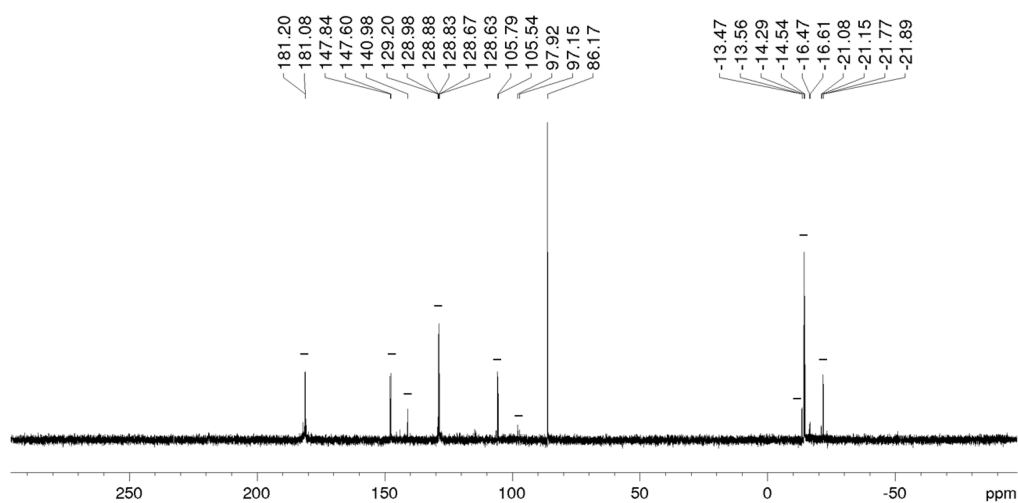


Figure S36. ^{31}P NMR spectrum (161.98 MHz) from a reaction mixture sample of $T_7Ph_7(ONa)_3$ with PCl_3 in thf, stirred overnight. Unidentified byproducts are marked with a minus sign -.

2. Crystallographic data

2.1 Refinement Details for T₇Ph₇P-BPh₃ 2

The data set was collected using a Bruker X8 Apex diffractometer. Graphite-monochromated MoK α radiation ($\lambda = 0.71073$ Å) was used. Data were collected at 152(2) K and corrected for absorption effects using the multi-scan method. The structure was solved by direct methods using SHELXS-97^[S1] and was refined by full matrix least squares calculations on F^2 (SHELXL2018^[S2]) in the graphical user interface Shelxle.^[S3]

All non H-atoms were located in the electron density maps and refined anisotropically. C-bound H atoms were placed in positions of optimized geometry and treated as riding atoms. Their isotropic displacement parameters were coupled to the corresponding carrier atoms by a factor of 1.2 (CH, CH₂) or 1.5 (CH₃). *Disorder*: One of the toluene solvent molecules lies over a center of inversion and hence, was split over two positions using the PART -1 command of SHELX. Its site occupation factors were constraint to 0.5. A $\text{dfix} = 1.39$ (0.01) Å was used to restraint the C-C bond lengths. One solvent toluene was split over two positions ($\text{fvar } 2: 0.82 / 0.18$).

Acknowledgements. Instrumentation and technical assistance for this work were provided by the Service Center X-ray Diffraction, with financial support from Saarland University and German Science Foundation (project number INST 256/506-1).

Table S1. Crystal data and structure refinement for sh4115.

| | | |
|---|--|--------------------------------|
| Identification code | sh4115 | |
| Empirical formula | 2(C ₆₀ H ₅₀ B O ₁₂ P Si ₇), 7(C ₇ H ₈) | |
| Formula weight | 3047.75 | |
| Temperature | 152(2) K | |
| Wavelength | 0.71073 Å | |
| Crystal system | Triclinic | |
| Space group | P-1 | |
| Unit cell dimensions | $a = 11.8613(5)$ Å | $a = 80.0806(16)^\circ$. |
| | $b = 15.2142(8)$ Å | $b = 87.8072(13)^\circ$. |
| | $c = 23.0370(13)$ Å | $\gamma = 76.4972(12)^\circ$. |
| Volume | $3981.9(4)$ Å ³ | |
| Z | 1 | |
| Density (calculated) | 1.271 Mg/m ³ | |
| Absorption coefficient | 0.201 mm ⁻¹ | |
| $F(000)$ | 1598 | |
| Crystal size | $0.344 \times 0.251 \times 0.169$ mm ³ | |
| Theta range for data collection | 1.396 to 29.265° . | |
| Index ranges | $-16 \leq h \leq 16$, $-20 \leq k \leq 20$, $-31 \leq l \leq 31$ | |
| Reflections collected | 146482 | |
| Independent reflections | 21619 [$R(\text{int}) = 0.0515$] | |
| Completeness to $\theta = 25.242^\circ$ | 100.0 % | |
| Absorption correction | Semi-empirical from equivalents | |

| | |
|--------------------------------------|------------------------------------|
| Max. and min. transmission | 0.7458 and 0.7219 |
| Refinement method | Full-matrix least-squares on F^2 |
| Data / restraints / parameters | 21619 / 370 / 1051 |
| Goodness-of-fit on F^2 | 1.013 |
| Final R indices [$I > 2\sigma(I)$] | $R1 = 0.0399$, $wR2 = 0.0919$ |
| R indices (all data) | $R1 = 0.0729$, $wR2 = 0.1096$ |
| Extinction coefficient | n/a |
| Largest diff. peak and hole | 0.463 and -0.368 e.Å ⁻³ |

2.2 Refinement Details for T₇Ph₇P-B(C₆F₅)₃ 3.

The data set was collected using a Bruker D8 Venture diffractometer with a microfocus sealed tube and a Photon II detector. Monochromated MoK α radiation ($\lambda = 0.71073$ Å) was used. Data were collected at 133(2) K and corrected for absorption effects using the multi-scan method. The structure was solved by direct methods using SHELXT^[S4] and was refined by full matrix least squares calculations on F^2 (SHELXL2018^[S2]) in the graphical user interface Shelxle.^[S3]

All non H-atoms were located in the electron density maps and refined anisotropically. C-bound H atoms were placed in positions of optimized geometry and treated as riding atoms. Their isotropic displacement parameters were coupled to the corresponding carrier atoms by a factor of 1.2 (CH) or 1.5 (CH₃). *Disorder*: One phenyl-group is split over two positions (fvar 2: 0.67/0.33).

Acknowledgements. Instrumentation and technical assistance for this work were provided by the Service Center X-ray Diffraction, with financial support from Saarland University and German Science Foundation (project number INST 256/506-1 (D8 Venture) and 256/582-1 (Synergy-S)).

Table 1. Crystal data and structure refinement for sh4494_a.

| | | |
|---------------------------------|---|--------------------------|
| Identification code | sh4494_a | |
| Empirical formula | C ₈₁ H ₅₉ B F ₁₅ O ₁₂ P Si ₇ | |
| Formula weight | 1747.69 | |
| Temperature | 133(2) K | |
| Wavelength | 0.71073 Å | |
| Crystal system | Monoclinic | |
| Space group | P2 ₁ /n | |
| Unit cell dimensions | $a = 16.5251(10)$ Å | $a = 90^\circ$. |
| | $b = 23.3893(14)$ Å | $b = 107.336(2)^\circ$. |
| | $c = 21.9647(13)$ Å | $c = 90^\circ$. |
| Volume | $8103.9(8)$ Å ³ | |
| Z | 4 | |
| Density (calculated) | 1.432 Mg/m ³ | |
| Absorption coefficient | 0.233 mm ⁻¹ | |
| $F(000)$ | 3576 | |
| Crystal size | 0.320 x 0.263 x 0.048 mm ³ | |
| Theta range for data collection | 1.994 to 27.000°. | |

| | |
|-----------------------------------|---|
| Index ranges | -20<=h<=21, -28<=k<=29, -28<=l<=28 |
| Reflections collected | 119722 |
| Independent reflections | 17680 [R(int) = 0.0935] |
| Completeness to theta = 25.242° | 100.0 % |
| Absorption correction | Semi-empirical from equivalents |
| Max. and min. transmission | 0.7461 and 0.6278 |
| Refinement method | Full-matrix least-squares on F ² |
| Data / restraints / parameters | 17680 / 290 / 1114 |
| Goodness-of-fit on F ² | 1.029 |
| Final R indices [I>2sigma(I)] | R1 = 0.0573, wR2 = 0.1263 |
| R indices (all data) | R1 = 0.1070, wR2 = 0.1578 |
| Extinction coefficient | 0.00133(13) |
| Largest diff. peak and hole | 0.903 and -0.607 e.Å ⁻³ |

References

- [S1] G. M. Sheldrick, *Acta Cryst.* **2008**, *A64*, 112-122.
[S2] G. M. Sheldrick, *Acta Cryst.* **2015**, *C71*, 3-8.
[S3] C. B. Hübschle, G. M. Sheldrick, B. Dittrich, *J. Appl. Crystallogr.* **2011**, *44*, 1281-1284.
[S4] G.M. Sheldrick, *Acta Cryst.* **2015**, *A71*, 3-8.

7 Permission of Redistribution and Licensing

Reproduced Articles:

M. Hunsicker, N. E. Poitiers, V. Huch, B. Morgenstern, M. Zimmer, D. Scheschkewitz, Interlinkage of a siliconoid with a silsesquioxane: en route to a molecular model system for silicon monoxide, *Z. Anorg. Allg. Chem.* **2022**, 648, e202200239.

(<https://doi.org/10.1002/zaac.202200239>)

This article has been published by Wiley-VCH Verlag GmbH & Co. KGaA as an “Open Access” Article and is licensed under a “Creative Commons Attribution-NonCommercial-NoDerivatives 4.0 International (CC BY-NC-ND-4.0)” License (<https://creativecommons.org/licenses/by-nc-nd/4.0/>).

M. Hunsicker, Ankur, B. Morgenstern, M. Zimmer, D. Scheschkewitz, Polyhedral Oligomeric Silsesquioxane D_{3h} -(RSiO_{1.5})₁₄, *Chem. Eur. J.* **2024**, 30, e202303640.

(<https://doi.org/10.1002/chem.202303640>)

This article has been published by Wiley-VCH Verlag GmbH & Co. KGaA as an “Open Access” Article and is licensed under a “Creative Commons Attribution-NonCommercial-NoDerivatives 4.0 International (CC BY-NC-ND-4.0)” License (<https://creativecommons.org/licenses/by-nc-nd/4.0/>).

M. Hunsicker, J. Krebs, M. Zimmer, B. Morgenstern, V. Huch, D. Scheschkewitz, Synthesis and Ligand Properties of Silsesquioxane-Caged Phosphite T₇Ph₇P, *Z. Anorg. Allg. Chem.* **2024**, 650, e202400068.

(<https://doi.org/10.1002/zaac.202400068>)

This article has been published by Wiley-VCH Verlag GmbH & Co. KGaA as an “Open Access” Article and is licensed under a “Creative Commons Attribution-

NonCommercial-NoDerivatives 4.0 International (CC BY-NC-ND-4.0)" License (<https://creativecommons.org/licenses/by-nc-nd/4.0/>).

Reproduced Figures:

Figure 4a from A. Hirata, S. Kohara, T. Asada, M. Arao, C. Yogi, H. Imai, Y. Tan, T. Fujita, M. Chen, Atomic-scale disproportionation in amorphous silicon monoxide, *Nat. Commun.* **2016**, 7, 11591; excerpt of the original.


(<https://doi.org/10.1038/ncomms11591>)

This article has been published by Springer Nature as an „Open access“ article and is licensed under a „Creative Commons Attribution 4.0 International (CC-BY-4.0)“ License (<https://creativecommons.org/licenses/by/4.0/>). Copyright © 2016, The Authors.

Figure 1 from T. Kudo, K. Machida, M. S. Gordon, Exploring the Mechanism for the Synthesis of Silsesquioxanes. 4. The Synthesis of T₈, *J. Phys. Chem. A* **2005**, 109, 5424-5429.

(<https://doi.org/10.1021/jp040731b>)

Reprinted with permission from T. Kudo, K. Machida, M. S. Gordon, *J. Phys. Chem. A* **2005**, 109, 5424-5429. Copyright © 2005, American Chemical Society.



ACS Publications
Most Trusted. Most Cited. Most Read.

Exploring the Mechanism for the Synthesis of Silsesquioxanes. 4. The Synthesis of T₈

Author: Takako Kudo, Kazuya Machida, Mark S. Gordon

Publication: The Journal of Physical Chemistry A

Publisher: American Chemical Society

Date: Jun 1, 2005

Copyright © 2005, American Chemical Society

PERMISSION/LICENSE IS GRANTED FOR YOUR ORDER AT NO CHARGE

This type of permission/license, instead of the standard Terms and Conditions, is sent to you because no fee is being charged for your order. Please note the following:

- Permission is granted for your request in both print and electronic formats, and translations.
- If figures and/or tables were requested, they may be adapted or used in part.
- Please print this page for your records and send a copy of it to your publisher/graduate school.
- Appropriate credit for the requested material should be given as follows: "Reprinted (adapted) with permission from {COMPLETE REFERENCE CITATION}. Copyright {YEAR} American Chemical Society." Insert appropriate information in place of the capitalized words.
- One-time permission is granted only for the use specified in your RightsLink request. No additional uses are granted (such as derivative works or other editions). For any uses, please submit a new request.

If credit is given to another source for the material you requested from RightsLink, permission must be obtained from that source.

BACK
CLOSE WINDOW

Figure 15 from A. Hohl, T. Wieder, P. A. Van Aken, T. E. Weirich, G. Denninger, M. Vidal, S. Oswald, C. Deneke, J. Mayer, H. Fuess, An interface clusters mixture model for the structure of amorphous silicon monoxide (SiO), *J. Non-Cryst. Solids* **2003**, 320, 255-280.

(<https://www.sciencedirect.com/science/article/abs/pii/S0022309303000310>;

DOI: 10.1016/S0022-3093(03)00031-0)

Reprinted from “An interface clusters mixture model for the structure of amorphous silicon monoxide (SiO)”, Volume 320, A. Hohl, T. Wieder, P. A. van Aken, T. E. Weirich, G. Denninger, M. Vidal, S. Oswald, C. Deneke, J. Mayer, H. Fuess, Figure 15 / Discussion, pages 255-280, Copyright © 2003, with permission from Elsevier.

7 Permission of Redistribution and Licensing

ELSEVIER LICENSE TERMS AND CONDITIONS

Oct 24, 2024

This Agreement between Marc Christian Hunsicker ("You") and Elsevier ("Elsevier") consists of your license details and the terms and conditions provided by Elsevier and Copyright Clearance Center.

| | |
|---|--|
| License Number | 5895370306196 |
| License date | Oct 24, 2024 |
| Licensed Content Publisher | Elsevier |
| Licensed Content Publication | Journal of Non-Crystalline Solids |
| Licensed Content Title | An interface clusters mixture model for the structure of amorphous silicon monoxide (SiO) |
| Licensed Content Author | A Hohl, T Wieder, P.A van Aken, T.E Weirich, G Denninger, M Vidal, S Oswald, C Deneke, J Mayer, H Fuess |
| Licensed Content Date | Jun 1, 2003 |
| Licensed Content Volume | 320 |
| Licensed Content Issue | 1-3 |
| Licensed Content Pages | 26 |
| Start Page | 255 |
| End Page | 280 |
| Type of Use | reuse in a thesis/dissertation |
| Portion | figures/tables/illustrations |
| Number of figures/tables/illustrations | 1 |
| Format | both print and electronic |
| Are you the author of this Elsevier article? | No |
| Will you be translating? | No |
| Title of new work | Functionalization of Silsesquioxanes: From Linkage of Unsaturated Silicon Clusters and Framework Expansion to Lewis Acid-Base Chemistry |
| Institution name | University of Saarland |
| Expected presentation date | Oct 2024 |
| Order reference number | 2 |
| Portions | Figure 15 |
| The Requesting Person / Organization to Appear on the License | Marc Christian Hunsicker |
| Requestor Location | Mr. Marc Christian Hunsicker University of Saarland, Campus C4.1 Saarbrücken, 66123 Germany Attn: University of Saarland GB 494 6272 12 |
| Publisher Tax ID | |
| Total | 0.00 EUR |
| Terms and Conditions | |

INTRODUCTION

1. The publisher for this copyrighted material is Elsevier. By clicking "accept" in connection with completing this licensing transaction, you agree that the following terms and conditions apply to this transaction (along with the Billing and Payment terms and conditions established by Copyright Clearance Center, Inc. ("CCC"), at the time that you opened your RightsLink account and that are available at any time at <https://myaccount.copyright.com>).

GENERAL TERMS

2. Elsevier hereby grants you permission to reproduce the aforementioned material subject to the terms and conditions indicated.

3. Acknowledgement: If any part of the material to be used (for example, figures) has appeared in our publication with credit or acknowledgement to another source, permission must also be sought from that source. If such permission is not obtained then that material may not be included in your publication/copies. Suitable acknowledgement to the source must be made, either as a footnote or in a reference list at the end of your publication, as follows:

"Reprinted from Publication title, Vol /edition number, Author(s), Title of article / title of chapter, Pages No., Copyright (Year), with permission from Elsevier [OR APPLICABLE SOCIETY COPYRIGHT OWNER]." Also Lancet special credit - "Reprinted from The Lancet, Vol. number, Author(s), Title of article, Pages No., Copyright (Year), with permission from Elsevier."

4. Reproduction of this material is confined to the purpose and/or media for which permission is hereby given. The material may not be reproduced or used in any other way, including use in combination with an artificial intelligence tool (including to train an algorithm, test, process, analyse, generate output and/or develop any form of artificial intelligence tool), or to create any derivative work and/or service (including resulting from the use of artificial intelligence tools).

5. Altering/Modifying Material: Not Permitted. However figures and illustrations may be altered/adapted minimally to serve your work. Any other abbreviations, additions, deletions and/or any other alterations shall be made only with prior written authorization of Elsevier Ltd. (Please contact Elsevier's permissions helpdesk [here](#)). No modifications can be made to any Lancet figures/tables and they must be reproduced in full.

6. If the permission fee for the requested use of our material is waived in this instance, please be advised that your future requests for Elsevier materials may attract a fee.

7. Reservation of Rights: Publisher reserves all rights not specifically granted in the combination of (i) the license details provided by you and accepted in the course of this licensing transaction, (ii) these terms and conditions and (iii) CCC's Billing and Payment terms and conditions.

8. License Contingent Upon Payment: While you may exercise the rights licensed immediately upon issuance of the license at the end of the licensing process for the transaction, provided that you have disclosed complete and accurate details of your proposed use, no license is finally effective unless and until full payment is received from you (either by publisher or by CCC) as provided in CCC's Billing and Payment terms and conditions. If full payment is not received on a timely basis, then any license preliminarily granted shall be deemed automatically revoked and shall be void as if never granted. Further, in the event that you breach any of these terms and conditions or any of CCC's Billing and Payment terms and conditions, the license is automatically revoked and shall be void as if never granted. Use of materials as described in a revoked license, as well as any use of the materials beyond the scope of an unrevoked license, may constitute copyright infringement and publisher reserves the right to take any and all action to protect its copyright in the materials.

9. Warranties: Publisher makes no representations or warranties with respect to the licensed material.

10. Indemnity: You hereby indemnify and agree to hold harmless publisher and CCC, and their respective officers, directors, employees and agents, from and against any and all claims arising out of your use of the licensed material other than as specifically authorized pursuant to this license.

11. No Transfer of License: This license is personal to you and may not be sublicensed, assigned, or transferred by you to any other person without publisher's written permission.

12. No Amendment Except in Writing: This license may not be amended except in a writing signed by both parties (or, in the case of publisher, by CCC on publisher's behalf).

13. Objection to Contrary Terms: Publisher hereby objects to any terms contained in any purchase order, acknowledgment, check endorsement or other writing prepared by you, which terms are inconsistent with these terms and conditions or CCC's Billing and Payment terms and conditions. These terms and conditions, together with CCC's Billing and Payment terms and conditions (which are incorporated herein), comprise the entire agreement between you and publisher (and CCC) concerning this licensing transaction. In the event of any conflict between your obligations established by these terms and conditions and those established by CCC's Billing and Payment terms and conditions, these terms and conditions shall control.

14. Revocation: Elsevier or Copyright Clearance Center may deny the permissions described in this License at their sole discretion, for any reason or no reason, with a full refund payable to you. Notice of such denial will be made using the contact information provided by you. Failure to receive such notice will not alter or invalidate the denial. In no event will Elsevier or Copyright Clearance Center be responsible or liable for any costs, expenses or damage incurred by you as a result of a denial of your permission request, other than a refund of the amount(s) paid by you to Elsevier and/or Copyright Clearance Center for denied permissions.

LIMITED LICENSE

The following terms and conditions apply only to specific license types:

15. Translation: This permission is granted for non-exclusive world English rights only unless your license was granted for translation rights. If you licensed translation rights you may only translate this content into the languages you requested. A professional translator must perform all translations and reproduce the content word for word preserving the integrity of the article.

16. Posting licensed content on any Website: The following terms and conditions apply as follows: Licensing material from an Elsevier journal: All content posted to the web site must maintain the copyright information line on the bottom of each image; A hyper-text must be included to the Homepage of the journal from which you are licensing at <http://www.sciencedirect.com/science/journal/xxxxx> or the Elsevier homepage for books at <http://www.elsevier.com>; Central Storage: This license does not include permission for a scanned version of the material to be stored in a central repository such as that provided by Heron/XanEdu.

Licensing material from an Elsevier book: A hyper-text link must be included to the Elsevier homepage at <http://www.elsevier.com>. All content posted to the web site must maintain the copyright information line on the bottom of each image.

7 Permission of Redistribution and Licensing

Posting licensed content on Electronic reserve: In addition to the above the following clauses are applicable: The web site must be password-protected and made available only to bona fide students registered on a relevant course. This permission is granted for 1 year only. You may obtain a new license for future website posting.

17. For journal authors: the following clauses are applicable in addition to the above:

Preprints:

A preprint is an author's own write-up of research results and analysis, it has not been peer-reviewed, nor has it had any other value added to it by a publisher (such as formatting, copyright, technical enhancement etc.). Authors can share their preprints anywhere at any time. Preprints should not be added to or enhanced in any way in order to appear more like, or to substitute for, the final versions of articles however authors can update their preprints on arXiv or RePEc with their Accepted Author Manuscript (see below).

If accepted for publication, we encourage authors to link from the preprint to their formal publication via its DOI. Millions of researchers have access to the formal publications on ScienceDirect, and so links will help users to find, access, cite and use the best available version. Please note that Cell Press, The Lancet and some society-owned have different preprint policies. Information on these policies is available on the journal homepage.

Accepted Author Manuscripts: An accepted author manuscript is the manuscript of an article that has been accepted for publication and which typically includes author-incorporated changes suggested during submission, peer review and editor-author communications.

Authors can share their accepted author manuscript:

- immediately
 - via their non-commercial person homepage or blog
 - by updating a preprint in arXiv or RePEc with the accepted manuscript
 - via their research institute or institutional repository for internal institutional uses or as part of an invitation-only research collaboration work-group
 - directly by providing copies to their students or to research collaborators for their personal use
 - for private scholarly sharing as part of an invitation-only work group on commercial sites with which Elsevier has an agreement
- After the embargo period
 - via non-commercial hosting platforms such as their institutional repository
 - via commercial sites with which Elsevier has an agreement

In all cases accepted manuscripts should:

- link to the formal publication via its DOI
- bear a CC-BY-NC-ND license - this is easy to do
- if aggregated with other manuscripts, for example in a repository or other site, be shared in alignment with our hosting policy not be added to or enhanced in any way to appear more like, or to substitute for, the published journal article.

Published journal article (JPA): A published journal article (JPA) is the definitive final record of published research that appears or will appear in the journal and embodies all value-adding publishing activities including peer review co-ordination, copy-editing, formatting, (if relevant) pagination and online enrichment.

Policies for sharing publishing journal articles differ for subscription and gold open access articles:

Subscription Articles: If you are an author, please share a link to your article rather than the full-text. Millions of researchers have access to the formal publications on ScienceDirect, and so links will help your users to find, access, cite, and use the best available version.

Theses and dissertations which contain embedded JPAs as part of the formal submission can be posted publicly by the awarding institution with DOI links back to the formal publications on ScienceDirect.

If you are affiliated with a library that subscribes to ScienceDirect you have additional private sharing rights for others' research accessed under that agreement. This includes use for classroom teaching and internal training at the institution (including use in course packs and courseware programs), and inclusion of the article for grant funding purposes.

Gold Open Access Articles: May be shared according to the author-selected end-user license and should contain a [CrossMark logo](#), the end user license, and a DOI link to the formal publication on ScienceDirect.

Please refer to Elsevier's [posting policy](#) for further information.

18. For book authors the following clauses are applicable in addition to the above: Authors are permitted to place a brief summary of their work online only. You are not allowed to download and post the published electronic version of your chapter, nor may you scan the printed edition to create an electronic version. **Posting to a repository:** Authors are permitted to post a summary of their chapter only in their institution's repository.

19. Thesis/Dissertation: If your license is for use in a thesis/dissertation your thesis may be submitted to your institution in either print or electronic form. Should your thesis be published commercially, please reapply for permission. These requirements include permission for the Library and Archives of Canada to supply single copies, on demand, of the complete thesis and include permission for Proquest/UMI to supply single copies, on demand, of the complete thesis. Should your thesis be published commercially, please reapply for permission. Theses and dissertations which contain embedded JPAs as part of the formal submission can be posted publicly by the awarding institution with DOI links back to the formal publications on ScienceDirect.

Elsevier Open Access Terms and Conditions

You can publish open access with Elsevier in hundreds of open access journals or in nearly 2000 established subscription journals that support open access publishing. Permitted third party re-use of these open access articles is defined by the author's choice of Creative Commons user license. See our [open access license policy](#) for more information.

Terms & Conditions applicable to all Open Access articles published with Elsevier:

Any reuse of the article must not represent the author as endorsing the adaptation of the article nor should the article be modified in such a way as to damage the author's honour or reputation. If any changes have been made, such changes must be clearly indicated.

The author(s) must be appropriately credited and we ask that you include the end user license and a DOI link to the formal publication on ScienceDirect.

If any part of the material to be used (for example, figures) has appeared in our publication with credit or acknowledgement to another source it is the responsibility of the user to ensure their reuse complies with the terms and conditions determined by the rights holder.

Additional Terms & Conditions applicable to each Creative Commons user license:

CC BY: The CC-BY license allows users to copy, to create extracts, abstracts and new works from the Article, to alter and revise the Article and to make commercial use of the Article (including reuse and/or resale of the Article by commercial entities), provided the user gives appropriate credit (with a link to the formal publication through the relevant DOI), provides a link to the license, indicates if changes were made and the licensor is not represented as endorsing the use made of the work. The full details of the license are available at <http://creativecommons.org/licenses/by/4.0>.

CC BY NC SA: The CC BY-NC-SA license allows users to copy, to create extracts, abstracts and new works from the Article, to alter and revise the Article, provided this is not done for commercial purposes, and that the user gives appropriate credit (with a link to the formal publication through the relevant DOI), provides a link to the license, indicates if changes were made and the licensor is not represented as endorsing the use made of the work. Further, any new works must be made available on the same conditions. The full details of the license are available at <http://creativecommons.org/licenses/by-nc-sa/4.0>.

CC BY NC ND: The CC BY-NC-ND license allows users to copy and distribute the Article, provided this is not done for commercial purposes and further does not permit distribution of the Article if it is changed or edited in any way, and provided the user gives appropriate credit (with a link to the formal publication through the relevant DOI), provides a link to the license, and that the licensor is not represented as endorsing the use made of the work. The full details of the license are available at <http://creativecommons.org/licenses/by-nc-nd/4.0>. Any commercial reuse of Open Access articles published with a CC BY NC SA or CC BY NC ND license requires permission from Elsevier and will be subject to a fee.

Commercial reuse includes:

- Associating advertising with the full text of the Article
- Charging fees for document delivery or access
- Article aggregation
- Systematic distribution via e-mail lists or share buttons

Posting or linking by commercial companies for use by customers of those companies.

20. Other Conditions:

v1.10

Questions? E-mail us at customercare@copyright.com.